ISSN 0031 - 9465

PHYTOPATHOLOGIA MEDITERRANEA

Plant health and food safety

Volume 64 • No. 1 • April 2025

The international journal of the
Mediterranean Phytopathological Union

FIRENZE UNIVERSITY PRESS

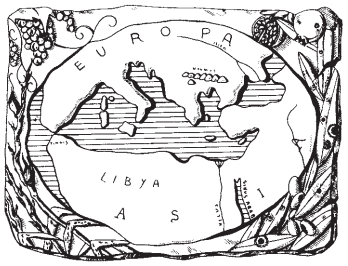

PHYTOPATHOLOGIA MEDITERRANEA

Plant health and food safety

The international journal edited by the Mediterranean Phytopathological Union
founded by A. Ciccarone and G. Goidànich

Phytopathologia Mediterranea is an international journal edited by the Mediterranean Phytopathological Union. The journal's mission is the promotion of plant health for Mediterranean climate and regions, safe food production, and the transfer of knowledge on diseases and their sustainable management.
The journal deals with all areas of plant pathology, including epidemiology, disease control, biochemical and physiological aspects, and utilization of molecular technologies. All types of plant pathogens are covered, including fungi, nematodes, protozoa, bacteria, phytoplasmas, viruses, and viroids. Papers on mycotoxins, biological and integrated management of plant diseases, and the use of natural substances in disease and weed control are also strongly encouraged. The journal focuses on phytopathology and closely related fields in the Mediterranean agro-ecological regions. The journal includes three issues each year, publishing Reviews, Original research papers, Short notes, New or unusual disease reports, News and opinion, Current topics, Commentaries, and Letters to the Editor.

PHYTOPATHOLOGIA MEDITERRANEA

The international journal of the Mediterranean Phytopathological Union

Volume 64, April, 2025

Firenze University Press

Phytopathologia Mediterranea. The international journal of the Mediterranean Phytopathological Union
https://www.fupress.com/pm
ISSN 0031-9465 (print) | ISSN 1593-2095 (online)
Published three times a year

Published by Firenze University Press

Firenze University Press
Università degli Studi di Firenze
via Cittadella, 7, 50144 Firenze, Italy
www.fupress.com

Phytopathologia Mediterranea
The international journal of the
Mediterranean Phytopathological Union

Firenze University Press
www.fupress.com/pm

New or Unusual Disease Reports

First report of *Calosphaeria pulchella* causing canker and branch dieback of sour cherry trees (*Prunus cerasus*) in North Macedonia

Sasa MITREV[1,*], Dzoko KUNGULOVSKI[2], Emilija ARSOV[1], Biljana KOVACEVIK[1]

[1] *Department for Plant Protection and Environment, Faculty of Agriculture, Goce Delcev University - Stip, UNILAB laboratory, Krste Misirkov, 10-A, P.O. 201, 2000, Stip, Republic of North Macedonia*
[2] *Department of Microbiology and Microbial Biotechnology, Institute of Biology, Faculty of Natural Sciences and Mathematics-Skopje, Ss. Cyril and Methodius University in Skopje, Republic of North Macedonia*
*Corresponding author. E-mail: sasa.mitrev@ugd.edu.mk

Summary. Symptoms of Calosphaeria canker were observed on sour cherry trees in the Stip region of North Macedonia. Fungal isolates were obtained from the infected twigs and branches showing external symptoms of twig dieback, occasionally followed by amber-coloured gummy exudates and brown to black vascular streaking in tissue cross-sections. The fungus was identified as *Calosphaeria pulchella* (Pers.: Fr.) J. Schröt (syn. *Calosphaeriophora pulchella* Réblová, L. Mostert, W. Gams & Crous), based on its morphology, and this identification was confirmed by sequence comparison in the GenBank database using the internal transcribed spacer region (RBK02_ITS1-ITS4) of the rDNA. The sequences had 100% identity and 100% query coverage with *C. pulchella* reference isolate SJC-6+ITS Internal transcribed spacer 1. Pathogenicity tests conducted on sour cherry and apricot trees showed that the obtained isolates were pathogenic to sour cherry, but not to apricot. This is the first report of *Calosphaeria pulchella* on sour cherry trees in North Macedonia, and in the Balkan region. This study increases understanding of the status of *C. pulchella* as a pathogen in this region.

Keywords. ITS, fungus, Calosphaeria canker.

OPEN ACCESS

Citation: Mitrev, S., Kungulovski, D., Arsov, E. & Kovacevik, B. (2025). First report of Calosphaeria pulchella causing canker and branch dieback of sour cherry trees (*Prunus cerasus*) in North Macedonia. *Phytopathologia Mediterranea* 64(1): 3-8. doi: 10.36253/phyto-15660

Accepted: January 10, 2025

Published: May 15, 2025

Data Availability Statement: All relevant data are within the paper and its Supporting Information files.

Competing Interests: The Author(s) declare(s) no conflict of interest.

Editor: José R. Úrbez Torres, Agriculture and Agri-Food Canada, Summerland, British Columbia, Canada.

ORCID:
SM: 0000-0003-2004-4687
DK: 0009-0002-0825-7487
EA: 0000-0002-8978-4635
BK: 0000-0002-3361-0759

INTRODUCTION

Trunk and branch canker diseases have been reported in many countries, particularly indicating the prevalence of these diseases among *Prunus* spp., and the increasing concerns among related fruit production industries. Common symptoms of these diseases include wood necroses and cankers on the plant trunks or scaffold branches, necroses of woody tissues, and gummoses. As a result of host zylem and phloem disruption, movement of water and nutrients may cease, resulting in death of cambial and bark tissues and shoot and branch dieback. Over time, significant parts of affected trees or whole trees may die, while other trees in an orchard may remain unaffected.

Literature has reported that Cytospora canker, also known as perennial canker, Eutypa dieback, and Calosphaeria canker, are the most common diseases in cherry trees (Trouillas *et al*. 2012). Most studies referred to canker in sweet cherries, while information on the disease in sour cherries is scarce. Pruning wounds are the main entry points for the pathogens causing these diseases. *Calosphaeria pulchella* (Pers.: Fr.) J. Schröt (syn. *Calosphaeriophora pulchella* Réblová, L. Mostert, W. Gams & Crous) is associated with Calosphaeria canker in sweet cherry trees, and has been reported on sweet cherry in Spain (Berbegal *et al*., 2014; Berbegal and Armengol, 2018), Australia (Trouillas *et al*., 2012), California (Trouillas *et al.* 2010), France (Réblová *et al*., 2004), Italy (Cainelli *et al*., 2017), Germany (Bien and Damm, 2020), Chile (Auger *et al*. 2020), and in Turkey (Özben and Uzunok, 2023). The fungus also occurs on peach (*Prunus persica*) (Grinbergs *et al*., 2023), nectarine (*P. persica*) (Trouillas *et al*., 2012), and almond (*P. dulcis*) (Arzanlou and Dokhanchi, 2013). Relevance of the pathogen on other *Prunus* spp. is insufficiently explored. Perithecia of the pathogen are commonly produced beneath the periderms of dead and diseased branches. Asexual fruiting bodies of the pathogen have not been observed in nature, but an *Acremonium*-like anamorph was observed in culture by Réblová *et al.* (2004), for which *Calosphaeriophora* was proposed.

Rain and sprinkle irrigation favour the release of *C. pulchella* ascospores, which are the primary inocula (Trouillas *et al*., 2012). Canker has been noticed in established sour cherry orchards in the region of Stip during the last 10 years., in the Eastern part of North Macedonia. Although symptoms of canker are commonly observed on individual trees in sour cherry orchards in the Republic of North Macedonia, no study has identified the causal pathogens in this country. There is also no literature on occurrence of canker in sour cherries in the rest of the Balkan Peninsula, nor in Serbia, which are important areas for sour cherry production in the Balkans and Europe.

The aim of the present study was to characterize the causal agent of sour cherry canker in orchards of the Stip province, using phenotypic characteristics and provide description of morphological and molecular features of the pathogen.

MATERIALS AND METHODS

Experimental sites

The investigated commercial sour cherry tree orchards were located in the region of Stip, covering the area of 60 ha in the Eastern part of North Macedonia. During 2019, symptoms of canker were observed in approx. 10% of the cv. Oblachinska trees, which is a leading sour cherry variety grown in North Macedonia and the Balkan region. Harvested fruit is mainly used for industrial processing, although fresh consumption is also important because the fruit have high sugar and antioxidant contents (Karakashova *et al*., 2022). The trees were 5 to 10 years old at the time of the investigation. Spacings between trees in the orchards were 2.5 m within rows and 4 m between rows. Regular agrotechnical measures applied to the orchards include drip irrigation and annual pruning in early spring. Winter treatments included copper fungicides and insecticidal oil applications, while growing season regular protection was applied against *Monilinia*, using fungicides based on boscalid, pyraclostrobin, captan, or dithianon.

Pathogen isolation and pathogenicity tests

Symptomatic branches, suggesting canker disease, were collected from ten sour cherry trees. The bark was removed, and small pieces of wood were cut between diseased and healthy tissues. These wood samples were sterilized using 56% ethanol for approx. 30 s, double rinsed in sterile distilled water, dried, and then placed in Petri dishes containing potato dextrose agar (PDA; Biolife). The dishes were then maintained in the dark at 25°C until mycelium developed. Cultures were purified by transferring single hyphal tips onto new sterile PDA Petri plates. The fungal isolates obtained have been deposited in the culture collection of the UNILAB laboratory.

Pathogenicity of the isolates was assessed by inoculating healthy 5-year-old sour cherry plants (cv. Oblachinska) in May 2019. Circular injuries were made on the scaffold branches using a sterile knife. Inoculations were made using water suspension (10^8 CFU) from actively growing 7-d-old mycelium cultures, after which the inoculated wounds were covered with sterile cotton and plastic film (Figure 5 A). Water suspensions of sterile PDA were used as a negative inoculation control, following the same procedure for inoculation. Inoculated branches and trees were examined for symptoms every 2 weeks for the following 3 months. Pathogenicity of the isolates to apricots (cv. 'Roxana') was also assessed, using the procedures described above.

Morphological characterization of isolated fungi

Isolates were tentatively identified using available literature (Réblová *et al.,* 2004; Trouillas *et al*., 2012). Colony morphology was assessed after 20 d incubation on PDA at

25°C, with cultures maintained in the dark to characterize the fungus anamorph. Colony colour was assessed, and size, colour and shape of conidiophores, phialides, and conidia were observed using an Olympus BX41 light microscope. Measurements fungus characteristics (n = 100) were conducted in water at ×1,000 magnification using an ocular micrometer. Images of the fungi captured using a digital camera (Olympus U-CMAD3, Mini Vid, LW Scientific).

DNA extraction, PCR amplification and sequencing

Identification of the isolates was achieved using polymerase chain reaction (PCR) by amplification of the internal transcribed spacer region (ITS) of the rDNA. Total genomic DNA was extracted according to the protocol of Möller *et al.* (1992). DNA amplification of the ITS region (Internal Transcribed Spacer region of the rDNA) was achieved using primers ITS1 (*5′TCCGTAGGTGAACCTGCGG3′*) and ITS4 (*5′TCCTCCGCTTATTGATATGC3′*) (Ferrer *et al*., 2001). PCR reactions were carried out in a thermal cycler (Eppendorf AG, No.5332) as follows: initial denaturation for 3 min at 95°C; amplification for 40 cycles of of 30 sec each; denaturation at 95°C, 1 min of primer annealing at 55–60°C and 45 sec for extension at 72°C, followed by a final step at 72°C for 5 min (Ferrer *et al*., 2001). PCR fragments were separated on 1.5% agarose gel (UltraPure™ Agarose, Invitrogen), stained in ethidium bromide and visualized under UV light. PCR-amplified fragments were used to construct libraries with rapid barcoding for Oxford Nanopore sequencing on the MinION device, using a Flongle flow cell. Total genomic DNA was extracted according to the protocol of Moller *et al.* (1992). The sequencing run produced 1,354 sample-specific reads in FASTQ format, which were then analyzed for taxonomic classification through the wf-metagenomics workflow on the EPI2ME platform. This workflow leveraged the NCBI Targeted Loci database, encompassing 16S rDNA, 18S rDNA, and ITS regions, to ensure accurate taxonomic assignment. Additionally, a consensus FASTA sequence of the ITS region was generated using the Medaka pipeline (https://github.com/nanoporetech/medaka), and BLASTn analysis was carried out to identify sequences with significant alignments.

RESULTS AND DISCUSSION

Disease symptoms on naturally infected sour cherry trees

Canker symptoms were observed on cv. 'Oblachinska' sour cherry trees that had been growing under stress conditions (lack of water), with the symptoms appearing on wood and bark of twigs, branches and trunks. Trees in early stages of disease showed less visible symptoms, particularly in old scaffold branches and trunks, whereas symptoms on young twigs were more noticeable, including twig dieback and dead buds, occasionally with amber-coloured gummy exudate (Figure 1 B). Cankers were usually observed on host plant scaffold branches and trunks in latter stages of infections, and were often accompanied by gum exudation that leached from the cankers. Brown to black vascular streaking was visible in branch cross-sections, as circular discolouration within the tissue which advanced gradually from the heartwood into the sapwood (Figure 1 A). Symptoms of dead arm, twig, and branch dieback, and leaf desiccation were also observed (Figure 1 D). In severe cases and mostly in older trees, periderm was detached from the phloem, and perithecia bodies in circinate groups were present (Figure 1, C and F). Occasionally, large parts of affected trees were evident, and some trees were dead. These observed symptoms indicated the presence of Calosphaeria canker.

Morphological and cultural features of isolated fungi

Ten fungal isolates were obtained from sour cherry trees which had trunk or branch cankers and symptomatic young twigs. All the isolates had similar appearances, and their colonies were slow growing and distinct. After 15 d at 25°C, the isolate colonies had ceramide red moderate aerial mycelium with white margins.. After 30 d incubation, the colony colour became more intense dark purple (Figure 1 G). Young hyphae were hyaline with red pigmentation developing in cells, which had striped appearance when examined with light microscopy (Figure 2 A). Well-developed hyphae were completely red (Figure 2, A, B, and D). Individual hyphae grew in circular formations, giving a unique appearance (Figure 2 B). Conidiophores were phialidic, unbranched, and hyaline while conidiogenous cells (phialides) were hyaline, terminal or lateral, and monophialidic. Two types of phialides, which differed in size and shape, were observed on aerial mycelium. Type I phialides were the shortest, and were vase shaped adelophialides (Figure 2 F). Type II phialides were elongate ampulliform and slightly attenuated at the bases (Figure 2, D, and E). Conidia were hyaline, aseptate, allantoid to suballantoid in shape, with mean dimensions 2.7–9.3 × 1.3–2.5 μm (Figure 2 G). Perithecia were black, flask-shaped, with elongated necks, and were arranged in dense circinate groups beneath the periderm (Figure 1 F).

Morphological characteristics of the anamorph observed in culture, and teleomorph structures found

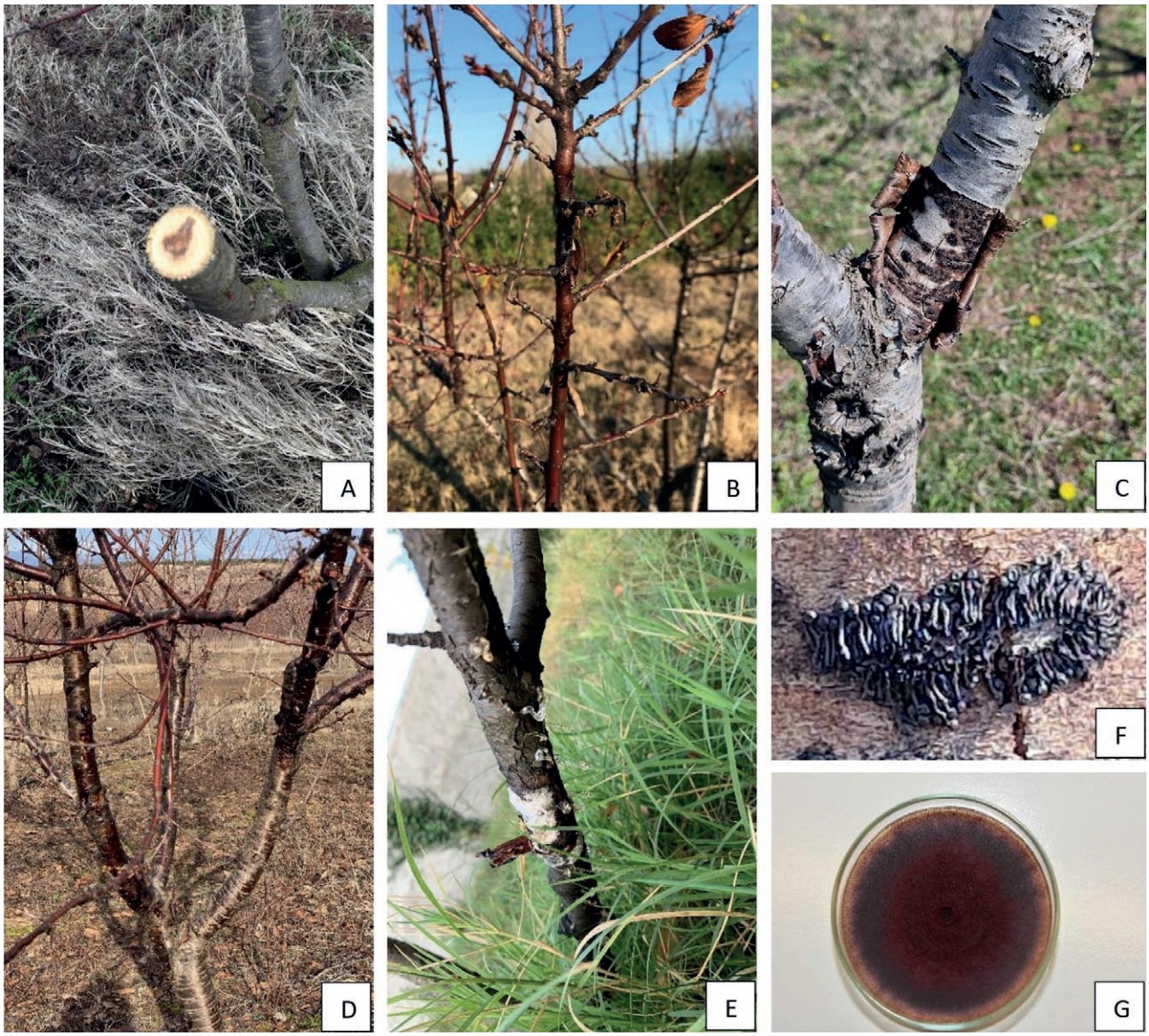

Figure 1. Symptoms of Calosphaeria canker on sour cherry observed in the field (A to D), and after inoculation (E). A, Internal wood necrosis and vascular discolouration. B, Twig dieback and dead buds. C and F, Bark cracking and appearance of circinate groups of perithecia on the scaffold branches beneath the periderm. D. Symptoms of dead arm. E. Gummy exudate on an inoculated trunk. G, Colony of isolate on PDA after 21 d incubation at 25°C.

in the field, accorded with those described as *Calosphaeria pulchella* by Réblová *et al.* (2004) and Trouillas *et al.* (2012).

Molecular identification of isolates

PCR fragments were separated on 1.5% agarose gel, stained in ethidium bromide, and visualized under UV light. The PCR products corresponded to size 330 bp for ITS. Three out of four samples indicated of *C. pulchella*. The identity of the fungus was further confirmed by sequencing, using one representative isolate. The taxonomic assignment conducted using the wf-metagenomics workflow identified a single hit corresponding to *C. pulchella*. Subsequent BLASTn analysis of the consensus sequence revealed a significant match to *C. pulchella* isolate SJC-61. Identification of *C. pulchella* isolates was confirmed by sequence comparison in the GenBank database using the internal transcribed spacer region (RBK02_ITS1-ITS4) of the rDNA. Sequences

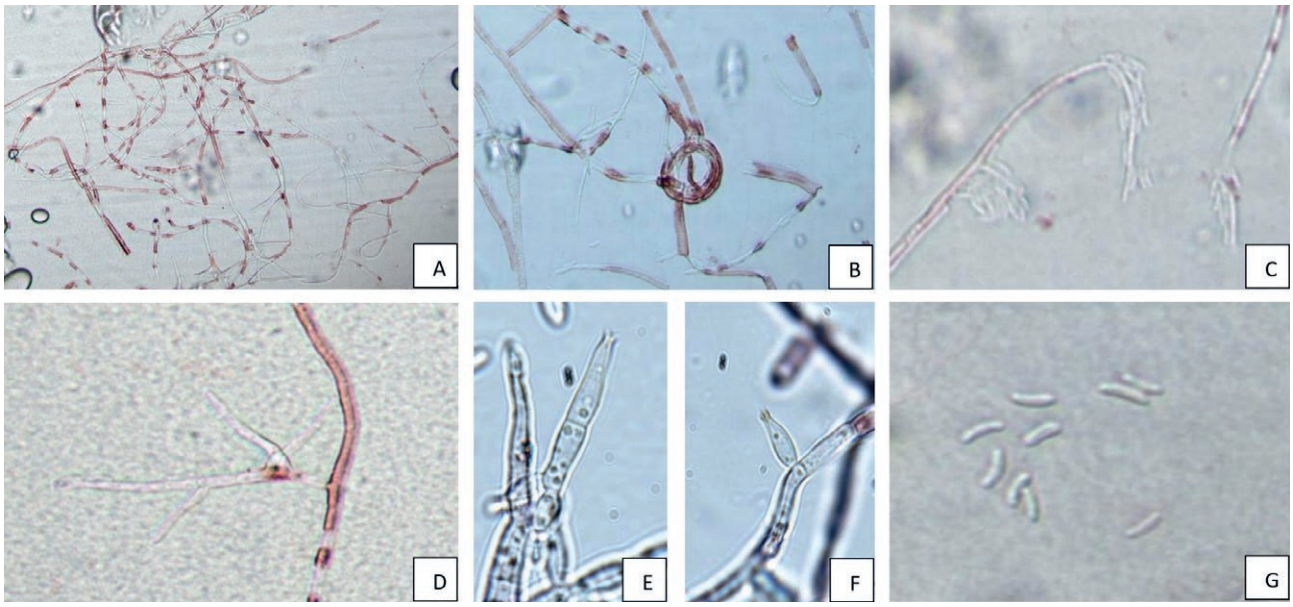

Figure 2. Morphology of *Calosphaeria pulchella*. A, Hyphae on PDA after 21 d incubation at 25°C. B, Coiled hyphae. C, Conidia forming in bunches. D, Two phialides. E, Type II phialide. F, Adelophialide. G, Allantoid to suballantoid hyaline conidia formed on PDA.

showed 100% identity and 100% query coverage with *C. pulchella* reference isolate SJC-6+ITS Internal transcribed spacer 1. The ITS sequence of one of the isolates obtained in this study was deposited into the GenBank (AN PP063991.1).

Pathogenicity tests

Pathogenicity tests showed that the *C. pulchella* isolates were pathogenic to sour cherry, but not to apricot. Observed symptoms on inoculated trees were very similar to the naturally occurring symptoms. Cankers appeared on inoculated trunks and scaffold branches, showing extensive hyaline gummy exudate (Figure 1 E), followed by dieback and gummoses on shooting twigs, as well as leaf decay and dieback of inoculated trunks. Development of the *C. pulchella* teleomorph was not observed on the inoculated branches. The pathogen was re-isolated from symptomatic twigs at 100% recovery rate, and its identity was confirmed, thus fulfilling Koch's postulates. No recovery of *C. pulchella* was obtained from the non-inoculated branches.

CONCLUSIONS

Disease symptoms, and the morphological and molecular analyses in this study confirmed the presence of *C. pulchella* on sour cherry in North Macedonia, and this fungus and its anamorph are well-known as plant pathogenic *Ascomycetes*. The circinate groups of perithecia that occurred on host trunks and beneath the periderm are important signs for easy and quick diagnoses of Calosphaeria canker in the field. Pathogenicity of *C. pulchella* is well documented on sweet cherry, peach, nectarine and almond, but its relevance on sour cherry and on the other *Prunus* spp. is sinsufficiently explored. Only the study of Bien and Damm (2020) has reported isolation of *C. pulchella* from sour cherry, and that described a phylogenetic analysis of wood pathogens on *Prunus* trees in Germany.

Results from the present study confirm the pathogenicity of the *C. pulchella* isolates to sour cherry, and have shown that these isolates were not pathogenic to apricot. These results are the first identification of *Calosphaeria pulchella* (syn. *Calosphaeriophora pulchella*) causing canker on sour cherry in North Macedonia, in the Balkan region, and elsewhere in Central Europe.

Further research is required to determine the potential impacts of Calosphaeria canker on sour cherry and its potential to cause dieback diseases. It was observed that trees grown under stress conditions, particularly excess water, promote disease development. Winter treatments with copper fungicides and insecticidal oils, as well as chemical treatments based on the multi-site contact fungicides captan and dithianon, and the succinate-dehydrogenase inhibitor boscalid and the quinone outside inhibitor pyraclostrobin, which are

used for regular protection against *Monilinia* in investigated general area of this study, have been shown to be ineffective against *C. pulchella*. Therefore, specific management strategies must be developed to reduce the impact of Calosphaeria canker, to provide sustainability in sour cherry production. If *C. pulchella* is not managed, it could result in substantial economic losses for sour cherry producers.

This research has increased knowledge of the aetiology of canker diseases affecting sour cherry trees and suggest that more attention should be given to Calosphaeria canker disease on sour cherries in the Balkans.

LITERATURE CITED

Auger J., Pozo L., Rubilar M., Briceño N., Osorio-Navarro C., Esterio M., 2020. First Report of canker and branch dieback of sweet cherry trees caused by *Calosphaeria pulchella* in Chile. *Plant Disease* 105(1): 2017. https://doi.org/10.1094/PDIS-05-20-1026-PDN

Arzanlou M., Dokhanchi H., 2013. Calosphaeria canker of almond caused *by Calosphaeria pulchella* in Iran. *Archives of Phytopathology and Plant Protection* 46(2): 215–226. https://doi.org/10.1080/03235408.2012.737256

Berbegal M., García-Jiménez J., Armengol J., 2014. First report of *Calosphaeria pulchella* causing canker and branch dieback of sweet cherry trees in Spain. *Plant Disease* 98: 1008–1009. https://doi.org/10.1094/PDIS-01-14-0027-PDN

Berbegal M., Armengol J., 2018. Pruning practices influence infection and dissemination of *Calosphaeria pulchella*, the cause of Calosphaeria canker of sweet cherry. *Phytopathologia Mediterranea* 57(1): 3–7. https://doi.org/10.14601/Phytopathol_Mediterr-21185

Bien S., Damm U., 2020. Prunus trees in Germany—a hideout of unknown fungi? *Mycological Progress* 19(7): 667–690. https://doi.org/10.1007/s11557-020-01586-4

Cainelli C., Longa C.M.O., Franchini S., Angeli G., Prodorutti D., 2017. Calosphaeria canker of sweet cherry in Trentino (north-eastern Italy). *IOBC/WPRS BULLETIN* 123: 195-197.

Grinbergs D., Chilian J., Isla M., Otarola J., 2023. First report of *Calosphaeria pulchella* causing cankers in peach (*Prunus persica*) in Chile. *Plant Disease* 107(10): 3314.

Ferrer C., Colom F., Frases S., Mulet E., Abad L.J., Alio J.L., 2001. Detection and identification of fungal pathogens by PCR and by ITS2 and 5.8S ribosomal DNA typing in ocular infections. *Journal of Clinical Microbiology* 39(8): 2873–2879. https://doi.org/10.1128/JCM.39.8.2873-2879.2001

Karakashova L., Bogdanovska V., Stojanov M., Milenkovska F.B., Velkoska-Markovska L., ... Durmishi N., 2022. Total anthocyanins in fresh fruit and compote of "Oblacinska" sour cherry (*Prunus cerasus* L.). *Journal of Agricultural, Food and Environmental Sciences* 76(3): 25–30. https://doi.org/10.55302/jafes22763025k

Möller E.M., Bahnweg G., Sandermann H., Geiger H.H., 1992. A simple and efficient protocol for isolation of high molecular weight DNA from filamentous fungi, fruit bodies, and infected plant tissues. *Nucleic Acids Research,* 1992, Vol. 20, No. 22, 6115-6116.

Özben S., Uzunok S., 2023. First report of *Calosphaeria pulchella* causing canker and branch

dieback of cherry in Turkey. *Journal of Plant Pathology* 105:339 https://doi.org/10.1007/s42161-022-01255-3

Réblová M., Mostert L., Gams W., Crous, P.W., 2004. New genera in the *Calosphaeriales*: *Togniniella* and its anamorph *Phaeocrella*, and *Calosphaeriophora* as anamorph of *Calosphaeria*. *Studies in Mycology* 50(2): 533-550.

Trouillas F.P., Lorber J.D., Peduto F., Grant J., Coates W.W., ... Gubler W.D., 2010. First report of *Calosphaeria pulchella* associated with branch dieback of sweet cherry trees in California. *Plant Disease* 94:1167. https://doi.org/10.1094/pdis-94-9-1167a

Trouillas F.P., Peduto F., Lorber J.D., Sosnowski M.R., Grant J., ... Gubler W.D., 2012. Calosphaeria canker of sweet cherry caused by *Calosphaeria pulchella* in California and South Australia. *Plant Disease* 96(5):648-658. https://doi.org/10.1094/PDIS-03-11-0237

Phytopathologia Mediterranea
The international journal of the
Mediterranean Phytopathological Union

Firenze University Press
www.fupress.com/pm

Research Papers

Root and crown rot caused by *Fusarium pseudograminearum* in the euhalophyte *Salicornia europaea*: pathogenicity and mycotoxin production in plants grown in soilless culture

Emiliano DELLI COMPAGNI[1,*], Alberto PARDOSSI[1,2], Susanna PECCHIA[1,2]

[1] *Department of Agriculture, Food and Environment, University of Pisa, Via del Borghetto 80, I-56124 Pisa, Italy*
[2] *Interdepartmental Research Center Nutrafood "Nutraceuticals and Food for Health", University of Pisa, Via del Borghetto 80, I-56124 Pisa, Italy*
*Corresponding author. E-mail: emiliano.dellicompagni@phd.unipi.it

Summary. *Salicornia europaea* L. is a euhalophyte increasingly cultivated as a high-value green vegetable. In July 2021, root and crown rot occurred on 6-month-old *S. europaea* plants grown in peat-filled pots under a greenhouse, affecting 25% of plants. The causal agent was identified as *Fusarium pseudograminearum* O'Donnell & T. Aoki using morphological and molecular analyses. An experiment to assess the pathogenicity of this fungus to *S. europaea* was conducted with 96 seedlings in hydroponic culture. Half of these plants were inoculated with a conidial suspension of *F. pseudograminearum*. At 24 days post inoculation (dpi), half of the plants were transferred into a new hydroponic system, while the other plants were transplanted into pots. At 80 dpi, all inoculated plants grown in pots had shoot browning and desiccation symptoms, while these symptoms developed more slowly in 70% of the hydroponically grown inoculated plants. A qualitative symptom severity assessment scale showed that disease severity was greater (63%) in pot-grown plants than in hydroponically grown plants (46%). *Fusarium pseudograminearum* was consistently reisolated from diseased plants in both cultivation systems (62% from pots and 83% from hydroponics) fulfilling Koch's postulates. Production of deoxynivalenol (DON) and zearalenone (ZEA) was investigated *in vitro* and *in planta*. Traces of DON (0.029 ± 0.012 mg kg^{-1}) were found in severely damaged plants grown in hydroponics. In the *in vitro* test, *F. pseudograminearum* isolates from wheat crops in Spain (isolate ColPat-351) and Italy (isolate PVS Fu-7) were also assessed, and all tested isolates produced considerable amounts of ZEA. *Fusarium pseudograminearum* isolates obtained from *S. europaea* produced more DON (6.81 ± 0.24 mg kg^{-1}, on average) than the Italian isolate PVS Fu-7 (0.37 ± 0.06 mg kg^{-1}), while DON production by the Spanish isolate ColPat-351 was less than the limit of detection (< 0.25 mg kg^{-1}). This is the first report of root and crown rot caused by *F. pseudograminearum* on *S. europaea*.

Keywords. Deoxynivalenol, fungi, glasswort, hydroponic system, plant disease, zearalenone.

OPEN ACCESS

Citation: Delli Compagni, E., Pardossi, A. & Pecchia, S. (2025). Root and crown rot caused by *Fusarium pseudograminearum* in the euhalophyte *Salicornia europaea*: pathogenicity and mycotoxin production in plants grown in soilless culture. *Phytopathologia Mediterranea* 64(1): 9-23. doi: 10.36253/phyto-15597

Accepted: January 21, 2025

Published: May 15, 2025

Data Availability Statement: All relevant data are within the paper and its Supporting Information files.

Competing Interests: The Author(s) declare(s) no conflict of interest.

Editor: Adeline Picot, Université de Bretagne Occidentale, LUBEM, Plouzané, France.

ORCID:
EDC: 0000-0003-4357-4277
AP: 0000-0001-9927-4017
SP: 0000-0002-9017-4738

INTRODUCTION

Salicornia europaea L. (syn. *Salicornia perennans* Willd. subsp. *perennans*, *Amaranthaceae*), commonly known as glasswort or sea asparagus, is a euhalophyte that is widespread in many regions of the Northern Hemisphere, especially in the Mediterranean region (Lombardi *et al*., 2022). This plant thrives in saline ecosystems and can tolerate up to 1000 mM NaCl, with optimal growth at 200–400 mM NaCl (Cárdenas-Pérez *et al*., 2021). For this reason, it has received considerable interest as an alternative crop in saline agriculture, especially in desert areas and marginal lands (Araus *et al*., 2021). *Salicornia europaea* has a wide range of applications as a food and non-food crop. This plant is a good candidate for biodiesel production because of its high seed oil contents, for the remediation of saline soils, and for pharmaceutical purposes (Ventura and Sagi, 2013; Cárdenas-Pérez *et al*., 2021). It has edible shoots, raw or cooked, and is increasingly cultivated as a high-priced green vegetable (Araus *et al*., 2021; Cárdenas-Pérez *et al*., 2021). Despite the broad range of agronomic usages of *S. europaea*, little attention has been paid to phytopathological issues for this plant.

In July 2021, at the University of Pisa, severe root and crown rot symptoms were observed in pot-grown *S. europaea* plants purchased from a nursery in northern Italy (Figure 1, a, b, and c). Symptoms appeared on 25% of 6-month-old seed-propagated plants. The causal agent of the disease was identified as *Fusarium pseudograminearum* O'Donnell & T. Aoki. This fungus was previously described as *F. graminearum* Schwabe Group 1 and was identified for the first time in Australia in 1983 (Burgess *et al*., 1987). Subsequently, Aoki and O'Donnell (1999a) described the novel species *F. pseudograminearum*, based on morphological and molecular observations.

Fusarium pseudograminearum is a heterothallic Ascomycete, although the formation of perithecia by the teleomorph *Gibberella coronicola* T. Aoki & O'Donnell has been rarely observed (Aoki and O'Donnell, 1999b). This fungus is a soil-borne pathogen, primarily causing Fusarium crown rot (FCR) on small grain cereals, which is a common disease in warm, dry regions (Chakraborty *et al*., 2006; Poole *et al*., 2013; Sabburg *et al*., 2015). The fungus is widespread in Asia, especially China where it is becoming the predominant cause of FCR (Xu *et al*., 2017; Zhou *et al*., 2019; Deng *et al*., 2020), and in Australia (Obanor *et al*., 2013; Kazan and Gardiner, 2018). In Europe, the occurrence of *F. pseudograminearum* is unclear, as the pathogen has only been reported a few times. It was first identified as the cause of root rot on durum wheat in Foggia, southern Italy, by Balmas (1994), when it was still designated as *F. graminearum* Group 1. In 2016, *F. pseudograminearum* was found in Cordoba, southern Spain, causing FCR on *Triticum aestivum* (Agustí-Brisach *et al*., 2018). The pathogen has been described on wheat in the Mediterranean countries Algeria (Abdallah-Nekache *et al*., 2019), Syria (Alkadri *et al*., 2013), Tunisia (Kammoun *et al*., 2009), and Turkey (Tunali *et al*., 2008). However, Akinsanmi *et al.* (2007) noted that some alternative host plants (monocots and dicots) were infected by *F. pseudograminearum*, indicating that the pathogen is not host-specific. In Croatia, this fungus was first recorded on naturally infected rotted apples (Sever *et al*., 2012), and seeds of the wild legume *Vicia cracca* (Miličević *et al*., 2013). An endophytic *F. pseudograminearum* was also isolated from coastal dunegrass (*Leymus mollis*), improving plant growth and salinity resistance (Shan *et al*., 2021). Due to the uncertainty of the occurrence of the pathogen, the European Food Safety Authority (EFSA) has recently proposed to designate *F. pseudograminearum* as a potential quarantine pathogen for the European Union (EFSA Panel Health, 2022).

A key feature in several *Fusarium* species (including *F. culmorum*, *F. graminearum*, and *F. pseudograminearum*) is their ability to produce trichothecene B mycotoxins. This class of mycotoxins includes deoxynivalenol (DON), nivalenol (NIV), and acetylated derivatives (3-acetyldeoxynivalenol, 3ADON; 15-acetyldeoxynivalenol, 15ADON). Based on the type of trichothecene produced, each isolate can be assigned to a specific chemotype (3ADON, 15ADON, NIV). Each chemotype is determined by the trichothecene gene cluster (*tri*), composed of ten to 12 contiguous genes. The number of functional genes in this cluster varies depending on the species and chemotype (Pasquali and Migheli, 2014). Zearalenone (ZEA) is another mycotoxin of interest that exhibits strong estrogenic effects in mammals. ZEA is a polyketide mycotoxin synthesized from the acetate-polymalonate pathway, in which four genes are involved: *pks4*, *pks13*, *zeb1*, and *zeb2* (Nahle et al. 2021). Determining the mycotoxins produced by an isolate is essential for studying the dynamics of a fungal population in a specific agricultural area, and to evaluate toxigenic risks of specific chemotypes in food and feed.

Root and crown rot caused by *F. pseudograminearum* on cultivated *S. europaea* plants has not been previously described. Therefore, the aims of the present study were: (i) to assess the pathogenicity and evaluate disease severity caused by a selected isolate of *F. pseudograminearum* towards *S. europaea* plants grown in two different growing systems (pots and hydroponics); and (ii) to determine the mycotoxins produced by three isolates of

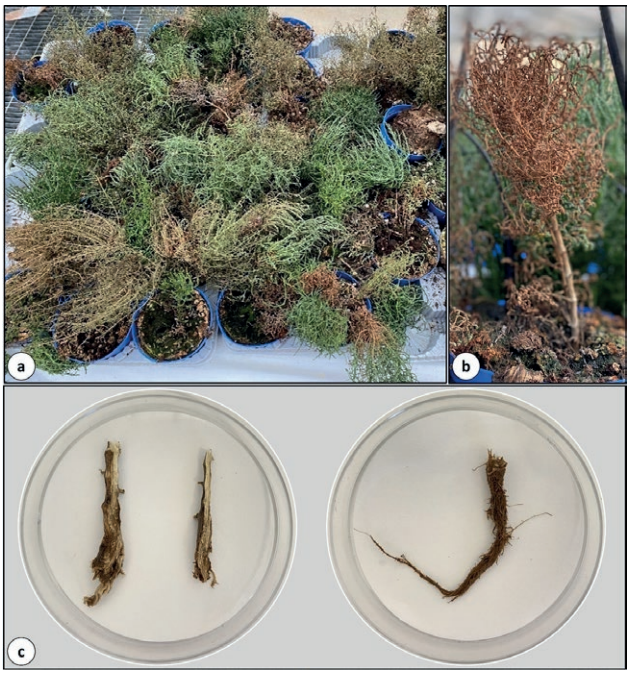

Figure 1. Diseased *Salicornia europaea* plants grown in pots. a) Overview of the pots on a greenhouse bench. b) A completely desiccated plant. c) Diseased plant crowns and roots.

F. pseudograminearum from *S. europaea* compared to two other European isolates of *F. pseudograminearum*.

MATERIALS AND METHODS

Origin of infected samples and isolation of fungal isolates

Severe root and crown rot symptoms were observed on seed-propagated *S. europaea* plants (approx. 6 months old) that had been purchased from a commercial nursery in northern Italy. The plants were grown in pots filled with peat (Figure 1, a and b). Symptoms affected 25% of the plants.

To isolate the putative causal agent, the roots and crowns of affected plants were gently washed under running tap water. Symptomatic tissues (Figure 1 c) were then cut into small pieces and surface sterilized with sodium hypochlorite (NaOCl; 1% available chlorine) for 2 min, rinsed twice for 2 min in sterile distilled water, and then plated onto Potato Dextrose Agar plates (PDA, 42 g L^{-1}, BioLife, Milan, Italy) amended with streptomycin (0.3 g L^{-1}, Sigma-Aldrich, Saint Louis, MO, USA). The plates were then incubated at 25 ± 1°C under fluorescent light and checked daily for mycelium development. After 4 days of incubation, hyphae emerging from infected plant tissues were transferred onto new PDA plates.

Monoconidial cultures and storage conditions

Colony morphology, and macroconidia shapes observed under an optical microscope indicated that the putative causal agent of the disease belonged to the genus *Fusarium*. Further analyses, both morphological and molecular, were carried out by generating monoconidial cultures of three selected isolates (designated 3B, PD-A, and PD-B), each obtained from a different diseased plant. An isolate of *F. oxysporum* (DAFE SP21-23), a fungus often associated with *S. europaea* plant tissues but not pathogenic, was included in the study as a negative control. For preservation of the isolates, PDA plugs derived from the above-described monoconidial cultures were transferred onto Synthetic Nutrient-poor Agar (SNA), which contained: 1 g L^{-1} KH_2PO_4; 1 g L^{-1} KNO_3; 0.5 g L^{-1} $MgSO_4 \cdot 7H_2O$; 0.5 g L^{-1} KCl; 0.2 g L^{-1} glucose; 0.2 g L^{-1} sucrose; and 20 g L^{-1} agar (Nirenberg, 1981). The cultures were stored at 4°C. All the chemicals used in the culture medium were obtained from Sigma-Aldrich (Saint Louis, MO, USA).

Species identification

Morphological observations

The three monoconidial isolates, derived from three different plants, were identified at species level by combining a morphological and molecular approach. Colony morphology, pigmentation, and macroconidia sizes were compared to the published descriptions of Aoki and O'Donnell (1999a). Suspensions of macroconidia were obtained by rinsing 2-week-old PDA plates, which had been incubated at 25 ± 1°C in complete darkness, with 10 mL of sterile distilled water and gently scraping the mycelium with a sterile glass Drigalski spatula. The suspensions were then filtered through a layer of sterile Miracloth (Calbiochem, San Diego, CA, USA) and were observed using an optical microscope (model Dialux 22, Leitz, Wetzlar, Germany). Micrograph images were captured using a Leica DFC 450C digital camera, and fungal structures were measured using the software Leica Application Suite X Version 3.1.1.17751 (Leica Microsystems Ltd., Heerbrugg, Switzerland). For each isolate, at least 50 macroconidia with different numbers of septa (1- 3- and 5-septa) were measured.

DNA extraction and molecular identification of isolates

Five agar discs (diam. 6 mm) were cut from 1-week-old monoconidial PDA plates and were inoculated into 50 mL tubes each containing 25 mL of Yeast Malt

Broth: 3 g L^{-1} yeast extract; 3 g L^{-1} malt extract; 5 g L^{-1} peptone; 10 g L^{-1} glucose. The tubes were then kept for 5 days at room temperature (22–25°C) under constant stirring at 60 rpm on the Multi-RS 60 programmable rotator (Biosan, Riga, Latvia), with a rotation angle of 75°. Mycelium was then collected by filtering each liquid culture through a layer of sterile Miracloth (Calbiochem, San Diego, CA, USA), washed twice with sterile distilled water, dried on sterile filter paper, and then stored at -20°C for DNA extraction.

Genomic DNA was extracted with the Genesig® Easy DNA/RNA extraction kit (Primer Design Ltd, UK), using the method described by Spada *et al.* (2023). DNA was quantified using the Qubit™ DNA BR Assay Kit in a Qubit™ 4 Fluorometer (Invitrogen by Thermo Fisher Scientific Inc., Eugene, OR, USA). A fragment of the *ef-1α* gene was amplified according to O'Donnell *et al.* (1998), using the EF-1/EF-2 primer pair. PCR was carried out in a 25 µL reaction mix with GoTaq Green Master Mix 2X (Promega Corporation, Madison, WI, USA), 0.1 µM of each primer, 30-50 ng of DNA, and adding nuclease-free water to the volume. PCR conditions were: initial denaturation at 95°C for 8 min, followed by 35 cycles of 95°C for 30 sec, 53°C for 1 min, and 72°C for 1 min, and final extension at 72°C for 5 min. A negative control (no DNA) was included in the reaction. PCR products were analyzed by electrophoresis in 0.5× Tris-Borate-EDTA (TBE) buffer with 1% (w/v) agarose gels and detected by UV fluorescence after GelRed™ staining (Biotium Inc., CA, USA) according to the manufacturer's instructions. The 100 bp DNA ladder (Promega, Madison, WI, USA) was used as a molecular size marker. Amplicons were purified with the QIAquick PCR purification kit (QIAGEN, Milan, Italy), following the manufacturer's instructions. The purified amplicons were sent to BMR Genomic (Padua, Italy) for Sanger sequencing in both directions, with the same set of primers used for amplification. Consensus sequences were edited with BioEdit v 7.7 and used as queries in BLASTn searches of the GenBank database hosted by NCBI. To further confirm the species, the species-specific primers Fp1-1 and Fp1-2 were used, targeting a 523 bp fragment in the *ef-1α* gene (Aoki and O'Donnell, 1999a). As described above, each PCR was conducted in a 25 µL reaction mix using 0.24 µM of each primer and setting the thermal conditions described by the authors.

Artificial inoculations of Salicornia europaea *seedlings grown in pots and in hydroponics*

To assess the pathogenicity of *F. pseudograminearum*, inoculations of *S. europaea* plants were carried out. The plants were grown in pots and hydroponics (floating raft system). One isolate (*F. pseudograminearum* 3B) was used in this experiment. Seeds of *S. europaea* were purchased from Alsagarden (Niederhaslach, France), and were sown into polystyrene trays containing stone wool plugs (Grodan, Roermond, The Netherlands), which were kept under a greenhouse for germination (Figure 2 a). Plants were selected for phenotypic uniformity based on height and number of shoots. At 46 days after sowing (das), seedlings (n = 96) were removed from stone wool plugs and transferred to a small-scale floating raft system (Figure 2 b). This consisted of polystyrene rafts (7 x 10 cm, each containing eight plants) placed in a 200 mL dark-colored polypropylene tank filled with nutrient solution. The solution contained 14.0 mM NO_3, 2.0 mM NH_4, 2.0 mM H_2PO_4, 10.0 mM K, 4.5 mM Ca, 2.0 m M Mg, 5.0 mM SO_4, 40.0 µM Fe, 40.0 µM B, 3.0 µM Cu, 10.0 µM Zn, 10.0 µM Mn, and 1.0 µM Mo. The nutrient solution in each hydroponic tank was continuously aerated to supply oxygen to the plants and maintain the inoculum in a homogeneous suspension. The plants were maintained in a growth chamber (25.0 ± 1.5°C, PAR 150 µmol m^2 s^{-2} from LED tubes) for 11 days to promote root development. Subsequently, at 57 das, plant (n = 48) roots were inoculated with a suspension of *F. pseudograminearum* macroconidia (final concentration 10^5 macroconidia mL^{-1}) (Figure 2 c1), and the other half with an equal volume of sterile distilled water (Figure 2 c2). Macroconidia suspensions were obtained as described above. At 24 days post inoculation (dpi; 81 das), half of the inoculated plants (n = 24) were transferred into 1 L pots filled with sterile peat, and the other half were transferred into 50 L tanks filled with 25 L of nutrient solution. The same method was used for control plants (those treated with sterile distilled water), and all plants were moved under a greenhouse (Figure 2 d). The plants had been randomly selected for transplanting in pots or hydroponics. The pots were sub-irrigated daily with nutrient solution, while in the hydroponic tanks, the nutrient solution was periodically added to maintain the initial volume.

The trial lasted until 80 dpi (corresponding to 137 das), when disease symptoms (shoot browning) were assessed using a six-point empirical qualitative ordinal scale (0 to 5): 0 = no symptoms; 1 = browning on the main stem; 2 = browning on the basal lateral shoots; 3 = complete browning of the main stem and primary lateral shoots; 4 = almost complete browning, pale-green secondary shoots; and 5 = completely desiccated (dead) plant (Figure 3, a to e). A score was assigned to each plant and, for each treatment (i.e. potted-inoculated plants, hydroponics-inoculated plants, potted-non-inoc-

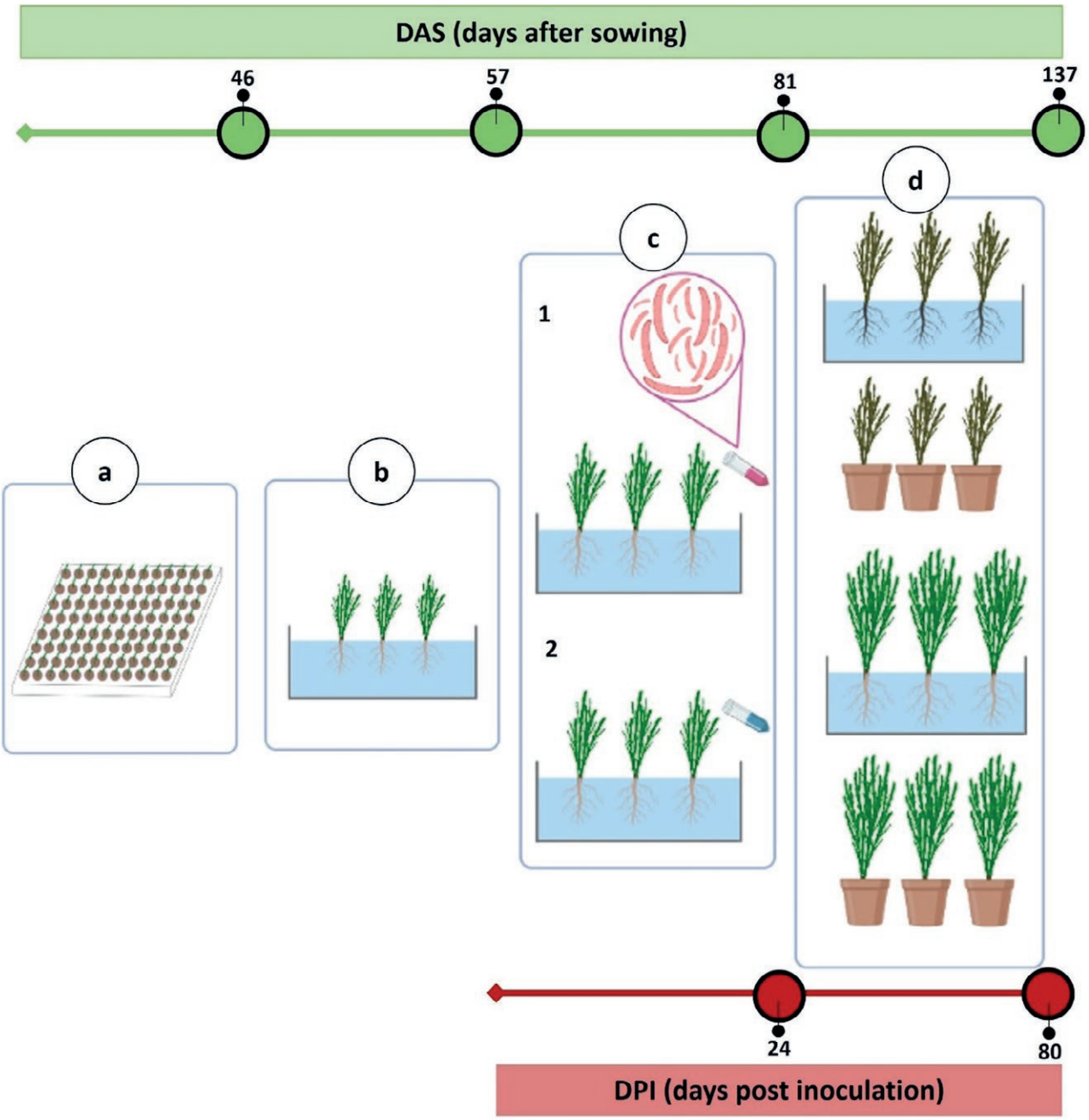

Figure 2. Diagram describing the protocol used for artificial inoculations of *Salicornia europaea* plants with *Fusarium pseudograminearum* isolate 3B. a) Sowing of *S. europaea* seeds in a seedling tray. b) Hydroponic cultivation of plants for root development. c) Inoculation of plants with *F. pseudograminearum* macroconidia (c 1) or sterile distilled water (control plants) (c 2). d) Greenhouse cultivation in pots or hydroponics.

ulated plants, and hydroponic-non-inoculated plants), the plants (n = 24) were randomly divided into three groups of eight plants each. The McKinney Index (MKI; McKinney, 1923), which incorporates disease incidence and severity, was calculated for each group using the following formula:

$$MKI = \frac{\sum(d \times f)}{N \times D} \times 100$$

where d = disease score, f = disease frequency (for a given group of plants), N = total number of observed plants, and D = the greatest level of disease infection on the empirical qualitative ordinal scale. Disease incidence

was determined by counting the plants showing symptoms of at least 1 on the empirical scale.

At 80 dpi, re-isolations were carried out (as previously described) from plant tissues for the fulfillment of Koch's postulates. In addition to plant roots and crowns, the first nine segments of the main stem and the two basal lateral shoots were plated, and the development of resulting organisms was assessed.

At 80 dpi, control and inoculated plants were also assessed for shoot fresh weight (SFW), shoot dry weight (SDW), and shoot succulence. For the inoculated plants, samples were collected from asymptomatic plants grown in hydroponics and from plants grown in pots with a disease severity score of 1. Shoot dry weights were measured after drying the fresh samples in a ventilated oven at 70°C until constant weight. Shoot succulence was calculated as the ratio of shoot water content to SDW.

Mycotoxins production: fungal isolates and culture conditions

The following isolates were used in the experiment on mycotoxin production: the three *F. pseudograminearum* isolates (3B, PD-A, and PD-B) from *S. europaea*, *F. pseudograminearum* ColPat-351 from wheat (Agustí-Brisach *et al.*, 2018), *F. pseudograminearum* PVS Fu-7 from wheat (Balmas, 1994), and the non-pathogenic *F. oxysporum* DAFE SP21-23 isolate, obtained from *S. europaea* plant tissues in the present study, used as a negative control since this species does not produce DON or ZEA. The isolate DAFE SP21-23 was also used as further confirmation that only *F. pseudograminearum* isolates were DON and ZEA producers. All fungi were grown on PDA plates and maintained on SNA, as described before.

Amplification of mycotoxin-related genes

To determine whether *F. pseudograminearum* isolates were potentially mycotoxigenic, we first investigated if they had the gene pool required for mycotoxin biosynthesis. The *tri5* gene and the *pks4* gene were assessed in each isolate, as *tri5* is involved in the biosynthesis of DON (Proctor *et al.*, 1995; Desjardins *et al.*, 1996), and *pks4* is involved in the biosynthesis of ZEA (Lysøe *et al.*, 2006).

A 650 bp fragment of the *tri5* gene was amplified using the Tox5-1/Tox5-2 primer pair (Niessen and Vogel, 1998), and a 280 bp fragment of the *pks4* gene using the PKS4F/PKS4R primers (Meng *et al.*, 2010). PCR was carried out in a 25 µL reaction mix with GoTaq Green Master Mix 2X (Promega Corporation, Madison, WI, USA), 0.4 µM of each primer for *tri5* and 0.5 µM for *pks4*, 30–50 ng of DNA, and adding nuclease-free water to the volume. Negative controls (no DNA) were included. The amplification conditions used were those described by the respective authors (cited above). Amplicons were purified and sequenced, and consensus sequences were generated as previously described. Amplification of fragments of the *tri3* and *tri12* genes (Starkey *et al.*, 2007) was carried out in a multiplex PCR to find out whether the isolates belonged to a specific DON-chemotype (i.e. nivalenol, NIV; and acetylated forms of DON: 3-acetyldeoxynivalenol, 3ADON; and 15-acetyldeoxynivalenol, 15ADON). Primers 3CON, 3NA, 3D15A, and 3D3A were used to target the *tri3* gene. Primers 12CON, 12NF, 12-15F, and 12-3F were used for the *tri12* gene. Multiplex PCRs were carried out following the methods described by the authors.

In vitro *production of mycotoxins*

Production of DON and ZEA was evaluated *in vitro* in a model system that consisted of growing the *F. pseudograminearum* isolates on moistened barley grains. This system method was chosen so that the fungi were grown in optimal conditions for mycotoxin production (Blaney and Dodman, 2002; Clear *et al.,* 2006; Kokkonen *et al.,* 2010). Thus, 30 g of dried barley grains, obtained from a local organic farm, were rinsed overnight in 25 mL of sterile distilled water in 500 mL flasks and sterilized twice at 121°C for 20 min with 24 hours between the two heat treatments. Each flask was then inoculated with a PDA disk (diam. 10 mm) cut from an actively growing culture of each isolate. A mycelium-free PDA disk was used as a control. An experiment was established consisting of five biological replicates for each isolate. The fungi were grown for 3 weeks at room temperature, and the cultures were manually shaken to avoid grain clumps. After incubation, the grains were dried under a laminar flow cabinet for 48 hours and were ground with a coffee grinder.

Mycotoxin production was evaluated for DON and ZEA with the immunochromatographic RIDA® QUICK RQA ECO tests (R-Biopharm AG, Milan, Italy), according to the manufacturer's instructions. The limits of detection (LOD) were 0.25 mg kg^{-1} for DON and 0.05 for ZEA, and the maximum measurable amounts were 50 mg kg^{-1} for DON and 1 mg kg^{-1} for ZEA. Sequential 10-fold dilutions were made, with the appropriate solvent, for samples outside these ranges until measurable amounts of mycotoxin were obtained. The DON test does not discriminate between acetylated forms of DON.

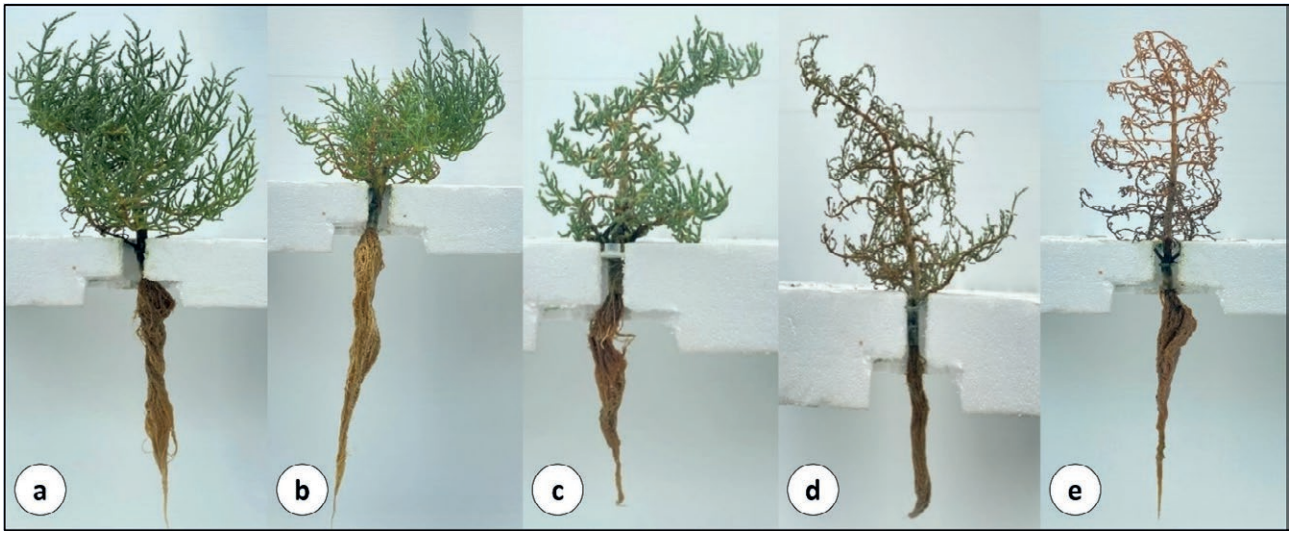

Figure 3. The empirical qualitative ordinal scale of disease symptoms (1 to 5) in *Salicornia europaea* plants grown hydroponically (floating raft system) and inoculated with *Fusarium pseudograminearum* isolate 3B. The photographs were taken 80 days post inoculation. a) Browning on the main stem (score 1). b) Browning on basal lateral shoots (score 2). c) Complete browning of the main stem and primary lateral shoots (score 3). d) Almost complete browning, pale-green secondary shoots (score 4). e) Completely desiccated (dead) plant (score 5).

In planta *production of mycotoxins*

Mycotoxin production in *S. europaea* plants was assessed using LC-MS/MS, which is a commonly used multi-mycotoxin method to determine levels in feeds and foods to overcome specific matrix effects (De Santis *et al*., 2017; Iqbal, 2021). The method used (protocol: MP 213, rev. 3, 2022) detects 17 mycotoxins, including NIV, ZEA, DON, and the acetylated forms 3- and 15-acetyldeoxynivalenol.

According to the empirical scale of host plant symptoms (Figure 3), the plants were pooled and divided into three groups: no symptoms (score 0); mild symptoms (scores 1 to 2), and severe symptoms (scores 3 to 5). The plants were also divided based on the growing methods (i.e. in pots or hydroponics). For each group of plants, the analyses were carried out on three biological replicates. Therefore, at 80 dpi, the above-ground parts of each plant were cut and freeze-dried. Samples were sent to Biochemie Lab s.r.l. (Campi Bisenzio, Florence, Italy; Accredia No. 0195; https://www.accredia.it/) for LC-MS/MS analyses.

Statistical analysis

Data were subjected to 1-way ANOVA using CoStat 6.4 statistical software (Cohort Software, Monterey, CA, USA). Percentage data (disease incidence and MKI) were $arcsin\sqrt{\%}$ transformed before ANOVA. In the artificial inoculation experiment, for each cultivation method, plants (n = 24) were randomly divided into 3 groups (eight plants each), and disease incidence and MKI values were calculated for each group. The normality of the data was assessed using the Shapiro–Wilk test and homoscedasticity was tested using Bartlett's test. Means were separated using Tukey's honestly significant difference post-hoc (HSD) test ($P \leq 0.05$).

Artificial inoculations of *F. pseudograminearum* on *S. europaea* plants were repeated twice in pots, using the same protocol, and both inoculations gave similar results. In addition, in the first experiment carried out in pots, the *F. oxysporum* isolate DAFE SP21-23 was also inoculated, but the inoculation did not cause any symptoms (data not shown). Only the results of the experiment conducted to compare the two growing methods (i.e. pots and hydroponics) are presented in this paper.

RESULTS

Identification

Fusarium pseudograminearum colonies were isolated from 64% of the total specimens of diseased stems, roots, and crowns collected from *S. europaea* plants. *Fusarium oxysporum* colonies were also frequently observed, representing 45% of the total plated samples. On PDA, colonies appeared whitish to brownish-yellow on the upper surface, especially during the first few days of growth. After

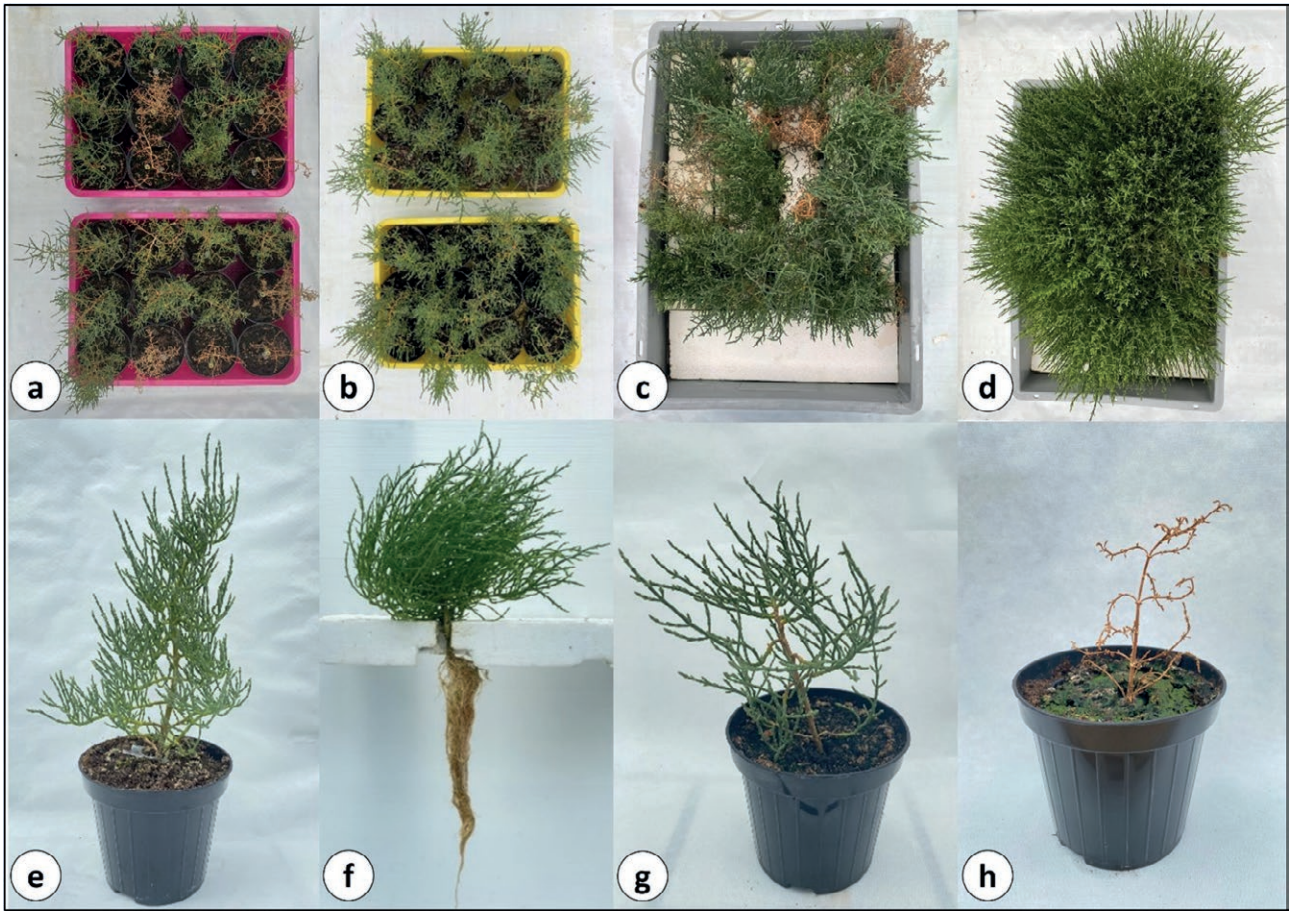

Figure 4. *Salicornia europaea* plants grown in pots (a and b) and hydroponics (c and d), and inoculated with *Fusarium pseudograminearum* isolate 3B, at 80 days post inoculation (a and c). Control plant in a pot (e) and hydroponics (f). Plants with disease severity score 1 (g) and score 5 (h), grown in pots.

one week, reddish to dull-red pigmentation was visible. The reverse colony pigmentation ranged from pale brown to brownish yellow, becoming red, reddish-brown, and ruby after 2 weeks. Abundant and floccose aerial mycelium was typically observed during colony growth. The size of macroconidia was comparable to that described by Aoki and O'Donnell (1999a) (Table S1), although no 7-septate macroconidia were observed. Microconidia were absent. Three isolates (3B, PD-A, and PD-B) were selected for morphological and molecular studies.

The consensus sequences of the partial translation elongation factor 1 alpha (*ef-1α*) gene were 100% similar, in whole length, to those of *F. pseudograminearum* [GenBank accession numbers (AN) MG670539 to MG670541 and OM746828 to OM746837]. These sequences were deposited in GenBank under the AN PQ045864 to PQ045866. A species-specific PCR, with the Fp1-1/Fp1-2 primer pair, confirmed that the three isolates belonged to *F. pseudograminearum* (Figure S1).

Artificial inoculations and plant disease assessments

No symptoms were observed in control plants (Figure 4, b, d, e, and f). The plants cultivated in pots and hydroponics had different growth patterns (Table 1). The pot-cultivated plants tended to be woodier than those in hydroponics, especially at the base of the stem. In these cases, desiccation of at least 50% of the main stem of each affected plant was considered as score 1 on the empirical qualitative ordinal scale of disease symptoms (Figure 4 g). In addition to the control plants, asymptomatic inoculated plants (i.e. score 0), grown in hydroponics, and potted plants with a score of 1, were collected for the determination of shoot fresh weight (SFW), shoot dry weight (SDW), and succulence. Differences between inoculated and non-inoculated plants, within the same cultivation method, were statistically significant ($P \leq 0.05$) for potted plants, but not for plants grown hydroponically (Table 1).

Table 1. Mean shoot fresh weight, dry weight, and succulence of *Salicornia europaea* plants grown in pots or hydroponics, sampled at 80 days post inoculation with *Fusarium pseudograminearum* isolate 3B. Shoot succulence was calculated as the ratio between shoot water content and shoot dry weight. For inoculated plants, measurements were carried out on asymptomatic plants in hydroponics and on pot-grown plants with a score of 1 on the empirical qualitative scale of disease symptoms (browning on the main stems). Within each growing system, means (n = 4; ± SE) accompanied by the same letters are not significantly different according to Tukey's HSD post-hoc test ($P \leq 0.05$).

Parameter	Hydroponics		Pots	
	Inoculated	Non-inoculated	Inoculated	Non-inoculated
Shoot fresh weight (g/plant)	56.3 ± 6.4 a	62.9 ± 4.9 a	7.3 ± 0.8 a	16.7 ± 0.5 b
Shoot dry weight (g/plant)	6.4 ± 0.6 a	6.8 ± 1.1 a	1.4 ± 0.2 a	2.6 ± 0.2 b
Succulence (g/g)	7.8 ± 0.4 a	7.7 ± 1.2 a	4.2 ± 0.3 a	5.4 ± 0.3 b

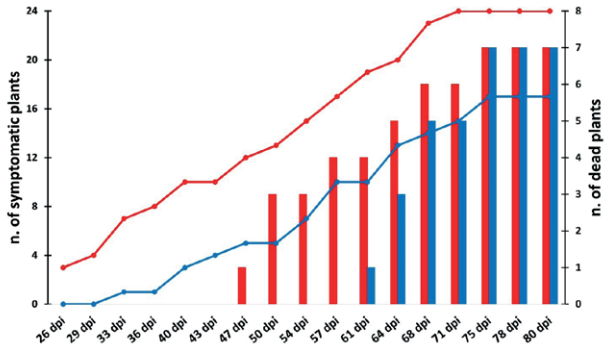

Figure 5. Progression of symptom emergence (lines) and plant death (histograms) in *Salicornia europaea* plants inoculated with *Fusarium pseudograminearum* isolate 3B, in pots (red) or hydroponics (blue), at different days post inoculation (dpi).

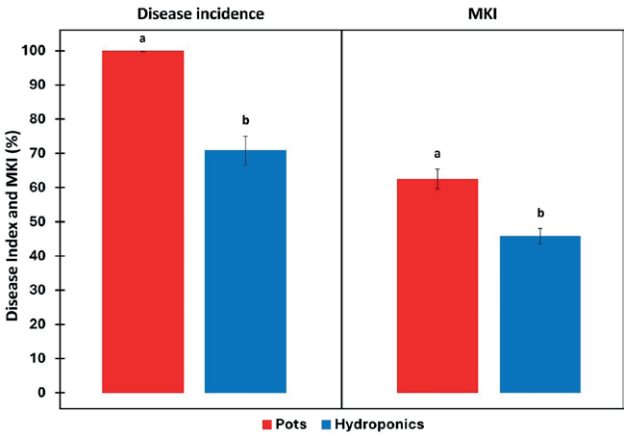

Figure 6. Disease incidence and McKinney Index for potted (red bars) and hydroponically grown (blue bars) *Salicornia europaea* plants that were inoculated with *Fusarium pseudograminearum* isolate 3B. Different letters above the bars indicate significant differences between the mean values (n = 3; ± SE), according to Tukey's HSD post-hoc test ($P \leq 0.05$). Statistical analyses were conducted separately for each disease measurement.

Symptoms of aerial parts of plants were characterized by acropetal patterns, initially affecting the stems and basal lateral shoots (Figure 4, a and c), following damage to the roots. The disease had a long asymptomatic phase. Initial wilting symptoms were observable at 24 dpi, when the plants were transplanted into pots or in hydroponics. There was no clear evidence of root or crown rot before transplanting. Clear signs of disease in the aboveground portions (i.e. desiccation of the main stems) were observed in pots 2 days after transplanting (26 dpi). The plants in hydroponics showed evidence of desiccation at 1 week after transplanting (31 dpi). These different rates of symptom appearance were very obvious at 80 dpi. First plant death in pots was recorded at 47 dpi (Figure 4 h) and at 61 dpi in hydroponics (Figure 5).

In pots, 100% (24/24) of the inoculated plants showed symptoms attributable to at least class 1 in the empirical qualitative ordinal scale of disease symptoms. In hydroponics, disease only affected 70.8% (17/24) of the plants, and seven out of 24 plants were asymptomatic and were assigned scores of zero. The number of dead plants (score 5) was the same at 80 dpi (seven) in pots and in hydroponics. Accordingly, disease incidence and McKinney Index were significantly greater in pot-grown plants than in those grown hydroponically (Figure 6).

Koch's postulates were fulfilled by reisolating *F. pseudograminearum* from below- and above-ground tissues collected from both groups of plants, regardless of disease severity. The pathogen was mainly present in the roots and crowns. In pot-grown plants, *F. pseudograminearum* was re-isolated from 96% of sampled roots and 100% of sampled crown tissues, and 87% of root and 82% of crown samples of hydroponically grown plants. Pathogen re-isolation from above-ground tissues of potted plants was 41% from stems, 91% from first lateral branches, and 59% from second lateral branches. In hydroponics, re-isolations of *F. pseudograminearum* in above-ground plant tissues were higher, 85% from stems, 91% from first lateral branches, and 64% from second

lateral branches (Table S2). Overall, re-isolations of *F. pseudograminearum* were greater from plants grown in the hydroponic system (83% of total plated tissues) than those grown in pots (62%). *Fusarium pseudograminearum* was also re-isolated from asymptomatic hydroponically grown plants.

Production of mycotoxins in vitro *and* in planta

In this experiment, in addition to the three isolates of *F. pseudograminearum* (3B, PD-A, and PD-B), two further isolates of *F. pseudograminearum*, PVS-Fu 7 (Balmas, 1994) and ColPat-351 (Agustí-Brisach *et al*., 2018) and one isolate of *F. oxysporum* (DAFE SP-21-23) isolated from *S. europaea* plants were included.

First, we tested whether the isolates had the gene pool required for the production of deoxynivalenol (DON) and zearalenone (ZEA) by amplifying a fragment of the *tri5* (Niessen and Vogel, 1998) and *pks4* (Meng *et al*., 2010) genes. All the isolates, except for *F. oxysporum* DAFE SP21-23, were positive for the 650 bp fragment of the *tri5* gene (Figure S2), and the 280 bp fragment of the *pks4* gene (Figure S3). Consensus sequences were used for BLASTn search to verify sequence identity and were deposited under the GenBank AN PQ045872 to PQ045876 for *tri5* and PQ045867 to PQ045871 for *pks4*. For *tri5*, the sequences exhibited 98.65% (isolates 3B, PD-A, and PD-B) and 98.80% (isolates ColPat-351 and PVS-Fu 7) identity with the *tri5* gene of *F. pseudograminearum* strains NRRL 28334, NRRL 28338, and 28062 (respectively, AN AY102583, AY102585, and AY102580). Lower sequence similarity was found for *pks4*. The sequences showed 95.02% (isolates 3B, PD-A, and PD-B), 95.37% (isolate ColPat-351), and 94.66% (isolate PVS-Fu 7) similarity with the *pks4* gene of *F. pseudograminearum* CS3096 (AN: XM_009259983). The amplification of *tri3* and *tri12* genes (Starkey *et al*., 2007), with a multiplex PCR developed to determine the DON-chemotype, failed to produce any amplicons. Although several attempts were made, such as modifying the annealing temperature, concentration of DNA, primers combinations, and $MgCl_2$ in the reaction mixture, the multiplex PCR yielded no results. Therefore, no specific DON-chemotype (i.e. NIV, 3ADON, 15ADON) could be assigned to the isolates.

The mycotoxigenic ability of the *F. pseudograminearum* isolates was assessed by growing them on barley grains. Table 2 shows the results for DON and ZEA production, assessed using the respective immunochromatographic test kits (Figures S4 and S5). Zearalenone was detected in all the samples with considerable yields. The PD-B isolate produced the least amount of toxin (40.01 ± 1.05 mg kg^{-1}) while isolate ColPat-351 produced the greatest amount (69.1 ± 5.45 mg kg^{-1}). In contrast, in the latter isolate the production of DON was below the LOD (0.25 mg kg^{-1}), while isolate PVS-Fu 7 produced only a small amount of this mycotoxin (0.37 ± 0.06 mg kg^{-1}). Interestingly, the *F. pseudograminearum* isolates obtained from *S. europaea* were higher DON producers, each with comparable yields. As expected, the *F. oxysporum* isolate DAFE SP21-23 did not produce the tested mycotoxins.

Mycotoxin production *in planta* was low. Deoxynivalenol was detected by LC-MS/MS only at 0.029 ± 0.012 mg kg^{-1} in severely damaged *S. europaea* plants (disease scores 3 to 5) grown in hydroponics, while all samples were negative for ZEA, NIV, 3ADON, and 15ADON. Since *S. europaea* plants were inoculated with the *F. pseudograminearum* 3B isolate, the results were consistent with those obtained from the molecular analyses, which did not identify any specific DON chemotype.

Table 2. Mean amounts of deoxynivalenol (DON) and zearalenone (ZEA) produced by five isolates of *Fusarium pseudograminearum* on barley grains after 21 days. Data are shown as mg of toxin per kg of substrate. Mycotoxin production was evaluated with immunochromatographic RIDA® QUICK RQA ECO kits. The limit of detection (LOD) was 0.25 mg kg^{-1} for DON and 0.05 mg kg^{-1} for ZEA. Means (n = 5; ± SE) accompanied by the same lowercase letters are not significantly different, according to Tukey's HSD post hoc test ($P \leq 0.05$).

Isolate	DON (mg kg^{-1})	ZEA (mg kg^{-1})
F. pseudograminearum 3B	6.93 ± 0.43 a	61.10 ± 2.17 ab
F. pseudograminearum PD-A	6.72 ± 0.11 a	52.94 ± 2.93 abc
F. pseudograminearum PD-B	6.79 ± 0.19 a	40.01 ± 1.05 c
F. pseudograminearum ColPat-351	< LOD c	69.10 ± 5.45 a
F. pseudograminearum PVS Fu-7	0.37 ± 0.06 b	47.48 ± 4.49 bc
F. oxysporum DAFE SP21-23	< LOD c	< LOD d
Control	< LOD c	< LOD d

DISCUSSION

This is the first report of root and crown rot caused by *F. pseudograminearum* on cultivated *S. europaea* plants. There are very few records of diseases affecting *Salicornia* species (Delli Compagni *et al*., 2024). The only report regarding cultivated species is for *S. bigelovii,* which was found to be susceptible to *Botrytis cinerea* in Mexico (Rueda Puente *et al*., 2014). Pathogenicity of this fungus was confirmed by spraying a conidial suspension on detached branches. There are no documented artificial inoculation experiments on *S. europaea*, since the pathogenic species found on this halophyte have only

been described in wild plants (Delli Compagni *et al*., 2024). In the present study, artificial inoculations were carried out on seed-propagated plants of *S. europaea*.

The pathogenicity test showed that root and crown rot caused by *F. pseudograminearum* was less severe when test plants were grown hydroponically (MKI = 46%) than when grown in potting soil (MKI = 63%) and all the pot-grown plants developed browning symptoms. Disease incidence was less in the hydroponic system, with seven out of 24 plants remaining asymptomatic (Figure 6). These results indicate that disease severity depended on the cultivation method. At 80 dpi, SFW, SDW, and shoot succulence of inoculated, asymptomatic plants (i.e. score 0) grown in the hydroponic system resembled parameters measured for the control plants, whereas the same parameters in score 1 potted plants were significantly different from the respective controls (Table 1). Moreover, the potted plants also had disease symptoms soon after transplanting, while in hydroponics symptom development was delayed (Figure 5). However, mortality rates were the same between the two groups of plants (each with seven out of 24 plants), although in hydroponics the first plant death occurred 2 weeks later than in pots (Figure 5).

Hydroponic cultivation can reduce plant susceptibility to infectious diseases compared to soil cultivation. In a similar experiment, Maurer *et al*., (2023) found that sweet basil plants grown in a static hydroponic solution were much less sensitive to downy mildew caused by *Peronospora belbahrii* than those grown in soil. They stated that the higher antioxidant content in hydroponically grown basil plants could alleviate symptom development. Moulin *et al*. (1994) showed that several *Pythium* species (*P. aphanidermatum*, *P. intermedium*, *P. irregulare*, *P. sylvaticum*, and *P. ultimum* var. *ultimum*) caused damping-off of cucumber when grown in sand-peat soil, but only *P. aphanidermatum* caused disease in substrate (stone wool) and in hydroponic culture. These authors reported that symptoms were milder in hydroponics than in substrate. Moreover, inoculations with *Streptomyces scabies* resulted in less infection of potato plants grown hydroponically compared to pot-grown plants (Khatri *et al*., 2011). Similarly, rice artificially inoculated with *Xanthomonas oryzae* pv. *oryzae*, the causative agent of bacterial leaf blight, had lower disease severity in hydroponic culture than in soil (Song *et al*., 2016).

In the present study, the greater growth rate of hydroponically grown plants than those in potting soil, was likely due to the better supply of water and minerals, and oxygenation of roots compared to soil cultivation, which may have resulted in the reduced rate of development of *F. pseudograminearum* root and crown rot on *S. europaea*. In addition, *F. pseudograminearum* is a soil-borne pathogen and causes disease in warm and dry climates (Poole *et al*., 2013), with increased virulence in drought conditions (Kazan and Gardiner, 2018). In agricultural areas characterized by low moisture and high temperatures, *F. pseudograminearum* was found to be predominant compared to other *Fusarium* species (e.g. *F. culmorum*), which prefer cool and humid regions (Poole *et al*., 2013).

Little information is available on mycotoxins on *Salicornia* species. Lopes *et al*. (2020) reported that several *S. ramosissima* and *Salicornia* sp. samples were contaminated by aflatoxins in Portugal. These compounds were detected in plants collected in the wild, and also in those cultivated with conventional and organic methods, but no mycotoxins were detected from greenhouse and hydroponically cultivated plants.

In the present study, DON was detected in low amounts from inoculated plants. Traces of DON (0.029 ± 0.012 mg kg^{-1}) were detected only in severely damaged (score 3–5) plants grown hydroponically. This result could be due to the greater water content of these plants compared to those grown in potting soil since high levels of water activity (a_w) have been shown to be necessary for optimal production of trichothecenes by *Fusarium* spp. (Hope *et al*., 2005; Han *et al*., 2018; Rybecky *et al*., 2018; Belizán *et al*., 2019). Therefore, one hypothesis is that the inoculated *F. pseudograminearum* isolate produced the mycotoxin only in suitable conditions (such as high plant water content) and during an advanced stage of disease development. In wheat kernels, the most favorable conditions for DON and ZEA production by *F. pseudograminearum* were an a_w of 0.97 and a temperature of 25°C (Cui *et al*., 2022).

When inoculated on barley grains, all the tested *F. pseudograminearum* isolates produced ZEA with considerable yields, similar to those documented by other authors (Blaney and Dodman, 2002; Clear *et al*., 2006; Alkadri *et al*., 2013). Furthermore, only the three *F. pseudograminearum* isolates obtained from *S. europaea* were high DON producers, each with similar production (Table 2). The other two European isolates had different mycotoxigenic activities. Low production of DON was detected in the Italian isolate *F. pseudograminearum* (PVS Fu-7), while production of DON by the Spanish isolate (ColPat-351), was below the LOD (Table 2). In addition, PCR targeting the *tri3* and *tri12* genes to discriminate between NIV and acetylated derivatives of DON producers (i.e. 3ADON and 15ADON) did not identify any specific DON chemotype. Deng et al. (2020), in a molecular analysis to determine the DON chemotypes of 372 isolates of *F. pseudograminearum*,

showed that 196 isolates did not produce any fragments in *tri3* and *tri12* PCR assays, with the same primers used in this study. After LC-MS/MS analysis, isolates without a chemotype marker were assigned to the putative 15-ADON chemotype (Deng *et al*., 2020).

The present study is the first to record root and crown rot of *S. europaea* caused by *F. pseudograminearum*. This study also provides an important contribution to the current distribution and host range of this pathogenic fungus in Europe. In addition, the mycotoxin deoxynivalenol was detected in diseased plants, although only in small quantities and under specific conditions. Further studies are ongoing to assess the environmental conditions (e.g. salinity and temperature) that may promote mycotoxigenic activity in *F. pseudograminearum* and to determine potential mycotoxin exposure risk in *S. europaea*.

ACKNOWLEDGEMENTS

This research was funded by the project "HALOphytes grown in saline Water for the production of INnovative ready-to-eat salad – HALOWIN", funded by the University of Pisa (project code PRA_2020_43). The authors are grateful to Grazia Puntoni (University of Pisa) for the technical support, and Prof. Virgilio Balmas (University of Sassari) and Prof. Carlos Agustí-Brisach (University of Cordoba) for providing the *F. pseudograminearum* isolates used in this study.

LITERATURE CITED

Abdallah-Nekache N., Laraba I., Ducos C., Barreau C., Bouznad Z., Boureghda H., 2019. Occurrence of *Fusarium* head blight and *Fusarium* crown rot in Algerian wheat: identification of associated species and assessment of aggressiveness. *European Journal of Plant Pathology* 154(3): 499–512. https://doi.org/10.1007/s10658-019-01673-7

Agustí-Brisach C., Raya-Ortega M.C., Trapero C., Roca L.F., Luque F., … Trapero A., 2018. First report of *Fusarium pseudograminearum* causing crown rot of wheat in Europe. *Plant Disease* 102(8): 1670. https://doi.org/10.1094/PDIS-11-17-1840-PDN

Akinsanmi O.A., Chakraborty S., Backhouse D., Simpfendorfer S., 2007. Passage through alternative hosts changes the fitness of *Fusarium graminearum* and *Fusarium pseudograminearum*. *Environmental Microbiology* 9(2): 512–520. https://doi.org/10.1111/j.1462-2920.2006.01168.x

Alkadri D., Nipoti P., Döll K., Karlovsky P., Prodi A., Pisi A., 2013. Study of fungal colonization of wheat kernels in Syria with a focus on *Fusarium* species. *International Journal of Molecular Science* 14(3): 5938–5951. https://doi.org/10.3390/ijms14035938

Aoki T., O'Donnell K., 1999a. Morphological and molecular characterization of *Fusarium pseudograminearum* sp. nov., formerly recognized as the Group 1 population of *F. graminearum*. *Mycologia* 91(4): 597–609. https://doi.org/10.1080/00275514.1999.12061058

Aoki T., O'Donnell K., 1999b Morphological characterization of *Gibberella coronicola* sp. nov., obtained through mating experiments of *Fusarium pseudograminearum*. *Mycoscience* 40(6): 443–453. https://doi.org/10.1007/BF02461021

Araus J.L., Rezzouk F.Z., Thushar S., Shahid M., Elouafi I.A., … Serret M.D., 2021. Effect of irrigation salinity and ecotype on the growth, physiological indicators and seed yield and quality of *Salicornia europaea*. *Plant Science* 304: 110819. https://doi.org/10.1016/j.plantsci.2021.110819

Balmas V., 1994. Root rot of wheat in Italy caused by *Fusarium graminearum* Group I. *Plant Disease* 78: 317A. https://doi.org/10.1094/PD-78-0317A

Belizán M.M.E., Gomez A. de los, Terán Baptista Z.P., Jimenez C.M., Sánchez Matías M. del H., … Sampietro D.A., 2019. Influence of water activity and temperature on growth and production of trichothecenes by *Fusarium graminearum sensu stricto* and related species in maize grains. *International Journal of Food Microbiology* 305: 108242. https://doi.org/10.1016/j.ijfoodmicro.2019.108242

Blaney B.J., Dodman R.L., 2002. Production of zearalenone, deoxynivalenol, nivalenol, and acetylated derivatives by Australian isolates of *Fusarium graminearum* and *F. pseudograminearum* in relation to source and culturing conditions. *Australian Journal of Agricultural Research* 53(12): 1317–1326. https://doi.org/10.1071/AR02041

Burgess L.W., Klein T.A., Bryden W.L., Tobin N.F., 1987. Head blight of wheat caused by *Fusarium graminearum* Group 1 in New South Wales in 1983. *Australasian Plant Pathology* 16: 72–78. https://doi.org/10.1071/APP9870072

Cárdenas-Pérez S., Piernik A., Chanona-Pérez J.J., Grigore M.N., Perea-Flores M.J., 2021. An overview of the emerging trends of the *Salicornia* L. genus as a sustainable crop. *Environmental and Experimental Botany* 191: 104606. https://doi.org/10.1016/j.envexpbot.2021.104606

Chakraborty S., Liu C.J., Mitter V., Scott J.B., Akinsanmi O.A., … Simpfendorfer S., 2006. Pathogen population

structure and epidemiology are keys to wheat crown rot and *Fusarium* head blight management. *Australasian Plant Pathology* 35: 643–655. https://doi.org/10.1071/AP06068

Clear R.M., Patrick S.K., Gaba D., Roscoe M., Demeke T., ... Turkington T.K., 2006. Trichothecene and zearalenone production, in culture, by isolates of *Fusarium pseudograminearum* from western Canada. *Canadian Journal of Plant Pathology* 28(1): 131–136. https://doi.org/10.1080/07060660609507279

Cui H., Wang S., Yang X., Zhang W., Chen M., ... Wang S., 2022. Predictive models for assessing the risk of *Fusarium pseudograminearum* mycotoxin contamination in post-harvest wheat with multi-parameter integrated sensors. *Food Chemistry: X* 16:100472. https://doi.org/10.1016/j.fochx.2022.100472

De Santis B., Debegnach F., Gregori E., Russo S., Marchegiani F., ... Brera C., 2017. Development of a LC-MS/MS method for the multi-mycotoxin determination in composite cereal-based samples. *Toxins* 9(5): 169. https://doi.org/10.3390/toxins9050169

Delli Compagni E., Pardossi A., Pecchia S., 2024. Fungal and fungal-like diseases of halophytes in the Mediterranean basin: a state-of-the-art review. *Horticulturae* 10(4): 313. https://doi.org/10.3390/horticulturae10040313

Deng Y.Y., Li W., Zhang P., Sun H.Y., Zhang X.X., ... Chen H.G., 2020 *Fusarium pseudograminearum* as an emerging pathogen of crown rot of wheat in eastern China. *Plant Pathology* 69(2):240–248. https://doi.org/10.1111/ppa.13122

Desjardins A.E., Proctor R., Bai G., McCormick S., Shaner G., ... Hohn T.M., 1996 Reduced virulence of trichothecene-nonproducing mutants of *Gibberella zeae* in wheat field tests. *Molecular Plant-Microbe Interactions*. 9(9): 775. http://doi.org/10.1094/MPMI-9-0775

EFSA Panel on Plant Health (PLH), Bragard C, Baptista P, Chatzivassiliou E, Di Serio F, Gonthier P, ... Reignault P.L., 2022 Pest categorisation of *Fusarium pseudograminearum*. *EFSA Journal* 20:e07399. https://doi.org/10.2903/j.efsa.2022.7399

Han Z., Shen Y., Di Mavungu J.D., Zhang D., Nie D., Jiang K., ... Zhao Z., 2018. Relationship between environmental conditions, TRI5 gene expression and deoxynivalenol production in stored *Lentinula edodes* infected with *Fusarium graminearum*. *World Mycotoxin Journal* 11(2): 177–186. https://doi.org/10.3920/WMJ2017.2245

Hope R., Aldred D., Magan N., 2005. Comparison of environmental profiles for growth and deoxynivalenol production by *Fusarium culmorum* and *F. graminearum* on wheat grain. *Letters in Applied Microbiology* 40(4): 295–300. https://doi.org/10.1111/j.1472-765X.2005.01674.x

Iqbal S.Z., 2021. Mycotoxins in food, recent development in food analysis and future challenges; a review. *Current Opinion in Food Science* 42: 237–247. https://doi.org/10.1016/j.cofs.2021.07.003

Kammoun L.G., Gargouri S., Hajlaoui M.R., Marrakchi M., 2009. Occurrence and distribution of *Microdochium* and *Fusarium* species isolated from durum wheat in northern Tunisia and detection of mycotoxins in naturally infested grain. *Journal of Phytopathology* 157(9): 546–551. https://doi.org/10.1111/j.1439-0434.2008.01522.x

Kazan K., Gardiner D.M., 2018. *Fusarium* crown rot caused by *Fusarium pseudograminearum* in cereal crops: recent progress and future prospects. *Molecular Plant Pathology* 19(7): 1547–1562. https://doi.org/10.1111/mpp.12639

Khatri B.B., Tegg R.S., Brown P.H., Wilson C.R., 2011. Temporal association of potato tuber development with susceptibility to common scab and *Streptomyces scabiei*-induced responses in the potato periderm. *Plant Pathology* 60(4): 776–786. https://doi.org/10.1111/j.1365-3059.2011.02435.x

Kokkonen M., Ojala L., Parikka P., Jestoi M., 2010. Mycotoxin production of selected *Fusarium* species at different culture conditions. *International Journal of Food Microbiology* 143(2): 17–25. https://doi.org/10.1016/j.ijfoodmicro.2010.07.015

Lombardi T., Bertacchi A., Pistelli L., Pardossi A., Pecchia S., ... Sanmartin C., 2022. Biological and agronomic traits of the main halophytes widespread in the Mediterranean region as potential new vegetable crops. *Horticulturae* 8(3): 195. https://doi.org/10.3390/horticulturae8030195

Lopes M., Castilho M., Sanches-Silva A., Freitas A., Barbosa J., ... Ramos F., 2020. Evaluation of the mycotoxins content of *Salicornia* spp.: a gourmet plant alternative to salt. *Food Additives & Contaminants: Part B* 13(3): 162–170. https://doi.org/10.1080/19393210.2020.1741692

Lysøe E., Klemsdal S.S., Bone K.R., Frandsen R.J.N., Johansen T., ... Giese H., 2006. The PKS4 gene of *Fusarium graminearum* is essential for zearalenone production. *Applied Environmental Microbiology* 72(6): 3924–3932. https://doi.org/10.1128/AEM.00963-05

Maurer D., Sadeh A., Chalupowicz D., Barel S., Shimshoni J.A., Kenigsbuch D., 2023. Hydroponic versus soil-based cultivation of sweet basil: impact on plants' susceptibility to downy mildew and heat stress, storability and total antioxidant capacity. *Journal of the*

Science of Food and Agriculture 103(15): 7809–7815. https://doi.org/10.1002/jsfa.12860

McKinney H.H., 1923. Influence of soil temperature and moisture on infection of wheat seedlings by *Helminthosporium sativum*. *Journal of Agricultural Research* 26: 195–218.

Meng K., Wang Y., Yang P., Luo H., Bai Y., Yao B., 2010. Rapid detection and quantification of zearalenone-producing *Fusarium* species by targeting the zearalenone synthase gene PKS4. *Food Control* 21(2): 207–11. https://doi.org/10.1016/j.foodcont.2009.05.014

Miličević T., Kaliterna J., Ivić D., Stričak A., 2013. Identification and occurrence of *Fusarium* species on seeds of common vetch, white lupin and some wild legumes. *Poljoprivreda* 19(1): 25–32.

Moulin F., Lemanceau P., Alabouvette C., 1994. Pathogenicity of *Pythium* species on cucumber in peat-sand, rockwool and hydroponics. *European Journal of Plant Pathology* 100: 3–17. https://doi.org/10.1007/BF01871963

Nahle S., El Khoury A., Atoui A., 2021. Current status on the molecular biology of zearalenone: its biosynthesis and molecular detection of zearalenone producing *Fusarium* species. *European Journal of Plant Pathology* 159: 247–258. https://doi.org/10.1007/s10658-020-02173-9

Niessen M.L., Vogel R.F., 1998. Group specific PCR-detection of potential trichothecene-producing *Fusarium*-species in pure cultures and cereal samples. *Systematic and Applied Microbiology* 21(4): 618–631. https://doi.org/10.1016/S0723-2020(98)80075-1

Nirenberg H.I., 1981. A simplified method for identifying *Fusarium* spp. occurring on wheat. *Canadian Journal of Botany* 59(9): 1599–1609. https://doi.org/10.1139/b81-217

O'Donnell K., Kistler H.C., Cigelnik E., Ploetz R.C., 1998. Multiple evolutionary origins of the fungus causing Panama disease of banana: concordant evidence from nuclear and mitochondrial gene genealogies. *Proceedings of the National Academy of Science* 95(5): 2044–2049. https://doi.org/10.1073/pnas.95.5.2044

Obanor F., Neate S., Simpfendorfer S., Sabburg R., Wilson P., Chakraborty S., 2013. *Fusarium graminearum* and *Fusarium pseudograminearum* caused the 2010 head blight epidemics in Australia. *Plant Pathology* 62(1): 79–91. https://doi.org/10.1111/j.1365-3059.2012.02615.x

Pasquali M., Migheli Q., 2014. Genetic approaches to chemotype determination in type B-trichothecene producing *Fusaria*. *International Journal of Food Microbiology*. 189: 164-182. https://doi.org/10.1016/j.ijfoodmicro.2014.08.011

Poole G.J., Smiley R.W., Walker C., Huggins D., Rupp R., ... Paulitz T.C., 2013. Effect of climate on the distribution of *Fusarium* spp. causing crown rot of wheat in the Pacific Northwest of the United States. *Phytopathology* 103(11): 1130–1140. https://doi.org/10.1094/PHYTO-07-12-0181-R

Proctor R.H., Hohn T.M., McCormick S.P., 1995. Reduced virulence of *Gibberella zeae* caused by disruption of a trichothecene toxin biosynthetic gene. *Molecular Plant-Microbe Interactions* 8(4): 593–601. https://doi.org/10.1094/mpmi-8-0593

Rueda Puente E.O., Hernandez Montiel L.G., Holguin Peña J., Murillo Amador B., Rivas Santoyo F.J., 2014. First report of *Botrytis cinerea* Pers. on *Salicornia bigelovii* Torr. in North-West México. *Journal of Phytopathology* 162(7-8): 513–515. https://doi.org/10.1111/jph.12205

Rybecky A.I., Chulze S.N., Chiotta M.L., 2018. Effect of water activity and temperature on growth and trichothecene production by *Fusarium meridionale*. *International Journal of Food Microbiology* 285: 69–73. https://doi.org/10.1016/j.ijfoodmicro.2018.07.028

Sabburg R., Obanor F., Aitken E., Chakraborty S., 2015. Changing fitness of a necrotrophic plant pathogen under increasing temperature. *Global Change Biology* 21(8): 3126–3137. https://doi.org/10.1111/gcb.12927

Sever Z., Ivić D., Kos T., Miličević T., 2012. Identification of *Fusarium* species isolated from stored apple fruit in Croatia. *Archives of Industrial Hygiene and Toxicology* 63(4): 463–470. https://doi.org/10.2478/10004-1254-63-2012-2227

Shan X., Zhu Y., Redman R., Rodriguez R.J., Yuan Z., 2021. The chromosome-scale genome resource for two endophytic *Fusarium* species, *F. culmorum* and *F. pseudograminearum*. *Molecular Plant-Microbe Interactions* 34(6): 703–706. https://doi.org/10.1094/MPMI-07-20-0205-A

Song A., Xue G., Cui P., Fan F., Liu H., ... Liang Y., 2016. The role of silicon in enhancing resistance to bacterial blight of hydroponic- and soil-cultured rice. *Scientific Reports* 6: 24640. https://doi.org/10.1038/srep24640

Spada M., Pugliesi C., Fambrini M., Palpacelli D., Pecchia S., 2023. Knockdown of BMP1 and PLS1 virulence genes by exogenous application of RNAi-Inducing dsRNA in *Botrytis cinerea*. *International Journal of Molecular Sciences* 24(5): 4869. https://doi.org/10.3390/ijms24054869

Starkey D.E., Ward T.J., Aoki T., Gale L.R., Kistler H.C., O'Donnell K., 2007. Global molecular surveillance

reveals novel *Fusarium* head blight species and trichothecene toxin diversity. *Fungal Genetics and Biology* 44(11): 1191–1204. https://doi.org/10.1016/j.fgb.2007.03.001

Tunali B., Nicol J.M., Hodson D., Uçkun Z., Büyük O., ... Bağci H., 2008. Root and crown rot fungi associated with spring, facultative, and winter wheat in Turkey. *Plant Disease* 92(9): 1299–1306. https://doi.org/10.1094/PDIS-92-9-1299

Ventura Y., Sagi M., 2013. Halophyte crop cultivation: the case for *Salicornia* and *Sarcocornia*. *Environmental and Experimental Botany* 92: 144–153. https://doi.org/10.1016/j.envexpbot.2012.07.010

Xu F., Song Y.L., Wang J.M., Liu L.L., Zhao K., 2017. Occurrence of *Fusarium* crown rot caused by *Fusarium pseudograminearum* on barley in China. *Plant Disease* 101(5): 837. https://doi.org/10.1094/PDIS-10-16-1436-PDN

Zhou H., He X., Wang S., Ma Q., Sun B., Ding S., ... Li H., 2019. Diversity of the *Fusarium* pathogens associated with crown rot in the Huanghuai wheat-growing region of China. *Environmental Microbiology* 21(8): 2740–2754. https://doi.org/10.1111/1462-2920.14602

Phytopathologia Mediterranea
The international journal of the
Mediterranean Phytopathological Union

Firenze University Press
www.fupress.com/pm

Research Papers

Aphelenchoididae nematodes in a centennial *Pinus pinea* tree, and a review of *Bursaphelenchus* species from this host

Luís FONSECA[1,2*], Hugo SILVA[1], Joana M.S. CARDOSO[1], Ricardo M.F. DA COSTA[1,3], Filipe CAMPELO[1], Joana VIEIRA[1,4], Isabel ABRANTES[1]

[1] *Centre for Functional Ecology-CFE, Associate Laboratory for Sustainable Land Use and Ecosystem Services-TERRA, Department of Life Sciences, University of Coimbra, Coimbra, Portugal*
[2] *FITOLAB – Laboratory for Phytopathology, Instituto Pedro Nunes (IPN), Coimbra, Portugal*
[3] *Molecular Physical-Chemistry R&D Unit, Department of Chemistry, LAQV-REQUIMTE, University of Coimbra, Coimbra, Portugal*
[4] *COLAB ForestWISE, Collaborative Laboratory for Integrated Forest and Fire Management, Vila Real, Portugal*
*Corresponding author. E-mail: luis.fonseca@uc.pt

Summary. A "monumental" centennial *Pinus pinea* L. tree of public interest with severe wilting symptoms was felled in Coimbra, Portugal. A survey was carried out to detect *Aphelenchoididae* nematodes (including *Bursaphelenchus* spp.) in the tree tissues. Nematode isolates were characterised/identified based on species-specific morphological characteristics, and on molecular data. *Bursaphelenchus xylophilus* was not detected. Three other *Bursaphelenchus* species (*B. arthuri*, *B. fungivorus* and *B. sexdentati* Type II) were found co-occurring in the tree. Other *Aphelenchoididae* nematodes, *Potensaphelenchus stammeri* and *Cryptaphelenchus* sp., were also identified. An annotated checklist of *Bursaphelenchus* spp. on *P. pinea* is also presented, demonstrating the wide variability of *Bursaphelenchus* species in this host. These results have shown that centennial wilted pine trees can be reservoirs of nematode diversity impacting forest health.

Keywords. Nematode diversity, stone pine, urban tree.

Citation: Fonseca, L., Silva, H., Cardoso, J. M. S., da Costa, R. M. F., Campelo, F., Vieira, J. & Abrantes, I. (2025). *Aphelenchoididae* nematodes in a centennial *Pinus pinea* tree, and a review of *Bursaphelenchus* species from this host. *Phytopathologia Mediterranea* 64(1): 25-39. doi: 10.36253/phyto-15829

Accepted: February 18, 2025

Published: May 15, 2025

Data Availability Statement: All relevant data are within the paper and its Supporting Information files.

Competing Interests: The Author(s) declare(s) no conflict of interest.

Editor: Jean-Michel Savoie, INRA Villenave d'Ornon, France.

ORCID:
LF: 0000-0001-7405-8916
HS: 0000-0002-0046-4716
JMSC: 0000-0002-6594-4892
RMFdC: 0000-0002-5426-412X
FP: 0000-0001-6022-9948
JV: 0000-0003-1021-4101
IA: 0000-0002-8761-2151

INTRODUCTION

Centennial trees play important ecological roles contributing to climate change mitigation by sequestering large amounts of carbon (Stephenson *et al.*, 2014). Their unique dendrometric characteristics, such as cavities, dry and hollow branches, intricate crowns, and complex branching, also create biodiversity hotspots that support a wide variety of organisms, including fungi, insects, plants, bacteria, and nematodes (Lindenmayer, 2017; Paillet *et al.*, 2017; Azuma *et al.*, 2022). Beyond their ecological significance, these trees can hold historical, cultural, and religious values (Dafni, 2006; Lopes *et al.*,

2019; Rivers *et al*., 2022). In recent years, however, many of these trees in Europe have been lost due to natural and human-induced factors such as fires, invasive plant species, abandonment, improper pruning, a lack of protective legislation, or pathogens (San-Miguel-Ayanz *et al*., 2012; Stara and Tsiakiris, 2019).

In 1938, Portugal introduced the "Trees of Public Interest Law," establishing one of the earliest tree protection laws in Europe. Over the course of the 20th century, this law evolved, leading to the creation of a National Registry, which catalogues and classifies 100-year-old trees of public interest as "monumental trees" and "living monuments" (Lopes *et al*., 2019). Due to their age and size, upon their senescence and eventual death, these may become reservoirs for invasive pathogens, such as bacteria, fungi, insects, and nematodes (Stara and Tsiakiris, 2019). To prevent the spread of these pathogens to adjacent areas, dead and affected trees are removed from the field.

The present study examined a classified "monumental" centennial stone pine (*Pinus pinea* L.) with severe wilting symptoms, felled at the Health Sciences Campus of the University of Coimbra, Portugal. *Pinus pinea* is a medium-sized coniferous tree widely distributed across the Mediterranean basin, from Portugal to Syria. It is most abundant in southwestern Europe, particularly in the Iberian Peninsula, southern France, and Italy (Viñas *et al*., 2016).

The primary economic value of *P. pinea* are its nutritious and edible seeds (pine nuts), with secondary uses in furniture and rosin production. Additionally, stone pine trees stabilise sand dunes, and are commonly used as ornamental trees in warm European regions. As for other Mediterranean pines, stone pine is vulnerable to forest fires but is considerably less fire-sensitive than other Mediterranean pines due to its thick bark and high crown without low branches. Moreover, *P. pinea* is a slow-growing species with some resistance to pests and diseases (Viñas *et al*., 2016). Nevertheless, it is susceptible to several fungal diseases, including blister rust (*Cronartium flaccidum*), twisting rust (*Melampsora populnea*), needle rust (*Coleosporium tussilaginis*), diplodia tip blight (*Diplodia sapinea*), and Pestalotiopsis disease (*Pestalotiopsis pini*) (Fady *et al*., 2004; Viñas *et al*., 2016; Silva *et al*., 2020). Severe damage can also be caused by insects such as boring beetles (*Ernobius* spp.), snout moths (*Dioryctria* spp.), pine tortoise scale (*Toumeyella parvicornis*) and western conifer seed bug (*Leptoglossus occidentalis*) (Bracalini *et al*., 2013; Özçankaya *et al*., 2013; EPPO, 2015; Viñas *et al*., 2016; Sousa *et al*., 2017; Farinha *et al*., 2018).

Regarding the species *Monochamus galloprovincialis*, the European insect vector of the quarantine pinewood nematode (PWN), *Bursaphelenchus xylophilus*, the European pine species *P. pinaster* Aiton (maritime pine), *P. nigra* J. F. Arnold (black pine), *P. sylvestris* L. (Scots pine), and *P. halepensis* Mill. (Aleppo pine) are also hosts of this insect (EPPO, 2024). For *P. pinea*, laboratory tests have shown that adult *M. galloprovincialis* feed on fresh shoots, but this host was the least preferred species among other European pines tested, with few eggs laid, and few or no young adults emerging (Sanchez-Husillos *et al*., 2013; Naves *et al*., 2006). Furthermore, *P. pinea* volatile compounds are not attractive for *M. galloprovincialis* that is particularly attracted to alpha-pinene. Compared to other European pines, *P. pinea* has a greater proportion of limonene and consequently lower levels of alpha- and beta-pinene, which may explain its reduced attractiveness to insects (Pajares *et al*., 2004; Ibeas *et al*., 2007; Rodrigues *et al*., 2017; Gaspar *et al*., 2020; van Halder *et al*., 2022).

Pines susceptibility to PWN infection varies among species, with *P. pinea* being one of the less susceptible species (EPPO, 2024). Artificial PWN inoculation assays on *P. pinea* seedlings have consistently demonstrated its low susceptibility (Nunes da Silva *et al*., 2015; Menéndez-Gutiérrez *et al*., 2017; Pimentel *et al*., 2017; Estorninho *et al*., 2022). Contrasting to other European pine species, *P. pinea* showed almost no wilting symptoms and maintained physiological performance under stressful conditions such as high temperatures and low water availability (Estorninho *et al*., 2022). Resistance to PWN infection could be linked to drought-resistance of *P. pinea*, which is associated with slow growth rates, constitutive defences and high production of phenolics and tannins (Awada *et al*., 2003; Tapias *et al*., 2004; Pimentel *et al*., 2017).

Santos *et al.* (2012), using high-throughput sequencing, analysed the responses of *P. pinaster* and *P. pinea* to PWN infection, and showed that there was upregulation of genes involved in activating plant defence mechanisms, including general stress response genes such as ricin B-related lectin, phytoalexins like chalcone synthase, antioxidant enzymes (e.g. malic oxidoreductase), and disease resistance proteins that protect against a variety of plant pathogens. Resistant pine species demonstrate defence mechanisms including reactive oxygen species (ROS) detoxification, increased cell wall lignification related genes, and the production of secondary metabolites (polyphenols, terpenes flavonoids, stilbenoids, tannins), which hinder PWN mobility and survival (Modesto *et al*., 2022; Rodrigues *et al*., 2024).

Although Portugal has extensive stone pine forests, no cases of PWN infection or significant attacks of *M. galloprovincialis* have been reported on *P. pinea* in the field. However, other *Bursaphelenchus* species, which

are mycetophagous and insect-dispersed, have been previously recorded to be associated with *P. pinea*, including *B. hylobianum*, *B. leoni*, *B. minutus*, *B. pinasteri*, *B. sexdentati*, *B. teratospicularis* and *B. tusciae* (Ryss *et al.*, 2005; Errico *et al.*, 2015).

In the present study, a dendrochronological analysis of the classified "monumental" centennial *P. pinea* tree, which had severe wilting symptoms, was carried out by determining the tree age and the *Aphelenchoididae* diversity within the tree. Five nematode isolates were obtained from this tree and characterised using morphological and molecular characterisation. An updated checklist of *Bursaphelenchus* spp. reported on *P. pinea* is also presented in this paper.

MATERIALS AND METHODS

Dendrochronological characterisation of the Pinus pinea *tree*

The "monumental" *P. pinea* displaying severe wilting symptoms (Figure 1 A) was felled at the Health Sciences Campus (40°13'07"N, 8°25'02"W) of the University of Coimbra, Portugal.

A circular cross-section from the base of the main trunk (Figure 1 B) was cut from the felled tree with a chainsaw for dendrochronological examination. A mechanical hand-held circular sander was used to prepare the wood surface along the longest section radius (Figure 1 B) until the tree-ring limits were clearly visible. Tree rings were visually identified using standard dendrochronology methods (Stokes and Smiley, 1996), and the age of the tree was determined.

Wood sampling

Wood samples (100 g each) were collected from four different zones of the trunk, using an electric drill with a 20 mm diam. bit, and several branches were cut into small pieces (≈ 1 cm) using pruning scissors (EPPO, 2023). The samples, from the trunk and branches, were combined for nematode extraction.

Nematode extraction and nematode isolate establishment

Nematodes were extracted from the wood samples using the tray method (Whitehead and Hemming, 1965; EPPO, 2023) and were observed under an Olympus CKX41SF inverted stereomicroscope (Olympus). Ten nematodes (males and females), exhibiting the same morphological characteristics, were selected, individually picked, and transferred to malt extract agar (MEA) plates colonised with *Botrytis cinerea*. The plates were then incubated at 25°C, and five nematode isolates were established. These were maintained by transferring small culture plugs containing nematodes to new MEA plates colonised with *B. cinerea* at 3-week intervals (Fonseca *et al.*, 2008). Nematodes from the five isolates were collected by washing the *B. cinerea* plates with sterilised distilled water, for subsequent morphological and molecular characterisation.

Figure 1. (A) The *Pinus pinea* tree exhibiting severe wilting symptoms at Health Sciences Campus of the University of Coimbra, Portugal. (B) Main trunk cross section of the tree.

Morphological characterisation

Female and male nematodes from each isolate were individually selected and placed on glass microscope slides in drops of water. The slides were heated (to kill the nematodes), and the nematodes were immediately photographed with a microscope DM 2500; Leica, using a digital camera (DFC 450; Leica). Nematode genus identification was based on the morphological characters of females and males.

Molecular characterisation/identification

DNA extraction and amplification of ITS rDNA regions

Nematode DNA was extracted from mixed developmental nematode stages collected from MEA culture plates using the DNeasy Blood and Tissue Mini Kit (Qiagen), following the manufacturer's instructions, and were quantified using Nanodrop 2000C (ThermoScientific). The Internal Transcribed Spacer (ITS) rDNA regions containing partial 18S and 28S and complete ITS1, 5.8S and ITS2 sequences were amplified using 50 ng of extracted DNA and 1 U of Dream Taq DNA polymerase (Fermentas) in 1× Dream Taq buffer, 0.2 mM each dNTP, and 1 µM primers 18SF 5′-CGTAACAAGGTAGCTGTAG-3′ (Ferris *et al.* 1993) and 28SR 5′-TTTCACTCGCCGTTACTAAGG-3′ (Vrain, 1993). PCR reactions were carried out in a Thermal Cycler (Bio-Rad), with an initial denaturation step of 95°C for 2.5 min, followed by 40 reaction cycles each of 95°C for 30 s, annealing at 55°C for 30 s, extension at 72°C for 1 min, and final extension at 72°C for 5 min.

Restriction fragment length polymorphism analysis

The resulting amplification products were purified using the NucleoSpin Gel and PCR Clean-up Kit (Macherey-Nagel), according to manufacturer's instructions, and were used for restriction fragment length polymorphism (RFLP) analysis for *Bursaphelenchus* species characterisation/identification, according to Burgermeister *et al.* (2009) and EPPO (2023). The RFLP analysis of amplified ITS rDNA PCR products was carried out for isolates BfungPt2 and BsexPt2, using a combination of eight restriction endonucleases: *Afa*I, *Alu*I, *Hae*III, *Hinf*I, *Msp*I, *Mfe*I, *BsrB*I and *Hpy*188I (Amersham Biosciences), with restriction reactions performed according to the manufacturer's instructions. Restriction products were separated by electrophoresis on 2% agarose gel, fragment sizes were estimated via Hyper Ladder II (Bioline), and these were compared to previously described RFLP patterns. When the species identification was not possible from analysis of the RFLP patterns, the ITS rDNA PCR product was sequenced.

Sequencing and phylogenetic analyses

For the isolate CryPt1, which was morphologically characterised as *Cryptaphelenchus* sp., the ITS rDNA PCR product was sequenced in both strands in an Automatic Sequencer 3730xl under BigDye™ terminator cycling conditions at Macrogen Company (Seoul, Korea), using the same primers as used in the PCR. Sequence analyses were carried out using BioEdit (Hall, 1999). Homologous sequences in the databases were searched by BLAST (Altschul *et al.*, 1997), and selected sequences were used for sequence alignment. Phylogenetic analyses were carried out in MEGA 11 (Tamura *et al.*, 2021) by the Neighbor-Joining method (Saitou and Nei, 1987) with 1000 replications of bootstrap (Felsenstein, 1985) and Jukes-Cantor as substitution model (Jukes and Cantor, 1969), with all ambiguous positions removed for each sequence pair (pairwise deletion option), using the ITS rDNA sequence alignments.

RESULTS

Pinus pinea *dendrochronology*

The identification and quantification of the tree rings in the circular wood section from the base of the main trunk of the diseased tree indicated that the tree was of approx. 160 years old.

Nematode isolates

Five nematode isolates, corresponding to five different species, were designated as BaPt1 (*B. arthuri*); BfungPt2 (*B. fungivorus*); BsexPt2 (*B. sexdentati*); PsPt1 (*Potensaphelenchus stammeri*) and CryPt1 (*Cryptaphelenchus* sp.). These isolates have been maintained at the Laboratory of Nematology (NEMATO-lab), Department of Life Sciences, University of Coimbra, Portugal.

Morphological, morphometrical and molecular characterisation of PsPt1 were described by Silva *et al.* (2023), and of BaPt1 by Silva *et al.* (2024). Morphological and molecular characterisation/identifications of the other three isolates (BfungPt2, BsexPt2 and CryPt1) are presented below.

Morphological characterisation

Nematodes from the five isolates had main characteristic of *Aphelenchoididae* as described by Nickle (1970), including: i) body slender with variable length; ii) lips often slightly offset; iii) stylet with knobs ranging from absent, to slightly thickened, to well-developed; iv) oesophagus with overlapping glands; and v) spicules characteristically rosethorn-shaped with caudal papillae.

Nematodes of the isolates BfungPt2 and BsexPt2 had main morphological characters of the *Bursaphelenchus* genus (Ryss *et al*., 2015; EPPO, 2023), including: i) vermiform; ii) cephalic region offset by a constriction; iii) stylet length with weak basal knobs; iv) strong median bulb oval to quadrangular; v) oesophageal glands overlapping the intestine; vi) female with vulva posterior, with or without an anterior vulval flap, rounded tail or with a smooth or mucronate terminus; and vii) male with hook-like spicules with a prominent rostrum, and a capitulum, sometimes with a cucullus in the distal end, and a ventrally arched tail terminus.

The main morphological diagnostic characters of the nematodes of the isolate BfungPt2 were: i) cephalic region offset by a constriction with six lips; ii) stylet with weak basal knobs; iii) median bulb well developed (Figure 2 A); iv) males with ventrally curved tails with compact spicules without cucullus (Figure 2 B); v) females with vulvae without flaps and long ventrally bent tails (Figure 2, C and D). These characteristics are in accordance with those described for *B. fungivorus* (Franklin and Hooper, 1962; Ambrogioni *et al*., 2003; Arias *et al*., 2005; Oliveira *et al*., 2011; Fonseca *et al*., 2014; Torrini *et al*., 2020b).

The main morphological diagnostic characters for isolate BsexPt2 nematodes were: i) cephalic region offset by a constriction with six lips; ii) stylet with weak basal knobs, median bulb well developed (Figure 3 A); iii) male spicules each with a sharply pointed rostrum, and well-developed broadly truncate condylus with a small cucullus (Figure 3 B); and iv) females each with a small vulval flap and with a gradually tapering tail (Figure 3, C and D). These characteristics are in accordance with those previously described for *B. sexdentati* (Lange *et al*., 2006; 2008; Penas *et al*., 2008; Slonin *et al*., 2018). According to Lange *et al*. (2006) and considering the condylus and female tail shapes, isolate BsexPt2 belongs to *B. sexdentati* Type II (South European isolates).

Nematodes of isolate CryPt1 had main morphological diagnostic characters of *Cryptaphelenchus* (Figure 4) (Pedram, 2017; Gu *et al*., 2024), including: i) short body length (≤ 500 µm), C-shaped, not slender; ii) lips rounded forming a cap, slightly offset; iii) stylet delicate (≤ 10 µm), with small rounded basal knobs (Figure 4 A); iv) males with arcuate spicules, and prominent and narrow rostrum; condylus well developed; v) bursa absent and tail gradually attenuated to point (Figure 4 B); and vi) females with vulva posterior (V ≥ 75%) without vulvar flap, tail short and conical (Figure 4 C).

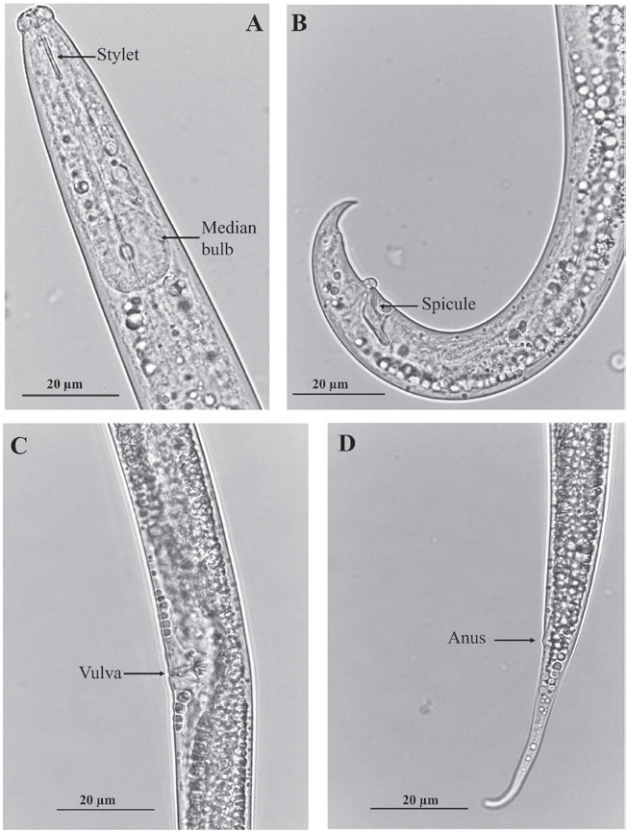

Figure 2. Light microscope photographs of the nematode isolate BfungPt2. (A) Anterior region. (B) Male tail. (C) Female vulvar region. (D) Female tail.

Molecular characterisation/identification

Amplification of ITS rDNA region amplifications from isolate BfungPt2 yielded a single product of approx. 1050 bp. The restriction endonuclease patterns with five enzymes (*Afa*I, *Alu*I, *Hae*III, *Hinf*I and *Msp*I) (Figure 5 A) agree with patterns previously reported for *B. fungivorus* (Arias *et al*., 2005; Burgermeister *et al*., 2009; Oliveira *et al*., 2011; Fonseca *et al*., 2014), confirming the identifications of isolate BfungPt2 as *B. fungivorus*.

Isolate BsexPt2 ITS rDNA region amplification yielded a single product of approx. 960 bp. ITS-RFLP analysis with the five enzymes (*Afa*I, *Alu*I, *Hae*III, *Hinf*I and *Msp*I) produced a restriction pattern similar to

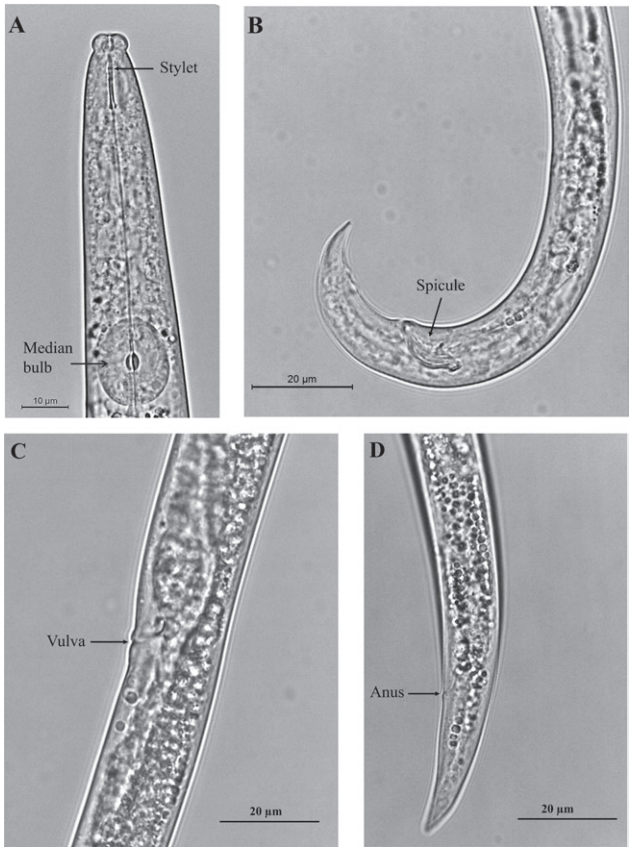

Figure 3. Light microscope photographs of the nematode isolate BsexPt2. (A) Anterior region. (B) Male tail. (C) Female vulvar region. (D) Female tail.

B. sexdentati isolates (Figure 5 B) (Penas *et al*., 2006; Burgermeister *et al*., 2009; Dayi *et al*., 2014). *Bursaphelenchus sexdentati* Type I isolates could not be distinguished from Type II isolates using these five restriction enzymes. Three additional restriction enzymes, *Mfe*I (isochizomer of *Mun*I), *BsrB*I (isochizomer of *Mbi*I) and *Hpy*188I were selected according to Lange *et al*. (2006, 2008). Isolate BsexPt2 had a restriction pattern correspondent to the southern European isolates (Type II) (Figure 5 C).

After sequencing, an 813 bp sequence corresponding to the CryPt1 rDNA region, containing partial 18S and 28S and complete ITS1, 5.8S and ITS2 sequences, was submitted to the NCBI database under accession number PQ408586. The phylogenetic analysis, from multiple sequence alignment of sequences available in GenBank of *Cryptaphelenchus* species, showed that isolate CryPt1 was included in a large phylogenetic group corresponding to *Cryptaphelenchus* species. This group included *C. minutus*, *C. orientalis*, *C. recticaudatum* and *C. tumidus*, and other unidentified *Cryptaphelenchus* species from Israel, forming a separate phylogenetic group from the other isolates analysed (Figure 6).

DISCUSSION

After the detection of *B. xylophilus* (EPPO A2 quarantine list) associated with *P. pinaster* in the Setúbal peninsula, Portugal, in 1999 (Mota *et al*., 1999), official surveys have been conducted to evaluate nematode diversity associated with *Pinus* spp. In Portugal, *B. xylophilus* was also reported in *P. nigra* (Inácio *et al*., 2015) and *P. sylvestris* (Fonseca *et al*., 2024), and in Spain, in *P. pinaster* (Abelleira *et al*., 2011) and *P. radiata* D. Don (Zamora *et al*., 2015).

In Portugal, from 1999 to the present, several other *Bursaphelenchus* species have been reported in *P. pinaster*, including *B. hellenicus*, *B. hylobianum*; *B. leoni*, *B. mucro-*

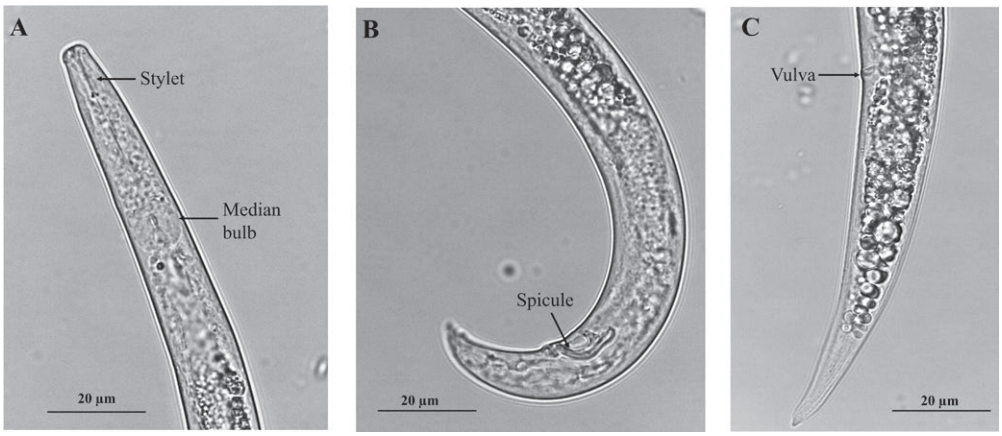

Figure 4. Light microscope photographs of the nematode isolate CryPt1. (A) Anterior region. (B) Male tail (C) Female vulvar region and tail.

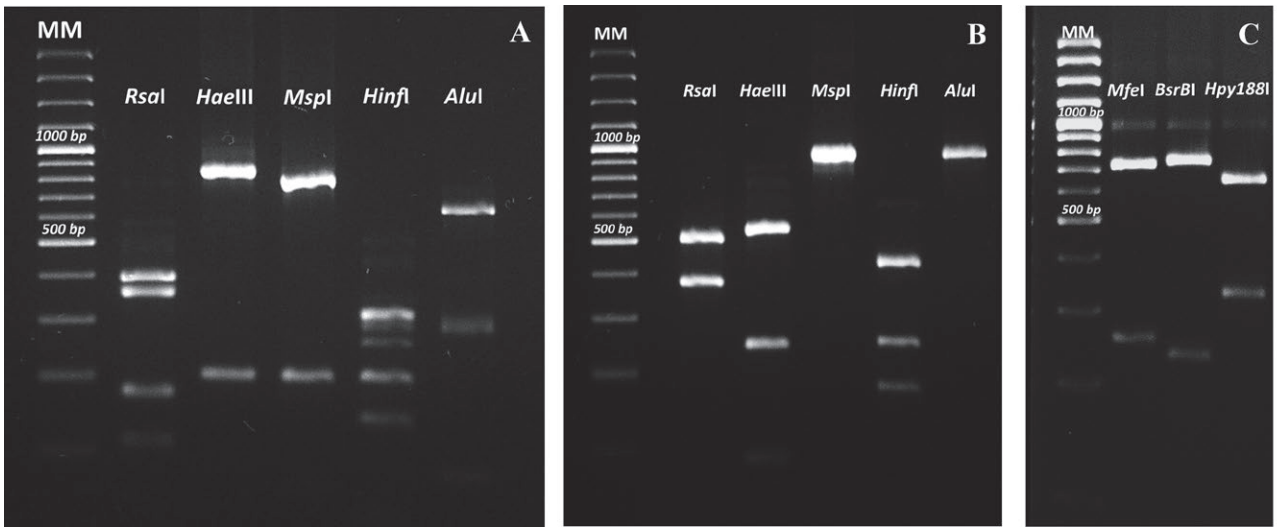

Figure 5. ITS-RFLP patterns of two *Bursaphelenchus* isolates. **(**A) Isolate BfungPt2. (B) and (C) Isolate BsexPt2. MM is the DNA size marker (Hyper Ladder II; Bioline).

natus, *B. pinasteri*, *B. pinophilus*, *B. sexdentati*, *B. teratospicularis*, *B. tusciae* (Penas *et al*., 2004, 2006), *B. fungivorus* (Fonseca *et al*., 2014) and *B. luxurosiae* (Inácio *et al*., 2017). From *P. pinea*, nine *Bursaphelenchus* species have been reported in the Mediterranean region (Table 1).

Species of *Bursaphelenchus* are primarily mycetophagous and include nematodes that are associated with insects and dead or dying coniferous trees (Ryss *et al*., 2005). In forestry areas, the most significant vectors of *Bursaphelenchus* spp. belong to *Cerambycidae*, *Curculionidae*, *Scolytidae*, and *Buprestidae* (Linit *et al*., 1983; Linit, 1988).

In Portugal, three *Bursaphelenchus* species have now been identified in association with *P. pinea*: i) *B. arthuri* (Silva *et al*., 2024); ii) *B. fungivorus* isolate BfungPt2; and iii) *B. sexdentati* isolate BsexPt2 (this study) (Table 1). These species, as mycetophagous, can be maintained in the laboratory in fungus cultures.

Bursaphelenchus arthuri was first detected in Portugal and Europe associated with *P. pinea*, in 2024 (Silva *et al*., 2024). This nematode was previously reported in coniferous packaging wood imported from Taiwan, South Korea, United States of America, China, and Japan (Burgermeister *et al*., 2005; Gu *et al*., 2006, 2008).

Bursaphelenchus fungivorus was first reported in the United Kingdom, in rotting gardenia buds (*Gardenia* sp.) infected by *Botrytis cinerea* (Franklin and Hooper, 1962). It was later found in: i) a bark-based growing medium in Germany (Braasch *et al*., 1999); ii) coniferous bark imported from the Czech Republic and Russia (Braasch *et al*., 2002); iii) Chinese *Callitris columellaris* F. Muell. packaging wood imported to Italy (Ambrogioni *et al*., 2003); iv) *Pinus* species, in Spain, associated with the bark beetle *Orthotomicus erosus* (Arias *et al*., 2004; 2005); v) wood chips and sawdust in Germany (Schonfeld *et al*., 2008); vi) fibrous husk of *Cocos nucifera* L. in Brazil (Oliveira *et al*., 2011); vi) *P. pinaster* bark in Portugal (Fonseca *et al*., 2014); and vii) associated with *Crocus sativus* L. in Italy (Torrini *et al*., 2020b). The present report is the first for presence of *B. fungivorus* on *P. pinea*.

Bursaphelenchus sexdentati is a cosmopolitan species with broad geographic range across European pine forests. This nematode has been divided into two distinct Types based on morphological characteristics, molecular features, and geographical distribution: Type I has been mainly found in Central Europe (Germany, Switzerland); and Type II is mostly distributed in Southern Europe (Cyprus, Greece, Portugal, Spain) (Lange *et al*., 2006, 2008). The isolate BsexPt2 is of the Type II (Lange *et al*., 2006; 2008; Penas *et al*., 2006; Burgermeister *et al*., 2009; Dayi *et al*., 2014). In the Mediterranean region, *B. sexdentati* has been associated with several pine species, including *P. brutia* Ten., *P. halepensis*, *P. nigra*, *P. pinea*, *P. pinaster*, *P. radiata*, and *P. sylvestris*, which are typically colonised by bark beetles (Errico *et al*., 2015). *Bursaphelenchus sexdentati* has also been described as vectored by insects such as *Ips sexdentatus*, *Tomicus piniperda*, and *O. erosus*. Furthermore, *O. erosus* has been reported as a vector for other *Bursaphelenchus* species, including *B. erosus, B. fuchsi*, *B. minutus* and *B. fungivorus* (Slonim *et al*., 2018).

Three *Bursaphelenchus* species were found co-existing within the *P. pinea* tree assessed in the present study. The co-existence of multiple *Bursaphelenchus* species within a single tree has also been reported by Caroppo

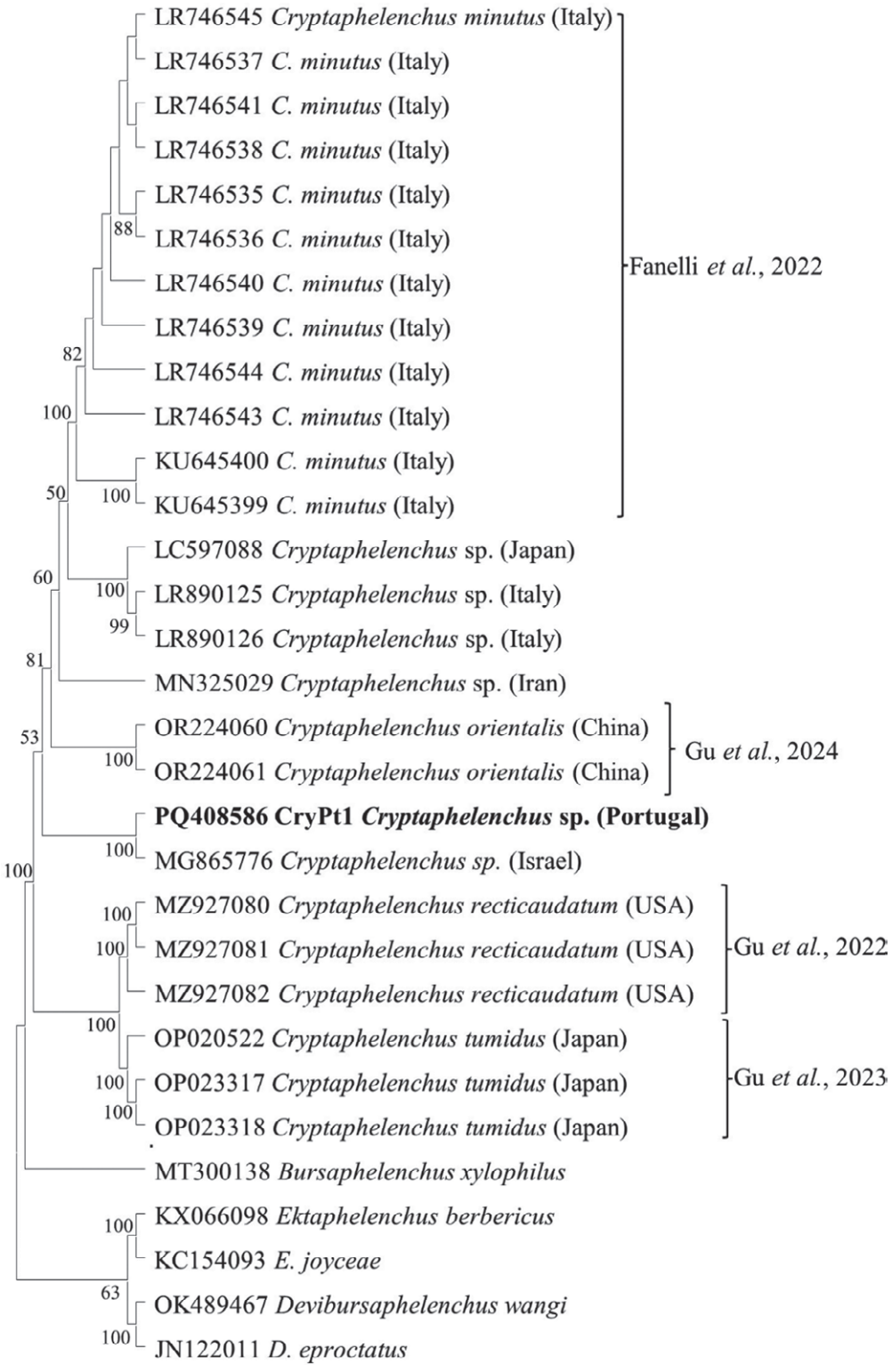

Figure 6. Phylogenetic tree generated by the Neighbour-Joining method using the multiple sequence alignment of 5.8S gene, ITS1 and ITS2 regions and partial regions of 18S and 28S genes sequences conducted in MEGA11. The percentages of replicate trees in which the associated taxa clustered together in the bootstrap test (100 replicates) are shown next to the branches. Evolutionary distances were computed using the Jukes-Cantor method. The analysis involved 31 nucleotide sequences with all ambiguous positions removed for each sequence pair (pairwise deletion option).

Table 1. *Bursaphelenchus* species associated with *Pinus pinea*.

Bursaphelencaahus species	Country	Reference
B. arthuri	**Portugal**	Silva *et al.* (2024)
B. fungivorus	**Portugal**	**The present study**
B. hylobianum	Spain	Escuer *et al.* (2004)
B. leoni	Cyprus	Philis (1996); Philis and Braasch (1996)
	Italy	Ambrogioni *et al.* (1994); Palmisano and Ambrogioni (1994); Ambrogioni and Caroppo (1998); Caroppo *et al.* (1998); Carletti (2008); Torrini *et al.* (2020a)
	Spain	Arias *et al.* (2004); Escuer *et al.* (2004)
B. minutus	Italy	Carletti (2008); Torrini *et al.* (2017
B. pinasteri	Spain	Escuer *et al.* (2004)
B. sexdentati	Italy	Ambrogioni and Caroppo (1998); Caroppo *et al.* (1998); Carletti (2008); Torrini *et al.* (2020a)
	Portugal	**The present study**
	Spain	Arias *et al.* (2004); Escuer *et al.* (2004)
B. teratospicularis	Italy	Ambrogioni and Caroppo (1998); Caroppo *et al.* (1998)
	Spain	Arias *et al.* (2004)
B. tusciae	Italy	Ambrogioni and Palmisano (1998); Carletti (2008); Torrini *et al.* (2020a)

et al. (1998), Braasch (2001) and Karmezi *et al.* (2022). Despite the *Bursaphelenchus* species reported, other nematode isolates of *Cryptaphelenchus* (this study) and of *Potensaphelenchus stammeri* (Silva *et al.*, 2023) were characterised and identified.

Cryptaphelenchus genus is known for its fungal-feeding species and has received little attention due to its small body size, resulting in fewer species being described. However, in the past decade, interest in *Cryptaphelenchus* species has grown, leading to the identification of more than 20 nominal species in countries including Germany, Italy, Iran, the United States of America, Japan, and China (Pedram, 2017; Fanelli *et al.*, 2022; Gu *et al.*, 2022; 2023; 2024). *Cryptaphelenchus* species have been isolated directly from bark or wood packaging materials and have been extracted from insect bodies (Kanzaki *et al.*, 2021; Gu *et al.*, 2022, 2023, 2024). Isolate CryPt1 showed the main morphological characters of this genus, belongs to the phylogenetic group of *Cryptaphelenchus* species, and clustered with an unidentified species from Israel (Fanelli *et al.*, 2022; Gu *et al.*, 2022, 2023, 2024). Further morphological, morphometrical and molecular characterisation is required to identify the CryPt1 isolate.

Potensaphelenchus stammeri was also found associated with the *P. pinea* tree. This is the first report of this nematode in Portugal and in *P.* pinea (Silva *et al.*, 2023). This nematode was first isolated from the insect *Spondylis buprestoides* and was described as *Aphelenchoides stammeri* (Körner, 1954). Later, it was found widely distributed in German coniferous forests in *S. buprestoides* breeding sites and in trunks of declining *Pinus* and *Picea* trees (Braasch, 1998), in China from PWN infected *P. massoniana* Lamb. (Huang and Ye, 2006), in Slovenia from *P. sylvestris* (Urek *et al.*, 2007), and in Turkey and China from *P. massoniana* (Dayi *et al.*, 2019; Gu *et al.*, 2021).

CONCLUSIONS

The present study has assessed the diversity of *Aphelenchoididae* nematodes within a classified "monumental" centennial *P. pinea* tree and has reported three *Bursaphelenchus* species co-existing simultaneously with two other *Aphelenchoididae* nematodes. This knowledge emphasises the role of large, catalogued trees as biodiversity hotspots for nematodes from different trophic groups, including plant parasites. The enduring stability of these habitats supports nematofauna, insect galleries, as well as bacteria and fungi. Diseased and dead trees should be removed from plant communities to prevent pathogen spread to nearby healthy areas. These "monumental" trees impact forest health, nutrient cycling, and microbial communities in forest areas.

AUTHORS CONTRIBUTIONS

Luís Fonseca (conceptualisation, methodology, writing, review, and editing of the manuscript, research supervision, project administration, funding acquisition), Hugo Silva (methodology, writing, review, and editing of the manuscript), Joana M. S. Cardoso (meth-

odology, writing, review, and editing of the manuscript), Ricardo M. C. da Costa (methodology, writing, review, and editing of the manuscript, funding acquisition), Filipe Campelo (methodology, writing, review, and editing of the manuscript), Joana Vieira (methodology, writing, review, and editing of the manuscript), and Isabel Abrantes (conceptualisation, writing, review, and editing of the manuscript, supervision, funding acquisition).

FUNDING

This research was supported by the Portuguese Foundation for Science and Technology ("Fundação para a Ciência e Tecnologia – FCT") through national funds, and co-funding by FEDER, PT2020 and COMPETE 2020 under the following projects: POINTERS- PTDC/ASP-SIL/31999/2017 (POCI-01-145-FEDER-031999); PineWALL, PTDC/ASP-SIL/3142/2020 (https://doi.org/10.54499/PTDC/ASP-SIL/3142/2025), UIDB/04004/2025 (https://doi.org/10.54499/UIDB/04004/2025), UIDB/00070/2020 (https:/doi.org/10.54499/UIDB/00070/2025); Project ReNATURE – Valorization of the Natural Endogenous Resources of the Centro Region (Centro 2020, Centro-01-0145-FEDER-000007) and "Instituto do Ambiente, Tecnologia e Vida". Hugo Silva (Grant—2023. 03527.BD) is funded by FCT, the European Social Fund (ESF), under the "Programa Demografia, Qualificações e Inclusão" (PDQI)—Portugal2030.

DATA AVAILABILITY

Genomic data presented in this study related to the *Cryptaphelenchus* sp. isolate can be found in NCBI database under the accession number PQ408586.

LITERATURE CITED

Abelleira A., Picoaga A., Mansilla J.P., Aguin O., 2011. Detection of *Bursaphelenchus xylophilus*, causal agent of pine wilt disease on *Pinus pinaster* in Northwestern Spain. *Plant Disease* 95: 776. https://doi.org/10.1094/PDIS-12-10-0902

Altschul S.F., Madden T.L.., Schaffer AA., Zhang J., Zhang Z., Miller W., Lipman D.J., 1997. Gapped BLAST and PSI-BLAST: a new generation of protein database search programs. *Nucleic Acids Research* 25: 3389–3402. https://doi.org/10.1093/nar/25.17.3389

Ambrogioni L., Caroppo S., 1998. Morphology and morphometrics of Italian populations of *Bursaphelenchus* species. *Nematologia Mediterranea* 26: 97–116.

Ambrogioni L., Cerchiarini G., Irdani T., Tossani N., 1994. Indagine preliminare sulla diffusione di *Bursaphelenchus* spp. (Nematoda) in pinete italiane. *Redia* 77: 273–278.

Ambrogioni L., Irdani T., Caroppo S., 2003. Records of *Bursaphelenchus* species on coniferous wood imported from Asian Russia and China to Italy. *Redia* 86: 139–146.

Ambrogioni L., Palmisano M.A., 1998. Description of *Bursaphelenchus tusciae* sp. n. from *Pinus pinea* in Italy. *Nematologia Mediterranea* 26: 243–254.

Arias M., Escuer M., Bello A., 2004. Nematodos asociados a madera y árboles de coníferas en pinares españoles. *Boletín de Sanidad Vegetal – Plagas* 30: 581–593.

Arias M., Robertson L., Garcia-Alvarez A., Arcos S.C., Escuer M., Sanz R., Mansilla J.P., 2005. *Bursaphelenchus fungivorus* (Nematoda: Aphelenchida) associated with *Orthotomicus erosus* (Coleoptera: Scolitydae) in Spain. *Forest Pathology* 35: 375–383. https://doi.org/10.1111/j.1439-0329.2005.00422.x

Awada T., Radoglou K., Fotelli M.N., Constantinidou H.I.A., 2003. Ecophysiology of seedlings of three Mediterranean pine species in contrasting light regimes *Tree Physiology* 23: 33–41. https://doi.org/10.1093/treephys/23.1.33

Azuma W.A., Komada N., Ogawa Y., Ishii H., Nakanishi A., Noguchi Y., Kanzaki M., 2022. One large tree crown can be defined as a local hotspot for plant species diversity in a forest ecosystem: a case study in temperate old-growth forest. *Plant Ecology* 223: 99–112. https://doi.org/10.1007/s11258-021-01192-8

Braasch H., 1998. *Aphelenchoides stammeri* Körner, 1954–ein in Deutschland weit verbreiteter. *Nachrichtenblatt für den Deutschen Pflanzenschutzdienst* 50: 317–319.

Braasch H., 2001. *Bursaphelenchus* species in conifers in Europe: Distribution and morphological relationships. *Bulletin OEPP/EPPO Bulletin* 31: 127–142. https://doi.org/10.1111/j.1365-2338.2001.tb00982.x

Braasch H., Bennewitz A., Hantusch W., 2002. *Bursaphelenchus fungivorus* – a nematode of the wood nematode group in growing substrate of a greenhouse and in imported wood on bark. *Nachrichtenblatt für den Deutschen Pflanzenschutzdienst* 54: 1–4.

Braasch H., Metge K., Burgermeister W., 1999. *Bursaphelenchus* species (Nematoda: Parasitaphelenchidae) found in coniferous trees in Germany and their ITS-RFLP patterns. *Nachrichtenblatt für den Deutschen Pflanzenschutzdienst* 51: 312–320.

Bracalini M., Benedettelli S., Croci F., Terreni P., Tiberi R., Panzavolta T., 2013. Cone and seed pests of *Pinus pinea*: Assessment and characterization of damage. *Journal of Economic Entomology* 106: 229-234. https://doi.org/10.1603/EC12293

Burgermeister W., Gu J., Braasch H., 2005. *Bursaphelenchus arthuri* sp. n. (Nematoda: Parasitaphelenchidae) in packaging wood from Taiwan and South Korea-a new species belonging to the fungivorus group. *Journal of Nematode Morphology and Systematics* 8: 7–17.

Burgermeister W., Braasch H., Metge K., Gu J., Schröder T., Woldt E., 2009. ITS-RFLP analysis, an efficient tool for differentiation of *Bursaphelenchus* species *Nematology* 11: 649–668. https://doi.org/10.1163/156854108/399182

Carletti B., 2008. *Bursaphelenchus* species with their natural vectors in Italy: Distribution and essential diagnostic features. *Redia* 91: 111–117.

Caroppo S., Ambrogioni L., Cavalli M., Coniglio D., 1998. Occurrence of pinewood nematodes *Bursaphelenchus* and their possible vectors in Italy *Nematologia Mediterranea* 26: 87–92.

Dafni A., 2006. On the typology and the worship status of sacred trees with a special reference to the Middle East. *Journal of Ethnobiology and Ethnomedicine* 2: 26. https://doi.org/10.1186/1746-4269-2-26

Dayi M., Calin M., Akbulut S., Gu J., Schröder T., Vieira P., Braasch H., 2014. Morphological and molecular characterisation of *Bursaphelenchus andrassyi* sp. n. (Nematoda: Aphelenchoididae) from Romania and Turkey. *Nematology* 16: 207-218. https://doi.org/10.1163/15685411-00002759

Dayi M., Uludamar E.B.K., Akbulut S., Elekcioğlu I.L., 2019. First record of *Aphelenchoides stammeri* (Nematoda: Aphelenchoididae) from Turkey. *Journal of Nematology* 51: 1-6. https://doi.org/10.21307/jofnem-2019-070

EPPO, 2015. *EPPO Global Database*. Retrieved from: https://gd.eppo.int (September 9, 2024).

EPPO, 2023. PM 7/4 (4) *Bursaphelenchus xylophilus*. *Bulletin OEPP/EPPO Bulletin* 53: 156–183. https://doi.org/10.1111/epp.12915

EPPO, 2024. *Bursaphelenchus xylophilus. EPPO datasheets on pests recommended for regulation*. Retrieved from: https://gd.eppo.int/taxon/BURSXY (September 9, 2024).

Errico G., Carletti B., Schröder T., Mota M., Vieira P., Roversi P.F., 2015. An update on the occurrence of nematodes belonging to the genus *Bursaphelenchus* in the Mediterranean area. *Forestry* 88*:* 509–520. https://doi.org/10.1093/forestry/cpv028

Escuer M., Arias M., Bello, A., 2004. Occurrence of the genus *Bursaphelenchus* Fuchs, 1937 (Nematoda: Aphelenchida) in Spanish conifer forests. *Nematology* 6: 155–156. https://doi.org/10.1163/156854104323073035

Estorninho M., Chozas S., Mendes A., Colwell F., Abrantes I., … Antunes C., 2022. Differential impact of the pinewood nematode on *Pinus* species under drought conditions. *Frontiers in Plant Science* 13: 841707. https://doi.org/10.3389/fpls.2022.841707

Fady B., Fineschi S., Vendramin G.G., 2004. EUFORGEN Technical guidelines for genetic conservation and use for Italian stone pine (*Pinus pinea*) *International Plant Genetic Resources Institute*, Rome, Italy.

Fanelli E., Troccoli A., Sacchi S., Castillo P., Gaffuri F., Cavagna B., De Luca F., 2022. Occurrence of *Cryptaphelenchus minutus* and other nematode species associated with the bark of unidentified coniferous tree in Italy. *European Journal of Plant Pathology* 163: 155-165. https://doi.org/10.1007/s10658-022-02465-2

Farinha A.O., Durpoix C., Valente S., Sousa E., Roques A., Branco M., 2018. The stone pine, *Pinus pinea* L., a new highly rewarding host for the invasive *Leptoglossus occidentalis*. *NeoBiota* 41: 1–18. https://doi.org/10.3897/neobiota.41.30041

Felsenstein J., 1985. Confidence limits on phylogenies: An approach using the bootstrap *Evolution* 39: 783-791. https://doi.org/10.2307/2408678

Ferris V.R., Ferris J.M., Faghihi J., 1993. Variation in spacer ribosomal DNA in some cyst-forming species of plant parasitic nematodes. *Fundamental and Applied Nematol*ogy 16: 177–184.

Fonseca L., Cardoso J.M.S., Moron-Lopez J., Abrantes., 2014. *Bursaphelenchus fungivorus* from *Pinus pinaster* bark in Portugal. *Forest Path*ology 44: 131–136. https://doi.org/10.1111/efp.12077

Fonseca L., Santos M.C.V., Santos M.S., Curtis R.H.C., Abrantes I., 2008. Morpho-biometrical characterisation of Portuguese *Bursaphelenchus xylophilus* isolates with mucronate, digitate or round tailed females *Phytopathologia Mediterranea* 47: 223–233. https://doi.org/10.14601/Phytopathol_Mediterr-2726

Fonseca L., Silva H., Cardoso J.M.S., Esteves I., Maleira C., Lopes S., Abrantes I., 2024. *Bursaphelenchus xylophilus* in *Pinus sylvestris*—The first report in Europe. *Forests* 15: 1556. https://doi.org/10.3390/f15091556

Franklin M.T., Hooper D.J., 1962. *Bursaphelenchus fungivorus* n. sp. (Nematoda: Aphelenchoidea) from rotting gardenia buds infected with *Botrytis cinerea*. *Nematologica* 8: 136-142.

Gaspar M.C., Agostinho B., Fonseca L., Abrantes I., de Sousa H.C., Braga M.E.M., 2020. Impact of the

pinewood nematode on naturally emitted volatiles and scCO2 extracts from *Pinus pinaster* branches: a comparison with *P. pinea*. *Journal of Supercritical Fluids* 159: 104784. https://doi.org/10.1016/j.supflu.2020.104784

Gu J., Liu L., Abolafia J. Pedram M., 2021. A revision of the taxonomy of *Aphelenchoides stammeri* Körner, 1954 (Rhabditida: Aphelenchoididae) and proposal for a new genus. *Nematology* 23: 215–228. https://doi.org/10.1163/15685411-bja10039

Gu J., Braasch H, Burgermeister W., Zhang J., 2006. Records of *Bursaphelenchus* spp. intercepted in imported packaging wood at Ningbo, China *Forest Patholo*gy 36: 323–333. https://doi.org/10.1111/j.1439-0329.2006.00462.x

Gu J., Castillo P., Ma X., Munawar M., 2024. Unveiling novel and know *Cryptaphelenchus* species from China and USA. *Nematology* 26: 731-752. https://doi.org/10.1163/15685411-bja10335

Gu J., Fang E., Ma X., 2022. Description of *Cryptaphelenchus recticaudatus* n. sp. (Aphelenchoidea: Ektaphelenchinae) in *Pinus elliottii* from the USA. *Nematology* 24: 465-473. https://doi.org/10.1163/15685411-bja10142

Gu J., Ma X., Castillo P., Munawar M., 2023. Description of two new *Cryptaphelenchus* species from China and Japan. *Nematology* 25: 479-493. https://doi.org/10.1163/15685411-bja10234

Gu J., Zhang J, Chen X. Braasch H., Burgermeister W., 2008. *Bursaphelenchus* spp. in wood packaging intercepted in China. In: *Pine Wilt Disease: A Worldwide Threat to Forest Ecosystems* (M. Mota, P. Vieira, eds), Springer. pp. 83–88.

Hall T.A., 1999. BioEdit: a user-friendly biological sequence alignment editor and analysis program for Windows 95/98/NT. *Nucleic Acids Symposium Series* 41: 95–98.

Huang R.E., Ye J.R., 2006. *Seinura lii* n. sp. and *S. wuae* n. sp. (Nematoda: Seinuridae) from pine wood in China. *Nematology* 8: 749–759. https://doi.org/10.1163/156854106778877848

Ibeas F., Gallego D., Diez J.J., Pajares A., 2007. An operative kairomonal lure for managing pine sawyer beetle *Monochamus galloprovincialis* (Coleoptera: Cerymbycidae). *Journal of Applied Entomology* 131: 13–20. https://doi.org/10.1111/j.1439-0418.2006.01087.x

Inácio M.L., Nóbrega F., Mota M., Vieira P., 2017. First detection of *Bursaphelenchus luxuriosae* associated with *Pinus pinaster* in Portugal and in Europe. *Forest Pathology* 45: 1-4. https://doi.org/10.1111/efp.12296

Inácio M.L., Nóbrega F., Vieira P., Bonifácio L., Naves P., Sousa E., Mota M., 2015. First detection of *Bursaphelenchus xylophilus* associated with *Pinus nigra* in Portugal and in Europe. *Forest Pathology* 45: 235–238. https://doi.org/10.1111/efp.12162

Jukes T.H., Cantor C.R., 1969. Evolution of protein molecules. In: *Mammalian protein metabolism* (H.N. Munro, ed),. New York Academic Press. pp. 21-132.

Karmezi M., Bataka A., Papachristos D., Avtzis D.N., 2022. Nematodes in the pine forests of Northern and Central Greece. *Insects* 13: 194. https://doi.org/10.3390/insects13020194

Kanzaki N., Ekino T., Daegawa Y., 2021. *Cryptaphelenchus abietis* n. sp. (Tylenchomorpha: Aphelenchoididae) isolated from *Cryphalus piceae* (Ratzeburg) (Coleoptera: Scolytinae) emerged from *Abies veitchii* Lindl. (Pinaceae) from Nagano, Japan. *Nematology* 24: 65–84. https://doi.org/10.1163/15685411-bja10112

Körner H., 1954. Die Nematoden fauna des vergehenden Holzes und ihre Beziehungen zu den Insekten. *Zoologische Jahrbücher Abteilung für Systematik, Geographie und Biologie der Tiere* 82: 245–353.

Lange C., Burgermeister W., Metge K., Braasch H., 2006. Phylogenetic analysis of isolates of the *Bursaphelenchus sexdentati* group using intergenic transcribed spacer DNA sequences. *Journal of Nematode Morphology and Systematics* 9: 95–109.

Lange C, Burgermeister W, Metge K., Braasch H., 2008. Molecular characterization of isolates of the *Bursaphelenchus sexdentati* group using ribosomal DNA sequences and ITS-RFLP. In: *Pine Wilt Disease: A Worldwide Threat to Forest Ecosystems* (M. Mota, P. Vieira, ed), Springer. pp. 165–174.

Lindenmayer D.B., 2017. Conserving large old trees as small natural features. *Biological Conservation* 211: 51-57. https://doi.org/10.1016/j.biocon.2016.11.012

Linit M.J., 1988. Nematode-vector relationships in the pine wilt disease system. *Journal of Nematology* 20: 227–235.

Linit M.J., Kondo E., Smith M.T., 1983. Insect associated with the pine wood nematode, *Bursaphelenchus xylophilus*, in Missouri. *Environmental Entomology* 12: 467–470. https://doi.org/10.1093/ee/12.2.467

Lopes R.P., Reis C.S., Trincão P.R., 2019. Portugal's trees of public interest: their role in botany awareness. *Finisterra* 110: 19-36. https://doi.org/10.18055/Finis14564

Menéndez-Gutiérrez M., Alonso M., Toval G., Diaz R., 2017. Variation in pinewood nematode susceptibility among *Pinus pinaster* Ait. provenances from the Iberian Peninsula and France. *Annals of Forest Science* 74: 1–15. https://doi.org/10.1007/s13595-017-0677-3

Modesto I., Mendes A., Carrasquinho I., Miguel C.M., 2022. Molecular defense response of pine trees

(*Pinus* spp.) to the parasitic nematode *Bursaphelenchus xylophilus*. *Cells* 11: 3208. https://doi.org/10.3390/cells11203208

Mota M.M., Braasch H., Bravo M.A., Penas A.C., Burgermeister W., Sousa E., 1999. First report of *Bursaphelenchus xylophilus* in Portugal and in Europe *Nematology* 1: 727–734. https://doi.org/10.1163/156854199508757

Naves P.M., Sousa E.M., Quartau J.A., 2006. Feeding and oviposition preferences of *Monochamus galloprovincialis* for certain conifers under laboratory conditions. *Entomologia Experimentalis et Applicata* 120: 99–104. https://doi.org/10.1111/j.1570-7458.2006.00430.x

Nickle W.R., 1970. A taxonomic review of the genera of the Aphelenchoidea (Fuchs 1937) Thorne 1949 (Nematoda: Tylenchida). *Journal of Nematology* 2: 375-392.

Nunes da Silva M., Solla A., Sampedro L., Zas R., Vasconcelos M.W., 2015. Susceptibility to the pinewood nematode (PWN) of four pine species involved in potential range expansion across Europe *Tree Physiology* 35: 987–999. https://doi.org/10.1093/treephys/tpv046

Oliveira C.M.G., Eulálio J., Bessi R., Harakava R., 2011. Caracterizações morfológica e molecular de *Bursaphelenchus fungivorus* (Nematoda: Aphelenchida), detectado pela primeira vez no Brasil. *Nematologia Brasileira* 35: 63–70.

Özçankaya I.M., Balay S.N., Bucak C., 2013. Effects of pests and diseases on stone pine (Pinus pinea L.) conelet losses in Kozak catchment area. In: *Mediterranean Stone Pine for Agroforestry* (S. Mutke, M. Piqué, R. Calama, ed), CIHEAM. pp. 29-33.

Paillet Y., Archaux F., Boulanger V., Debaive N., Fuhr N., Gilg O., Gosselin F., Guilbert E., 2017. Snags and large trees drive higher tree microhabitat densities in strict forest reserves. *Forest Ecology and Management* 389: 176-186. https://doi.org/10.1016/j.foreco.2016.12.014

Pajares J.A., Ibea F., Diez J.J., gallego D., 2004. Attractive responses by *Monochamus galloprovincialis* (Col Cerambycidae) to host and bark beetle semiochemicals. *Journal of Applied Entomology* 128: 633–638. https://doi.org/10.1111/j.1439-0418.2004.00899.x

Palmisano A.M., Ambrogioni L., 1994. Aphelenchoidoidea nematodes associated with *Pinus* spp. *Redia* 77: 225-240.

Pedram M., 2017. *Cryptaphelenchus varicaudatus* n. sp. (Rhabditida: Ektaphelenchinae) from Tehran Province, Iran. *Journal of Nematology* 49: 223-230. https://doi.org/10.21307/jofnem-2017-066

Penas A.C., Bravo M.A., Naves P., Bonifácio L., Sousa E., Mota M., 2006. Species of *Bursaphelenchus* Fuchs, 1937 (Nematoda: Parasitaphelenchidae) and other nematode genera associated with insects from *Pinus pinaster* in Portugal. *Annals of Applied Biology* 148: 121-131. https://doi.org/10.1111/j.1744-7348.2006.00042.x

Penas A.C., Bravo M.A., Valadas V., Mota M., 2008. Detailed morphobiometric studies of *Bursaphelenchus xylophilus* and characterisation of other *Bursaphelenchus* species (Nematoda: Parasitaphelenchidae) associated with *Pinus pinaster* in Portugal. *Journal of Nematode Morphology and Systematics* 10: 137–163.

Penas A., Correia P., Bravo M.A., Mota M., Tenreiro R., 2004. Species of *Bursaphelenchus* Fuchs, 1937 (Nematoda: Parasitaphelenchidae) associated with maritime pine in Portugal. *Nematology* 6: 437–453. https://doi.org/10.1163/1568541042360573

Philis J., 1996. An outlook on the association of *Bursaphelenchus leoni* with wilting pines in Cyprus. *Nematologia Mediterranea* 24: 221–225.

Philis J., Braasch H., 1996. Occurrence of *Bursaphelenchus leoni* (Nematoda, Aphelenchoididae) in Cyprus and its extraction from pine wood. *Nematologia Mediterranea* 24*:* 119–123.

Pimentel C., Gonçalves E., Firmino P., Calvão T., Fonseca L., … Máguas C., 2017. Differences in constitutive and inducible defences in pine species determining susceptibility to pinewood nematode *Plant Pathology* 66: 131–139. https://doi.org/10.1111/ppa.12548

Rivers M., Newton A.C., Oldfield S., 2022. Global tree assessment contributors. Scientists' warning to humanity on tree extinctions. *Plants People Planet* 5: 466–482. https://doi.org/10.1002/ppp3.10314

Rodrigues A.M., Mendes M.D., Lima A.S., Barbosa P.M., Ascensão L., … Figueiredo A.C., 2017. *Pinus halepensis*, *Pinus pinaster*, *Pinus pinea* and *Pinus sylvestris* essential oils chemotypes and monoterpene hydrocarbon enantiomers before and after inoculation with the pinewood nematode, *Bursaphelenchus xylophilus*. *Chemistry and Biodiversity* 14: e1600153. https://doi.org/10.1002/cbdv.201600153

Rodrigues A.M., Silva M.N.D., Vasconcelos M., António C., 2024. Metabolomics of *Pinus* spp. in response to pinewood nematode infection. In: *Monitoring Forest Damage With Metabolomics Methods* (C. António, ed.), John Wiley and Sons Inc. pp. 389-419. https://doi.org/10.1002/9781119868750.ch13

Ryss A, Vieira P., Mota M., Kulinich O., 2005. A synopsis of the genus *Bursaphelenchus* Fuchs, 1937 (Aphelenchida: Parasitaphelenchidae) with keys to species. *Nematology* 7: 393–458. https://doi.org/10.1163/156854105774355581

Saitou N., Nei M., 1987. The Neighbor-Joining method – a new method for reconstructing phylogenetic trees.

Molecular Biology and Evolution 4: 406–425. https://doi.org/10.1093/oxfordjournals.molbev.a040454

Sanchez-Husillos E., Alvarez-Baz G., Etxebeste I.A., Pajares A., 2013 Shoot feeding oviposition and development of *Monochamus galloprovincialis* on *Pinus pinea* relative to other pine species. *Entomologia Experimentalis et Applicata* 149: 1–10. https://doi.org/10.1111/eea.12105

San-Miguel-Ayanz J., Rodrigues M., de Oliveira S.S., Pacheco C.J.K., 2012. Land cover change and fire regime in the European Mediterranean region. In: *Post-fire Management and Restoration of Southern European Forests* (F. Moreira, M. Arianoutsou, P. Corona, J. De las Heras, ed), Springer. pp. 83–88.

Santos C.S., Pinheiro M., Silva A.I., Egas C., Vasconcelos M.W., 2012. Searching for resistance genes to *Bursaphelenchus xylophilus* using high throughput screening *BMC Genomics* 13: 599. https://doi.org/10.1186/1471-2164-13-599

Schonfeld U., Braasch H.W., Burgermeister W., 2008. Investigations on wood–inhabiting nematodes of the genus *Bursaphelenchus* in pine forests in the Brandenburg Province, Germany. In: *Pine Wilt Disease: A Worldwide Threat to Forest Ecosystems* (M. Mota, P. Vieira ed), Springer. pp. 69–73.

Silva A.C., Diogo E., Henriques J., Ramos A.P., Sandoval-Denis M., Crous P.W., Bragança H., 2020. *Pestalotiopsis pini* sp. nov., an emerging pathogen on stone pine (*Pinus pinea* L.). *Forests* 11: 805. https://doi.org/10.3390/f11080805

Silva H., Cardoso J.M.S., da Costa R.M.F., Abrantes I., Fonseca L., 2023. *Potensaphelenchus stammeri* (Körner, 1954) Gu, Liu, Abolafia & Pedram, 2021 (Nematoda: Aphelenchoididae) from *Pinus pinea* Linnaeus, 1753 in Portugal. *Forests* 14: 962. https://doi.org/10.3390/f14050962

Silva H., Cardoso J.M.S., da Costa R.M.F., Abrantes I., Fonseca L., 2024. *Bursaphelenchus arthuri* from *Pinus pinea*: first record in Europe and a new host. *Phytopathologia Mediterranea* 63: 385-391.

Slonim O., Bucki P., Mendel Z., Protasov A., Golan O., Vieira P., Braun-Miyara S., 2018. First report on *Bursaphelenchus sexdentati* (Nematoda: Aphelenchoididae) in Israel. *Forest Pathology* 48: e12431. https://doi.org/10.1111/efp.12431

Sousa E., Pimpão M., Valdiviesso T., 2017. Cone pests of s tone pine in the Mediterranean Basin. In: *Mediterranean Pine Nuts From Forests and Plantations* (I. Carrasquinho, A.C. Correia, S. Mutke ed), CIHEAM. pp. 91-107.

Stokes M.A., Smiley T.L., 1996. *An Introduction to Tree-ring Dating*. Tucson: University of Arizona Press.

Stara K., Tsiakiris R., 2019. Oriental planes *Platanus orientalis* L. and other monumental trees in central squares and churchyards in NW Greece: Sacred, emblematic, and threatened. *Acta Horticulturae et Regiotecturae* 22: 14–18. https://doi.org/10.2478/ahr-2019-0003

Stephenson N.L., Das A.J., Condit R., 2014. Rate of tree carbon accumulation increases continuously with tree size *Nature*. 507: 90-93. https://doi.org/10.1038/nature12914

Tamura K., Stecher G., Kumar S., 2021. MEGA 11: Molecular evolutionary genetics analysis version 11. *Molecular Biology and Evolution* 38: 3022–3027. https://doi.org/10.1093/molbev/msab120

Tapias R., Climent J., Pardo J., Gil L., 2004. Life histories of Mediterranean pines. *Plant Ecology* 171: 53–68. https://doi.org/10.1023/B:VEGE.0000029383.72609.f0

Torrini G., Strangi A., Paoli F., Binazzi F., Camerota M., Pennacchio F., Roversi P.F., 2017. A new phoretic association: *Bursaphelenchus minutus* (Nematoda: Parasitaphelenchidae) and *Orthotomicus erosus* (Coleoptera: Scolytidae) recorded on *Pinus pinea* (L.). *Scandinavian Journal of Forest Research* 32: 455–458. https://doi.org/10.1080/02827 581.2016.1254278

Torrini G., Paoli F., Mazza G., 2020a. First detection of *Bursaphelenchus abietinus* and *B. andrassyi* in Italy. *Forest Pathology* 50: e12627. https://doi.org/10.1111/efp.12627

Torrini G, Strangi A, Simoncini S., Luppino M., Roversi P.F., Marianelli L., 2020b. First report of *Bursaphelenchus fungivorus* (Nematoda: Aphelenchida) in Italy and an overview of nematodes associated with *Crocus sativus* L. *Journal of Nematology* 52: 1-11. https://doi.org/10.21307/jofnem-2020-023

Urek G., Širca S., Geri B., 2007. Morphometrical and molecular characterization of *Bursaphelenchus* species from Slovenia. *Helminthologia* 44: 37–42. https://doi.org/10.2478/s11687-007-0001-0

Van Halder I., Sacristan A., Martín-García J., 2022. *Pinus pinea*: a natural barrier for the insect vector of the pine wood nematode? *Annals of Forest Science* 79: 43. https://doi.org/10.1186/s13595-022-01159-3

Viñas A., Caudullo R., Oliveira G., de Rigo D., 2016. *Pinus pinea* in Europe: distribution, habitat, usage and threats. In: *European Atlas of Forest Tree Species* (S.M. Ayanz, D. Rigo, G. Caudullo, ed) Publications Officials of European Union. e01b4fc+.

Vrain T.C., 1993. Restriction Fragment Length Polymorphism separates species of the Xiphinema americanum group. *Journal of Nematology* 25: 361–364.

Whitehead A.G., Hemming R., 1965. A comparison of some quantitative methods of extracting small vermi-

form nematodes from soil. *Annals of Applied Biology* 55: 25–38. https://doi.org/10.1111/j.1744-7348.1965.tb07864.x

Zamora P., Rodríguez V., Renedo F., Sanz A.V., Domínguez J.C., ... Martín A.B., 2015. First report of *Bursaphelenchus xylophilus* causing pine wilt disease on *Pinus radiata* in Spain. *Plant Disease* 99: 1449. https://doi.org/10.1094/PDIS-03-15-0252-PDN

Phytopathologia Mediterranea
The international journal of the
Mediterranean Phytopathological Union

Firenze University Press
www.fupress.com/pm

Research Papers

Alternaria and *Curvularia* leaf spot pathogens show high aggressivity on watermelon, and are emerging pathogens in cucurbit production

Cristina PAREDES-MACHADO[1], Verëlindë BOGAJ[1], Viktor PAPP[2], Gábor BALÁZS[3], David PAPP[1,*]

[1] *Department of Fruit Growing, Institute of Horticulture, Hungarian University of Agriculture and Life Sciences, 2100 Budapest, Hungary*
[2] *Department of Botany, Institute of Agronomy, Hungarian University of Agriculture and Life Sciences, H-1118 Budapest, Hungary*
[3] *Department of Vegetable and Mushroom Growing, Institute of Horticulture, Hungarian University of Agriculture and Life Sciences, 2100 Budapest, Hungary*
*Corresponding author. E-mail: Papp.David@uni-mate.hu

Summary. Fungal leaf spot pathogens of cucurbits cause significant yield losses. They cause extensive leaf necroses and defoliation, reducing host photosynthesis. They increase risks of fruit sunscald, and can cause substantial crop damage. *Alternaria cucumerina* has been recognized as the causal agent of leaf spot disease of cucurbits, and recent studies have identified other *Alternaria* species, and other emerging pathogens such as *Curvularia*. This study characterized 25 isolates obtained from infected watermelon and cucumber leaves from Hungary, Spain, and Kosovo. Morphological characterization and molecular analyses using *TEF1-α, HIS3,* and ITS gene regions identified *Alternaria alternata* and *A. arborescens*, and for the first time on this host, the genus *Curvularia*. Detached leaf assays of ten isolates on 73 watermelon accessions showed variation in isolate pathogenicity. The tested *Curvularia* isolate was the most aggressive, followed by the *A. arborescens* and *A. alternata* isolates, although *A. alternata* was the most frequently identified species. These results highlight the potential for emerging fungal pathogens causing cucurbit leaf spot, such as *Curvularia* sp., and show that these fungi can cause damage on economically important plants. This study also showed differing resistance within the watermelon collection, indicating potential for the plant introduction (PI) accessions as sources of resistance breeding.

Keywords. *Alternaria alternata, Alternaria arborescens*, bar coding, leaf spot, *Citrullus* spp.

OPEN ACCESS

Citation: Paredes-Machado, C., Bogaj, V., Papp, V., Balázs, G. & Papp, D. (2025). *Alternaria* and *Curvularia* leaf spot pathogens show high aggressivity on watermelon, and are emerging pathogens in cucurbit production. *Phytopathologia Mediterranea* 64(1): 41-55. doi: 10.36253/phyto-15955

Accepted: March 11, 2025

Published: May 15, 2025

Data Availability Statement: All relevant data are within the paper and its Supporting Information files.

Competing Interests: The Author(s) declare(s) no conflict of interest.

Editor: Thomas A. Evans, University of Delaware, Newark, DE, United States.

ORCID:
CP-M: 0009-0006-6872-7224
VB: 0009-0005-3611-1241
VP: 0000-0001-6994-8156
GB: 0009-0001-0671-7649
DP: 0009-0002-8370-8604

INTRODUCTION

Watermelon (*Citrullus lanatus*, *Cucurbitaceae*) is an important food crop which has been cultivated for at least 5000 years since domestication in northeastern Africa (Paris, 2015; Chomicki *et al*., 2020). In 2022, world watermelon production was approx. 100 million tons, while the total area of

watermelon cultivation was approx. 2.9 million hectares, highlighting the extensive land use dedicated to this crop (FAO, 2022).

Watermelon plants are susceptible to several important fungal diseases, such as powdery mildew (*Podosphaera xanthii*, *Erysiphe cichoracearum*), downy mildew (*Pseudoperonospora cubensis*), anthracnose (*Colletotrichum orbiculare*), Fusarium wilt (*Fusarium oxysporum*) and gummy stem blight (*Didymella bryoniae*) (Egel *et al*., 2022). Fungal leaf spot of cucurbits has also been a growing concern during the last decade, resulting in significant economic losses for farmers due to reduced yields and increased production costs (Abu-Nasser and Abu-Naser, 2018; Ma *et al*., 2021; Shanthi Avinash *et al*., 2021).

Alternaria cucumerina has been identified as the causal agent of the Alternaria leaf spot of cucurbits, including watermelon (AA.VV., 2021; Kucharek, 1985). In recent decades, new *Alternaria* species have been reported as pathogens of cucurbits, including *A. alternata* f. sp. *cucurbitae* (Vakalounakis, 1990; Zhou and Everts, 2008; Ahmed *et al*., 2021), *A. tenuissima, A. infectoria,* and *A. gaisen* (Kwon *et al*., 2021; Ma *et al*., 2021).

The importance of these pathogens is indicated by *Alternaria* being among the ten most cited pathogenic fungal genera. This diverse genus includes more than 600 species, many of which are major plant pathogens causing leaf spots, blights, rots, and seed infections of a wide range of agricultural plants, including cereals, fruit crops, vegetables, and ornamentals (Bhunjun *et al*., 2022, 2024). New cucurbit host species and outbreaks of *Alternaria* diseases are being reported, highlighting the increasing threats of these pathogens to cucurbit production, especially in regions with extended periods of high humidity (Abu-Nasser and Abu-Naser, 2018; Matić *et al*., 2020; Shanthi Avinash *et al*., 2021). Alongside Alternaria leaf spot, more recent reports have shown that members of the related *Curvularia* genus can also affect cucurbits, including *Trichosanthes dioica* (pointed gourd), *Cucurbita argyrosperma* (kershaw, or silver-seed gourd), and *Cucumis melo* (melon) (Sarkar *et al*., 2018; Ayvar-Serna *et al*., 2022; Vanitha *et al*., 2024).

The *Pleosporaceae* includes 23 genera with *Alternaria* and *Curvularia* as two of the most important genera (Torres-Garcia *et al*., 2022; Hyde *et al*. 2024). *Curvularia* spp. are ubiquitous as pathogens and saprobes of plants, animals, and humans (Sivanesan, 1987; Marin-Felix *et al*., 2017), and many are known as causes of diseases of grasses and staple food crops, including rice, maize, wheat, and sorghum (Khan *et al*., 2023). More than 200 *Curvularia* species are recognized (Hyde *et al*. 2024). *Curvularia* and *Alternaria* have been described as "sister genera" within *Pleosporaceae*, due to their close evolutionary relationship (Bao and Roossinck, 2013). Therefore, they share morphological traits (Torres-Garcia *et al*., 2022), and cause similar symptoms on host plants (Rabaaoui *et al*., 2022), making species identification difficult. Results showing different capabilities of *Alternaria* species to cause disease on a given host have highlighted the importance of accurate species level diagnoses, for plant protection and resistance breeding (Fontaine *et al*., 2021).

Phylogenetic analyses utilizing barcoding markers are important for identification of fungi. In the last decade, *Alternaria* (Peever *et al*., 2004; Woudenberg *et al*., 2015; Dettman and Eggertson, 2021) and *Curvularia* (Manamgoda *et al*., 2012a; 2015; Marin-Felix *et al*., 2020; Connally *et al*., 2022) have undergone substantial taxonomic changes, with reclassification of several species and identification of new species based primarily on molecular genetic analyses. Considerable progress has been made in systematic revision of both genera through multi-locus sequence analyses, particularly using the genetic regions of Internal Transcribed Spacer (ITS), Translation Elongation Factor 1- α *(TEF1-α),* Glyceraldehyde-3-phosphate dehydrogenase *(GAPDH),* RNA polymerase II second largest subunit *(RPB2),* Histone H3 *(HIS3),* Small Subunit ribosomal RNA *(SSU, 18S rRNA),* and Large Subunit ribosomal RNA *(LSU, 28S rRNA)* (Dettman and Eggertson, 2021; Aung *et al*., 2024). Those phylogenetic analyses have often been refined, by using endopolygalacturonase gene *(endoPG)* and two anonymous genome regions (OPA1-3 and OPA2-1), which are suitable for functional studies and species delimitations (Woudenberg *et al*., 2015; Aung *et al*., 2024). Species delimitation within *Alternaria* has challenges, and is often considered to be difficult, emphasizing the need for integrated approaches combining morphological, ecological, and molecular data for species identifications.

Selection of host plants that are tolerant or resistant gene sources for the breeding requires accurate identification of the respective pathogens. Among germplasm collections, plant introductions (PIs, USDA) of watermelon offer a valuable source of genetic diversity for resistance breeding programmes, that contribute to reducing the reliance on fungicides, and can improve fruit quality and yield to increase crop profitability (Grumet *et al*., 2021). Currently, little is known about resistance watermelon towards leaf spot diseases caused by *Alternaria* or *Curvularia* spp.

The present study reports occurrence of a *Curvularia* sp. on watermelon. Furthermore, *A. alternata, A. arborescens,* and *Curvularia* isolates were characterized as causal agents of leaf spot disease in cucurbits, combining

morphological and phylogenetic analyses, and evaluation of their pathogenicity on a diverse collection of watermelon accessions.

MATERIALS AND METHODS

Collection and culturing of fungal isolates

Diseased watermelon and cucumber (*Cucumis sativus*) leaves were collected from plants grown in open fields and greenhouses in Hungary, Spain, and Kosovo, between June and September of 2024. A total of 25 single conidium isolates were obtained from collected leaves. Isolations were carried out according to Venkatesagowda *et al*. (2012), with some modifications. Fungal lesions were cut out from leaves, and were surface-sterilized in 4% sodium hypochlorite solution for 60 sec, then rinsed with distilled water for 10 sec. Leaf fragments were then dried on sterile paper, and placed on Potato Dextrose Agar (PDA) in Petri plates. After 24 h, hyphal tips resembling *Alternaria* sp. were aseptically cut under a stereo microscope, and placed on new PDA plates. From the developing cultures, after 4–5 d, conidia were harvested by mixing a small piece of sporulating mycelium with sterile distilled water containing 0.03% Tween 20, and filtering the suspension through double cheesecloth. Resulting conidium suspensions were then spread on the surface of 1.6% water agar, (and individual conidia were each picked up with a needle and transferred to a new PDA plate. Single conidium isolates were maintained on 25°C, and were subcultured every 10 d.

To obtain conidium suspensions for morphological characterization and for host inoculations, isolates were grown on a calcium carbonate-based sporulation medium as described by Shahin (1979), with sucrose omitted from the medium formulation. Seven-day-old conidia were collected from the surfaces of abundantly-sporulating isolates, by washing with sterile distilled water containing Tween 20, or using the tape touch method for microscope slide preparations (Harris, 2000).

Culture and conidium morphology

Photographs of 1-week-old PDA cultures of the isolates were taken to evaluate culture appearance, including colour according to RAL code system (RAL GmbH), and texture following the description of Nobles (1948). Colony growth rates (cm d^{-1}) were calculated from the age of cultures, and their final colony diameters measured with a vernier caliper.

Conidium length (µm), width (µm), and numbers of conidia in chains or clusters were assessed using a Zeiss Axio Imager A2 (Carl Zeiss Microscopy). Conidium characteristics were measured for at least 20 replicates per species, with isolates selected randomly, using the software ImageJ2 (Rueden *et al*., 2017).

Molecular analyses

To identify species of the collected isolates, their genetic sequences were analysed and a phylogenetic tree was constructed. To extract DNA, mycelia of each monospore isolate grown on PDA were cut and stored at -80 °C. Frozen samples were then ground in a mortar, and DNA was extracted using the E.Z.N.A. plant DNA kit (Norcoss), according to the manufacturer's recommendations. DNA concentrations were verified by staining and running the extracted DNA on 1% agarose gels (BioReagent, Sigma-Aldrich).

Three barcoding markers were used for the amplifications: the Internal Transcribed Spacer (ITS) region was amplified using the primers ITS1-F (5'-TCCGTAGGTGAACCTGCGG-3') and ITS4-R (3'-TCCTCCGCTTATTGATATGC-5') (White, 1990), Histone 3 *(HIS3)*, using HIS3-F (5'-ACTAAGCAGACCGCCGCGAAG-3'), and (HIS3-R (3'-GCGGGCGAGCTGGATGTCCTT-5') (Steenkamp *et al*., 2000), and the Translation Elongation Factor 1-alpha *(TEF1-α)* using TEF1-F (5'-CATCGAGAAGTTCGAGAAGG-3') and TEF1-R (5′-TACTTGAAGGAACCCTTACC-3′) (Wu *et al.,* 2013).

The polymerase chain reaction (PCR) was carried out for DNA samples and a negative control (without DNA), using a Thermal Cycler 2720 PCR machine (Applied Biosystems). The PCR mixture (final volume of 16 µL) was prepared with the DreamTaq Green PCR Master Mix (Fermentas). The PCR program was set according to the specified temperatures, times, and number of cycles as described in Table S1**.** Integrity of amplicons was evaluated by running them on 1% agarose gel (BioReagent, Sigma-Aldrich). Amplicons were sequenced using an ABI 3100 automatic sequencer. All generated sequences were uploaded to GenBank (Table S2).

The quality of the resulting chromatograms was checked using CodonCode Aligner 7.0.1 (CodonCode Corporation). Reference sequences for *Alternaria* and *Curvularia* from the GeneBank database were included in the analyses (Table S2). *HIS3* was only used for Blast analyses. Sequences of ITS and *TEF1-α*, together with sequences of related species downloaded from GenBank, were aligned separately with the online MAFFT v. 7.0, using the L-INS-i strategies (Katoh and Standley, 2013). The alignments were checked and edited by manual adjustment in Multiple sequence alignment, and manual corrections (cutting of low-quality edges, indels) were

achieved using AliView (Larsson, 2014). Maximum Likelihood (ML) analysis was performed using RAxML in raxmlGUI2.0 (Stamatakis, 2014; Edler *et al*., 2021), with 1,000 rapid bootstraps and the GTRGAMMA substitution model. The resulting phylogenetic tree was visualized in MEGA11 (Tamura *et al*., 2021).

Pathogenicity assays

Healthy watermelon leaf samples were collected from an open greenhouse located in Soroksár, Hungary (47°23′49″ N, 19°09′10″ E), containing a collection of 73 watermelon varieties. The collection included 71 plant introduction (PI) accessions from the United States of America, and the commercial *C. lanatus* cultivars 'Black Diamond' and 'Calhoun Grey'. The plant accessions originated from a wide geographic range, including Turkey, Spain, Zimbabwe, Democratic Republic of Congo, Senegal, Iran, Japan, Syria, Ghana, Zambia, South Africa, and the United States of America.

The leaf samples were put between wet sterile tissue for transport to the laboratory. Leaves were then washed gently in 1% sodium hypochlorite solution for 60 sec and immediately placed in sterile water for a further 60 sec. Young undamaged leaf sections (each of 6 mm) were cut with a cork borer and surface water was removed by placing these on sterile paper towels. the leaf sections were then placed adaxial surface upwards on 1% water agar.

Following identification of isolates to genus or species, pathogenicity tests were carried out using six representative isolates from watermelon in Spain, identified as *A. arborescens*, one isolate from watermelon in Hungary, identified as *Curvularia*, and three isolates from watermelon in Hungary, identified as *A. alternata*. These assays were each conducted using a conidium suspension (1×10^6 conidia mL^{-1}, with 5 µL of the suspension applied on each leaf disc. Each plate contained three inoculated leaf discs per plant accession, for biological replicates and one leaf disc mock-inoculated with 5 µL of sterile water. The plates were incubated at 25°C in dark conditions. Relative disease severity (DS) was estimated visually at 5 d post-inoculation (DPI), using a 0 to 9 scale (Singh *et al*., 2020) and an Olympus BX41 stereomicroscope (Olympus Corporation). Development of new conidium chains, hyphae, and the presence of necrotic tissues were considered compatible reactions (Figure S1).

Statistical analyses

Morphological features of conidia were evaluated using the Wilks's lambda MANOVA model to compare the mean lengths, widths, and conidium counts per chain, among the different species. This model had the assumptions of homogeneity of covariance matrices, multivariate normality, and homogeneous variances. Assumption of homogeneity of covariance matrices was tested by Box's M-test and multivariate normality with the Shapiro-Wilk test, while homogeneity of variances was tested using Bartlett's test. MANOVA was carried out with Wilk's Lambda test. After identifying statistically significant overall differences among species using Wilks' Lambda ($P < 0.05$), pairwise comparisons between species were subsequently made using estimated marginal means based on the fitted multivariate linear model. *P*-values were adjusted using the Bonferroni correction for multiple comparisons.

A Principal Component Analysis (PCA) was conducted on five morphological traits related for each culture (growth rate, appearance) and conidia (length, width, number per chain or cluster). Principal Components (PC) were computed, and proportion of variance explained by each function was assessed to determine their contributions to species discrimination. To visualize the relationship between the main two PC across species, a two dimension scatterplot was created.

For pathogenicity assessments, Disease Index (DI) was calculated from DS values using the formula described by Singh *et al*. (2020). A one-way ANOVA model was carried out to compare mean Disease Index (DI) across the different fungal species. This model had assumptions of independent samples, non-homogeneous variances, and normally distributed residuals. Normality was checked using the d'Agostino test, and graphically by histogram and QQ-plot, while homogeneity of variances was tested using Levene's test. Pairwise comparisons were calculated by the Games-Howell *post hoc* test. All statistical tests used were two-sided, and the significance level was set at $\alpha = 0.05$. All statistical analyses and visualizations were carried out using the software R (Version 4.4.1. R Foundation for Statistical Computing).

RESULTS

Based on morphology and genetic barcoding, three species of fungi were isolated from watermelon leaf spots from the sampled plant material (Table 1).

Morphology of isolates

The morphological analyses showed variations in culture colour and texture between the studied species (Table 2). *Alternaria alternata* isolates had colony colours

Table 1. Locations and host species for fungal isolates (n = 25) collected from cucurbit leaf spots.

Isolate species	Isolate code	Location of origin	Host species
Alternaria arborescens	cc_1[1]	Spain (La Puebla)	*Citrullus lanatus*
Alternaria arborescens	cc_2	Spain (La Puebla)	*Citrullus lanatus*
Alternaria alternata	cc_3[1]	Spain (La Puebla)	*Citrullus lanatus*
Alternaria arborescens	cc_4[1]	Spain (La Puebla)	*Citrullus lanatus*
Alternaria alternata	cc_6	Spain (La Puebla)	*Citrullus lanatus*
Alternaria alternata	cc_7[1]	Spain (La Puebla)	*Citrullus lanatus*
Alternaria arborescens	cc_8[1]	Spain (La Puebla)	*Citrullus lanatus*
Alternaria arborescens	cc_9	Spain (La Puebla)	*Citrullus lanatus*
Alternaria arborescens	cc_10	Spain (La Puebla)	*Citrullus lanatus*
Alternaria alternata	cc_11	Hungary (Buda)	*Cucumis sativus*
Alternaria alternata	cc_12	Hungary (Polgár)	*Cucumis sativus*
Alternaria alternata	cc_13	Hungary (Polgár)	*Cucumis sativus*
Alternaria alternata	cc_14	Hungary (Polgár)	*Cucumis sativus*
Alternaria alternata	cc_15	Hungary (Polgár)	*Cucumis sativus*
Alternaria alternata	cc_16	Hungary (Polgár)	*Cucumis sativus*
Alternaria alternata	cc_17	Hungary (Polgár)	*Cucumis sativus*
Alternaria alternata	cc_20	Hungary (Soroksár)	*Citrullus lanatus*
Alternaria alternata	cc_21	Hungary (Soroksár)	*Citrullus lanatus*
Curvularia sp.	cc_22[1]	Hungary (Soroksár)	*Citrullus lanatus*
Curvularia sp.	cc_24	Hungary (Soroksár)	*Citrullus lanatus*
Alternaria alternata	cc_25	Hungary (Soroksár)	*Citrullus lanatus*
Alternaria alternata	cc_36	Kosovo (Drenas)	*Citrullus lanatus*
Alternaria alternata	cc_41[1]	Hungary (Ócsa)	*Citrullus lanatus*
Alternaria alternata	cc_42[1]	Hungary (Ócsa)	*Citrullus lanatus*
Alternaria alternata	cc_45[1]	Hungary (Jászszentandrás)	*Citrullus lanatus*

[1] Isolates used for leaf disc assays.

Table 2. Culture and conidium morphologies of *Alternaria* and *Curvularia* species.

Species	Texture[a]	RAL colour[b]	Mean growth rate (cm d^{-1})	Mean conidium length (µm)	Mean conidium width (µm)	Number of conidia
Alternaria alternata	Cottony	RAL 7013	1.14 ± 0.10	23.51 ± 3.55	9.76 ± 1.59	7[1]
Alternaria arborescens	Cottony	RAL 7002	1.21 ± 0.04	21.83 ± 2.92	9.59 ± 1.16	5[1]
Curvularia sp.	Velvety	RAL 8000	1.23 ± 0.07	28.03 ± 3.57	8.99 ± 1.12	8[2]

[a] Predominant texture among the studied strains.
[b] Predominant RAL colour among the studied strains.
[1] Mean number (± standard deviation) of conidia per chain.
[2] Mean number (± standard deviation) of conidia per cluster.

ranging from grey to black, with cottony textures, and generally smooth regular margins. The *A. arborescens* isolates had colony colours of various tones of grey, with a predominantly cottony appearance, and regular and irregular colony margins. Colonies of *Curvularia* isolates were green-brown in colour, of velvety texture, and had smooth margins. Differences between *A. alternata*, *A. arborescens*, and *Curvularia* sp. were further quantified based on conidium features.

Alternaria alternata and *A. arborescens* had dark-coloured conidia, that were multicellular, ovoid or obclavate, and with short conical or cylindrical beaks. The average conidium dimensions of *A. alternata* were 23.5 ± 3.6 µm × 9.8 ± 1.6 µm, while those of *A. arborescens* were 21.8 ± 2.9 µm × 9.6 ± 1.2 µm. Conidia were produced in chains on conidiophores. The *Curvularia* sp. conidia were dark, ellipsoid, and each had three transverse septa. The average conidium dimensions of

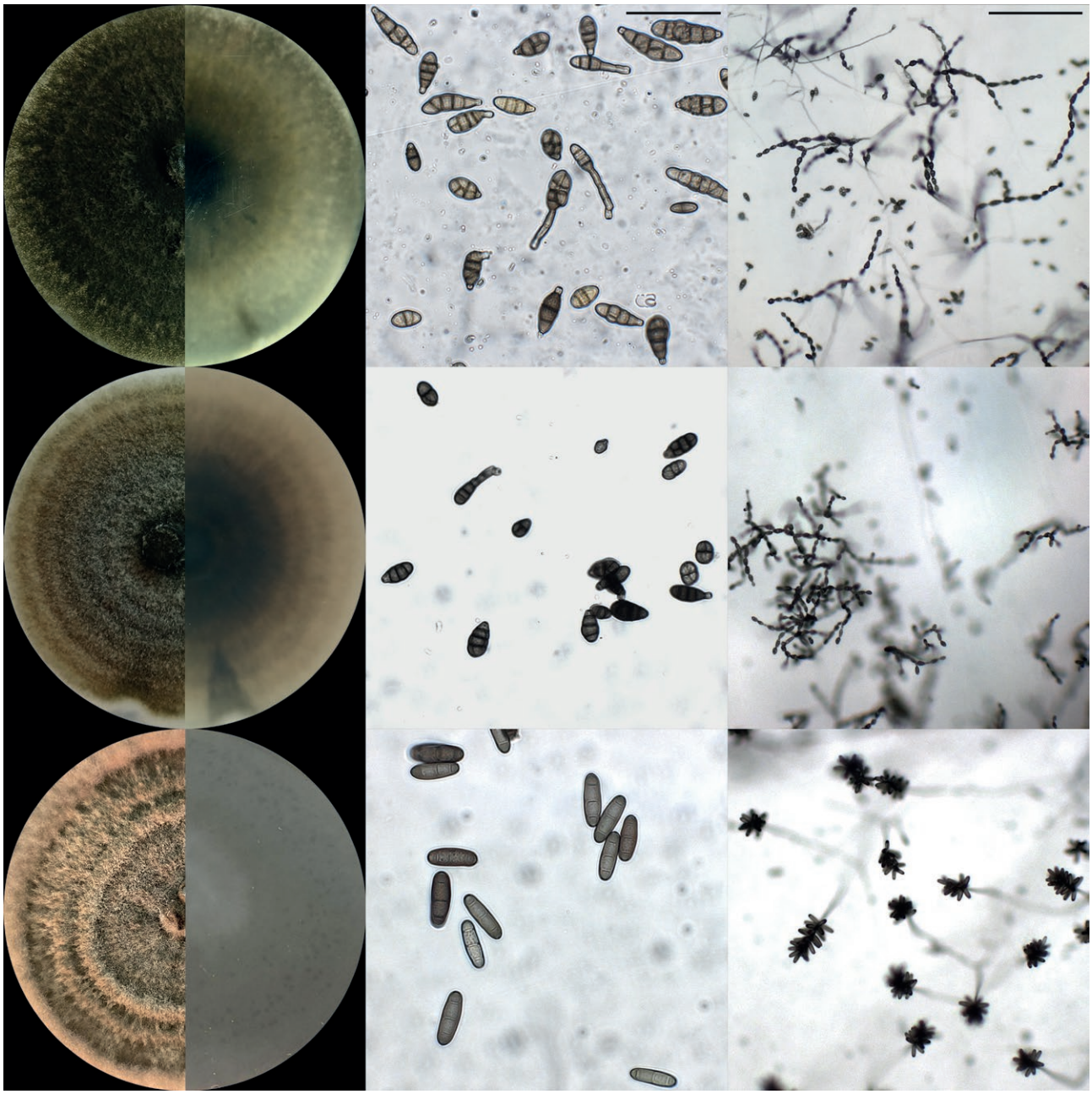

Figure 1. Cultures (left), conidia (middle), and conidium chains or clusters (right) of *Alternaria alternata* (upper images), *Alternaria arborescens* (middle), and *Curvularia* sp. (lower). Culture plates (right) were 9 cm diam. Scale bars = 50 μm (left) or 200 μm (right).

Curvularia sp. were 28.0 ± 3.6 μm × 9.0 ± 1.1 μm. These conidia developed close together in chains, appearing as clusters (Figure 1).

Evaluation of morphological traits of conidia using MANOVA Wilk's Lambda test showed statistically significant differences in mean lengths, widths, and numbers of conidia per chain across the three fungal species (Wilks' $F(6,168) = 14.60$; $P < 0.0001$). Pairwise comparisons using estimated marginal means, based on the multilinear model, showed significant differences in length, width, and number of conidia per chain between all pairs *Curvularia* sp. and *A. alternata* ($P < 0.01$), *Curvularia* sp. and *A. arborescens* ($P < 0.0001$), and *A. alternata* and *A. arborescens* ($P < 0.001$).

Morphological variations among the three species, *A. alternata*, *A. arborescens*, and *Curvularia* sp., based on

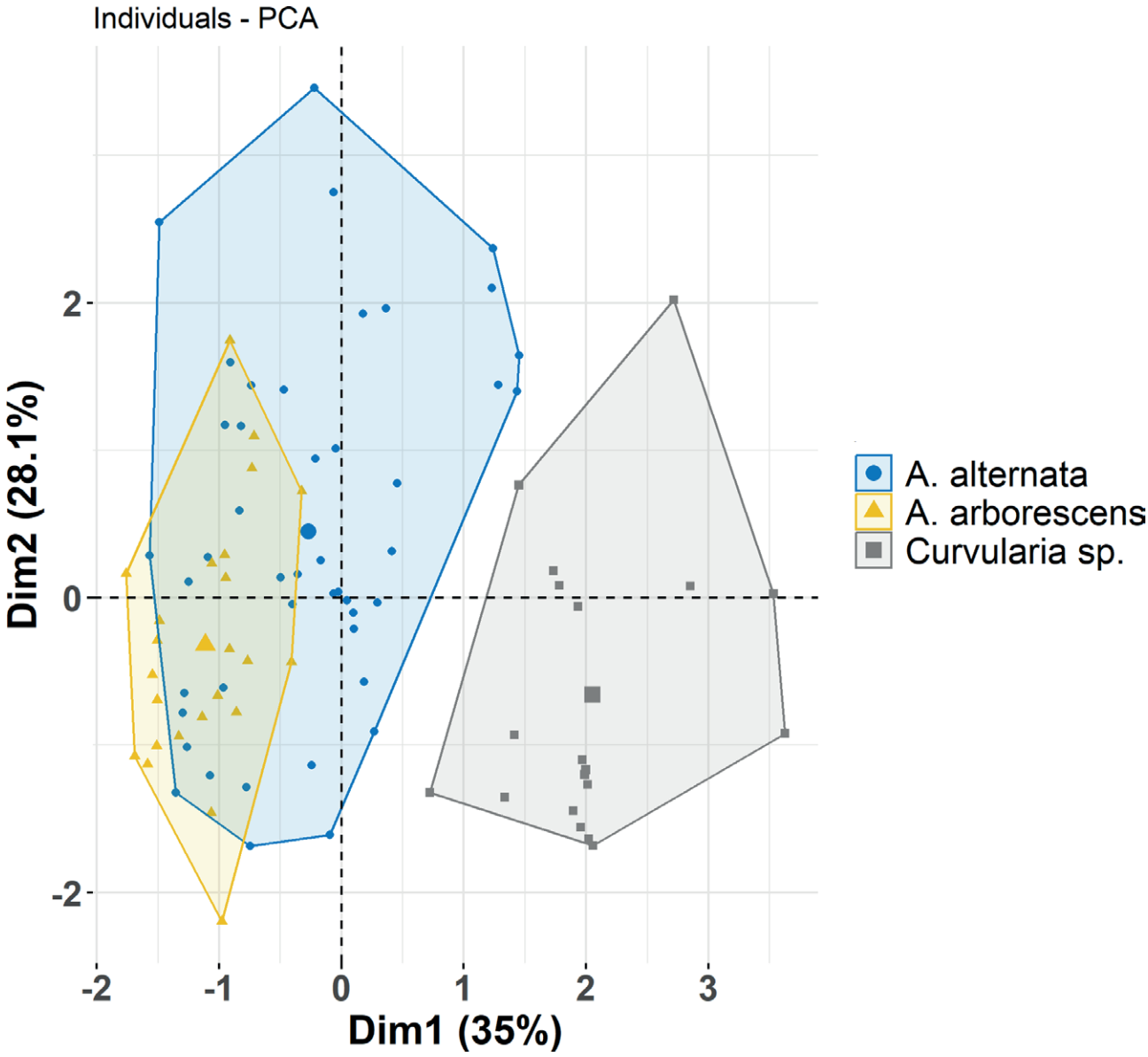

Figure 2. Principal component analyses of fungal isolates (n =25) obtained in this study, based on their morphological traits (colony growth rate, texture, conidium length, conidium width, and numbers of conidia per chain or cluster). The percentage of explained variability of the first two principal components (Dim 1 and Dim 2) is indicated in the parentheses.

the first two principal components (35.0% Dim. 1 and 28.1% Dim.2) are shown in Figure 2. *Curvularia* sp. was clearly distinct from the other two species, forming a separate cluster along the first principal component. In contrast, *A. alternata* and *A. arborescens* had overlapping clusters, indicating some morphological similarities and shared traits. Also, *A. alternata* had greater variability across both dimensions, reflecting high morphological diversity, while *A. arborescens* had a narrow cluster that indicated less variability within the species.

Phylogenetic analyses of fungal isolates

The phylogenetic analyses based on ITS sequences placed the studied isolates into two well-supported and clearly differentiated clades (Figure 3). Isolates cc_22 and cc_24 clustered with the type strains of *Curvularia buchloes, C. hawaiiensis, C. rouhanii,* and *C. spicifera.* BLAST analysis of *TEF1-α* sequences from the Hungarian *Curvularia* isolates (cc_24 and cc_24) identified the closest match with a *C. hawaiiensis* strain (GenBank no.

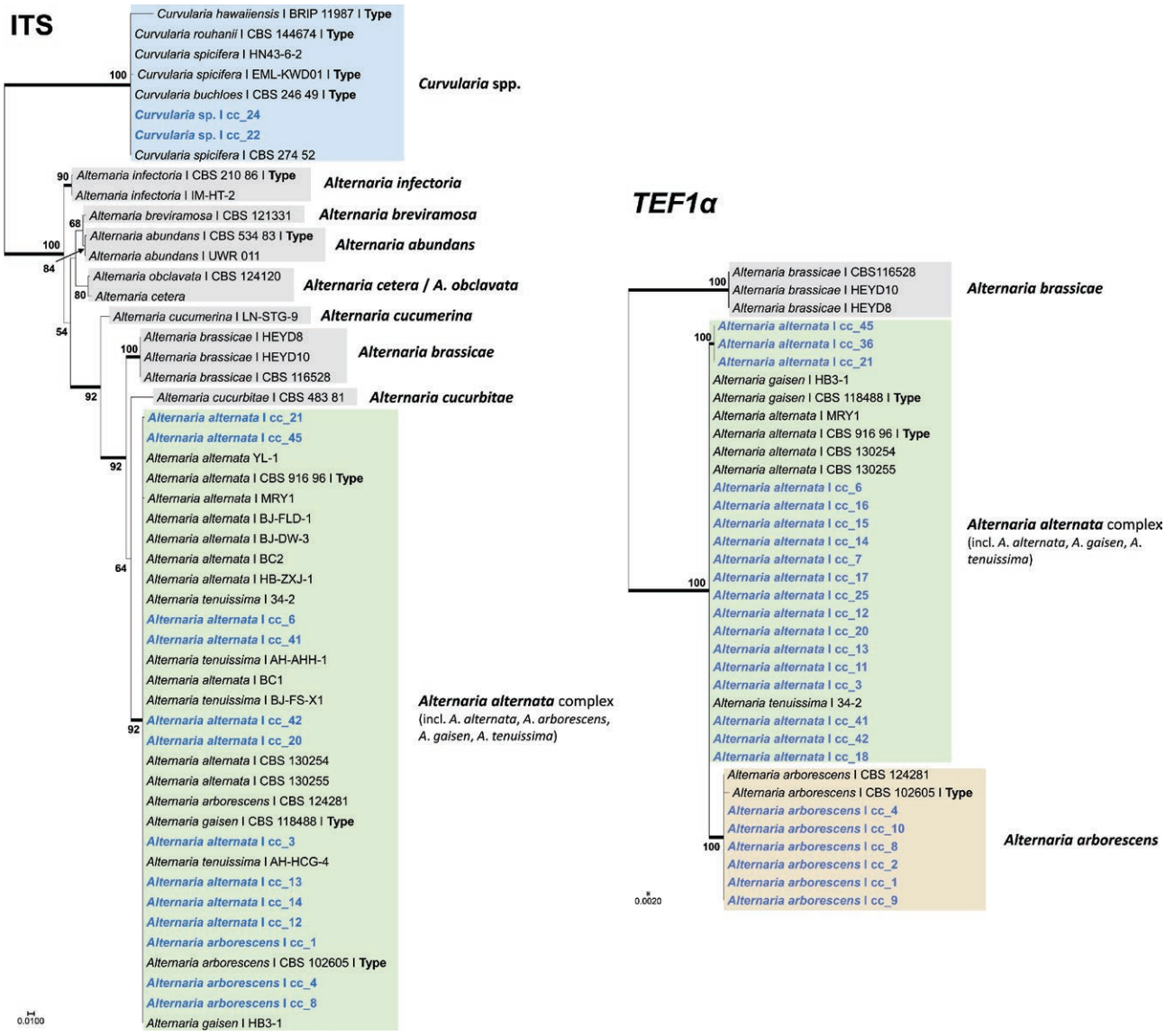

Figure 3. Internal Transcribed Spacer (ITS; left) and Translation elongation factor 1-α (*TEF1-α*; right) phylogenies of *Alternaria* and *Curvularia* isolates obtained in this study. Coloured boxes indicate different taxonomic groups. The obtained isolates are highlighted by blue font, and numbers on branches indicate bootstrap probabilities.

OR841149.1), showing 96% sequence similarity. In contrast, no relevant *Curvularia* sequences for *HIS3* were available in GenBank. Consequently, the Hungarian *Curvularia* isolates (cc_22 and cc_24) were reliably identified only to genus level.

In addition to the two *Curvularia* isolates, all the other isolates examined in this study were classified within the *Alternaria alternata* species complex, based on ITS sequence analysis (Figure 3). To achieve more precise species-level identifications within the complex, *TEF* sequence analysis was conducted. Six isolates (cc_1, cc_2, cc_4, cc_8, cc_9, and cc_10) formed a strongly supported clade (ML = 100%) with the type strain of *A. arborescens*, clearly separating them from other members of the *A. alternata* species complex (Figure 3). To further differentiate *A. alternata* s. str. from *A. tenuissima*, *HIS3* sequences were also analysed. However, none of the examined isolates showed sequence identity with *A. tenuissima*, indicating their affiliation with *A. alternata* s. str.

For species frequencies, 68% of the isolates were identified as *A. alternata*, 24% as *A. arborescens*, and 8% as *Curvularia* sp. The majority of *A. alternata* isolates were obtained from Hungary (77%), with smaller proportions from Spain (18%) and Kosovo (6%). In contrast,

A. arborescens isolates were all (100%) collected in Spain, and *Curvularia* sp. isolates were all (100%) collected in Hungary.

Pathogenicity assays

Leaf disc assays showed variations in host resistance to the pathogens, expressed by the disease index (DI) for the 73 different plant accessions and the ten fungal isolates (Figure 4). A one-way ANOVA showed differences in mean DI between the investigated groups of fungal species ($F(2,77.22) = 521.7$; $P < 0.0001$). According to Welch's ANOVA *post hoc* test, DI evaluated upon infection by *A. alternata*, *Curvularia* sp., and *A. arborescens* differed between all species ($P < 0.0001$). *Curvularia* sp. was the most aggressive with a meanDI of 63.69±26.0, followed by *A. arborescens* 50.75±26.04, and the least severe infection was caused by *A. alternata* 42.59±20.89 (Figure S2).

To focus on the pathogenicity of *Alternaria* and *Curvularia* species, and to draw conclusions about their aggressiveness to two reference cultivars with practical relevance, statistical analyses were narrowed to evaluate pathogenicity of *Alternaria* and *Curvularia* species using 'Calhoun Grey' and 'Black Diamond' as reference host cultivars. There was a statistically significant difference in mean DI between fungal species ($F(2,5.5) = 21.368$; $P < 0.01$). The Games- Howell *post hoc* test showed that *Curvularia* sp. (DI = 59.3 ± 6.4) and *A. arborescens* (DI 59.3 ± 26.1) were both more aggressive to watermelon than *A. alternata* (DI 33.3 ± 6.6) ($P < 0.05$). For 'Black Diamond', no statistically significant differences ($P > 0.05$) in mean DI were observed among the three fungal species. However, a consistent pattern was observed, with *Curvularia* sp. giving the greatest mean disease index (DI = 51.9, ± 12.8), followed by *A. arborescens* (DI = 46.9±16.4), and *A. alternata* (DI = 46.3 ± 16.7). Resistant plant accessions were identified with lower DI values than their commercial counterparts.

Based on the lowest recorded mean DI, which falls within the first quartile of the assessed plant accessions, the most resistant watermelon PIs were identified with a mean DI of 37.3 ± 2.9. These included accession PI512398 (from Spain), PI271775 (South Africa), PI512388 (Spain), PI167125 (Turkey), PI512346 (Spain), PI512350 (Spain), PI167059 (Turkey), PI482283 (Zimbabwe), PI512400 (Spain), PI175657 (Turkey), PI165002 (Turkey), PI167219 (Turkey), PI512401 (Spain), PI512383 (Spain), PI169292 (Turkey), PI169294 (Turkey), and accession PI512397 (from Spain).

No statistically significant differences ($P > 0.05$) in mean DIs were detected across the plant accessions orig-

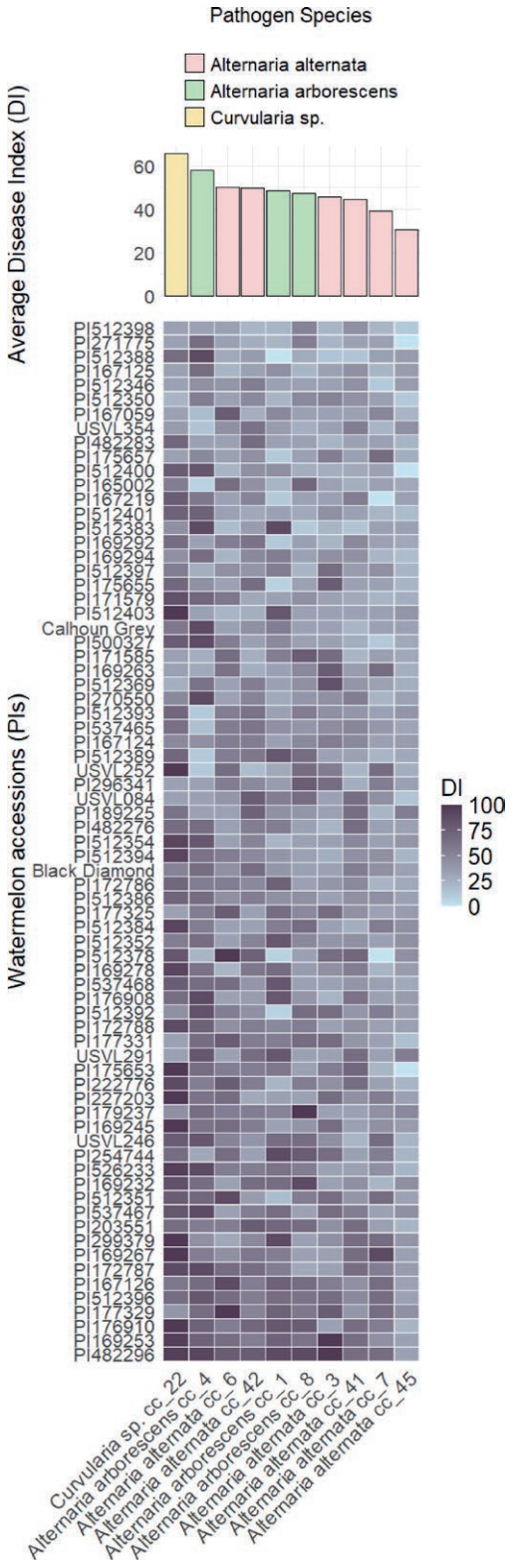

Figure 4. Mean Disease Indices (DIs) on leaf discs after inoculations of 73 watermelon accessions with *Curvularia* and *Alternaria* isolates (histogram), and heatmap of DI distribution across the watermelon accessions.

inating from different countries , indicating that country of origin did not affect resistance to leaf spots caused by *Alternaria* and *Curvularia* isolates among the studied watermelon collection.

DISCUSSION

Fungal leaf spot diseases pose increasing threats to cucurbit production (Abu-Nasser and Abu-Naser, 2018; Ma *et al*., 2021; Shanthi Avinash *et al*., 2021). Theses diseases cause premature losses of green leaf area through necroses and defoliation, as the infections progress, reducing photosynthetic rates, increasing fruit susceptibility to sunscald, and ultimately leading to important yield losses (Singh *et al.,* 2011; Kaniyassery *et al.,* 2024). Identifying the causal agents of these diseases is often challenging, as it requires distinction between closely related pathogen taxa that cause similar host symptoms and share similar morphological features (Rabaaoui *et al*., 2022; Torres-Garcia *et al*., 2022). Consequently, understanding the differences in pathogenicity among these fungi has been limited. The present study aimed to evaluate the morphology, genetic backgrounds, and pathogenicity of *Alternaria* and *Curvularia* species associated with leaf spot diseases in cucurbits collected from different geographical regions during 2024.

The most frequently isolated fungal leaf spot pathogen from infected leaves in the sampled locations was *A. alternata*, followed by *A. arborescens*, and *Curvularia* sp. The majority of *A. alternata* isolates were obtained from Hungary, while most *A. arborescens* isolates were collected from Spain, and *Curvularia* sp. isolates were exclusively from Hungary. Detection of *Curvularia* sp. in Hungary is notable since this is the first report of *Curvularia* sp. as a causal agent of fungal leaf spot on watermelon.

In the last decade, there have been few reports of *Curvularia* species affecting the cucurbits pointed gourd (Sarkar *et al*., 2018), kershaw (Ayvar-Serna *et al*., 2022), and melon (Vanitha *et al*., 2024). This limited number of reports suggests that the impacts of *Curvularia* on cucurbits may not be widespread, or may not have been consistently studied. In the present study, the observed symptoms of leaf spot diseases caused by *Curvularia* sp. on watermelon were similar to those described by Ayvar-Serna *et al*. (2022) and Sarkar *et al*. (2018), rather than blight symptoms reported by Vanitha *et al*. (2024).

The general morphological description of *Curvularia* sp. in the present study fits with other descriptions, for culture appearance and conidium size, septum number, and shape, and colony growth pattern (Ayoubi *et al*., 2017; Cui *et al*., 2020; Garganese *et al*., 2015). *Curvularia* species have been previously described considering only morphology, including conidium hila, septa, ontogeny, and wall structure, as well as culture colony appearance (Sivanesan, 1987). More recent studies have documented *Curvularia* spp. features including colony growth rates and conidium size and shape, which can depend on the culture conditions (dos Santos *et al*., 2018; Sun *et al*., 2003), which might lead to inaccurate pathogen identification. In the present study, species identification based on morphological characterization was challenging. To overcome these limitations multi-locus sequence analyses targeting ITS, *TEF1-α, GAPDH, RPB2, HIS3, SSU, LSU, endoPG,* OPA1-3, and OPA2-1 have been recommended (Dettman and Eggertson, 2021; Woudenberg *et al*., 2015; Aung *et al*., 2024). ITS, as the main barcoding marker for fungi, has been frequently employed for identifying *Curvularia* species (Ayoubi *et al*., 2017). However, recent studies have highlighted limitations in the use of ITS for species-level identification within *Pleosporales* (Bhunjun *et al*., 2020), suggesting the need for additional markers for more accurate delimitation of *Curvularia* species. Therefore, both *HIS3* and *TEF1-α* were included in the present study, based on previous research indicating their suitability to delineate *Curvularia* species (Manamgoda *et al*., 2011; 2012a; 2012b; 2015). However, in the present case, the two barcoding markers were not sufficient to determine the species identity of the isolates. BLAST results for ITS suggested *C. hawaiensis*, while *TEF1-α* suggested *C. spicifera* as the species, but with low support for both species. To confirm this identification or to describe our isolates as a new species, multilocus sequencing is recommended.

During sampling in Soroksár, Hungary, morphologically similar symptoms caused by *Curvularia* sp. and *Alternaria* spp. were observed co-occurring on the same leaves, raising the possibility that *Curvularia* may cause opportunistic infections. Recent studies have also reported the occurrence of *Curvularia* spp. along with other fungal pathogens suggesting that *Curvularia* spp. may be secondary pathogens infecting stressed plants, especially under environmental conditions of high temperatures and poor water quality (Katushova *et al*., 2021; Bessadat *et al*., 2023).

The present study fulfilled Koch's postulates for *Curvularia* as a pathogen of watermelon, using assays with 'Black Diamond' leaf disk, indicating pathogenicity. Furthermore, pathogenicity assessments were carried out for 73 watermelon accessions originating from 12 different countries. These assays showed statistically significant differences in DIs among the studied fungi, with *Curvularia* sp. having greatest pathogenicity, followed by *A. arborescens*, and *A. alternata* being the least pathogenic.

Several new host species has been recently reported for *Curvularia* spp. causing leaf blight and leaf spot diseases, many of which are important crops including sorghum (Akram *et al*., 2014), strawberry (Ayoubi *et al*., 2017), Chinese fir (Cui *et al*., 2020), maize (Garcia-Aroca *et al*., 2018; Manzar *et al*., 2024), citrus (Garganese *et al*., 2015), tomato (Huang *et al*., 2023), coffee (Nam *et al*., 2024), lettuce (Pornsuriya *et al*., 2018), rice (Majeed *et al*., 2015; Ren *et al*., 2022), vetiver (Sari *et al*., 2023), and dates (Rabaaoui *et al*., 2022). Previous reports have reported that within *Pleosporaceae,* the pathogenicity profiles and host ranges often depend on the production of host-specific toxins (HSTs) and non-host-specific toxins (nHSTs) (Akimitsu *et al*., 2014; Gao *et al*., 2014; Meena *et al*., 2017). *Alternaria* isolates produce several nHSTs, and low molecular weight HSTs that have host specificity. In contrast, *Curvularia* isolates have only been associated with nHSTs, which affect broader ranges of hosts (Meena *et al*., 2017; Rabaaoui *et al*., 2022). Understanding these differences will provide insights into the pathogenicity mechanisms and host-pathogen interactions of these fungi.

The present study results highlight the different host resistances within watermelon germplasm accessions, which could be utilized to select promising PI accessions, such as the Spanish PI512398, PI512350, and PI512388 which showed greater resistance than other accessions to *Alternaria* and *Curvularia*. The accession PI512398 has been used as a source of resistance to gummy stem blight (caused by *Stagonosporopsis cucurbitacearum*), so could be utilized as having multiple disease resistance (Gusmini *et al*., 2005; Rivera-Burgos *et al*., 2021). Additionally, during field sampling in the present study, PI512350 and PI512388 (both from Spain) were strongly tolerant to gummy stem blight under greenhouse conditions in Hungary (unpublished data, 2024). This suggests that some watermelon accessions classified as resistant in the present study may also possess resistance to a broader range of pathogens.

CONCLUSIONS

This study investigated morphology, phylogeny, and pathogenicity of *Alternaria* and *Curvularia* isolates associated with fungal leaf spots of cucurbits. *Alternaria alternata* occurred most frequently in the sampled locations, but was less aggressive in leaf disc assays with a diverse watermelon collection than the other fungi assessed. In contrast, only a relatively low number of *Curvularia* sp. isolates were detected, but the assessed isolate was the most aggressive in the leaf disc assays. This study is the first report of *Curvularia* sp. as a causal agent of fungal leaf spot disease on watermelon. This highlights the importance of considering species diversity and pathogenicity when managing leaf spot diseases of cucurbits. The present study also identified promising watermelon germplasm accessions among the plant material studied, that had resistance against *Alternaria* and *Curvularia* pathogens. Therefore, future research should focus on screening the watermelon germplasm collection under controlled and field conditions, and to further select resistant plant accessions. This knowledge will aid development of sustainable management strategies aimed at protecting cucurbit production from these emerging pathogens.

ACKNOWLEDGMENTS

Dr Maxim Byatets and Jeszenszky Szilvia, of the Watermelon Breeding Team, Syngenta Research Station, Ócsa, Hungary, donated samples and plant material, and strongly supported this research. Their expertise and guidance were instrumental in completion of this study.

AUTHOR CONTRIBUTIONS

C.P.; writing (original draft), visualization, validation, software, methodology, investigation, formal analysis, data curation, and conceptualization; V.P.; software, investigation, and formal analysis; V.B.; methodology, investigation; G.B.; methodology, resources, D.P.; supervision, writing, visualization, validation, software, methodology, investigation, formal analysis, data curation, conceptualization, resources, project administration, and funding acquisition. All the authors have read and agreed to the published version of the manuscript.

LITERATURE CITED

Abu-Nasser B. S., Abu-Naser S. S., 2018. Rule-Based System for Watermelon Diseases and Treatment. *International Journal of Academic Information Systems Research* 2(7): 1–7. https://hal.science/hal-01855441

Ahmed M. Z., Saeed S., Hassan A., Ghuffar S., Abdullah A., … Shafique M. S., 2021. *Alternaria alternata* causing Alternaria Leaf Spot of *Cucumis melo* (Muskmelon) in Pakistan. *Plant Disease* 105(6): 1853. https://doi.org/10.1094/PDIS-05-20-0973-PDN

Akimitsu K., Tsuge T., Kodama M., Yamamoto M., Otani H., 2014. *Alternaria* host-selective toxins: Determi-

nant factors of plant disease. *Journal of General Plant Pathology* 80(2): 109–122. https://doi.org/10.1007/S10327-013-0498-7

Akram W., Anjum T., Ahmad A., Moeen R., 2014. First Report of *Curvularia lunata* Causing Leaf Spots on *Sorghum bicolor* from Pakistan. *Plant Disease* 98(7): 1007. https://doi.org/10.1094/PDIS-12-13-1291-PDN

Aung S. L. L., Liu F. Y., Gou Y. N., Nwe Z. M., Yu Z. H., Deng J. X., 2024. Morphological and phylogenetic analyses reveal two new *Alternaria* species (Pleosporales, *Pleosporaceae)* in *Alternaria* section from *Cucurbitaceae* plants in China. *MycoKeys* 107: 125–139. https://doi.org/10.3897/MYCOKEYS.107.124814

Ayoubi N., Soleimani M. J., Zare R., Zafari D., 2017. First report of *Curvularia inaequalis* and *C. spicifera* causing leaf blight and fruit rot of strawberry in Iran. *Nova Hedwigia* 105(1–2): 75–85. https://doi.org/10.1127/nova_hedwigia/2017/0402

Ayvar-Serna S., Díaz-Nájera J. F., Vargas-Hernández M., Mena-Bahena A., Mora-Romero G. A., Leyva-Madrigal K. Y., Tovar-Pedraza J. M., 2022. *Curvularia brachyspora* causing leaf spot on *Cucurbita argyrosperma* in Mexico. *Journal of General Plant Pathology* 88(5): 331–335. https://doi.org/10.1007/S10327-022-01078-1

Bao X., Roossinck M. J., 2013. Multiplexed Interactions: Viruses of Endophytic Fungi. *Advances in Virus Research* 86: 37–58. https://doi.org/10.1016/B978-0-12-394315-6.00002-7

Bessadat N., Hamon B., Bataillé-Simoneau N., Hamini-Kadar N., Kihal M., Simoneau P., 2023. Identification and characterization of fungi associated with leaf spot/blight and melting-out of turfgrass in Algeria. *Phytopathologia Mediterranea* 62(1): 73–93. https://doi.org/10.36253/PHYTO-14169

Bhunjun C. S., Dong Y., Jayawardena R. S., Jeewon R., Phukhamsakda C., … Sheng J. (2020). A polyphasic approach to delineate species in *Bipolaris. Fungal Diversity* 102(1): 225–256. https://doi.org/10.1007/S13225-020-00446-6

Bhunjun C. S., Niskanen T., Suwannarach N., Wannathes N., Chen Y. J., … Lumyong S., 2022. The numbers of fungi: are the most speciose genera truly diverse? *Fungal Diversity* 114(1): 387–462. https://doi.org/10.1007/S13225-022-00501-4

Bhunjun C. S., Chen Y. J., Phukhamsakda C., Boekhout T., Groenewald J. Z., … Crous P. W., 2024. What are the 100 most cited fungal genera? *Studies in Mycology* 108: 1–411. https://doi.org/10.3114/sim.2024.108.01

Chomicki G., Schaefer H., Renner S. S., 2020. Origin and domestication of Cucurbitaceae crops: insights from phylogenies, genomics and archaeology. *New Phytologist* 226(5): 1240–1255. https://doi.org/10.1111/nph.16015

Connally A., Smith D., Marek S., Wu Y., Walker N., 2022. Phylogenetic evaluation of *Bipolaris* and *Curvularia* species collected from turfgrasses. *International Turfgrass Society Research Journal* 14(1): 916–930. https://doi.org/10.1002/ITS2.16

Cui W. L., Lu X. Q., Bian J. Y., Qi X. L., Li D. W., Huang L., 2020. *Curvularia spicifera* and *Curvularia muehlenbeckiae* causing leaf blight on *Cunninghamia lanceolata. Plant Pathology* 69(6): 1139–1147. https://doi.org/10.1111/PPA.13198

Dettman J. R., Eggertson Q., 2021. Phylogenomic analyses of *Alternaria* section *Alternaria:* A high-resolution, genome-wide study of lineage sorting and gene tree discordance. *Mycologia* 113(6): 1218–1232. https://doi.org/10.1080/00275514.2021.1950456

dos Santos P. R. R., Leão E. U., Aguiar R. W. de S., de Melo M. P., dos Santos G. R., 2018. Morphological and molecular characterization of *Curvularia lunata* pathogenic to andropogon grass. *Bragantia* 77(2): 326–332. https://doi.org/10.1590/1678-4499.2017258

Edler D., Klein J., Antonelli A., Silvestro D., 2021. RaxmlGUI 2.0: A graphical interface and toolkit for phylogenetic analyses using RAxML. *Methods in Ecology and Evolution* 12: 373–377. https://doi.org/10.1111/2041-210X.13512

Egel D. S., Adkins S. T., Wintermantel W. M., Keinath A. P., D'Arcangelo K. N., … Quesada-Ocampo L. M., 2022. Diseases of Cucumbers, Melons, Pumpkins, Squash, and Watermelons. In: *Handbook of Vegetable and Herb Diseases. Handbook of Plant Disease Management* (W. H. Elmer, M. McGrath, R. J. McGovern ed.), Springer, Cham, 1–105. https://doi.org/10.1007/978-3-030-35512-8_33-1

AA.VV., 2021. Alternaria leaf blight. Available at: http://ephytia.inra.fr/en/C/7941/Melon-Alternaria-cucumerina

FAOSTAT, 2022. FAOSTAT: Crops and livestock products. Available at: https://www.fao.org/faostat/en/#data/QCL. Accessed January 30, 2025.

Fontaine K., Fourrier-Jeandel C., Armitage A., Boutigny A. L., Crépet M., … Aguayo J., 2021. Identification and pathogenicity of *Alternaria* species associated with leaf blotch disease and premature defoliation in French apple orchards. *PeerJ* 9: e12496. https://doi.org/10.7717/PEERJ.12496

Gao S., Li Y., Gao J., Suo Y., Fu K., Li Y., Chen J., 2014. Genome sequence and virulence variation-related transcriptome profiles of *Curvularia lunata*, an important maize pathogenic fungus. *BMC Genomics* 15(1): 1–18. https://doi.org/10.1186/1471-2164-15-627

Garcia-Aroca T., Doyle V., Singh R., Price T., Collins K., 2018. First report of Curvularia leaf spot of corn, caused by *Curvularia lunata,* in the United States. *Plant Health Progress* 19(2): 140–142. https://doi.org/10.1094/PHP-02-18-0008-BR

Garganese F., Sanzani S. M., Mincuzzi A., Ippolito A., 2015. First report of *Curvularia spicifera* causing brown rot of citrus in Southern Italy. *Journal of Plant Pathology* 97(3): 543. https://doi.org/10.4454/JPP.V97I3.001

Grumet R., McCreight J. D., McGregor C., Weng Y., Mazourek M., … Fei Z., 2021. Genetic resources and vulnerabilities of major cucurbit crops. *Genes* 12(8): 1222. https://doi.org/10.3390/genes12081222

Gusmini G., Song R., Wehner T. C., 2005. New Sources of Resistance to Gummy Stem Blight in Watermelon. *Crop Science* 45(2): 582–588. https://doi.org/10.2135/CROPSCI2005.0582

Harris J. L., 2000. Safe, Low-Distortion Tape Touch Method for Fungal Slide Mounts. *Journal of Clinical Microbiology* 38(12): 4683. https://doi.org/10.1128/JCM.38.12.4683-4684.2000

Huang Y., Jones C., Urbina H., Zhang S., 2023. First Report of Leaf Blight Caused by *Curvularia aeria* and *C. senegalensis* on Tomato *(Solanum lycopersicum)* in Florida, U.S.A. *Plant Disease* 107(12): 4027. https://doi.org/10.1094/PDIS-06-23-1209-PDN

Hyde K.D., Noorabadi M.T., Thiyagaraja V., He M.Q., Johnston P.R., … Zvyagina E., 2024. The 2024 Outline of Fungi and fungus-like taxa. *Mycosphere* 15(1): 5146–6239. https://doi.org/10.5943/mycosphere/15/1/25

Kaniyassery A., Hegde M., Sathish S. B., Thorat S. A., Udupa S., … Muthusamy A., 2024. Leaf spot-associated pathogenic fungi alter photosynthetic, biochemical, and metabolic responses in eggplant during the early stages of infection. *Physiological and Molecular Plant Pathology* 133: 102320. https://doi.org/10.1016/j.pmpp.2024.102320.

Katoh K., Standley D.M., 2013. MAFFT multiple sequence alignment software version 7: improvements in performance and usability. *Molecular Biology and Evolution* 30(4): 772-80. https://doi.org/10.1093/molbev/mst010

Katushova M., Beloshapkina O., Tarakanov R., Shipulin A., Dzhalilov F., 2021. Fungi of the genus *Curvularia* sp. - new pathogens of turfgrass in Russia. *IOP Conference Series: Earth and Environmental Science* 663(1): 012007. https://doi.org/10.1088/1755-1315/663/1/012007

Khan N. A., Asaf S., Ahmad W., Jan R., Bilal S., … Al-Harrasi A., 2023. Diversity, lifestyle, genomics, and their functional role of *Cochliobolus, Bipolaris,* and *Curvularia* species in environmental remediation and plant growth promotion under biotic and abiotic stressors. *Journal of Fungi* 9(2): 254. https://doi.org/10.3390/JOF9020254

Kucharek T., 1985. Alternaria Leaf Spot of Cucurbits. University of Florida, Insitute of Food and Agricultural Sciences, Plant Pathology Department, Plant Pathology Fact Sheet. PP-32. https://original-ufdc.uflib.ufl.edu/UF00066896

Kwon O. K., Jeong A. R., Jeong Y. J., Kim Y. A., Shim J., … Park C. J., 2021. Incidence of *Alternaria* species associated with watermelon leaf blight in Korea. *Plant Pathology Journal* 37(4): 329–338. https://doi.org/10.5423/PPJ.OA.02.2021.0018

Larsson A., 2014. AliView: a fast and lightweight alignment viewer and editor for large datasets. *Bioinformatics* 30(22): 3276–3278. https://doi.org/10.1093/BIOINFORMATICS/BTU531

Ma G., Bao S., Zhao J., Sui Y., Wu X., 2021. Morphological and molecular characterization of *Alternaria* species causing leaf blight on watermelon in China. *Plant Disease* 105(1): 60–70. https://doi.org/10.1094/PDIS-01-20-0130-RE

Majeed R. A., Shahid A. A., Ashfaq M., Saleem M. Z., Haider M. S., 2015. First Report of *Curvularia lunata* Causing Brown Leaf Spots of Rice in Punjab, Pakistan. *Plant Disease* 100(1): 219. https://doi.org/10.1094/PDIS-05-15-0581-PDN

Manamgoda D. S., Cai L., Bahkali A. H., Chukeatirote E., Hyde K. D., 2011. *Cochliobolus:* An overview and current status of species. *Fungal Diversity* 51: 3–42. https://doi.org/10.1007/S13225-011-0139-4

Manamgoda D. S., Cai L., McKenzie E. H. C., Crous P. W., Madrid H., … Hyde K. D., 2012a. A phylogenetic and taxonomic re-evaluation of the *Bipolaris - Cochliobolus - Curvularia* Complex. *Fungal Diversity* 56(1): 131–144. https://doi.org/10.1007/S13225-012-0189-2

Manamgoda D. S., Cai L., McKenzie E. H. C., Chukeatirote E., Hyde K. D., 2012b. Two new *Curvularia* species from northern Thailand. *Sydowia* 2(64): 255–267.

Manamgoda D. S., Rossman A. Y., Castlebury L. A., Chukeatirote E., Hyde K. D., 2015. A taxonomic and phylogenetic re-appraisal of the genus *Curvularia (Pleosporaceae):* Human and plant pathogens. *Phytotaxa* 212(3): 175–198. https://doi.org/10.11646/PHYTOTAXA.212.3.1

Manzar N., Kashyap A. S., Sharma P. K., Srivastava A. K., 2024. First Report of Leaf Spot on Maize Caused by Curvularia verruculosa in India. *Plant Disease*

108(3): 793. https://doi.org/10.1094/PDIS-07-23-1410-PDN

Marin-Felix Y., Senwanna C., Cheewangkoon R., Crous P. W., 2017. New species and records of *Bipolaris* and *Curvularia* from Thailand. *Mycosphere* 8(9): 1555–1573. https://doi.org/10.5943/mycosphere/8/9/11

Marin-Felix Y., Hernández-Restrepo M., Crous P. W., 2020. Multi-locus phylogeny of the genus *Curvularia* and description of ten new species. *Mycological Progress* 19(6): 559–588. https://doi.org/10.1007/S11557-020-01576-6

Matić S., Tabone G., Garibaldi A., Gullino M. L., 2020. Alternaria leaf spot caused by *Alternaria* species: an emerging problem on ornamental plants in Italy. *Plant Disease* 104(8): 2275–2287. https://doi.org/10.1094/PDIS-02-20-0399-RE

Meena M., Gupta S. K., Swapnil P., Zehra A., Dubey M. K., Upadhyay R. S., 2017. *Alternaria* toxins: Potential virulence factors and genes related to pathogenesis. *Frontiers in Microbiology* 8(1451): 1-14. https://doi.org/10.3389/FMICB.2017.01451

Nam H. S., Park H. S., Kim Y. C., 2024. First report of coffee leaf spot caused by *Curvularia geniculata*. *Journal of Phytopathology* 172(1): e13245. https://doi.org/10.1111/JPH.13245

Nobles M. K., 1948. Studies in forest pathology: VI. Identification of cultures of wood-rotting fungi. *Canadian Journal of Research* 26(3): 281–431. https://doi.org/doi.org/10.1139/cjr48c-026

Paris H. S., 2015. Origin and emergence of the sweet dessert watermelon, *Citrullus lanatus*. *Annals of Botany* 116(2): 133–148. https://doi.org/10.1093/aob/mcv077

Peever T. L., Su G., Carpenter-Boggs L., Timmer L. W., 2004. Molecular systematics of citrus-associated *Alternaria* species. *Mycologia* 96(1): 119–134. https://doi.org/10.1080/15572536.2005.11833002

Pornsuriya C., Ito S., Sunpapao A., 2018. First report of leaf spot on lettuce caused by *Curvularia aeria*. *Journal of General Plant Pathology* 84(4): 296–299. https://doi.org/10.1007/S10327-018-0782-7

Rabaaoui A., Masiello M., Somma S., Crudo F., Dall'Asta C., ... Moretti A., 2022. Phylogeny and mycotoxin profiles of pathogenic *Alternaria* and *Curvularia* species isolated from date palm in southern Tunisia. *Frontiers in Microbiology* 13: 1034658. https://doi.org/10.3389/FMICB.2022.1034658

Ren X., Chen S., Guo J., Wang M., Liu X., Wei Z. Z., 2022. First Report of *Curvularia lunata* Causing Leaf Spot on *Oryza sativa* in Sabah, Malaysian Borneo. *Plant Disease* 107(7): 2234. https://doi.org/10.1094/PDIS-08-22-1939-PDN

Rivera-Burgos L. A., Silverman E., Sari N., Wehner T. C., 2021. Evaluation of Resistance to Gummy Stem Blight in a Population of Recombinant Inbred Lines of Watermelon × Citron. *HortScience* 56(3): 380–388. https://doi.org/10.21273/HORTSCI15599-20

Rueden C. T., Schindelin J., Hiner M. C., DeZonia B. E., Walter A. E., Arena E. T., Eliceiri K. W., 2017. ImageJ2: ImageJ for the next generation of scientific image data. *BMC Bioinformatics* 18(1): 1–26. https://doi.org/10.1186/S12859-017-1934-Z

Sari M. P., Wahyuno D., Hardiyanti S., Miftakhurohmah., 2023. First report of Curvularia akaiiensis as a causal agent of leaf spot disease on Vetiver. *Australasian Plant Disease Notes* 18(1): 1–4. https://doi.org/10.1007/S13314-023-00516-Z

Sarkar T., Chakraborty P., Das S., Saha D., Saha A., 2018. Curvularia leaf spot of pointed gourd in India. *Canadian Journal of Plant Pathology* 40(4): 594–600. https://doi.org/10.1080/07060661.2018.1504822

Shahin E. A., 1979. An Efficient Technique for Inducing Profuse Sporulation of *Alternaria* Species. *Phytopathology* 69(6): 618. https://doi.org/10.1094/PHYTO-69-618

Shanthi Avinash T., Jai Shanker Pillai H. P., Biradar M., Shinde V. M., 2021. A Review on Fungal Diseases of *Cucurbitaceae* and their Management. *International Journal of Current Microbiology and Applied Sciences* 10(08): 653–672. https://doi.org/10.20546/ijcmas.2021.1008.075

Singh M. P., Erickson J. E., Boote K. J., Tillman B. L., Jones J. W., van Bruggen A. H. C., 2011. Late Leaf Spot Effects on Growth, Photosynthesis, and Yield in Peanut Cultivars of Differing Resistance. *Agronomy Journal* 103(1): 85-91 https://doi.org/10.2134/agronj2010.0322

Singh S. P., Khan N., Singh R., Singh H., Prasad S., Dwivedi D., 2020. Documentation variation for Alternaria blight resistance in varieties of Rapeseed mustard. International *Journal of Chemical Studies* 8(4): 1397–1400. https://doi.org/10.22271/CHEMI.2020.V8.I4M.9793

Sivanesan A., 1987. Graminicolous species of *Bipolaris, Curvularia, Drechslera, Exserohilum* and their teleomorphs. *Mycological Papers* 158: 154–185.

Stamatakis A., 2014. RAxML version 8: A tool for phylogenetic analysis and post-analysis of large phylogenies. *Bioinformatics* 30(9): 1312-1313. https://doi.org/10.1093/bioinformatics/btu033

Steenkamp E., Britz H., Coutinho T., Wingfield B., Marasas W., Wingfield M., 2000. Molecular characterization of *Fusarium subglutinans* associated with mango malformation. *Molecular Plant Pathol-*

ogy 1(3): 187–193. https://doi.org/10.1046/J.1364-3703.2000.00024.X

Sun G., Oide S., Tanaka E., Shimizu K., Tanaka C., Tsuda M., 2003. Species separation in *Curvularia "geniculate"* group inferred from *Brn1* gene sequences. *Mycoscience* 44(3): 239–244. https://doi.org/10.1007/S10267-003-0104-5

Tamura K., Stecher G., Kumar S., 2021. MEGA11: Molecular Evolutionary Genetics Analysis Version 11, *Molecular Biology and Evolution* 38(7): 3022–3027. https://doi.org/10.1093/molbev/msab120

Torres-Garcia D., García D., Cano-Lira J. F., Gené J., 2022. Two Novel Genera, *Neostemphylium* and *Sclero-myces (Pleosporaceae)* from Freshwater Sediments and Their Global Biogeography. *Journal of Fungi* 8(8): 868. https://doi.org/10.3390/JOF8080868

Vakalounakis D. J., 1990. *Alternaria alternata* f. sp. *cucurbitae,* the cause of a new leaf spot disease of melon *(Cucumis melo). Annals of Applied Biology* 117(3): 507–513. https://doi.org/10.1111/J.1744-7348.1990.TB04817.X

Vanitha S., Kavitha M., Ragul S., Mohanapriya S., Angappan K., … Rani C. I., 2024. First report of *Curvularia lunata* causing leaf blight on muskmelon *(Cucumis melo). New Disease Reports* 50(2): e12310. https://doi.org/10.1002/NDR2.12310

Venkatesagowda B., Ponugupaty E., Barbosa A. M., Dekker R. F. H., 2012. Diversity of plant oil seed-associated fungi isolated from seven oil-bearing seeds and their potential for the production of lipolytic enzymes. *World Journal of Microbiology and Biotechnology* 28(1): 71–80. https://doi.org/10.1007/S11274-011-0793-4

White T., Bruns T., Lee S., Taylor J., Innis M., … Sninsky J., 1990. Amplification and Direct Sequencing of Fungal Ribosomal RNA Genes for Phylogenetics. In: *PCR Protocols,* Academic Press, 315–322.

Woudenberg J. H. C., Groenewald J. Z., Binder M., Crous P. W., 2013. *Alternaria* redefined. *Studies in Mycology* 75: 171–212. https://doi.org/10.3114/sim0015

Woudenberg J. H. C., Seidl M. F., Groenewald J. Z., de Vries M., Stielow J. B., Thomma B. P. H. J., Crous P. W., 2015. *Alternaria* section *Alternaria:* Species, *formae speciales* or pathotypes? *Studies in Mycology* 82: 1–21. https://doi.org/10.1016/j.simyco.2015.07.001

Wu Q., Li Y., Li Y., Gao S., Wang M., Zhang T., Chen J., 2013. Identification of a novel fungus, *Leptosphaerulina chartarum* SJTU59 and characterization of its xylanolytic enzymes. *PLoS ONE* 8(9): e73729. https://doi.org/10.1371/journal.pone.0073729

Zhou X. G., Everts K. L., 2008. First report of *Alternaria alternata* f. sp. *cucurbitae* causing Alternaria leaf spot of melon in the Mid-Atlantic region of the United States. *Plant Disease* 92(4): 652. https://doi.org/10.1094/PDIS-92-4-0652B

Phytopathologia Mediterranea
The international journal of the
Mediterranean Phytopathological Union

Firenze University Press
www.fupress.com/pm

Research Papers

Orange oil postharvest dips for control of grey mould (*Botrytis cinerea*) of plums and strawberries, and green mould (*Penicillium digitatum*) of citrus

Ncumisa NJOMBOLWANA-SWARTZ[1,2], Julia MEITZ-HOPKINS[1,*], Sara MONTEIRO[3], Cheryl LENNOX[1]

[1] *Department of Plant Pathology, Stellenbosch University, Stellenbosch, South Africa*
[2] *Oro Agri SA (Pty) Ltd, 1 Henry Vos Close, Asla Park, Strand, South Africa*
[3] *ORO AGRI EUROPE S.A.Estrada Municipal 533, Zona de Biscaia, Estr. Do Lau, 2950-401, Palmela, Portugal*
*Corresponding author. E-mail: juliam@sun.ac.za

Summary. Orange oil has antibacterial properties for uses in food and pharmaceutical industries. This study evaluated the efficacy of orange oil dip applications and treatment periods for protective and curative effects against *Botrytis cinerea*, (which causes grey mould on plums and strawberries), and *Penicillium digitatum*, responsible for green mould of citrus. Pure orange oil and two orange oil-based formulations (OR007B and OR79) were tested on inoculated fruit, at oil concentrations from 0.05% to 1.00%, and were compared to the fungicides fludioxonil at 300 mg. L^{-1} for *B. cinerea*, or imazalil at 500 µg mL^{-1} for *P. digitatum*, the respective South African registered doses for these fungicides. Orange oil treatments failed to control green mould on lemons and oranges, with disease incidence exceeding 90% even after 120 sec of exposure. Two plum cultivars had different susceptibilities to grey mould, and orange oil reduced the disease incidence (24 to 14%) as the oil concentration increased in the curative treatments of cv. African Delight, outperforming 1% fludioxonil (24%). The OR007B and OR79 formulations both gave low incidence of grey mould, with 0.5% of orange oil in these formulations resulting in up to 12% incidence (from OR007B) and 17% (from OR79). Cv. Laetitia, in contrast, had >60% incidence of grey mould across all treatments, including fludioxonil. Protective treatments showed similar trends in both cultivars. On strawberries stored at 4°C for 14 d, grey mould incidence was reduced from 82% (control treatment) to 55% (for orange oil), 21% (for OR007B), and 44% (for OR79), with the orange oil treatments having efficacy comparable to fludioxonil. These results demonstrate the potential of orange oil treatments as alternatives for grey mould management in plums and strawberries.

Keywords. Fungicide sensitivity, natural antimicrobial products, plant extracts, soft chemicals.

OPEN ACCESS

Citation: Njombolwana-Swartz, N., Meitz-Hopkins, J., Monteiro, S. & Lennox, C. (2025). Orange oil postharvest dips for control of grey mould (*Botrytis cinerea*) of plums and strawberries, and green mould (*Penicillium digitatum*) of citrus. *Phytopathologia Mediterranea* 64(1): 57-70. doi: 10.36253/phyto-15613

Accepted: March 7, 2025

Published: May 15, 2025

Data Availability Statement: All relevant data are within the paper and its Supporting Information files.

Competing Interests: The Author(s) declare(s) no conflict of interest.

Editor: Lluís Palou, Valencian Institute for Agricultural Research, Valencia, Spain.

ORCID:
NN-S: 0009-0002-2189-8318
JM-H: 0000-0002-8127-6978
SM: 0000-0002-7069-0591
CL: 0000-0002-6350-253X

INTRODUCTION

Occurrence of fruit losses due to decay, long distances to markets, and cold chain interruptions are major drawbacks for fruit industries (Nelson,

2010; Stander and Dyk, 2017; Cherono and Workneh, 2018), and use of synthetic fungicides is the most effective management strategy for control of postharvest decay-causing fungal pathogens. *Penicillium digitatum* (Pers.) Sacc., a causal agent of green mould, is responsible for citrus production losses of up to 90% (Macarisin *et al*., 2007; Costa *et al.,* 2019). This disease is managed using the fungicide imazalil (Smilanick *et al*., 1997, Smilanick *et al*., 2005; Erasmus *et al*., 2011). *Botrytis cinerea* Pers. (which causes grey mould) is responsible for postharvest fungal decay of up to 73% on stone fruit (Fourie and Holz, 1985). The fungicide fludioxonil is registered for postharvest application on stone fruit and is used to control grey mould infections (Förster *et al*., 2007).

Safety concerns over human health and environmental pollution threaten the use of synthetic chemicals for plant disease management. Synthetic fungicides, including some of those used postharvest (e.g. imazalil), are regarded as unsafe for human health and environmental toxic to the environment (e.g. fludioxonil), and consumers have become more aware of the impacts of these substances on their health (Sişman and Türkez, 2010; Tao *et al*., 2020; European chemical agency-ECHA, 2024). These increasing concerns have necessitated international and national regulatory authorities to formulate policies for phasing out and prohibiting the use of these products (Commission delegated regulation (EU) 2023/1656, 2023; Department of Agriculture, Forestry, and Fisheries DAFF, 2010). Recent consumer demands in important fruit export markets (including Europe) have caused some supermarkets to introduce lower fungicide residue limits than those set by government regulatory authorities. New systems such as the Globally Harmonized System (GHS) for safety classification of chemicals have identified highly hazardous substances at categories 1A and 1B, subsequently leading to their phasing out (Mudzunga, 2022). These pressures have resulted in a pesticide market shift from development of novel synthetic substances to investments in biopesticide development (Lucintel, 2024). Authorities have also instituted regulatory pathways specifically focused on biopesticides, ensuring fast-tracked processes with minimum delays (DALRRD, 2023).

Biopesticides are defined as products that are of natural origin, either from plants or microorganisms, that are applied to crops to control, repel or prevent occurrence of specific pests and diseases (Hezakiel *et al*., 2023). They are "generally regarded as safe" (GRAS). Interest in these substances is largely due to their natural origins, and that they have been described as GRAS by the Food and Drug Administration (FDA, 2006). These products should have known or minimal toxicological effects on the environment and mammals and not be regulated for chemical residues on fresh produce (Palou *et al*., 2016). Essential oils are GRAS, and are liquid products extracted from plants through several methods, including, for oils from citrus, hydro distillation, steam distillation, and cold expression (Tao *et al*., 2009; Pejin *et al*., 2011; Botrel *et al*., 2015).

The complex composition of essential oils is an advantage for their use as antifungal products, since synergism of compounds has been shown against specific targets and pathogens (Sharifi-Rad *et al*.; 2017; Zareiyan and Khajehsharifi, 2021). Although limonene has been found as the largest proportion (76%), of the essential oil compounds from *Citrus sinensis*, other compounds including monoterpenes (geranial, neral), that are lesser components, also have antimicrobial activity and effectively inhibit fungal pathogen growth (Tsao and Zhou, 2000; Hanafy *et al*., 2021; Hamdan *et al*., 2024). This synergism would be advantageous in postharvest disease management, reducing the likelihood of target pathogens developing resistance to combined components (Tripathi and Dubey, 2004). Rammanee and Hongpattarakere (2011) showed that the individual components of essential oils were less effective than the natural essential oils, demonstrating synergism between different compounds.

It would be advantageous to incorporate essential oils into postharvest disease management, due to their high biodegradability, and to their likely lack of residue issues (Talibi *et al*., 2014). Therefore, the Environmental Protection Agency (EPA) and European Union have eliminated the need to establish permissible residue levels for sweet orange oil, when used during pre- and postharvest at less than 10% (Federal Register, 2014).

Citrus peel is produced as waste in large amounts during processing, so presents an opportunity for essential oil extraction (Zareiyan and Khajehsharifi, 2021). Orange oil is obtained from fruit rind via cold pressing and steam distillation of mature sweet orange fruit (*Citrus sinensis* Linnaeus) (Botrel *et al*., 2015). As is typical for all essential oils, orange oil is analysed using gas chromatography or mass spectrometry, and approx. 27 compounds have been identified. Monoterpene D-limonene is the principal component (> 70%) and with other monoterpene hydrocarbons they make up 90% of the total essential oil content (Droby *et al*., 2008; Tao *et al*., 2009; Regnier *et al*., 2014). As the main component, D-limonene has been classified as an insect repellent and a natural pesticide by the EPA (John *et al*., 2017). Although orange oil use is well documented for pharmaceutical and food industries for its antibacte-

rial and food preservation benefits (Guo *et al*., 2018; Jantrawut *et al*., 2018; De Andrade *et al*., 2022), little information is available on its efficacy against postharvest fruit pathogens, although several studies have previously tested its efficacy on other products including potato slices and cucumber, and one study evaluated its use on fresh-cut oranges (Radi *et al*., 2018; Shi *et al*., 2018; Ziedan *et al*., 2022).

The objective of the present study was to investigate post-harvest applications of orange oil as an alternative for the management of *B. cinerea* on plums and strawberries and *P. digitatum* on citrus. These applications were evaluated for curative and protective activities, and incubation times, and treatment bath exposure periods were also assessed.

MATERIALS AND METHODS

Treatments

Two orange oil-based products were obtained from ORO AGRI SA (Pty) Ltd, Strand, South Africa. One formulation (OR007B) contained 5% orange oil, and the second (OR-79) contained 10% orange oil. These products were compared as fruit dip applications. Pure essential orange oil, containing 97% d-limonene, was also obtained from Puris Natural Aroma Chemicals, Paarl, South Africa. Prior to treatments, fruit treated with the orange oil extracts was sent to HORTEC (Pty) Ltd, Somerset West, South Africa, for imazalil residue analyses, to validate the purity of the oil. Thyme oil (from *Thymus vulgaris* L.) containing > 40% of thymol and obtained from Clive Teubes Africa (Pty) Ltd, Johannesburg, South Africa, was used in these trials to compare with orange oil. Dip treatments in tap water were included in experiments as negative control treatments. The fruit industry standards for postharvest fungicide applications, fludioxonil (Teacher 230 SC) for plums, or imazalil sulfate (Imazacure; 750 g kg^{-1} SP) for citrus, were used as positive control treatments. These fungicide products were obtained from ICA International Chemicals (Pty) Ltd, Plankenburg, Stellenbosch, South Africa. Fludioxonil was applied as a dip at the recommended concentration of 300 mg L^{-1} for *B. cinerea* in plums, and imazalil (IMZ) at 500 mg L^{-1} for *P. digitatum* on citrus. Since no postharvest treatments are used commercially for strawberries, no commercial product was included in the experiments. All fruit used in the experiments was collected from local packhouses (near Stellenbosch, South Africa), and was used within a week after harvest.

Inoculation and treatment application

Citrus experiments

During the 2020 and 2021 fruit packing seasons, high quality export citrus fruit of 'Eureka' lemon [*Citrus* x *limon* (L.) Osbeck], and 'Midnight Valencia' orange [*Citrus* × *sinensis* (L.) Osbeck], were obtained from packhouses in the Citrusdal and Stellenbosch regions, Western Cape, South Africa. Fruit was washed upon arrival from packhouses, using a custom-built packline designed to mimic a commercial system to apply wash solution containing 200 mg L^{-1} of calcium hypochlorite. After washing, the fruit was dried in a drying tunnel.

To commence the experiments, inoculations were conducted as previously described in Njombolwana *et al.* (2022), using *P. digitatum* isolates previously classified as sensitive (isolate STE-U 6560) or resistant (isolate STE-U 6590) to IMZ (Erasmus *et al,.* 2011). The IMZ-resistant isolate was obtained from Citrus Research International (CRI), Nelspruit, South Africa, and the IMZ-sensitive isolate was obtained from a satsuma orchard at the Stellenbosch University experimental farm, Welgevallen, Stellenbosch, South Africa. These isolates were used to prepare conidium suspensions, following 2-week incubation on potato dextrose agar (Merck) containing streptomycin sulfate at 0.04 mg L^{-1} (PDA+). The conidium suspension was prepared in autoclaved deionized water amended with 0.01 mL L^{-1} Tween 20 (Sigma-Aldrich) and was filtered through two layers of sterile cheesecloth. A Neubauer improved haemocytometer was used to adjust the conidium suspension to 1×10^6 conidia mL^{-1}, according to Plaza *et al*. (2004). Ten unblemished fruits of similar size and colour per replicate were inoculated using a metallic rod wounding tool to create four wounds (0.5 mm deep and 2 mm wide) around each fruit stem end. Treatments were applied either 1 h before (protective) or 12 h after (curative).

The water bath solutions containing different treatments were prepared along with a negative control treatment (a bath containing water). In all the experiments, IMZ at 500 µg mL^{-1} was included as a standard disease control treatment (as conventionally used by industry). For orange oil only and thyme oil only treatments, the required concentrations of essential orange oil were premixed with 0.50% v/v Tween 80 to obtain suspensions of the oils in water. The essential oils were applied at 0.05, 0.1 0.5 or 1% concentrations. The OR-007B and OR-79 formulated products were adjusted to these concentrations. Treated fruit was submerged for 30 s in the aqueous solutions and allowed to dry for packing or inoculations depending on the treatment schedules.

In addition, 'Eureka' lemons and 'Midnight Valencia' oranges were used to evaluate effects of exposure times in the treatment bath. The fruit was submerged in the bath for 60, 90, or 120 s following a 12 h incubation period at 25°C. The preparation of the treatments and the procedures were as described above.

In all the experiments, the laboratory temperature was maintained. Fruit was stored in plastic crates on count SFT15 nectarine trays (AgriMark, Paarl, South Africa). Each crate was covered with a transparent polyethylene bag, which was sealed, and then incubated at 25°C for 4 d, after which the infected fruit wounds were evaluated. This was done using a light source (UV-A at 365 nm, Labino Mid-light; www.labino.com), with each wound visible as yellow fluorescence on the fruit surface. Six to 8 d later, incidence of conidium production was assessed, using the sporulation index described by Erasmus *et al.* (2011), which includes scores of 0 = absence of conidia, to 6 = conidia covering the whole fruit.

Plum experiments

Commercially harvested plums [*Prunus salicina* Lindley ('Angelino,' 'African Delight', 'Laetitia') were collected from packhouses in Wellington region, Western Cape, South Africa. The fruit was brought to the laboratory without receiving prior treatments at the packhouses. The plums were surface sterilized before the experiment, by submerging the fruit for 1 min in a waterbath containing 0.48 mg L^{-1} of sodium hypochlorite (Chlorguard sanitiser bleach), combined with 0.005% Tween 20 as a surfactant. The fruit was then allowed to dry on net stainless steel trays.

Inoculations for the experiments were carried out using a *B. cinerea* isolate STE-U 9254, obtained from the Stellenbosch University Plant Pathology culture collection. 1-week-old mycelium PDA+ cultures were grown for 4 d at 25ºC then for 3 d exposed to ultraviolet (UV) light to induce conidium production. Conidium suspensions were prepared as described above but were adjusted to concentration of 1×10^5 conidia mL^{-1} (Lopez-Reyes *et al*., 2013). Ten individual fruit per replication were wound inoculated using a metallic rod wounding tool (2 mm depth, and 2 mm wide). The wounded sections were carefully marked using an Artline 70 black permanent marker.

To evaluate the curative and protective effects of the treatments against *B. cinerea* on fruit of 'African Delight' and 'Laetitia', fludioxonil bath solution at the recommended commercial concentration for plums of 300 mg $^{-1}$ was used. All other treatments and applied concentrations were kept the as described above for the citrus experiments. Applications of thyme oil at all concentrations and 1% adjusted concentration of orange oil in the OR007B and OR79 treatments was discontinued due to the observed phytotoxicity in a pilot trial (data not shown). The fruit was submerged for 30 s in the aqueous solutions and allowed to dry for packing.

To evaluate the effect of incubation time on 'Angelino', a similar treatment procedure as described above was followed, but the fruit was treated after 8, 16, or 24 h. The fruit were allowed to dry, and were then packed on to SFT13 nectarine trays. For the duration of the trials, plums were kept in moisture chambers with temperature maintained at 25°C, and evaluations were carried out on day 7 and day 12 after the treatments were applied.

Form both application methods (preventative or curative), evaluations were made for disease incidence (total number of infected fruits per treatment replicate) and severity (lesion diameters, length and width at the inoculation site). Lesion size was measured using a digital calliper (Miyumoto, MTMA). A repeat of two trials per cultivar was conducted using 'African Delight' and 'Laetitia' cultivars.

Strawberry experiments

During the 2021 fruit packing season, strawberries *Fragaria* x *ananassa* (Duchesne ex Weston) Duchesne ex Rozier; 'Albion'), were collected from packhouses in Stellenbosch, Western Cape, South Africa. The fruit were surface sterilized using a 25 mg L^{-1} sodium hypochlorite solution for 3 mins, followed by a 5 min dip in sterile distilled water, and allowed to dry for 1 h in a laminar flow hood.

Fruit inoculations were carried out to evaluate curative effects of the treatments, after 3 h incubation. The fruit was treated by submerging in a bath containing orange oil, orange oil-based formulated products (using concentrations at 0.05, 0.1, 0.5 and 1% as described above for plums and citrus), and an untreated experimental control, with an exposure period of 30 s in the bath. No standard fungicide treatment was included, since this is not currently practiced by industry. Following treatments, the fruit was allowed to dry, and was then packed into plastic crates lined with black polystyrene pear trays (AgriMark). The fruit was stored at 4°C for 14 d, with monitoring for disease development in the untreated controls. On day 14, evaluations were carried out for appearance of superficial mycelia resembling grey mould, in the untreated fruit. The fruit was then transferred to 25°C and further development of the disease was evaluated on day 17 (i.e. after 3 d storage).

Statistical analyses of data

For disease incidence, severity, fungus sporulation, and control of *P. digitatum* or *B. cinerea* decay, data were analysed using appropriate analyses of variance (ANOVA) and generalized estimated models, using Statistica (v.13.5). These analyses were carried out by the Department for Statistical Analysis, Stellenbosch University. Dependant variables within the analyses were continuous, so Fisher's LSD was an appropriate method for detecting statistically significant differences (95% confidence interval).

RESULTS

Curative and protective efficacy of orange oil and orange oil-based dip applications

The curative and protective effects of the orange oil and orange oil-based treatments OR-007B and OR-79 were evaluated on plums and strawberries. In the preliminary investigations, thyme oil was incorporated and completely inhibited *B. cinerea* at 0.5 and 1%. However, heavy phytotoxicity symptoms were caused by these treatments, as fruit hardening and white patches, observed 24 h after application (Figure 1, B). These treatments were excluded from the main experiments.

On plums, for disease incidence and severity, the ANOVA analyses showed a statistically significant factor interaction of cultivar × action × treatment × day ($P < 0.001$). The interaction was attributed to differing levels of disease susceptibility between the cultivars (Table 1). In 'African Delight' plums, orange oil at all the tested concentrations reduced *B. cinerea* incidence, both curatively and as a protectant. There were statistically significant interactions for the incidence data ($P = 0.06$), and the severity data ($P < 0.001$), between cultivar, action (curative or preventative), and treatment.

Data for each plum cultivar are presented separately. Disease incidence for 'African Delight' was low in the untreated controls (mean = 50%; Table 1) in the curative experiments. The orange oil treatment decreased incidence with increasing concentration. The 0.5% concentration of orange oil (least mean incidence = 14%)

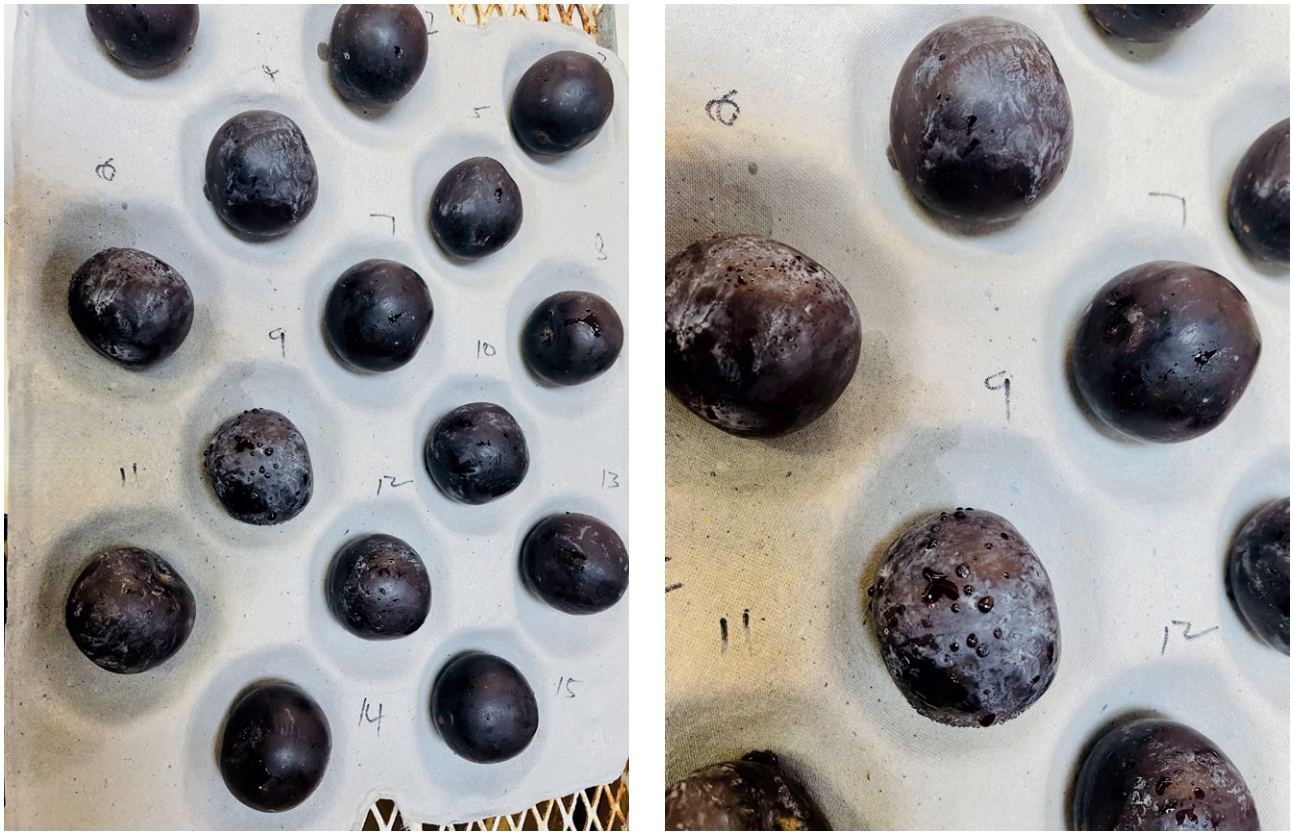

Figure 1. 'Angelino' plums treated with dip applications of thyme oil (0.05-0.5%) for control of *Botrytis cinerea*. White patches on the fruit surfaces indicate damage and hardened texture 24 h after oil application. **A,** thyme oil at 0.05%. **B,** thyme oil at 0.5%.

Table 1. Mean percent incidence of grey mould after 12 d incubation at 25°C, on plums of 'African Delight' and 'Laetitia' following curative or protective treatments, including: fludioxonil (300 mg L^{-1}, orange oil (0.05, 0.1, 0.5 or 1%), OR007B (5% orange oil) or OR79 (10% orange oil). The orange oil treatment rates were adjusted to give orange oil concentrations of 0.05, 0.1 or 0.5%.

Treatment	Mean grey mould incidence (%)			
	'African Delight'		'Laetitia'	
	Curative	Protective	Curative	Protective
Control	50 i-k	74 d-f	88 a-f	84 a-c
Fludioxonil 300 mg L^{-1}	24 I-p	33 l-n	68 e-h	72 b-g
Orange oil 0.05%	24 no	24 m-p	59 g-i	74 g-i
Orange oil 0.1%	23 no	49 i-k	75 g-i	80 b-g
Orange oil 0.5%	14 o-q	49 l-n	65 f-i	82 f-i
Orange oil 1%	22 m-o	25 m-p	55 h-j	79 b-g
OR007B 0.05%	7 q	32 k-m	78 c-f	96 a
OR007B 0.1%	26 m-o	24 m-o	80 d-f	83 b-f
OR007B 0.5%	12 pq	37 k-m	75 b-g	82 b-f
OR79 0.05%	35 j-o	26 m-o	77 d-g	91 ab
OR79 0.1%	24 op	19 n-p	78 c-f	83 b-f
OR79 0.5%	17 n-q	41 j-l	61 g-i	84 b-d

Means accompanied by the same letters are not significantly different ($P > 0.05$).

Table 2. Mean percent grey mould severity after 12 d incubation at 25°C on plums of cvs. 'African Delight' and 'Laetitia' following curative or protective treatments, including: fludioxonil (300 mg L^{-1}, orange oil (0.05, 0.1, 0.5, 1.0%), OR007B (5% orange oil) and OR79 (10% orange oil) adjusted to orange oil concentrations of 0.05, 0.1, 0.5%.

Treatment	Mean grey mould severity (%)			
	'African Delight'		'Laetitia'	
	Curative	Protective	Curative	Protective
Control	100 j-n	100 b-d	100 ab	100 a-c
Fludioxonil 300 mg L^{-1}	61 n-q	47 k-o	79 c-f	93 b-d
Orange oil 0.05%	64 m-p	81 l-o	68 e-i	91 b-d
Orange oil 0.1%	63 m-p	36 m-q	66 e-i	87 b-e
Orange oil 0.5%	36 q-r	69 f-j	73 d-g	97 a-c
Orange oil 1%	58 o- q	81 l-o	60 g-k	92 b-d
OR007B 0.05%	12 r	46 m-q	88 b-d	100 a
OR007B 0.1%	68 m- q	34 i-m	91 a-d	95 a-d
OR007B 0.5%	25 qr	55 m-q	83 b-e	94 a-d
OR79 0.05%	57 o- q	35 i-m	88 b-d	100 ab
OR79 0.1%	66 o-r	27 l-q	87 b-d	93 b-d
OR79 0.5%	29 p-r	60 h-l	67 e-h	95 a-d

Means accompanied by the same letters are not significantly different ($P > 0.05$).

provided control similar to fludioxonil (mean incidence = 24%). The OR007B and OR79 treatments also reduced disease incidence, in some cases to significantly less than the fludioxonil treatment (i.e. 7% from 0.05% OR007B). For the protective treatments in 'African Delight' plums, the untreated controls had mean grey mould incidence of 74%, while the orange oil treatments reduced incidence to between 24 and 49% (similar to the fludioxonil treatment). Fludioxonil resulted in 33% disease incidence, which was also similar to the OR007B and OR79 treatments, where mean incidence was the least (19%) from the 0.1% OR79 treatment.

Disease incidence for 'Laetitia' (untreated control mean = 88%) was greater compared to 'African Delight' (Table 1). Disease incidence in 'Laetitia' plums treated curatively with orange oil showed a trend of decreased grey mould incidence with increasing concentrations, similar to that from fludioxonil (mean incidence = 68%). None of the treatments effectively reduced grey mould incidence when applied protectively in 'Laetitia' plums, with the most effective treatment (0.05% orange oil) reducing mean disease incidence to 74%, compared with 84% from the untreated control).

Disease severity data showed similar trends to the incidence data in both cultivars (Table 2). In 'African Delight' plums treated curatively with 0.5% orange oil, mean severity was reduced to 35%, lower than from fludioxonil (61%), but this difference was not statistically significant. Similarly, 0.5% OR007B and 0.5% OR79 reduced mean incidence to, respectively, 25 and 28%. Fludioxonil reduced disease mean severity to 47%, when applied protectively. Orange oil alone did not consistently lower grey mould severity from the protective applications and demonstrated variable efficacy across oil concentrations. In 'Laetitia', plums, curative application of fludioxonil reduced severity to 79%. Orange oil at the greatest concentration tested (1%) reduced mean severity to 60%, which was significantly less than from the fludioxonil treatment. OR007B and OR79 gave similar results to fludioxonil, with greatest efficacy in the curative experiments from the 0.5% OR79 treatment (mean = 67% severity). Overall, all protective treatments of 'Laetitia' gave high mean grey mould severities (92 to 100%), with no effective disease control.

Although there was no statistically significant interaction between treatment and the day of evaluation ($P = 0.32$) for the dip applications of strawberries followed by 14 d of storage at 4°C, these results are discussed. There was a significant interaction ($P < 0.001$) between the evaluation days (i.e., day 14, the evaluation conducted at the end of cold storage, and day 17, 3 d at ambient temperature). On day 14, mean grey mould incidence was

reduced from 82% in the untreated control to means of 55% for OR79, 21% for OR007B, and 45% for orange oil alone (Table 3). On day 17, fruit became severely affected by grey mould.

Influence of incubation period for plums and lemon fruit

The incubation period experiments conducted with 'Angelino' plums gave significant interactions ($P < 0.0001$) between incubation period and treatment, for both severity and incidence of sporulation incidence data. Only fludioxonil at 8 h reduced disease level (mean = 69%), while the other treatments gave a disease incidence of > 80%. For disease incidence, fludioxonil reduced sporulation incidence with shorter incubation period (mean incidence = 20% after 8 h, and 37% after 24 h. The shorter incubation period for the OR007B and OR79 formulations resulted in decreased sporulation incidence, with increasing formulation the concentrations (means = 69 to 59% for OR007B, and 61 to 35% for OR79).

Table 3. Mean percent incidence of grey mould after 14 d at 4°C and 17 d (14 d plus 3 d incubation at 25°C) on strawberries following curative treatments with orange oil only at 0.05, 0.1, 0.5 or 1%, OR007B (%% orange oil) and OR79 (10% orange oil adjusted to orange oil concentrations of 0.05, 0.1 or 0.5%.

Treatment	Mean grey mould incidence (%)	
	Day 14	Day 17
Control	82 b	98 a
Orange oil 0.05%	42 c	98 a
Orange oil 0.1%	48 c	98 a
Orange oil 0.5%	45 cd	94 a
Orange oil 1%	64 c-e	98 a
OR007B 0.05%	36 de	94 a
OR007B 0.1%	35 e	97 a
OR007B 0.5%	21 c-e	95 a
OR79 0.05%	58 cd	98 a
OR79 0.1%	58 c-e	98 a
OR79 0.5%	55 b-d	98 a

Means accompanied by the same letters are not significantly different ($P > 0.05$).

Figure 2. Brown discolouration and rind damage for 'Eureka' lemons following thyme oil applications (0.05 to 0.5%), using dip applications, against *Penicillium digitatum*. **A,** thyme oil at 0.05%. **B,** thyme oil at 0.5%.

Table 4. Mean percent green mould incidence and sporulation incidence after 4 d at 25°C, on wound inoculated Eureka' lemons with either imazalil sensitive or resistant *Penicillium digitatum* isolates, after 8 h or 24 h incubation ', following curative treatments with imazalil (IMZ) at 500 mg.L $^{-1}$, or orange oil (0.05, 0.1, 0.5 or 1.0%), OR007B (5% orange oil) and OR79 (10% orange oil) adjusted to orange oil concentrations of 0.05, 0.1 and 0.5%.

Treatment	Mean green mould incidence (%)		Sporulating fruit (%)	
	IMZ-sensitive	IMZ-resistant	IMZ-sensitive	IMZ-resistant
8 h				
Control	96.6 a-d	96.6 a-d	99.4 ab	99.4 ab
Imazalil 500 µg mL ^{1}	0.0 n	28.6 l	16.2 e	95.7 e
Orange oil 0.05%	96.6 a-d	91.1 a-d	99.4 ab	99.4 ab
Orange oil 0.1%	96.6 a-d	96.6 a-d	99.4 ab	99.4 ab
Orange oil 0.5%	96.6 a-d	96.6 a-d	99.4 ab	99.4 ab
Orange oil 1.0%	96.6 a-d	95.9 a-d	99.4 ab	99.4 ab
OR-007B 0.05%	96.6 a-d	96.6 a-d	99.4 ab	99.4 ab
OR-007B 0.1%	84.5 gh	96.6 a-d	99.4 ab	99.4 ab
OR-007B 0.5%	77.2 ij	77.9 ij	99.4 ab	99.4 ab
OR-79 0.05%	96.6 a-d	96.6 a-d	99.4 ab	99.4 ab
OR-79 0.1%	96.6 a-c	93.8 b-e	99.4 ab	99.4 ab
OR-79 0. %	81.3 f-h	92.4 c-e	96.7 a-c	99.4 ab
24 h				
Control	100.0 a	100.0 a	100.0 a	100.0 a
Imazalil 500 µg mL ^{1}	5.5 m	52.7 k	19.6 e	93.1 cd
Orange oil 0.05%	100.0 a	100.0 a	100.0 a	100.0 a
Orange oil 0.1%	100.0 a	100.0 a	100.0 a	97.2 ab
Orange oil 0.5%	100.0 a	100.0 a	100.0 a	100.0 a
Orange oil 1.0%	97.9 a-c	100.0 a	100.0 a	100.0 a
OR-007B 0.05%	75.3 j	100.0 a	100.0 a	100.0 a
OR-007B 0.1%	85.4 gh	99.3 ab	100.0 a	92.5 d
OR-007B 0.5%	93.4 e-g	100 a	100.0 a	100.0 a
OR-79 0.0 %	99.3 a	99 a	100.0 a	100.0 a
OR-79 0.1%	97.2 a-c	100 a	100.0 a	95.8 ab
OR-79 0.5%	85.7 f-h	100 a	100.0 a	100.0 a

Means accompanied by the same letters are not significantly different ($P > 0.05$).

Table 5. Mean percent incidence of green mould after 4 d at 25°C on 'Eureka' lemons and 'Midnight Valencia' oranges that were wound inoculated with a imazalil (IMZ) sensitive or resistant *Penicillium digitatum* isolates and incubated for 12 h following dip treatments (60, 90 and 120 s exposure time), including: IMZ at 500 mg.L $^{-1}$, orange oil (0.5 or 1%), OR007B (5% orange oil) and OR79 (10% orange oil) adjusted to orange oil concentrations of 0.5 and 1.0%.

Treatment	Exposure time (s)	Mean green mould incidence (%)			
		'Eureka' lemon		'Midnight Valencia' orange	
		IMZ-sensitive	IMZ-resistant	IMZ-sensitive	IMZ-resistant
Control	0	100 a	100 a	99.3 a	100 a
IMZ	60	3.1 n	40.9 m	0.2 p	0.2 p
Orange oil 0.5%	60	99.6 ab	97.9 ab	99.1 a	96.9 a-c
Orange oil 1.0%	60	96.6 a-d	95.9 a-c	99.4 a	99.4 a
OR-007B 0.5%	60	93.4 a-g	82.9 d-i	77.3 j-m	90.1 a-g
OR-007B 1.0%	60	73.9 i-k	73.2 i-k	79.8 d-j	72.3 f-j
OR-79 0.5 %	60	94.7 a-d	81.5 e-j	84 g-k	77.4 i-n
OR-79 1.0 %	60	73.9 i-k	58.6 l	67.4 m-o	64.6 no
Orange oil 0.5%	90	99.6 ab	90.9 a-g	97.7 ab	95.5 a-e
Orange oil 1.0%	90	91.6 a-f	93.7 a-g	94.8 a-f	99.1 a
OR-007B 0.5%	90	87.2 b-h	80.9 g-j	90.2 a-h	85.3 c-i
OR-007B 1.0%	90	78.1 h-k	69.0 kl	68.9 g-l	70.5 j-n
OR-79 0.5 %	90	94.1 a-e	81.1 i-j	77.1 i-m	83.5 d-j
OR-79 1.0 %	90	76.7 i-k	45.5 m	64.2 no	61.1 o
Orange oil 0.5%	120	90.9 a-g	94.7 a-g	98.7 a	98.4 ab
Orange oil 1.0%	120	94.4 a-d	95.5 a-d	99.8 a	91.3 a-g
OR-007B 0.5%	120	84.0 f-j	81.2 c-i	84.2 g-k	83.1 ab
OR-007B 1.0%	120	87.3 a-h	66.8 j-l	80.5 k-o	75.5 k-o
OR-79 0.5 %	120	95.1 a-d	72.2 i-k	83.1 f-j	85.9 b-i
OR-79 1.0 %	120	76.3 h-k	70.0 j-l	74.7 i-n	68.0 l-o

Means accompanied by the same letters are not significantly different ($P > 0.05$).

Data for 'Eureka' lemon disease incidence data showed a significant disease incidence interaction ($P < 0.001$) between isolate, treatment, and incubation period. In preliminary tests, thyme oil was also assessed, to compare the effect on green mould with that from orange oil. Thyme oil was subsequently excluded from the main experiments due to host tissue damage observed immediately after treatment (Figure 2, A and B).

Imazalil showed reduced green mould control caused by the sensitive strain of *P. digitatum*, at both 8 h (mean = 0%) and 24 h (5%), while the resistant strain of the fungus was reduced to 29% at 8 h and 53% at 24 h (Table 4). Although disease levels were high from all the other treatments, the OR007B formulation showed decreasing mean levels of disease incidence (97 to 77%) with increasing concentration, for the sensitive strain after 8 h incubation. Greater amounts of sporulation incidence were observed following imazalil treatment except for the sensitive isolate.

Influence of exposure time (lemons and sweet oranges)

A statistically significant interaction for disease incidence ($P < 0.001$) was measured in 'Eureka' lemons between *P. digitatum* strains (sensitive or resistant) and

treatment type. In contrast, no significant interaction ($P = 0.83$) was detected for 'Valencia' oranges.

On 'Eureka' lemons, the untreated control fruit inoculated with the sensitive or resistant strains resulted in 100% disease incidence (Table 5). Disease symptomatic fruit inoculated with the sensitive strain and treated with imazalil were found at reduced disease incidence (mean = 3%), and the fruit inoculated with the resistant strain had mean incidence of 41%. While the resistant strain gave greater disease incidence, this was less from the orange oil and orange oil-based formulations 1% concentrations. The OR007B formulation resulted in decreasing mean disease incidence levels (73 to 66%) with increasing exposure times in the treatment bath. Similarly, the OR79 formulation gave disease incidence levels between 45 and 70%. However, this trend was not observed for the sensitive strain. 'Valencia' oranges showed comparable results to the OR79 formulation. The resistant strain resulted in reduced mean level of disease incidence, between 61 and 68%, and some reduction was also detected (64 and 74%) for the sensitive isolate treatments.

DISCUSSION

This study is the first comprehensive investigation of the efficacy of orange essential oil products as options for postharvest disease management in plums, strawberries, and citrus. The manufacturer of these products indicated that the orange oil batch used in this study contained 97% d-limonene. This corresponded with the previous studies that have investigated composition of citrus oil, including orange oil (Caccioni *et al*., 1998; Sharifi-Rad *et al*., 2017; Ramírez-Gómez *et al*., 2020). The results obtained here have demonstrated the potential of orange oil for management of grey mould on plums and strawberries, using the fruit dip applications. Although these experiments were conducted *in vitro*, several studies demonstrated comparable results following applications of orange oil against several pathogens, including *B. cinerea* and *Aspegillus niger* Tiegh (Sharma and Tripathi, 2006; Viuda-Martos *et al*., 2008). Lemon oil was also reported to induce reductions of grey mould severity when evaluated on tomatoes, strawberries, and cucumbers (Vitoratos *et al*., 2013).

The present study showed that orange oil and orange oil-based formulations were not capable of reducing green mould caused *P. digitatum* on citrus, similar to results of Rodríguez *et al*. (2015), Wuryatmo *et al*. (2014), or the *in vitro* study by Droby *et al*. (2008), which found the adverse effect of growth stimulation of *P. digitatum* by volatiles emitted from citrus rind. Rahman (2020) on the other hand found orange oil only effectively controls *P. digitatum* on citrus, provided it was UV irradiated. However, the orange oil formulated products used here (OR007B and OR79), at 1% adjusted oil concentration, exhibited an interesting phenomenon during the evaluation of exposure times. When these products were tested against the imazalil resistant isolate of *P. digitatum,* a reduced disease incidence on lemons and sweet oranges was found compared to results of trials with the sensitive isolate. This could have been due to synergism within the formulations. For instance, apart from surfactants and inert compounds that are incorporated in the formulation, orange oil contains terpenes that have been individually extracted and tested against an imazalil resistant *P. digitatum* strain. Ouyang *et al*. (2022) showed that α-Terpineol inhibited disease by this fungus at a minimum concentration of 4.00 $\mu L\ mL^{-1}$, but also disrupted cell membrane integrity, reduced ergosterol content, and inhibited squalene synthase (ERG9) gene expression. Additionally, aldehydes such as Trans-2-hexenal-β-cyclodextrin, which are present in most essential oils, could also overcome genetic mutation of *P. digitatum*. Yuan *et al*. (2023) showed that trans-2-hexenal-β-cyclodextrin interfered with the gene expression mediating the tricarboxylic acid cycle (an energy metabolism associated gene), glycolysis, and oxidative phosphorylation of an imazalil resistant strain. Since these results were not observed from the orange oil only treatments in the present study, it is likely that presence of surfactants within the formulations triggered the responses of the orange oil component compounds that were responsible for inhibition of the imazalil resistant pathogen strain. However, this concept requires further assessment to establish the mechanisms that are involved.

The attempt to incorporate thyme oil in the present study, by conducting pilot tests prior to the detailed investigation of potential bioactivity against green mould on citrus and grey mould on plums, was interrupted by elevated levels of phytotoxicity from thyme oil observed on the fruit, either directly after dip applications for citrus, or the day after treatment for plums. Although essential oils can cause phytotoxicity (Plaza *et al*., 2004), the present study is not the first to report phytotoxicity from thyme oil applications on fruit. Lopez-Reyes *et al*. (2013) demonstrated effects of thyme, oregano, savory oils against *B. cinerea* and *Monilinia laxa* on stone fruit. Although these treatments were highly effective, at 1% concentrations, phytotoxicity symptoms were observed, and at 10% the symptoms were exacerbated. Regnier *et al*. (2014) investigated seven essential oils (including thyme oil) for phytotoxicity, showing that of all the

oils, only those from *Mentha spicata* and *Geranium graveolens roseum* did cause browning or desiccation of the fruit rinds, and incorporation of essential oils with edible coatings did not result in rind damage.

Dip application was selected to apply the treatments in the present study. This method was used as a primary first step, to establish if orange oil was a potential postharvest disease management strategy against *B. cinerea* and *P. digitatum*. The fungicides fludioxonil and imazalil are registered for dip applications to, respectively, stone fruit and citrus. The industry norm in South Africa is to use atomiser sprays as postharvest applications of fludioxonil to plums. However, with the spray applications being preferred, it was important to assess whether dip application was a viable method for oranges. Erasmus *et al*. (2011) showed the superiority of dip application against green mould compared to spray application, and confirmed that the approved maximum residue limit for fludioxonil on plums (5 mg g^{-1}; DALRRD, 2021) was not exceeded. The residue level obtained in the present study was 1.03 mg g^{-1}. These results corresponded with those from previous studies on effectiveness of spray and dip applications, where spray application gave greater fruit residues than dip applications (Erasmus *et al*., 2011).

It is important to evaluate both curative and protective treatments when investigating postharvest disease management strategies, as fruit becomes injured during handling and packaging stages. Although disease incidence was high after the curative treatments, the orange oil gave similar control to that achieved with the registered standard, fludioxonil. The reduced performance of fludioxonil and orange oil treatments could have been due to the high inoculum levels used, meaning that the study was not a true depiction of commercial packhouse realities. Reducing the inoculum loads should be considered in future investigations.

Curative treatments of plums gave greater control compared to protective treatments. Du Plooy *et al*. (2009) reported similar results, following the application of several essential oils on citrus for control of *P. digitatum* causing green mould. Jenneker *et al*. (2024) also demonstrated efficacy against grey mould of thymol (the active compound in thyme oil) in edible coatings on plums. Thyme oil has also been reported to be fungistatic for *P. digitatum*, and has been successfully incorporated into packaging materials for oranges (Plaza *et al*., 2004). On citrus fruit in the present study, however, phytotoxicity of thyme oil was observed at all the tested concentrations in two separate experiments, so thyme oil was not used in the dip application investigations.

In a study on plums, preventive applications of fludioxonil gave poor control of postharvest decay compared to curative treatments with this fungicide (Förster *et al*., 2007). Edible fruit coatings are hydrophobic, and must act as barriers against moisture loss and entry by fungal pathogens (Njombolwana *et al*., 2013). Orange oil is lipophilic and hydrophobic, and should act as a barrier against *B. cinerea* when used as a protective treatment, although this was not assessed in the present study.

The 'African Delight' cultivar was less susceptible to grey mould than 'Laetitia'. Lopez-Reyes *et al*. (2013) also showed varying degrees of susceptibility of plum cultivars to grey mould. 'African Delight' is more prone to shrivelling than to grey mould (P. Rossouw, pers. comm.), and could have elevated epidermis resistance owing to a thicker cuticle, and increased levels of phenolics and pectin, differences which often occur between cultivars of the same species (Gradziel *et al*., 2003).

For strawberries, the industry heavily relies on synthetic fungicides for the control of *B. cinerea* during crop growth stages (Feliziani and Romanazzi, 2013; Fan *et al*., 2017). The available means for maintaining and preserving postharvest fruit quality are by direct cooling to 0 to 5°C directly after picking. (Haffner, 2002). The shelf life of strawberries is usually approx. 5 d, provided that temperatures are maintained between 0 and 4°C (Parvez and Wani, 2018). In the present study, beneficial effects were observed for orange oil and orange oil-based products to increased strawberry shelf-life period up to 14 days. Orange oil and commercial orange oil products could be recommended, as they pose no residue threats and are generally regarded as safe products. The 1% concentration of orange oil probably predisposed strawberries to postharvest disease, as the treated fruits y were generally softer than untreated fruit, a symptom that was suspected to be due to phytotoxicity. These results were similar to those of Lopez-Reyes *et al*. (2010; 2013) on long-term and cold storage evaluations of essential oils. They showed that these compounds could be useful for short storage periods. The present study evaluation conducted immediately after 14 d of cold storage at 4°C aligned closely with standard industry practices for maintaining strawberry quality. The observed loss of control during later evaluations (day 17) was anticipated, as strawberries are not typically exposed to ambient temperatures during supply chains.

This study adds to an expanding research database on the benefits of incorporating essential oils in postharvest disease management strategies for fruit products. However, their bioactivity is hampered by their volatility, which leads to oxidative deterioration especially when exposed to oxygen, light, moisture, and/or heat (Botrel *et al*., 2015; Maes *et al*., 2019). The next research step should focus on exploring fruit encapsulation, which

ensures that bioactivity of active ingredients is preserved, and less amounts are released, without causing harm to host tissues, but invasions by target fungi or bacteria are controlled (Pothakamury and Barbosa-Cánovas, 1995). Organoleptic characteristics of essential oil-based products and their volatile actives need to be evaluated through tasting panels of the treated fruit, unless methods are employed to remove strongly flavoured compounds, provided this does not reduce the antifungal activity of the respective essential oils. Once an appropriate formulation has been developed for oil application, trials can be upscaled to test large amounts of fruit (i.e., 500 fruit per treatment, and at commercial scales), including storage trials to simulate export conditions.

The present study forms part of a continuing effort to assess effects of orange oil against postharvest pathogens on selected fruit types. Orange oil has potential for post-harvest disease management. Future investigations should cover other plum cultivars, and for strawberries, should incorporate potential protective effects of orange oil and orange oil-based products.

ACKNOWLEDGMENTS

This study was funded by ORO AGRI SA (Pty) Ltd. The authors thank Elveresha Davids and Michell Leibrandt (Department of Plant Pathology, Stellenbosch University) for their technical support. The products used were supplied by ORO AGRI SA (Pty) Ltd and ICA International Chemicals (Pty) Ltd.

LITERATURE CITED

Andrade M.A., Barbosa C.H., Shah M.A., Ahmad N., Vilarinho F., … Ramos F., 2022. Citrus by-products: valuable source of bioactive compounds for food applications**.** *Antioxidants* 12: 38.

Botrel D.A., Fernandes R.V. de B., Borges S.V., 2015. Microencapsulation of Essential Oils Using Spray Drying Technology Chapter 12, In: *Microencapsulation and Microspheres for Food Applications,* pp. 235–251, Elsevier Academic Press, Amsterdam, The Netherlands, from https://doi.org/10.1016/B978-0-12-800350-3.00013-3

Caccioni D.R.L., Guizzardi M., Biondi, D.M., Renda A., Ruberto G., 1998. Relationship between volatile components of Citrus fruit essential oils and antimicrobial action on *Penicillium digitatum* and *Penicillium italicum*. *International Journal of Food Microbiology* 43: 1–2.

Cherono K. & Workneh T.S., 2018. A review of the role of transportation on the quality changes of fresh tomatoes and their management in South Africa and other emerging markets. *International Food Research* 25: 2211–2228.

Commission delegated regulation (EU) 2023/1656, 2023. amending Regulation (EU) No. 649/2012 of the European Parliament and of the Council as regards the listing of pesticides and industrial chemicals. Official Journal of the European Union 32023R1656.

Costa J.H., Bazioli J.M., de Moraes Pontes J.G., Fill T.P., 2019. *Penicillium digitatum* infection mechanisms in Citrus: What do we know so far? *Fungal Biology* 123: 584–593.

Department of Agriculture and Forestry (DAFF), 2010. Pesticide Management Policy (Act 36 of 1947). Pages 37–58.

DALRRD (Department of Agriculture Land Reform and Rural Development), 2021. Plums and prunes maximum residue limits (MRL) list. Food Safety and Quality Assurance. Available at https://dalrrd.gov.za/foodSafety

DALRRD (Department of Agriculture, Land Reform and Rural Development), 2023. Regulations relating to agricultural remedies. *Government Gazette* No. 3812.

Droby S., Eick A., Macarisin D., Cohen L., Rafael G. … Shapira R., 2008. Role of Citrus volatiles in host recognition, germination, and growth of *Penicillium digitatum* and *Penicillium italicum*. *Postharvest Biology and Technology* 49: 386–396.

Du Plooy W., Regnier T., Combrinck S., 2009. Essential oil amended coatings as alternatives to synthetic fungicides in Citrus postharvest management. *Postharvest Biology and Technology* 53: 117–122.

Erasmus A., Lennox C.L., Jordaan H., Smilanick J.L., Lesar K., Fourie P.H., 2011. Imazalil residue loading and green mould control in Citrus packhouses. *Postharvest Biology and Technology* 62: 193–203.

European Chemicals Agency, 2024. Classification, labelling and packaging. An agency of the European Union. Substance information: Imazalil sulphate. Available at https://echa.europa.eu/substance-information/-/substanceinfo/100.055.755

Fan F., Hamada M.S., Li N., Li G.Q., Luo C.X., 2017. Multiple fungicide resistance in *Botrytis cinerea* from greenhouse strawberries in Hubei Province, China. *Plant Disease* 101: 601–606.

Federal Register, 2014. Sweet orange peel tincture, exemption from the requirement of a tolerance. Environmental Protection Agency 40 CFR Part 80. Available at https://www.federalregister.gov/documents/2014/08/15/2014-19450/sweet-orange-peel-

tincture-exemption-from-the-requirement-of-a-tolerance

Feliziani E., Romanazzi G., 2013. Preharvest application of synthetic fungicides and alternative treatments to control postharvest decay of fruit. *Steward Postharvest Review* 3: 1–6.

Food and Drug Administration, 2006. How U.S. FDA's GRAS notification program works US Food and Drug Administration. Available at https://www.fda.gov/food/generally-recognized-safe-gras (02 September 2018).

Förster H., Driever G.F., Thompson D.C., Adaskaveg J.E., 2007. Postharvest decay management for stone fruit crops in California using the "reduced risk" fungicides fludioxonil and fenhexamid. *Plant Disease* 91: 209–215.

Fourie J.F., Holz G., 1985. Postharvest fungal decay of stone fruit in the South-Western Cape. *Phytophylactica* 17: 175–177.

Gradziel T.M., Bostock R.M., Adaskaveg J.E., 2003. Resistance to brown rot disease in peach is determined by multiple structural and biochemical components. *Acta Horticulturae* 622: 347–352.

Guo Q., Liu K., Deng W., Zhong B., Yang W., Chun J., 2018. Chemical composition and antimicrobial activity of Gannan navel orange (*Citrus sinensis* Osbeck cv. Newhall) peel essential oils. *Food Science and Nutrition* 6: 1431–1437.

Haffner K. 2002. Postharvest quality and processing of strawberries. *Acta Horticulturae* 567: 715–722.

Hamdan M., Jaradat N., Al-Maharik N., Ismail S., Qadi M., 2024.Chemical composition, cytotoxic effects and antimicrobial activity of combined essential oils from *Citrus meyeri, Citrus paradise*, and *Citrus sinensis* leaves. *Industrial Crops and Products* 210: 118096. https://doi.org/10.1016/j.indcrop.2024.118096

Hanafy S.M., El-Shafea Y.M.A., Saleh W.D., Fathy H.M. 2021. Chemical profiling, *in vitro* antimicrobial and antioxidant activities of pomegranate, orange and banana peel-extracts against pathogenic microorganisms. *Journal of Genetic Engineering and Biotechnology* 19: 80. https://doi.org/10.1186/s43141-021-00151-0

Hezakiel H.E., Thampi M., Rebello S. & Sheikhmoideen J.M. 2023. Biopesticides: a green approach towards agricultural pests. Applied biochemistry and biotechnology. *Pharmaceutics* 196: 5533–5562.

Jantrawut P., Boonsermsukcharoen K., Thipnan K., Chaiwarit T., Hwang K.M., Park E.S. 2018. Enhancement of antibacterial activity of orange oil in pectin thin film by microemulsion. *Nanomaterial* 8: 1–12.

Jenneker N., Silue Y., Meitz-Hopkins J.C., Lennox C.L., Opara U.L., Fawole O.A. 2024. Gum Arabic-incorporated thymol/salicylic acid composite coatings control grey mould and brown rot in 'Angeleno' plums. *European Journal of Plant Pathology* 170: 943–954. https://doi.org/1007/s10658-024-02888-z

John I., Muthukumar K., Arunagiri A., 2017. A review on the potential of Citrus waste for D-Limonene, pectin, and bioethanol production. *International Journal of Green Energy* 14: 599–612.

López-Reyes J.G., Spadaro D., Gullino M.L., Garibaldi A., 2010. Efficacy of plant essential oils on postharvest control of rot caused by fungi on four cultivars of apples *in vivo*. *Flavour and Fragrance Journal* 25: 171-177.

López-Reyes J.G., Spadaro D., Prelle A., Garibaldi A., Gullino M.L., 2013. Efficacy of plant essential oils on postharvest control of rots caused by fungi on different stone fruits *in vivo*. *Journal of Food Protection* 76: 631–639.

Lucintel, 2024. Pesticide Market: Trends, Opportunities and Competitive Analysis. 8951 Cypress Waters Blvd, Suite 160 Dallas, TX 75019, USA.

Macarisin D., Cohen L., Eick A., Rafael G., Belausov E., … Droby, S.. 2007. *Penicillium digitatum* suppresses production of hydrogen peroxide in host tissue during infection of Citrus fruit. *Phytopathology* 97: 1491–1500.

Maes C., Bouquillon S., Fauconnier M.L., 2019. Encapsulation of essential oils for the development of biosourced pesticides with controlled release: A review. *Molecules* 24: 1–15.

Mudzunga M.J., 2022. Phase-out of active ingredients and formulations that meet the criteria of carcinogenicity, mutagenicity, and reproductive toxicity categories 1A or 1B of the globally harmonized system of classification and labelling of chemicals. Agriculture, Land Reform and Rural Development of South Africa.

Nelson R.M., 2010. Quality challenges facing the South African avocado industry – An overview of the 2009 South African avocado season. *SAAGA* 33: 7–13.

Njombolwana N.S., Erasmus A., van Zyl J.G., du Plooy W., Cronje P.J.R., Fourie P.H., 2013. Effects of Citrus wax coating and brush type on imazalil residue loading, green mould control and fruit quality retention of sweet oranges. *Postharvest Biology and Technology* 86: 362–371.

Njombolwana N., Meitz-Hopkins J.C., Monteiro S., Lennox C. 2022. Postharvest decay control of plums using orange oil. *Proceedings V IS on Pomegranate and Minor Mediterranean Fruits. Acta Horticulturae* 1349: 189–194.

Ouyang Q., Liu Y., Chen Y., Tao N., 2022. Antifungal action of α-terpineol on imazalil-resistant *Penicillium digitatum* Pdw03. *Food Science* 43: 8–13.

Palou L., Ali A., Fallik E., Romanazzi G., 2016. GRAS, plant- and animal-derived compounds as alternatives to conventional fungicides for the control of postharvest diseases of fresh horticultural produce. *Postharvest Biology and Technology* 122: 41–52.

Parvez S. & Wani I.A., 2018. Postharvest Biology and Technology of Strawberry. In: *Postharvest Biology and Technology of Temperate Fruits* (Mir, S.A., Shah, M.A. and Mir, M.M., ed) Springer, Cham., Switzerland. pp. 331-348, from https://www.springerprofessional.de/en/postharvest-biology-and-technology-of-temperate-fruits/15801108

Pejin B., Vujisic L., Sabovljevic M., Tesevic V., Vajs V., 2011. Preliminary data on essential oil composition of the moss *Rhodobryum ontariense* (Kindb.) Cryptogamie. *Bryologie* 32: 113–117.

Plaza P., Torre, R. Usall, J. Lamarca N., Ninas I., 2004. Evaluation of the potential of commercial post-harvest application of essential oils to control Citrus decay. *Journal of Horticultural Science and Biotechnology* 79: 935–940.

Pothakamury U.R., Barbosa-Cánovas G. V., 1995. Fundamental aspects of controlled release in foods. *Trends In Food Science and Technology* 6: 397–406.

Radi M., Akhavan-Darabi S., Akhavan H.R., Amiri S., 2018. The use of orange peel essential oil microemulsion and nanoemulsion in pectin-based coating to extend the shelf life of fresh-cut orange. *Journal of Food Processing and Preservation* 42(2): e13441. https://doi.org/10.1111/jfpp.13441

Rahman M.M., Wills, R.B., Bowyer M.C., Golding J.B., Kirkman T., Pristijono P., 2020. Efficacy of orange essential oil and citral after exposure to UV-C irradiation to inhibit *Penicillium digitatum* in navel oranges. *Horticulturae* 6(4): 102. https://doi.org/10.3390/horticulturae6040102

Ramírez-Gómez X.S., Jiménez-García S.N., Campos V.B., Lourdes M. Campos G., 2020. Plant Metabolites in Plant Defence Against Pathogens. In: *Plant Disease-Current Threats and Management Trends.* (S. Topolovec-Pintaric, ed.) pp. 1-20. InTechOpen Ltd., London, UK, from: https://doi.org/10.5772/intechopen.87958

Rammanee K., Hongpattarakere T., 2011. Effects of tropical Citrus essential oils on growth, aflatoxin production, and ultrastructure alterations of *Aspergillus flavus* and *Aspergillus parasiticus*. *Food and Bioprocess Technology* 4: 1050–1059.

Regnier T., Combrinck S., Veldman W., du Plooy W., 2014. Application of essential oils as multi-target fungicides for the control of *Geotrichum citri-aurantii* and other postharvest pathogens of Citrus. *Industrial Crops and Products* 61: 151–159.

Rodríguez A., Shimada T., Cervera M., Redondo A., Alquézar B., Rodrigo M.J., …. López M.M., Peña L., 2015. Resistance to pathogens in terpene down-regulated orange fruits inversely correlates with the accumulation of D-limonene in peel oil glands. *Plant Signalling and Behaviour* 10: e1028704. https://doi.org/10.1080/15592324.2015.1028704.

Sharifi-Rad J., Sureda A., Tenore G.C., Daglia M., Sharifi-Rad M., Valussi M.,… Iriti M., 2017. Biological activities of essential oils: from plant chemoecology to traditional healing systems. *Molecules* 22: 70. https://doi.org/10.3390/molecules22010070

Sharma N., Tripathi A., 2006. Fungitoxicity of the essential oil of *Citrus sinensis* on postharvest pathogens. *World Journal of Microbiology and Biotechnology* 22: 587–593.

Shi Y., Huang S., He Y., Wu J., Yang Y., 2018. Navel orange peel essential oil to control food spoilage molds in potato slices. *Journal of Food Protection* 81(9): 1496–1502.

Sişman T., Türkez H., 2010. Toxicologic evaluation of imazalil with particular reference to genotoxic and teratogenic potentials. *Toxicology and Industrial Health* 26: 641–648.

Smilanick J.L., Michael I.F., Mansour M.F., Mackey B.E., Margosan D.A., … Weist C.F., 1997. Improved control of green mould of Citrus with imazalil in warm water compared with its use in wax. *Plant Disease* 81: 1299–1304.

Smilanick J.L., Mansour M.F., Margosan D.A., Gabler F.M., Goodwine W.R., 2005. Influence of pH and $NaHCO_3$ on effectiveness of imazalil to Inhibit germination of *Penicillium digitatum* and to control postharvest green mould on Citrus fruit. *Plant Disease* 89: 640–648.

Stander C., Van Dyk F.E., 2017. Maintaining cold chain integrity: Temperature breaks within fruit reefer containers in the Cape Town Container Terminal. *Southern African Business Review* 21:362–384.

Talibi I., Boubaker H., Boudyach E.H., Aoumar A.A. Ben, 2014. Alternative methods for the control of postharvest Citrus diseases. *Applied Microbiology* 117: 1–17.

Tao H., Bao Z., Jin C., Miao W., Fu Z., Jin Y., 2020. Toxic effects and mechanisms of three commonly used fungicides on the human colon adenocarcinoma cell line Caco-2. *Environmental Pollution* 263: 114660.

Tao N.G., Liu Y.J., Zhang M.L., 2009. Chemical composition and antimicrobial activities of essential oil from the peel of bingtang sweet orange (*Citrus sinensis* Osbeck). *International Journal of Food Science and Technology* 44: 1281–1285.

Tripathi P., Dubey N.K., 2004. Exploitation of natural products as an alternative strategy to control postharvest fungal rotting of fruit and vegetables. *Postharvest Biology and Technology* 32: 235–245.

Tsao R., Zhou T., 2000. Antifungal activity of monoterpenoids against postharvest pathogens *Botrytis cinerea* and *Monilinia fructicola*. *Journal of Essential Oil Research* 12: 113–121.

Vitoratos A., Bilalis D., Karkanis A., Efthimiadou A., 2013. Antifungal Activity of Plant Essential Oils Against *Botrytis cinerea*, *Penicillium italicum* and *Penicillium digitatum*. *Notulae Botanicae* 41: 86–92.

Viuda-Martos M., Ruiz-Navajas Y., Fernández-López J., Pérez-Álvarez J., 2008. Antifungal activity of lemon (*Citrus lemon* L.), mandarin (*Citrus reticulata* L.), grapefruit (*Citrus paradisi* L.) and orange (*Citrus sinensis* L.) essential oils. *Food Control* 19: 1130–1138.

Wuryatmo E., Able A.J., Ford C.M., Scott E.S., 2014. Effect of volatile citral on the development of blue mould, green mould, and sour rot on navel orange. *Australasian Plant Pathology* 43: 403-411.

Yuan X., Meng, K. Shi S., Wu Y., Chen X., ... Tao N., 2023. Trans-2-hexenal inhibits the growth of imazalil-resistant *Penicillium digitatum* Pdw03 and delays green mould in postharvest Citrus. *Postharvest Biology and Technology* 199: 112304. https://doi.org/10.1016/j.postharvbio.2023.112304

Zareiyan F., Khajehsharifi H., 2021. Analyzing bioactive compounds in essential oil of *Citrus maxima* and *Citrus sinensis* peel. *Journal of Essential Oil Bearing Plants* 24(4): 677–682.

Ziedan E. S. H., Saad M. M., El-Kafrawy A. A., Sahab A. F., Mossa A. T. H., 2022. Evaluation of essential oils nanoemulsions formulations on *Botrytis cinerea* growth, pathology, and grey mould incidence on cucumber fruits. *Bulletin of the National Research Centre* 46(1): 88.

Phytopathologia Mediterranea
The international journal of the
Mediterranean Phytopathological Union

Firenze University Press
www.fupress.com/pm

Short Notes

Pea seed-borne mosaic virus pathotypes isolated from Australian pea (*Pisum sativum*) seed

Joop VAN LEUR[1,*], Mohammad AFTAB[2], Angela FREEMAN[2]

[1] *New South Wales Department of Primary Industries and Regional Development, Tamworth Agricultural Institute, Tamworth, Australia*
[2] *Agriculture Victoria, The Grains Innovation Park, Horsham, Australia*
*Corresponding author. E-mail: joop.vanleur@dpi.nsw.gov.au

Summary. Pea seed lots (144) from Australian farms and research trials were assessed for pea seed-borne mosaic virus (PSbMV) seed transmission rates. High infection rates (up to 40%) were detected, particularly in the widely grown and highly PSbMV susceptible variety 'Kaspa', with only 12 out of 54 seed lots found to be free of the virus. PSbMV strains were isolated from 15 infected seed lots, and were pathotyped on a set of homogeneous *Pisum sativum* PSbMV differentials. Of the four pathotypes identified, P1 and P4 (eight and 20 isolates, respectively) were earlier reported in Australia. Pathotype P3, as yet unreported in Australia, was the most frequently identified pathotype (42 isolates). One PSbMV isolate was identified as the P2 pathotype, which has previously been isolated only from lentil seed. None of the isolated pathotypes could overcome the PSbMV resistance gene *sbm1*. The relevance of these findings for field pea breeding programmes and genomic studies of PSbMV are discussed.

Keywords. PSbMV, BYMV, virus resistance, pathogenicity test.

Citation: van Leur, J., Aftab, M. & Freeman, A. (2025). Pea seed-borne mosaic virus pathotypes isolated from Australian pea (*Pisum sativum*) seed. *Phytopathologia Mediterranea* 64(1): 71-76. doi: 10.36253/phyto-15934

Accepted: April 16, 2025

Published: May 15, 2025

Data Availability Statement: All relevant data are within the paper and its Supporting Information files.

Competing Interests: The Author(s) declare(s) no conflict of interest.

Editor: Arnaud G Blouin, Institut des sciences en production végétale IPV, DEFR, Agroscope, Nyon, Switzerland.

ORCID:
JvL: 0000-0003-4640-7423
MA: 0009-0003-8346-9743
AF: 0009-0003-2984-3087

INTRODUCTION

Pea seed-borne mosaic virus (PSbMV, *Potyvirus pisumsemenportati*) is present in field pea (*Pisum sativum*) in many countries, probably because the virus is seed transmitted at high rates. Distribution of this virus, seed transmission, host and vector range, and symptomatology have been reviewed extensively (Khetarpal and Maury, 1987; Congdon, 2017). Depending on the pea genotype, PSbMV symptoms can be difficult to identify in the field, and serological or molecular tests are required to determine its presence in host plants.

Cultivation of field pea, and of winter pulses in general, is recent in Australia (Siddique and Sykes, 1997), and it was not until 1991 that PSbMV was reported in commercial pea crops (Ligat *et al.*, 1991). Later surveys showed that the virus is widespread in Australia's pea crops, both in the western (Latham and Jones, 2001a, Congdon *et al.*, 2016) and eastern (Freeman *et al.*, 2013) regions of the country.

PSbMV causes considerable yield losses in Australian field peas, despite the generally mild symptoms it causes (Coutts *et al*., 2009), and the level of PSbMV infection in a pea crop is closely related to the level of seed-transmission in the seed stock used (Coutts *et al*., 2009; Freeman *et al*., 2013). Use of virus-free seed would therefore provide adequate control of PSbMV-induced yield losses. However, the virus can be introduced from neighbouring infested fields, and Australian pea growers generally save their own seed and rarely test the seed stocks for virus presence. Host resistance will provide a lasting control option, and the Australian field pea breeding programme has made the incorporation of PSbMV resistance in new varieties a priority (Rosewarne, 2016).

Breeding peas for PSbMV resistance is facilitated by the availability of single recessive genes in the host that provide immunity, and these can be identified in seedling tests using mechanical inoculations. Provvidenti and Alconero (1988) proposed four independent recessive resistance genes, *sbm1*, *sbm2*, *sbm3* and *sbm4*, to explain the differential reactions to the three PSbMV pathotypes, P1, P4 and P2, reported at the time (Alconero *et al*., 1986). The gene *sbm1* conferred resistance to P1, *sbm2* and *sbm3* conferred resistance to P2, and *sbm4* gave resistance to P4. These authors also reported strong linkages between gene *sbm2* and the *mo* resistance gene for bean yellow mosaic virus (BYMV) and between *sbm1*, *sbm3* and *sbm4* resistance genes. Johansen *et al*. (2001) showed that the differences between the three PSbMV pathotypes could be explained by the properties of two viral cistrons, and predicted the existence of a fourth pathotype, P3. The P3 pathotype was subsequently isolated from seed of a faba bean gene-bank accession originating from Nepal (Hjulsager *et al*., 2002). Gao *et al*. (2004) showed that only two recessive resistance genes were operating in the pea/PSbMV pathosystem. The *sbm1* gene (present in a range of germplasm of Indian and Ethiopian origin), confers resistance to all four PSbMV pathotypes (P1, P2, P3, P4), while a different allele of the *sbm1* gene, $sbm1^1$ (present in the germplasm accessions PI 269774 and PI 269818), gives resistance only to the P1 and P2 pathotypes, and the *sbm2* gene (in 'Dark Skin Perfection' and a large number of commercial pea lines) only provides resistance to pathotypes P2 and P3. The use of two differentials, one with the $sbm1^1$ gene and one with the *sbm2* gene, allows the classification of PSbMV to one of the four pathotypes (Table 1).

Within Australia, limited attention has been given to pathotyping of PSbMV strains. Ligat and Randles (1993) pathotyped three Australian isolates as P1 (one isolate) or P4 (two isolates), using a differential set of six pea genotypes. Torok and Randles (2007) pathotyped 14 Australian PSbMV isolates, and classified ten as P4 and four as the P1 pathotype.

Table 1. Differentiation of four PSbMV pathotypes by two pea genotypes with specific resistances (modified from Johansen *et al*., 2001, and Gao *et al*., 2004).

		sbm2 differential	
		Resistant	Susceptible
$sbm1^1$ differential	Resistant	P2	P1
	Susceptible	P3	P4

For pea breeding programmes to successfully incorporate PSbMV resistance, knowledge is required of the composition of the local PSbMV strain population. The present study isolated PSbMV strains from pea seed originating from geographically distinct locations in Australia, and pathotyped the isolates using a differential set of homogeneous pea genotypes.

MATERIAL AND METHODS

Tissue blot immunoassays (TBIA) were used for all virus diagnostics, as these provide a reliable, rapid, and cost-efficient methodology for processing large numbers of plant samples (Freeman *et al*., 2013; van Leur *et al*., 2013a). Samples were each blotted onto nitrocellulose membranes (Schleiger & Schuell Protran, 0.45 µm pore size), and were processed using a polyclonal PSbMV antibody (DSMZ, AS-0129), following the procedures described by Kumari *et al.* (2022).

PSbMV seed-to-plant transmission (PSbMV-SPT) rates were determined from 144 seed lots (92 harvested from farmer fields and 52 from trial fields), submitted to the Tamworth laboratory for PSbMV seed testing during 2006-2010. 'Kaspa' was the predominant cultivar in this evaluation, with 54 seed lots, followed by 'Excell' (18 seed lots), 'Morgan' (12), and 'Parafield' (nine).

Seeds were incubated on wet filter paper at 22°C in the dark for 7-10 d, after which plumules or radicles of the germinated seeds were tested for PSbMV presence by TBIA. Seed lots were first tested in batches of 30 seeds. A sequential sampling approach was later taken, with further tests made on seed lots that had low infection levels. For most seed lots, more than 90 seeds were tested. The PSbMV-SPT rate was calculated as:

100 × (total number of PSbMV positive germlings / total number of germinated seeds).

To isolate PSbMV strains, 20 seed lots were selected. This selection was based on PSbMV-SPT rates, but also included a range of varieties and seed sources, from three Australian states New South Wales (NSW), Western Australia (WA) and Victoria. For each selected seed lot, 20 small pots were sown with three seeds/pot, using a commercial potting mix, and the pots were then held in an aphid-proof, temperature-controlled (18–24°C) greenhouse. Two to 3 weeks after sowing, all emerged plants were tested by TBIA, and PSbMV positives were selected. The PSbMV strains were isolated by inoculating 2- to 3-week-old plants of the faba bean variety 'Fiesta' with individual PSbMV positive seedlings, using the inoculation methods described below. PSbMV presence in the faba bean plants was confirmed with TBIA prior to pathogenicity tests.

Three PSbMV pea lines with reported single resistance genes (Hjulsager *et al*., 2002; Gao *et al*., 2004), including PI 269774 (*sbm1*[1] gene), Dark Skin Perfection (*sbm2*) and PI 193835 (*sbm1*) were obtained from the Australian Grains Genebank (Horsham, Australia). To ensure host plant homogeneity, single plant selections were made from these lines prior to testing. For pathogenicity tests, four to five plants each of the three differentials, and a universally susceptible pea line ('Kaspa') were inoculated 10 to 14 d after sowing, by dusting first and second leaves of each plant with carborundum powder (silicon carbide # 400), and rubbing into the leaves a virus suspension from young virus-infected faba bean leaves. The suspension was prepared by homogenisation of the faba bean leaves in a cold 0.1 M sodium phosphate buffer (pH = 7.0). Each inoculation was repeated after one week on the third leaves of the plants. Two weeks after the second inoculation, the plants were TBIA-tested for virus presence. Virus isolates that gave variable results, or failed to infect the susceptible 'Kaspa' plants, were retested.

RESULTS AND DISCUSSION

PSbMV seed infections were common in the 144 submitted seed lots assessed, with 52 seed lots PSbMV-free and 47 having PSbMV-SPT rates greater than 5% (Table 2). 'Kaspa' and 'Excell' were found to be particularly susceptible to PSbMV seed infection, with only 12 (22%) 'Kaspa' seed lots PSbMV-free and 25 (46%) with infection levels greater than 5%. For 'Excell', five (27%) seed lots were PSbMV-free and six (33%) had infection levels greater than 5%. In contrast, ten out of 12 seed lots of 'Morgan' were PSbMV-free, although this variety does not contain any of the *sbm* genes for PSbMV resistance (van Leur *et al*., 2013a). The greatest PSbMV-SPT rate, 40%, was found in an 'Excell' seed lot from a trial plot at the Wagga Wagga Agricultural Institute, NSW. The greatest 'Kaspa' infection, 25%, was from a trial plot at the Plant Breeding Institute at Narrabri, NSW. Greater infection levels were found in seed originating from research stations as compared to farmer fields; out of nine 'Kaspa' seed lots harvested from trial fields, four (44%) had PSbMV-SPT levels >10%, while nine out of 45 'Kaspa' seed lots (20%) harvested in farmer fields had similar infection levels. Similarly, for all seed lots combined, 37 of 52 (71%) seed lots harvested from trial fields, and ten of 92 (11%) from farmer fields, had PSbMV-SPT levels >10%. These differences are probably a result of research stations growing a wide range of germplasm, including highly susceptible genotypes that can be inoculum reservoirs for viruses and virus vectors.

Table 2. Pea seed-borne mosaic virus seed-to-plant transmission (PSbMV-SPT) rates for 144 pea seed lots, tested during 2006 to 2010.

Variety	Harvested from farmer fields					Harvested from trial fields					Grand total
	Number of seed lots / PSbMV-SPT category				Total seed lots	Number of seed lots / PSbMV-SPT category				Total seed lots	
	0%	>0% ≤5%	>5% ≤10%	>10%		0%	>0% ≤5%	>5% ≤10%	>10%		
Kaspa	9	15	12	9	45	3	2	0	4	9	54
Excell	4	5	5	1	15	1	1	0	1	3	18
Morgan	9	1	1	0	11	0	1	0	0	1	12
Parafield	4	3	0	0	7	0	1	0	1	2	9
Other varieties[a]	8	5	1	0	14	14	11	8	4	37	51
Total	34	29	19	10	92	18	16	8	10	52	144

[a] Other varieties: 'Alezan', 'Alma', 'Bluey', 'Bonzer', 'Bundi', 'Collegian', 'Celine', 'Cooke', 'Cressy Blue', 'Derrimut', 'Dun', 'Dundale, 'Dunwa', 'Early Dunn', 'Glenroy', 'Helena', 'Jupiter', 'Laura', 'Moonlight', 'Mukta', 'Santi', 'Snowpeak', 'Soupa', 'Sturt', 'Wirrega'.

Table 3. Origins and pathotypes of the PSbMV isolates detected in this study.

Lot No.	Pea variety	Origin, State	Harvest year	% PSbMV-SPT	Isolates pathotyped	Isolates per pathotype			
						P1	P2	P3	P4
1	Kaspa	Farmer field, WA	2008	16	6			4	2
2	Kaspa	Farmer field, WA	2008	39	10			7	3
3	Kaspa	Farmer field, southern NSW	2010	3	2				2
5	Bluey	Trial field, Wagga Wagga, NSW	2005	13	4			1	3
7	Moonlight[a]	Trial field, Wagga Wagga, NSW	2007	13	4	3			1
8	Alezan	Trial field, Narrabri, NSW	2008	12	5	2		2	1
9	Parafield	Trial field, Horsham, Victoria	2006	14	4			3	1
10	Excell	Trial field, Wagga Wagga, NSW	2006	52	10	1		5	4
11	Kaspa	Trial field, Narrabri, NSW	2008	25	8	1		6	1
12	Kaspa	Farmer field, southern NSW	2008	15	7			6	1
13	Dundale	Trial field, Wagga Wagga, NSW	2005	19	4		1	2	1
14	Kaspa	Farmer field, Scaddan, WA	2006	20	2			2	
15	Parafield	Farmer field, Esperance, WA	2006	9	1			1	
16	Excell	Farmer field, southern NSW	2008	9	3			3	
18	Soupa[a]	Trial field, Wagga Wagga, NSW	2006	8	1	1			
Total number of isolates tested/pathotyped					71	8	1	42	20

[a] Indicates varieties resistant to bean yellow mosaic virus (van Leur *et al*., 2013a).

Out of the 20 selected seed lots, five did not yield PSbMV. From the remaining 15 seed lots, 88 PSbMV strains were isolated of which 71 were pathotyped (Table 3). None of the isolates infected PI 193835, confirming the effectiveness of the *sbm1* gene against all known PSbMV pathotypes. Both the P1 pathotype (with eight isolates identified), and the P4 pathotype (20 isolates identified), were previously reported in Australia (Ligat and Randles, 1993; Torok and Randles, 2007). The most frequently found pathotype was P3, with 42 isolates able to infect PI 269774 (containing *sbm1*^{1}), but not 'Dark Skin Perfection' (containing *sbm2*). The pathotype P3 has not been recorded in Australia previously, but previous studies (Ligat and Randles, 1993; Torok and Randles, 2007) may have missed this pathotype because they did not use a reliable *sbm2* differential. Ligat *et al.* (1991) compared symptom development of four Australian PSbMV isolates with an American isolate on a range of pea varieties, and noted that the Australian isolates did not infect the BYMV resistant pea variety 'Greenfeast'. This could indicate that the Australian isolates were P3 pathotypes.

Identification of a single P2 pathotype strain (isolate Ps11-13/19) from a 'Dundale' seed lot originating from the Wagga Wagga Agricultural Institute (NSW) field trial was unexpected. To date, P2 pathotypes have only been isolated from lentil seed (Hampton, 1982; Alconero *et al*., 1986; van Leur *et al*., 2013b). Wylie et al. (2011) reported a P2 pathotype (isolate W1) obtained from a pea plant grown at the Medina Research Station near Perth, WA (Latham and Jones, 2001a). Latham and Jones (2001b) noted severe PSbMV symptoms in germplasm plots at this station that could have been caused by exotic virus strains, and the W1 strain could have originated from imported lentil germplasm. Ashby *et al.* (1986) pathotyped a PSbMV strain isolated from peas in New Zealand using *sbm1*, *sbm1*^{1}, and *sbm2* differentials, and found that the strain reacted as a P2 pathotype. PSbMV is common in New Zealand lentil crops (Fletcher, 1993), and cross-infection of pea crops from lentil seed-borne PSbMV could have occurred. While isolate Ps11-13/19 originated from a pea seed, the seed was harvested at a research station where a wide range of legume germplasm, including lentils, is grown. The infection of the mother plant could have originated from a seed-infected lentil plant.

Identification of P3 and P2 pathotypes depends on their inability to infect *sbm2* differentials. Alconero *et al.* (1986) noted that their P4 strain had delayed and erratic infection in pea lines that had the *mo*/*sbm2* gene. The present study showed that infection of the 'Dark Skin Perfection' differential was occasionally not detected on all inoculated plants, despite the use of homogenous differentials derived from single seed progenies. However, the identities of the P2 and P3 pathotypes were confirmed with repeated inoculations of 'Dark Skin Perfection' and pea varieties such as 'Greenfeast' and 'Bundi', that showed BYMV resistance in previous trials (van Leur *et al*., 2013a).

Pathotyping of PSbMV strains is required for pea breeding programmes, but these biological tests are time consuming. Developments in the gathering and analyses of genetic information using molecular methods may enable rapid PSbMV pathotype identification. To date, phylogenetic analyses of PSbMV strains have been achieved for limited numbers of virus isolates. Safarova *et al.* (2008) examined eight pathotyped PSbMV isolates from the Czech Republic, and showed distinct grouping of P1 and P4 pathotypes. Wylie *et al.* (2011) analysed six pathotyped Australian PSbMV isolates; their P1 and P4 isolates clustered in two separate groups together with the Czech strains of the same pathotype, but their P2 isolate did not group with the published P2 pathotype strain (PSbMV-L1 isolate, GenBank accession code: AJ252242). Further development of pathotyping techniques would require analyses of large numbers of PSbMV strains for each pathotype, and the use of strains from diverse geographic backgrounds. Until that is achieved, pathotype identification should be based on biological indexing, and care must be taken not to propose pathotypes based solely on phylogenetic analyses.

The outcome of the present study is particularly relevant to pea breeding programmes. Firstly, the study confirmed the effectiveness of the *sbm1* gene against all four PSbMV pathotypes. This gene is widely used in the Australian pea breeding programme, and is present in currently grown varieties such as 'Yarrum' and 'PBA Wharton', although none of the commercial varieties are homogeneous for resistance (van Leur *et al.*, 2013a). Pea varieties that are heterogeneous for PSbMV resistance could provide enough protection for commercial purposes, but these varieties will require purification before being used as parents in breeding programmes. Secondly, given the prevalence of P3 pathotypes, varieties carrying the *mo/sbm2* gene may appear to be resistant to PSbMV. However, cultivation of these cultivars will result in selection for the P1 and P4 pathotypes, as is demonstrated by the absence of P3 pathotypes in the two tested seed lots harvested from the BYMV resistant varieties 'Moonlight' and 'Soupa'.

The present study results have shown how quickly PSbMV can spread. They also provide clear indications for differences in PSbMV seed transmission rates among host varieties that lack *sbm* resistance genes. While highly susceptible varieties (e.g. 'Kaspa' and 'Excell') are being replaced with new varieties, some carrying the *sbm1* gene, it remains important to monitor commercial seed lots for PSbMV transmission to identify varieties with high seed transmission rates for PSbMV.

ACKNOWLEDGEMENTS

This study was financially supported by the Grains Research and Development Corporation, Australia.

LITERATURE CITED

Alconero R., Provvidenti R., Gonsalves D., 1986. Three pea seedborne mosaic virus pathotypes from pea and lentil germ plasm. *Plant Disease* 70: 783–786. https://doi.org/10.1094/PD-70-783

Ashby J.W., Fletcher J.D., Jermyn W.A., Goulden D., 1986. Some properties of a strain of pea seed-borne mosaic virus isolated from field peas in New Zealand. *New Zealand Journal of Experimental Agriculture* 14: 209–213. https://doi.org/10.1080/03015521.1986.10426145

Congdon B.S., Coutts B.A., Renton M., Banovic M., Jones R.A.C., 2016. Pea seed-borne mosaic virus in field pea: widespread infection, genetic diversity, and resistance gene effectiveness. *Plant Disease* 100: 2475–2482. https://doi.org/10.1094/PDIS-05-16-0670-RE

Congdon B.S., 2017. *Understanding, Forecasting and Managing Pea Seed-borne Mosaic Virus in Field Pea*. PhD Thesis, The University of Western Australia. https://research-repository.uwa.edu.au/en/publications/understanding-forecasting-and-managing-pea-seed-borne-mosaic-viru. (accessed 03-01-25).

Coutts B.A., Prince R.T., Jones R.A.C., 2009. Quantifying effects of seedborne inoculum on virus spread, yield losses, and seed infection in the Pea seed-borne mosaic virus - field pea pathosystem. *Phytopathology* 99: 1156–1167. https://doi.org/10.1094/PHYTO-99-10-1156

Fletcher J.D., 1993 Surveys of virus diseases in pea, lentil, dwarf and broad bean crops in South Island, New Zealand. *New Zealand Journal of Crop and Horticultural Science* 21: 45–52. https://doi.org/10.1080/01140671.1993.9513745

Freeman A., Spackman M., Aftab M., McQueen V., King S., ... Rodoni B., 2013. Comparison of Tissue blot immunoassay and high throughput PCR for virus-testing samples from a southeastern Australian pulse virus survey. *Australasian Plant Pathology* 42: 675–683. https://doi.org/10.1007/s13313-013-0252-9

Gao Z., Johansen I.E., Eyers S., Thomas C.L., Ellis T.H.N., Maule A.J., 2004. The potyvirus recessive resistance gene, *sbm1*, identifies a novel role for translation initiation factor eIF4E in cell-to-cell trafficking. *The Plant Journal* 40: 376–385. https://doi.org/10.1111/j.1365-313X.2004.02215.x

Hampton R.O., 1982. Incidence of the lentil strain of Pea seedborne mosaic virus as a contaminant of *Lens culinaris* germ plasm. *Phytopathology* 72: 695–698. https://doi.org/10.1094/Phyto-72-695

Hjulsager C.K., Lund O.S., Johansen I.E., 2002. A new pathotype of Pea seedborne mosaic virus explained by properties on the P3-6k1- and viral genome-linked protein (VPg) - coding regions. *Molecular Plant-Microbe Interactions* 15: 169–171. https://doi.org/10.1094/MPMI.2002.15.2.169.

Johansen I.E., Lund O.S., Hjulsager C.K., Laursen J., 2001. Recessive resistance in *Pisum sativum* and potyvirus pathotype resolved in a gene-for-cistron correspondence between host and virus. *Journal of Virology* 75: 6609–6614. https://doi.org/10.1128/JVI.75.14.6609–6614.2001

Khetarpal R.K., Maury Y., 1987. Pea seed-borne mosaic virus: a review. *Agronomie* 7: 215–224. https://doi.org/10.1051/agro:19870401

Kumari, S.G., Moukahel A., El Miziani I, 2022. Diagnostic tools validated by ICARDA's Germplasm Health Unit (GHU) for detection of legume seed-borne pests. International Center for Agricultural Research in the Dry Areas (ICARDA), Beirut, Lebanon. https://hdl.handle.net/10568/126879 (accessed 03-01-25).

Latham L.J., Jones R.A.C., 2001a. Alfalfa mosaic and pea seed-borne mosaic viruses in cool season crop, annual pasture, and forage legumes: susceptibility, sensitivity and seed transmission. *Australian Journal of Agricultural Research* 52: 771–790. https://doi.org/10.1071/AR00165

Latham L.J., Jones R.A.C., 2001b. Incidence of virus infection in experimental plots, commercial crops, and seed stocks of cool season crop legumes. *Australian Journal of Agricultural Research* 52: 397-413. https://doi.org/10.1071/AR00079

Ligat J.S., Cartwright D., Randles J.W., 1991. Comparison of some pea seed-borne mosaic virus isolates and their detection by dot-immunobinding assay. *Australian Journal of Agricultural* Research 42: 441–451. https://doi.org/10.1071/AR9910441

Ligat J.S., Randles J.W., 1993. An eclipse of pea seed-borne mosaic virus in vegetative tissue of pea following repeated transmission through the seed. *Annals of Applied Biology* 122: 39–47. https://doi.org/10.1111/j.1744-7348.1993.tb04012.x

Provvidenti R., Alconero R., 1988. Inheritance of resistance to a third pathotype of pea seed-borne mosaic virus in *Pisum sativum*. *Journal of Heredity* 79: 76–77. https://doi.org/10.1093/oxfordjournals.jhered.a110457

Rosewarne G., 2016. DAV00118 - Pulse Breeding Australia: Field Pea Breeding Program. https://grdc.com.au/research/reports/report?id=6831 (accessed 03-01-25).

Safarova D., Navratil M., Petrusova J., Pokorny R., Piakova Z., 2008. Genetic and biological diversity of the pea seed-borne mosaic virus isolates occurring in Czech Republic. *Acta Virologica* 52: 53–57.

Siddique K.H.M., Sykes J., 1997. Pulse production in Australia past, present and future. *Australian Journal of Experimental Agriculture* 37: 103–111. https://doi.org/10.1071/EA96068

Torok V.A., Randles J.W., 2007. Discriminating between isolates of PSbMV using nucleotide sequence polymorphisms in the HC-Pro coding region. *Plant Disease* 91: 490–496. https://doi.org/10.1094/PDIS-91-5-0490

van Leur J.A.G., Kumari S.G., Aftab M., Leonforte A., Moore S., 2013a. Virus resistance of Australian pea (*Pisum sativum*) varieties. *New Zealand Journal of Crop & Horticultural Science* 41: 86–101. https://doi.org/10.1080/01140671.2013.781039

van Leur J.A.G., Freeman A., Aftab M., Spackman M., Redden B., Materne M., 2013b. Identification of seed-borne *Pea seed-borne mosaic virus* in lentil (*Lens culinaris*) germplasm and strategies to avoid its introduction in commercial Australian lentil fields. *Australasian Plant Disease Notes* 8: 75–77. https://doi.org/10.1007/s13314-013-0099-5

Wylie S.J., Couts B.A., Jones R.A.C., 2011. Genetic variability of the coat protein sequence of pea seed-borne mosaic virus isolates and the current relationship between phylogenetic placement and resistance groups. *Archive of Virology* 156: 1287–1290. https://doi.org/10.1007/s00705-011-1002-3

Phytopathologia Mediterranea
The international journal of the
Mediterranean Phytopathological Union

Firenze University Press
www.fupress.com/pm

Research Papers

Molecular detection and characterization of viruses infecting greenhouse-grown tomatoes in Albania

Magdalena CARA[1,2], Amani BEN SLIMEN[3], Enea MITRI[3], Orges CARA[2,3], Dajana FRASHERI[3], Jordan MERKURI[2], Giuseppe PARRELLA[4], Toufic ELBEAINO[2,3,4,*]

[1] *Agriculture University of Tirana, Rruga Paisi Vodica 1025, Tirana, Albania*
[2] *Nanobalkan, Academy of Sciences of Albania, Murat Toptani Avenue, 1000 Tirana, Albania*
[3] *International Centre for Advanced Mediterranean Agronomic Studies (CIHEAM of Bari), Valenzano, Italy*
[4] *Institute for Sustainable Plant Protection (IPSP), National Research Council of Italy (CNR), Portici, Italy*
*Corresponding author. E-mail: elbeaino@iamb.it

Summary. During the 2023–2024 growing season, a total of 45 tomato greenhouses were visited across five major production regions of Albania (Berat, Lushnje, Fier, Tirana, and Shkodra). A total of 196 greenhouse-grown tomato leaf samples, representing 31 varieties, were collected from plants showing virus-like symptoms. All samples were tested by RT-PCR and qPCR assays for the possible presence of significant tomato-infecting viruses and viroids, including alfalfa mosaic virus (AMV), cucumber mosaic virus (CMV), tomato brown rugose fruit virus (ToBRFV), tomato yellow leaf curl virus (TYLCV), tomato chlorosis virus (ToCV), tomato infectious chlorosis virus (TICV), tomato mottle mosaic virus (ToMMV), tomato spotted wilt virus (TSWV), tomato mild mottle virus (ToMMoV), tobacco mosaic virus (TMV), pepino mosaic virus (PepMV), potato viruses X and Y (PVX, PVY), potato leafroll virus (PLRV), tomato apical stunt viroid (TASVd), and potato spindle tuber viroid (PSTVd). In addition, Next-generation sequencing (NGS) using *Illumina* and *MinION* nanopore technologies were performed to characterize the complete genome of two Albanian ToBRFV isolates. RT-PCR and qPCR showed that ToCV, ToBRFV, AMV, and CMV were present in 25, 9.1, 4.1, and 4.1% of the samples, respectively, whereas all remaining viruses and viroids were absent. *Illumina* and *MinION* sequencing unveiled the complete genome sequences of ToBRFV (6,381 nucleotides) and of two additional viruses, i.e., Southern tomato virus, STV (3,437 nts) and tobacco vein clearing virus, TVCV (7,596 nts), both of which were not included in our initial screening. The two latter viruses were afterward diagnosed by PCR and found to be present in 2 and 3% of the tested samples, respectively. ToCV was most prevalent in Lushnje and Fier regions, while ToBRFV in Berat and Fier. The phylogenetic analyses predominantly clustered together the different Albanian viruses isolate, suggesting a local or regional origin. This study reports for the first time the presence of STV and TVCV in Albania and highlights the emergence of ToCV and ToBRFV in the country.

Keywords. RT-PCR, qPCR, next-generation sequencing, phylogenetic analysis, emerging viruses.

OPEN ACCESS

Citation: Cara, M., Ben Slimen, A., Mitri, E., Cara, O., Frasheri, D., Merkuri, J., Parrella, G. & Elbeaino, T. (2025). Molecular Detection and characterization of viruses infecting greenhouse-grown tomatoes in Albania. *Phytopathologia Mediterranea* 64(1): 77-86. doi: 10.36253/phyto-15811

Accepted: April 24, 2025

Published: May 15, 2025

Data Availability Statement: All relevant data are within the paper and its Supporting Information files.

Competing Interests: The Author(s) declare(s) no conflict of interest.

Editor: Joel L. Vanneste, Plant and Food Research, Sandringham, New Zealand.

INTRODUCTION

Tomato production in Albania has shown significant growth in recent years, with a total cultivated area reaching 6,663 hectares (FAO, 2022). Albania harbored ancient local tomato varieties, known for their potential to enhance agricultural diversity and emphasize rural economic prospects. Thanks to the dedicated efforts of Albanian farmers, the Plant Genetic Resources Institute (Agriculture University of Tirana) now houses 67 autochthon cultivated and inherited tomato varieties, reflecting the Albanian wealth agricultural heritage. In Albania, vegetable cultivation spans a total of 42,994 hectares (Dhuli, 2022), with 6,693 hectares dedicated to tomato farming, including 2,100 hectares for greenhouse-grown tomatoes. The country's annual vegetable production amounts to 1.3 million tons, of which tomatoes account for approximately 300,000 tons. In 2022, Albania exported an average of 29,760 tons of tomatoes, valued at approximately 26.2 million USD. The country's tomato cultivation is concentrated in five main regions, with Fier being the most productive. It accounts for 24.8% of the total cultivated area and 37.3% of total production, followed by Berat, which represents 14.7% of the cultivation area and 17.7% of production. Shkodra ranks third, with around 5.5% of both the cultivated area and total production (Dhuli, 2022).

In Albania, several viruses have been reported to infect tomatoes, causing various symptoms that impact both production and quality. Notably, tomato brown rugose fruit virus (ToBRFV), first detected in 2022, has emerged as a major concern due to its severe symptoms, including fruit deformation and plant stunting on different cultivars (Orfanidou *et al*., 2022a). The alfalfa mosaic virus (AMV), cucumber mosaic virus (CMV), tomato spotted wilt virus (TSWV) and potato virus Y (PVY), all identified for the first time in 2005 (Finetti-Sialer *et al*., 2005), together with tomato chlorosis virus (ToCV) in 2022 (Orfanidou *et al*., 2022b), were associated with different symptoms, i.e., yellowing, leaf curl, and yield reduction in the country. These viruses, together with many others uninvestigated previously in the country are of a significant concern for tomato farmers, particularly in greenhouse systems where conditions may favor the spread of viral diseases.

This study extensively investigates for the first time the presence and prevalence of some important tomato viruses and viroids, possibly infecting greenhouses-grown tomato plants in the country, i.e., ToCV, alfalfa mosaic virus (AMV), cucumber mosaic virus (CMV), tomato brown rugose fruit virus (ToBRFV), tomato yellow leaf curl virus (TYLCV), tomato infectious chlorosis virus (TICV), tomato mottle mosaic virus (ToMMV), tomato spotted wilt virus (TSWV), tomato mild mottle virus (TMMoV), tobacco mosaic virus (TMV), pepino mosaic virus (PepMV), potato viruses X and Y (PVX, PVY), potato leafroll virus (PLRV), tomato apical stunt viroid (TASVd), and potato spindle tuber viroid (PSTVd); for which the results are hereafter reported.

MATERIALS AND METHODS

Source and location of plant material

During the 2023-2024 growing season, a total of 45 tomato greenhouses across five regions, i.e., Berat (5), Lushnje (25), Fier (13), Tirana (1), and Shkodra (1), were visited. These regions are known for their significant tomato production, accounting for 70% of the national output. A total of 196 tomato leaf samples, representing 31 varieties (11 of which were local; Supplementary Table 1), were collected from plants exhibiting virus-like symptoms, such as yellowing, stunting, mottling, chlorosis, necrosis, deformed and brown fruits. The samples were placed in labeled plastic bags with wet filter paper and were transported in a cool box for laboratory processing.

Extraction of total nucleic acids (DNA and RNA)

Two protocols were adopted for extracting the total nucleic acids (TNA). The total RNAs were extracted from 0.1 g of leaf veins, homogenized in 1 mL grinding buffer (4.0 M guanidine thiocyanate, 0.2 M NaOAc pH 5.2, 25 mM EDTA, 1.0 M KOAc pH 5.0 and 2.5% w/v PVP-40), and purified using Silica particles, according to Foissac *et al*. (2001). The total DNAs were extracted from 1 g of leaf tissues, following the CTAB protocol (Doyle, 1991). The TNA quality was evaluated by NanoDrop™ One/OneC Microvolume UV–Vis Spectrophotometer (ThermoFisher Scientific, Waltham, MA, United States) and electrophoresis in 1.2% agarose gel of 1X TBE buffer (Tris-Borate-EDTA). The purified TNAs were then stored at -20°C until processing.

Complementary DNA synthesis (cDNA), PCR and qPCR assays

Total RNA (0.5 µg) was reverse-transcribed into cDNA using 1 µL of random hexamer primers (0.5 mg/

Table 1. List of primers used in RT-PCR and qPCR for detecting tomato viruses and viroids, and for complete genome PCR amplification and Sanger sequencing of ToBRFV, STV and TVCV. F and R: forward and reverse primers, respectively.

Virus	Primer sequence (5´ - 3´)	PCR amplicon (bp)	qPCR amplicon (bp)	Reference
Tomato brown rugose fruit virus (ToBRFV)	F-GTAAGGCTTGCAAAATTTCGTTCG R-CTTTGGTTTTTGTCTGGTTTCGG		79	(Panno *et al*., 2019)
	F-GAAGTCCCGATGTCTGTAAGG R-GTGCCTACGGATGTGTATGA	842		(Ling *et al*., 2019)
Pepino mosaic virus (PepMV)	F-ACTCCTAGAGCTGACCTCAC R-TCTCCAGCAACAGGTTGGTA		107	(Ling, 2007)
Tomato yellow leaf curl virus (TYLCV)	F-TGTTGTAAGGGCCCGTGACT R-GACGGGCGTGGAAATGATTA		62	(Papayiannis *et al*., 2010)
Tomato spotted wilt virus (TSWV)	F-GCTTGTTGAGGAAACTGGGAATT R-AGCCTCACAGACTTTGCATCATC		150	(Roberts *et al*., 2000)
Tomato chlorosis virus (ToCV)	F-TCTCGAACCTGCTTATGAAAAGAAA R-ATGCAAGTTGGTTAACGTTGTACAGT		80	(Lozano *et al*., 2006)
	F-AAGAGGGTGTCAGCAACAGG R-TGGGTTCTGAGGTTGAGAGT	760		(Hirota *et al*., 2010)
Tomato infectious chlorosis virus (TICV)	F-AAAGCGGGACATTTTTTATCATATG R-TGTTTCCAGACTAGATCGCATGAAT		89	(Vaira *et al*., 2002)
Tomato mosaic virus (ToMV)	F-TTGCCGTGGTGGTGTGAGT R-GACCCCAGTGTGGCTTCGT		72	(Boben *et al*., 2007)
Alfalfa mosaic virus (AMV)	F-TCGTCACGTCATCAGTGAGAC R-CCATCATGAGTTCTTCACAAAAG	351		(Xu and Nie, 2006)
	F-GTTGATGCTGCTGCTGCTG R-GCTGCTGCTGCTGCTGCTG		100	(Trucco *et al*., 2022)
Cucumber mosaic virus (CMV)	F-CTTTCGCGACTTAATAAGACGTT R-CACAGTAGAATCAAATTTCGGCA	230		(Srivastava *et al*., 2019)
	F-ATCCGGAGTTTTCGATTA R-GCATCATCATATATTCCAATTC		96	(Xinying *et al*., 2022)
Tomato mottle mosaic virus (ToMMV)	F-CTGGAGAAGACTGGGTCTAG R-TTCGGTAAGTTCAATGGGACCT		50	(Fowkes *et al*., 2022)
Tomato apical stunt viroid (ToASVd)	F-GGG ATC CCC GGG GAA AC R-AGCTTCAGTTGTATCCACCGGGT		196	(Verhoeven *et al*., 2012)
Tomato mild mottle virus (ToMMoV)	F-CGACCCTGTAGAATTAATAAATATT R-CACTCTGCGAGTGGCATCCAAT		289	(Sui *et al*., 2017)
Potato virus Y (PVY)	F-CCA ATC GTT GAGAATGCAAAAC R-ATA TACGCTTCTGCAACATCTGAC A		74	(Cárdenas *et al*., 2017)
Potato virus X (PVX)	F-AAGCCTGAGCACAAATTCGC R-GCTTCAGACGGTGCCG		101	(Agindotan *et al*., 2007)
Tobacco mosaic virus (TMV)	F-ATTAGACCCGCTAGTCACAGCAC R-GTGGGGT TCGCCTGATTTT		83	(Yang *et al*., 2012)
Tomato brown rugose fruit virus (ToBRFV)	1F-CAACTACAATACTTAACAAC 1R- CTCCTTCATGTAGACCTCTC	956		This study
	2F- AATACGTGTGCAAAACTTAC 2R- CATGGATGGTTCTTCAACAT	1097		
	3F- AGGGTGCACTAGTGGTTACT 3R- TGTACACATGACATGTCCTT	1079		
	4F- AGCCGACATTACCCACTATC 4R- GCTTTAATCATATGCCTGTA	1005		
	5F- GCTTGCAGATTTTGATTTTG 5R- ACACTCTTAACAGGTGTGAA	1081		
	6F- GGTAAAGTCAATATTAATGA 6R- AAATTGCCGTTGAACGGTTG	935		
	7F- TGGGCCGACCCTATAGAATT 7R- CGCCCCTACCGGGGGTTCCG	628		

(Continued)

Table 1. (Continued).

Virus	Primer sequence (5′ - 3′)	PCR amplicon (bp)	qPCR amplicon (bp)	Reference
Tobacco vein clearing virus (TVCV)	1F-ATATGTATGATTTATATGAT 1R-CATTTCCGTCTATTTCATTT	1009		This study
	2F-GATAAAGAGCTAGAATTAAC 2R-GTTGTACATCCAAATTGTGG	1061		
	3F-ATGGCACCACAATTTGGATG 3R-GCTTCCTGGTGCTAGTTCTA	989		
	4F-CTATAGAAAAAAGCGTAATT 4R-GGCATTCCTAATAACATATC	1120		
	5F-TGGTAGTAACAGGATTTAAT 5R-GTATTCCTAGAAATTCTATC	1080		
	6F-ATTCAGGTATAAGTTTAAGT 6R-TAGATTGTCCTGCTGTAGAT	1000		
	7F-GCATGACTATAAACATGCGG 7R-AGTCTATTCCAGTTGTACTC	1093		
	8F-GACTTGATGACCAGATACTG 8R-CATAATAAAGtTCATCTTGT	1005		
Southern tomato virus (STV)	1F- GATAAATTTAGTAAGCTACC 1R- CTGGAGCTCATCCTTCACAT	935		This study
	2F- AGCCTACTAGGAAGCAAGTC 2R- CCCACCCTTGCAGCAAAATA	905		
	3F- CTGATGGAGGATATCTACTG 3R- TTCTCCAAGTTCTCGTGAGA	1010		
	4F- CATAGGTGGGAGTACAGGTT 4R- GAAGACGCGCTACTCTAATA	878		

mL) and the M-MLV reverse transcriptase enzyme, following the manufacturer's instructions (Thermo Fisher). All samples were initially screened using qPCR assay, only positive samples were further tested by RT-PCR and confirmed via Sanger sequencing. Both PCR and qPCR were performed on the cDNA using a comprehensive set of sense and antisense primers designed to target all tomato-infecting viruses and viroids examined in this study (Table 1). PCR and qPCR primers, conditions, and cycles were applied according to each virus and viroid and relative reference (Table 1). PCR reactions, conducted for further sequencing, were carried out in a final volume of 25 µL, of which 2.5 µL of cDNA or total DNA were used as a template. Cycling conditions included 30 sec of denaturation at 95°C, followed by 40 cycles of PCR amplification at 95°C for 50 sec, annealing at 50–58°C (according to each virus and viroid primer pair) for 30 sec and an elongation at 72°C for 40 sec. qPCR based on iTaq Universal SYBR Green Supermix [2x concentrated, ready-to-use master reaction mix, optimized for dye-based quantitative PCR (qPCR)] was carried out for viruses and viroids detection (Table 1), using Rotor- Gene Q and CFX96 BioRad thermocyclers (Milan, Italy). Specific primer sets were designed based on NGS generated sequences for ToBRFV as well as Southern tomato virus (STV) and tobacco vein clearing virus (TVCV), both initially not included in our investigation (Table 1).

Cloning, sequencing and computer-assisted analysis

All the PCR amplicons obtained from different viruses were ligated into the StrataCloneTM PCR cloning vector pSC-A, subsequently cloned into *Escherichia coli* DH5 cells, and automatically sequenced (Eurofins Genomics, Koln, Germany). Nucleotide (nt) and amino acid (aa) sequences were analyzed with the assistance of Geneious Prime 2024.0.5 (San Diego, CA, USA). Search for nt and aa identities in the GenBank was carried out using BLASTX and BLASTP tools (http://www.ncbi.nlm.nih.gov/) (Altschul *et al*., 1990). Sequence alignment and tentative phylogenetic trees were performed using "Clustal Omega" and "Maximum Likelihood" packages included in Geneious Prime 2024.0.5.

Next-generation sequencing using Illumina and MinION nanopore technologies

Next-generation sequencing (NGS) was performed on two ToBRFV-infected samples using both *Illumina* and *MinION* nanopore technologies. This analysis aimed to determine the complete genome sequences of two Albanian isolates from the highly affected regions of Fier and Lushnje and to assess their phylogenetic relationships with homologous sequences reported in the GenBank. Accordingly, the total RNA was ribo-depleted, fragmented, and double-stranded (ds) cDNA was synthesized using random hexamers and used as input in the end-prep step in the direct cDNA sequencing kit (SQK-DCS109). The prepared library was loaded onto a *MinION* flow cell (FLO-MIN114), and sequencing was conducted using ONT *MinION* sequencing device with Flongle flow cells, generating real-time data. Raw reads were base-called, quality-controlled, and aligned to a reference genome. *Illumina* sequencing was conducted on the reverse-transcribed templates that were sequenced in a run of 2 × 150 bp paired-end mode (Eurofins Genomics, Germany). The reads were trimmed, error corrected and normalized using BBDuck package in Geneious Prime 2024.0. The Tadpole tool with different k-mers was used for *de novo* assembly of all the previously filtered reads into larger contigs. BLASTX (e-value with cut-off from 10^{-6} to 10^{-2}) and BLASTP were used for sequence homology screening of the assembled contigs.

RESULTS

PCR and qPCR detection of tomato viruses and viroids

PCR and qPCR assays conducted on 196 tomato samples identified the presence of only four viruses, i.e., ToCV, ToBRFV, AMV, and CMV, among those tested, while no viroids were detected. A total of 87 tomato plants were found to be infected, representing an overall infection rate of 44.4% (Table 2). The Fier region showed the highest infection rate at 47.2%, with 26 PCR-positive samples out of 55 tested, followed by Lushnje with a rate of 43.5%, based on 44 infected samples out of 101 collected. The analysis revealed that ToCV and ToBRFV were the most prevalent viruses, with ToCV being dominant in the Lushnje and Fier regions and ToBRFV more prevalent in Berat and Fier (Table 2). Among the infected samples, six plants exhibited double infections, while 81 had single infections.

Symptoms in greenhouses

The symptoms found associated with ToBRFV in greenhouses-tomato infected plants were varied and ranged from light to severe. Affected leaves exhibited moderate to severe mosaic patterns, accompanied by dark green wrinkling, blistering, narrowing, deformation, and necrotic spots (Figure 1a). On the fruit, irregular brown necrotic lesions, deformities, and yellowing spots were commonly observed, making the tomatoes unsuitable for market (Figure 1b). Plants infected with ToCV had the same type of symptoms, characterized by vein clearing, yellowing, crinkle and deformed leaves (Figure 1c). Light mottling and vein clearing symptoms were observed on TVCV-infected tomato plants (Figure 1d). Symptoms of both viruses were prevalent across numerous tomato plants in various locations. However, no symptoms suggestive of viral infection were observed and associated with AMV-, CMV-, and STV-infected plants.

Illumina and MinION nanopore sequencing

The NGS runs using *Illumina* and *MinION* platforms were performed on total RNA extracted from two ToBRFV-infected samples (Alb-L1 and Alb-F5). The *Illumina* runs yielded approximately 6.2 million paired-

Table 2. Detection and incidence analysis of tomato viruses in samples from five regions of Albania.

Region	Tomato samples	Infected samples	Infection rate %	ToCV	ToBRFV	AMV	CMV	STV	TVCV
Berat	32	12	37.5	3	6	1	0	2	1
Lushnje	101	44	43.5	26	4	3	8	2	4
Fier	55	26	47.2	18	6	3	0	0	1
Tirana	5	2	40	0	2	0	0	0	0
Shkodra	3	3	100	2	0	1	0	0	0
Total	196	87	44.4	49 (25%)	18 (9.1%)	8 (4.1%)	8 (4.1%)	4 (2%)	6 (3.1%)

Figure 1. Symptoms of viral infections in tomato plants: ToBRFV causes visible damage on both leaves and fruits (a, b), whereas ToCV (c) and TVCV (d) primarily affect the leaves. White arrows highlight symptom locations.

end reads per sample, while *MinION* produced approximately 0.71 million reads per sample. After quality filtering, these numbers were reduced to approximately 3.7 and 3.6 million high-quality reads for *Illumina* and 0.49 and 0.47 million high-quality reads for *MinION*. All high-quality reads were used for de novo assembly, generating around 12,334 and 11,259 contigs from *Illumina* and 3,108 and 3,548 contigs from *MinION,* with contig lengths ranging from 150 to 4,720 nucleotides. The alignment of high-quality *Illumina* and *MinION* reads to reference ToBRFV sequences from GenBank (Table 4) revealed that *Illumina* sequencing provided higher resolution for genome assembly, which is critical for accurate virus characterization. It successfully uncovered the complete genome sequences of ToBRFV in both samples, as well as the full genome sequences of STV and TVCV, which were not initially included in our screening (Table 3). The complete genome sequences of both ToBRFV isolates obtained in this study were identical, spanning 6,381 nts. They shared 99.8% identity with the Israeli isolate "6166394_2" (GenBank accession number OM515237). One representative sequence for ToBRFV (Alb-L1 isolate) has been deposited in GenBank under the accession number PQ643185.

Similarly, *Illumina* outperformed *MinION* in generating and fully covering the nucleotide sequences of the STV and TVCV genomes, each uniquely identified in two distinct samples using these platforms (Table 3). The complete genome sequences of TVCV and STV were 7,596 and 3,437 nts in length, respectively, sharing 95.3% identity with the Iraqi isolate Iraq-1 (accession number ON684329) and 99.8% identity with the German isolate JKI ID1904214/15 (accession number MK948545). The accuracy of the full genome sequences of ToBRFV, TVCV, and STV was verified by Sanger-sequencing of PCR-amplified amplicons using specific primers designed from the NGS-generated sequences (Table 1).

Sequence and phylogenetic analyses

The sequencing analysis of PCR amplicons generated distinct sequence types across different virus isolates from tested samples. Sequence types were obtained from 6 out of 8 samples for AMV, 4 out of 8 for CMV, 10 out of 18 for ToBRFV, 13 out of 49 for ToCV, 1 out

Table 3. Genomics features provided by *Illumina* and *MinION* sequencing. Alb-L1: sample from Lushnje region: Alb-F5:sample from Fier region.

Virus	Method	Sample	Reads	Coverage %	Genome sequence length (nts)	GenBank Accession number
ToBRFV	*Illumina*	Alb-L1	298,175	100	6,381	PQ643185
		Alb-F5	287,741			
	MinION	Alb-L1	110,112	98.9	6,310	
		Alb-F5	109,187	99.3	6,336	
TVCV	*Illumina*	Alb-L1	250,149	100	7,596	PQ643187
	MinION	Alb-L1	95,545	97.2	7,383	
STV	*Illumina*	Alb-F5	210,580	100	3,437	PQ643186
	MinION	Alb-F5	80,633	97.7	3,357	

Table 4. List of virus isolates sequenced in this study and their identity levels with homologue in the GenBank

Virus	Accession No. deposited in GenBank	Intraspecies identity of Albanian isolates (%)	Reference isolate (Accession No.)	Origin	Highest identity with homologue in GenBank (%)
AMV	PQ613741- PQ613746	95–98	Tec1 (FR715042)	Spain	98.7
CMV	PQ643215- PQ643218	96–99	SKO20ST1 (OL472046)	Slovenia	99.5
ToBRFV	PQ643188- PQ643197	98–100	Gr2 (OQ190155)	Greece	100
ToCV	PQ643201-PQ6432013	96–99	DSMZ PV-1242 (ON398513)	Greece	99.3
TVCV	PQ643187	100	Iraq-1 (NO684329)	Iraq	95.3
STV	PQ643186	100	Mexico-1 (NC_011591)	Mexico	98.7

of 6 for TVCV and 1 out of 4 for STV. The resulting clones exhibited varying degrees of sequence identity both among themselves and with reported isolates in the GenBank (Table 4).

The phylogenetic analyses of ToCV and ToBRFV, identified as the two most significant viruses in our study and among the most prevalent in Albania, revealed notable genetic similarities with isolates from various countries. Notably, ToCV isolates from Albania formed a distinct clade, indicating a high level of sequence conservation among strains within the country. These isolates were closely related to those from Greece (Gr-535, Acc. No. EU284744; DSMZ-PV-1242, Acc. No. ON398513) but more distantly related to isolates from China and Korea (Figure 2).

The phylogenetic allocation of ToBRFV isolates from Albania showed a pattern somewhat analogous to that of ToCV. The Albanian isolates displayed genetic proximity to one another but were distributed across two main clades. One clade included some of the Albanian isolates alongside isolates from Greece (Gr2, Acc. No. OQ190155) and Israel (41106995, Acc. No. OM515266), forming two closely related clusters. The second clade grouped other Albanian isolates into two clusters, along with isolates from Cyprus (DSMZ-PV-1300, Acc. No. OL311702), the United Kingdom (ToBRFV.21930919, Acc. No. MN182533), Belgium (GBVC-01, Acc. No. MZ945 419), and the Netherlands (39941430A, Acc. No. MN882046) (Fig. 2). Overall, the Albanian ToCV and ToBRFV isolates showed genetic clustering with isolates from geographically neighboring regions and countries such as Greece and Israel, suggesting the potential circulation of closely related and genetically homogeneous strains across these areas.

DISCUSSION AND CONCLUSION

This study provides an in-depth analysis of viruses affecting greenhouse-grown tomatoes in Albania, highlighting several significant findings. RT-PCR and qPCR assays performed on greenhouse-grown tomato plants from five Albanian tomato growing regions detected six viruses, i.e., AMV, CMV, STV, TVCV, ToCV, and ToBRFV. Both methods provided consistent results, with PCR amplicons enabling molecular analyses. Among the viruses tested, ToCV and ToBRFV emerged as the most prevalent, accounting for 25 and 9.1% of the infected samples, respectively. ToCV showed higher prevalence in Lushnje and Fier regions, whereas ToBRFV was dominant in Berat and Fier. Notably, STV and TVCV were identified in Albanian greenhouses for the first time, using *Illumina* and *MinION* sequencing. This study reports for the first time the complete genome sequences of ToBRFV (6,381 nts), STV (3,437 nts), and TVCV (7,596 nts) Albanian isolates. The prevalence of the two latter, although low, indicates the need for further monitoring and study of their epidemiological impact in the country. Notably, ToBRFV earlier reported in a few samples from the Fier and Berat regions (Orfanidou *et al*., 2022a), has now been detected in two additional regions, Lushnje and Tirana, suggesting its potential spread. Similarly, ToCV, which was detected in 10 out of 15 tested tomato plants from the Fier and Berat regions (Orfanidou *et al*., 2022b), was found in 49 out of 196 samples in our survey, indicating a higher infection rate of 25%.

Illumina provided 100% genome coverage for ToBRFV, STV, and TVCV, while *MinION* achieved slightly lower coverage (97.2-99.3%) and shorter sequences for STV and TVCV. Therefore, *Illumina's* higher accuracy makes it preferable for detailed viral characterization, whereas *MinION* 's could be more valuable for diagnostics when it deals with accuracy/speed efficiency ratio.

The phylogenetic analyses showed that the Albanian isolates of ToCV and ToBRFV are closely related to those from neighboring regions, such as Greece, suggesting regional movement of these pathogens. An analogous phylogenetic profile for AMV and CMV isolates had also emerged (data not shown).

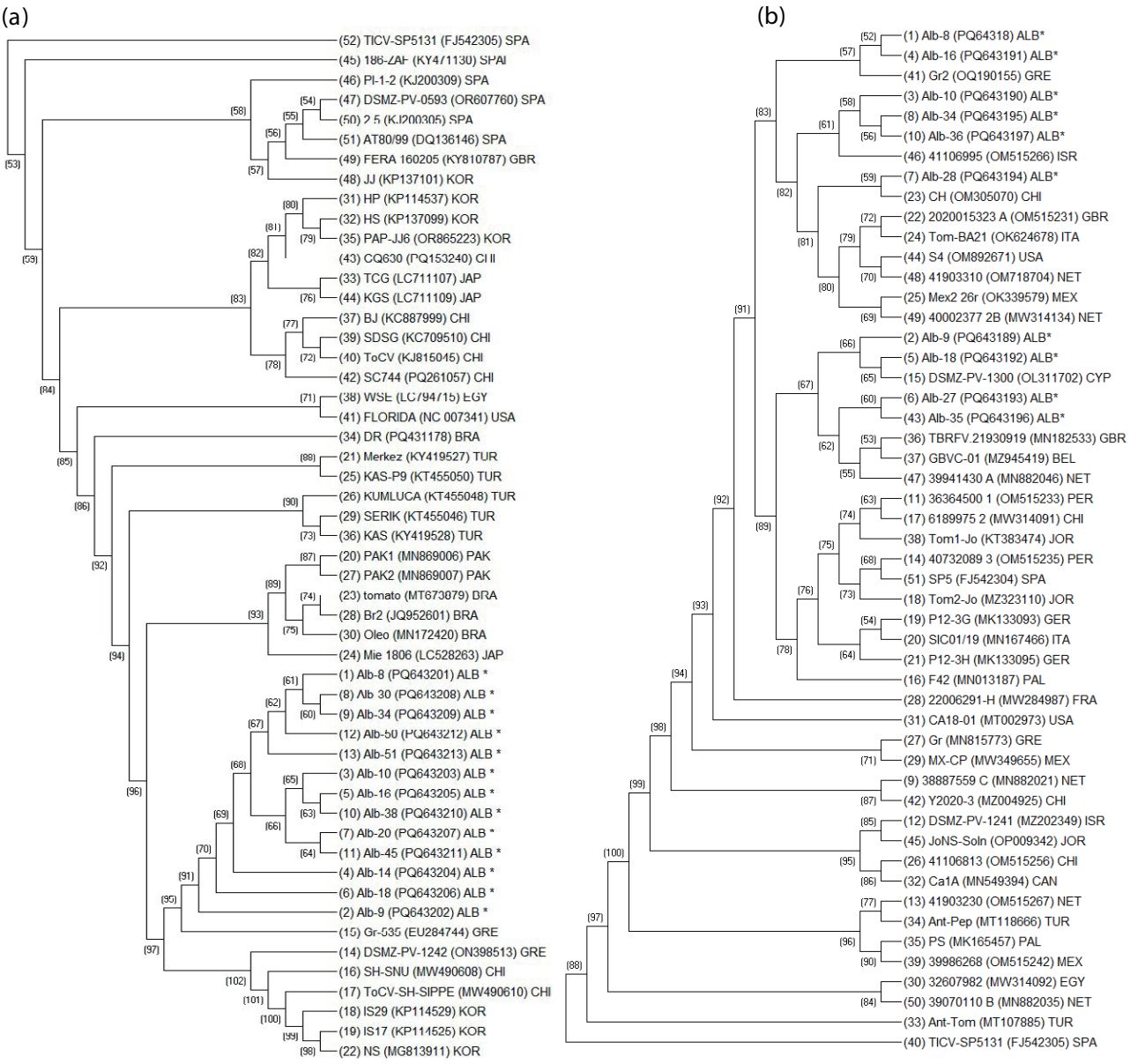

Figure 2. Phylogenetic trees constructed using nucleotide sequences of PCR amplicons of tomato chlorosis virus (a) and tomato brown rugose fruit virus (b) isolates from Albania (indicated with asterisks), along with sequences retrieved from GenBank for both viruses. Tomato infectious chlorosis was used as the outgroup species. Accession numbers of the sequences used are provided in brackets. The origins of the isolates are abbreviated as follows: Spain (SPA), United Kingdom (GBR), Korea (KOR), China (CHI), Japan (JAP), Egypt (EGY), United States of America (USA), Brazil (BRA), Turkey (TUR), Pakistan (PAK), Palestine (PAL), Mexico (MEX), Greece (GRE), Italy (ITA), France (FRA), Peru (PER), Germany (GER), Canada (CAN). Bootstrap values are indicated at branch nodes.

This study can be considered as a step toward sustainable tomato production in Albania, addressing emerging viral challenges while emphasizing the value of modern diagnostic technologies in agricultural research, such as NGS. Effective control measures, including managing insect vectors, using resistant varieties, ensuring virus-free seeds, and implementing strict sanitation practices, are essential to limit the spread of these viruses. Overall, the growing prevalence of viruses such as ToBRFV and ToCV, and the finding of new viruses never reported before in the country, underscores the need for improved disease management strategies in Albanian tomato production.

FUNDING

The study on ToBRFV was funded by the National Agency for Scientific Research of Albania as part of the project titled "Study of the Incidence of Tomato Brown Rugose Fruit Virus in Albania Using *MinION* Nanotechnology."

LITERATURE CITED

Agindotan B.O., Shiel P.J., Berger P.H., 2007. Simultaneous detection of potato viruses, PLRV, PVA, PVX and PVY from dormant potato tubers by TaqMan® real-time RT-PCR. *Journal of Virological Methods* 142: 1–9.

Altschul S.F., Gish W., Miller W., Myers E.W., Lipman D.J., 1990. Basic local alignment search tool. *Journal of Molecular Biology* 215: 403–410.

Boben J., Kramberger P., Petrovič N., Cankar K., Peterka M., Štrancar A., Ravnikar M., 2007. Detection and quantification of Tomato mosaic virus in irrigation waters. *European Journal of Plant Pathology* 118: 59–71.

Cárdenas H.M., Sánchez P.G., Montoya M.M., 2017. Detection and sequencing of Potato virus Y (PVY) and Potato leafroll virus (PLRV) in a volunteer plant of *Solanum tuberosum* L. cv. Diacol-Capiro. *Acta Agronómica* 66: 625–632.

Dhuli E., 2022. Vjetari Rajonal Statistikor 2022. *INSTAT*.

Doyle J., 1991. DNA protocols for plants. In: *Molecular Techniques in Taxonomy*. Springer, Berlin Heidelberg, D., 283-293.

FAO, 2022. Statistical Yearbook. Food and Agriculture Organization of the United Nations. Rome, Italy.

Finetti-Sialer M., Mërkuri J., Tauro G., Myrta A., Gallitelli D., 2005. Viruses of vegetable crops in Albania. *EPPO Bulletin* 35: 491–495.

Fowkes A., Botermans M., Frew L., de Koning P., Buxton-Kirk A., Westenberg M., Ward R., Schenk M., Webster G., Alraiss K., 2022. First report of Tomato mottle mosaic virus in *Solanum lycopersicum* seeds in The Netherlands and intercepted in seed imported from Asia. *New Disease Reports* 45.

Hirota T., Natsuaki T., Murai T., Nishigawa H., Niibori K., Goto K., Hartono S., Suastika G., Okuda S., 2010. Yellowing disease of tomato caused by Tomato chlorosis virus newly recognized in Japan. *Journal of General Plant Pathology* 76: 168–171.

Ling K.-S., 2007. Molecular characterization of two Pepino mosaic virus variants from imported tomato seed reveals high levels of sequence identity between Chilean and US isolates. *Virus Genes* 34: 1–8.

Ling K.-S., Tian T., Gurung S., Salati R., Gilliard A., 2019. First report of tomato brown rugose fruit virus infecting greenhouse tomato in the United States. *Plant Disease* 103: 1439.

Lozano G., Moriones E., Navas-Castillo J., 2006. Complete nucleotide sequence of the RNA2 of the crinivirus Tomato chlorosis virus. *Archives of Virology* 151: 581–587.

Orfanidou C.G., Cara M., Merkuri J., Papadimitriou K., Katis N.I., Maliogka V.I., 2022a. First report of tomato brown rugose fruit virus in tomato in Albania. *Journal of Plant Pathology* 104: 855–855.

Orfanidou C.G., Cara M., Merkuri J., Katis N.I., Maliogka V.I., 2022b. First report of tomato chlorosis virus in tomato in Albania. *Journal of Plant Pathology* 104, 1177.

Panno S., Caruso A., Davino S., 2019. First report of tomato brown rugose fruit virus on tomato crops in Italy. *Plant Disease* 103: 1443–1443.

Papayiannis L.C., Iacovides T.A., Katis N., Brown J., 2010. Differentiation of Tomato yellow leaf curl virus and Tomato yellow leaf curl Sardinia virus using real-time TaqMan® PCR. *Journal of Virological Methods* 165: 238–245.

Roberts C.A., Dietzgen R.G., Heelan L.A., Maclean D.J., 2000. Real-time RT-PCR fluorescent detection of tomato spotted wilt virus. *Journal of Virological Methods* 88: 1–8.

Srivastava N., Kapoor R., Kumar R., Kumar S., Saritha R., Kumar S., Baranwal V.K., 2019. Rapid diagnosis of Cucumber mosaic virus in banana plants using a fluorescence-based real-time isothermal reverse transcription-recombinase polymerase amplification assay. *Journal of Virological Methods* 270: 52–58.

Sui X., Zheng Y., Li R., Padmanabhan C., Tian T., Groth-Helms D., Keinath A.P., Fei Z., Wu Z., Ling K.-S., 2017. Molecular and biological characterization of tomato mottle mosaic virus and development of RT-PCR detection. *Plant Disease* 101: 704–711.

Foissac X., Svanella-Dumas L., Dulucq M., Candresse T., Gentit P., 2000. Polyvalent detection of fruit tree tricho, capillo and foveaviruses by nested RT-PCR using degenerated and inosine containing primers (PDO RT-PCR). *XVIII International Symposium on Virus and Virus-like Diseases of Temperate Fruit Crops-Top Fruit Diseases* 550: 37–44.

Trucco V., Castellanos Collazo O., Vaghi Medina C.G., Cabrera Mederos D., Lenardon S., Giolitti F., 2022. Alfalfa mosaic virus (AMV): Genetic diversity and a new natural host. *Journal of Plant Pathology* 104: 349–356.

Vaira A., Accotto G., Vecchiati M., Bragaloni M., 2002. Tomato infectious chlorosis virus causes leaf yellow-

ing and reddening of tomato in Italy. *Phytoparasitica* 30: 290–294.

Verhoeven J.T.J., Botermans M., Meekes E., Roenhorst J., 2012. Tomato apical stunt viroid in the Netherlands: most prevalent pospiviroid in ornamentals and first outbreak in tomatoes. *European Journal of Plant Pathology* 133: 803–810.

Xinying Y., Xin L., Lili Y., Qiuyue Z., Yongzhe P., Jijuan C., 2022. Detection of Cucumber green mottle mosaic virus in low-concentration virus-infected seeds by improved one-step pre-amplification RT-qPCR. *Plant Methods* 18: 70.

Xu H., Nie J., 2006. Identification, characterization, and molecular detection of Alfalfa mosaic virus in potato. *Phytopathology* 96: 1237–1242.

Yang J.-G., Wang F.-L., Chen D.-X., Shen L.-L., Qian Y.-M., Liang Z.-Y., Zhou W.-C., Yan T.-H., 2012. Development of a one-step immunocapture real-time RT-PCR assay for detection of Tobacco mosaic virus in soil. *Sensors* 12: 16685–16694.

Phytopathologia Mediterranea
The international journal of the
Mediterranean Phytopathological Union

Firenze University Press
www.fupress.com/pm

Research Papers

Isolation and identification of *Fusarium* spp. associated with Fusarium wilt of chickpea (*Cicer arietinum* L.) in Algeria

Ibrahim SEKKAL[1], Djamel MAHIOUT[1,*], Boubekeur Seddik BENDAHMANE[1], Tahar FARAH[2], Mohamed-Cherif BENTAHAR[3], Martina RICKAUER[4]

[1] *Plant Protection Laboratory, Abdelhamid Ibn Badis University of Mostaganem, 27000 – Algeria*
[2] *Laboratory protection, Valorization of Coastal Marine Resources and Molecular Systematics, Abdelhamid Ibn Badis University of Mostaganem, 27000 – Algeria*
[3] *Animal and Applied Physiology Laboratory, Abdelhamid Ibn Badis University of Mostaganem, 27000 – Algeria*
[4] *Research Center of Biodiversity and Ecology, UMR5300, CNRS- Paul Sabatier University- National Polytechnic Institute INP-ENSAT, Avenue de l'Agrobiopole 31326 Castanet-Tolosan, France*
*Corresponding author. E-mail: djamel.mahiout@univ-mosta.dz

Summary. Chickpea (*Cicer arietinum* L.) is an important vegetable crop in many Mediterranean countries, and *Fusarium* is known to cause wilt in these crops. *Fusarium oxysporum* f. sp. *ciceris* and *Fusarium redolens* are the only species which have been reported as the causes of Fusarium wilt in Algeria. *Fusarium* isolates (74) were obtained from roots of chickpea plants showing symptoms of wilting and necroses in xylem tissues. The plants were from 11 eleven principal provinces for chickpea crops in Algeria. Laboratory identifications for 31 isolates were achieved by sequencing their transcription elongation Factor 1- α (*Ef-1 α*) gene regions. Four principal species were identified including *F. oxysporum* (20 isolates), *F. redolens* (ten isolates), *F. solani* (one isolate) based on PCR using species-specific primers, and three *formae speciales* were identified within *Fusarium oxysporum*. *Fusarium redolens* and *F. oxysporum* f. sp. *ciceris* were dominant in the sampling sites. *Fusarium redolens* was identified in the western region of Algeria, and *F. oxysporum* f. sp. *ciceris* was not isolated from this region. In contrast, from the eastern region, *F. redolens* was not isolated but *F. oxysporum* f. sp. *ciceris* was detected. Pathogenicity tests showed that chickpea was susceptible to various *Fusarium* species. Inoculated plants exhibited gradual wilting that eventually affected entire plants. This study provides new knowledge of the distribution of *Fusarium species* causing chickpea wilt in Algeria. Precise identification and the localization of pathogen species is important for developing Fusarium wilt management strategies, including development of wilt resistant chickpea cultivars.

Keyswords. Koch's postulates, transcription elongation factor 1-α gene.

Abbreviations: FR: *Fusarium redolens*; **FS:** *Fusarium solani*; **FO:** *Fusarium oxysporum*; **FOC:** *Fusarium oxysporum* f. sp. *ciceris*; **FOL:** *Fusarium oxysporum* f. sp. *lactuceae*. Transcription elongation Factor 1-α gene (EF-1α).

OPEN ACCESS

Citation: Sekkal, I., Mahiout, D., Bendahmane, B. S., Farah, T., Bentahar, M.-C. & Rickauer, M. (2025). Isolation and identification of Fusarium spp. associated with Fusarium wilt of chickpea (*Cicer arietinum* L.) in Algeria. *Phytopathologia Mediterranea* 64(1): 87-99. doi: 10.36253/phyto-15328

Accepted: April 24, 2025

Published: May 15, 2025

Data Availability Statement: All relevant data are within the paper and its Supporting Information files.

Competing Interests: The Author(s) declare(s) no conflict of interest.

Editor: Diego Rubiales, Institute for Sustainable Agriculture, (CSIC), Cordoba, Spain.

ORCID:
IS: 0009-0004-9143-3123
DM: 0000-0002-1198-1444
BSB: 0000-0001-9959-2859
TF: 0000-0002-5806-4790
M-CB: 0000-0002-4708-4307
MR: 0000-0001-9217-6430

INTRODUCTION

Chickpea (*Cicer arietinum* L.) is an important pulse crop for human nutrition, and is a major component of food production systems that are resilient to climate change. Chickpea is a preferred food legumes (Siddique *et al*., 2000) in some regions because of its multiple uses. The high protein content of the seeds (approx. 40% of seed weight), has potential human health benefits, including reduced risk of diabetes, cardiovascular disease, and cancer (Merga and Haji, 2019). Chickpea also contributes to soil fertility by fixing atmospheric nitrogen in the soil through symbiosis with rhizobia, which is especially important in dry climate areas. However, chickpea crops are often affected by telluric diseases such as *Fusarium* wilt, *Verticillium* wilt and those caused by *Sclerotinia* sp. and *Rhizoctonia* sp. (Nene *et al*., 2012).

Fusarium wilt is now widespread in most chickpea production areas of Africa, southern Europe, the Americas, and Asia. This disease is caused by several *Fusarium* species, and accurate and rapid identification of the responsible pathogens is important for development of appropriate and efficient management of Fusarium wilt of chickpea (Tekeoğlu *et al*., 2017). In Algeria, Fusarium wilt of chickpea has been attributed to *Fusarium oxysporum* f. sp. *ciceris* (FOC), but in January 2022 Zaim and Bekkar (2022) reported a second pathogen, *F. redolens* (FR), causing this disease in the western region of the country.

Formal identification of the pathogen responsible for chickpea-wilt in Algeria was made using classical methods, including morphological characteristics and fulfilment of Koch's postulates. *Fusarium oxysporum* (FO) was defined by morphological criteria, including the shape of the microconidia, macroconidia and conidiophore structure (false head on short phialides formed on hyphae). This morphological identification is problematic, however, because of the diversity of non-pathogenic and saprophytic isolates in soil. *Fusarium* isolates are usually tested on the chickpea ILC-482 genotype, which is susceptible to all races of *F. oxysporum* f. sp. *ciceris* (Jimenez-Diaz *et al.,* 1989), and is supposed to confirm the identity of the pathogen.

Identification of *Fusarium* spp. based only on morphology is difficult, because informative morphological characteristics are limited, and microscopic traits can be influenced by environmental conditions, so that their plasticity and intergradation make them subject to misinterpretation (Leslie *et al*., 2001). For example, distinguishing *F. redolens* from *F. oxysporum* can be particularly challenging, because this relies on differences in size of their macroconidia (Gordon, 1952), and intermediate conidium forms may occur (Baayen and Gams, 1988). For these reasons, the taxonomic position of *F. redolens* has been problematic. Whereas Booth (1971) considered this fungus to be a variety of *F. oxysporum,* Nelson *et al*., (1983) considered *F. redolens* and *F. oxysporum* to be synonymous. The use of DNA-based methodologies now makes it possible to differentiate between different species of *Fusarium* (Jimenez-Gasco and Jimenez-Diaz., 2003; Jiménez-Fernandez *et al*., 2011).

During spring of 2020 and 2021, the present study investigated occurrence of *Fusarium* wilt of chickpea in the north of Algeria. Samples were collected from eleven provinces. Wilting and yellowing symptoms were observed on aerial parts of diseased chickpea plants, and 74 fungal isolates were obtained from roots. To identify these isolates, their translation elongation factor 1-alpha (EF-1α) gene regions were sequenced.

MATERIALS AND METHODS

Plant sampling, and isolation and maintenance of fungi

During the chickpea growing seasons of spring 2020 and 2021, chickpea plants with yellowing and wilting symptoms on their areal parts were collected from 23 farmer fields in different areas in north western and eastern Algeria. These areas were in to 11 provinces, five in the western region and six in the eastern region. The major chickpea sowing method in the west is strip sowing, whereas in the east it is broadcast sowing.

Tissue pieces (5 × 5 mm) were taken from diseased tap root tissues of wilted chickpea plants, and were surface-sterilized in 2% sodium hypochlorite for 30 sec, then rinsed three times in sterile distilled water, and dried on sterile paper. Samples were then plated on potato dextrose agar (PDA), and incubated at 27°C in the dark for 7 d. Growing tips of hyphae developing from in cultures were then transferred onto fresh PDA. Monoconidial isolates were prepared from cultures of fungi obtained from each region, and cultures were stored at 4°C.

A total of 74 *Fusarium* sp. isolates were obtained, of which 31 were sequenced using the EF-1α gene. The 31 isolates were chosen based on macroscopic characteristics (colony colour and appearance on PDA). Two to four representative isolates of the morphotypes from each province were considered.

DNA extractions

The selected fungal cultures were grown on PDA 25 ± 2°C in the dark for 7 d. For each extraction, 100 mg of mycelium was collected by scraping the colonies

from three plates per isolate. DNA of each isolate was extracted using a commercial NucleoSpin Plant II kit (Macherey-Nagel), following the supplier's instructions. The quality and concentration of extracted DNA were verified after 1% agarose gel electrophoresis, using a NanoDrop spectrophotometer (at 260/280 nm).

Molecular characterization of Fusarium *isolates*

The translation elongation factor-1alpha (EF-1α) gene region was amplified by PCR, using the universal primers EF-728F (CATYGAGAAGTTCGAGAAGG) and EF-2 (GGARGTACCAGTSATCATGTT) (Carbone and Kohn, 1999), in a 25 µL reaction volume containing 1.5 mM $MgCl_2$ (Promega), 0.2mM dNTPs (Invitrogen), 2 µg mL^{-1} fungal DNA, 0.5µM primers each, 1× Taq Buffer (Promega), and 1-unit Taq polymerase (Promega).

Amplifications were carried out in a thermal cycler (Icycler Bio-Rad), with an initial denaturation step for 5 min at 95°C, followed by 35 cycles each of 30 sec of denaturation at 95°C, 30 sec at annealing temperature (52°C), and 45 sec at 72°C, and an extension step of 7 min at 72°C. Amplification products were separated by electrophoresis on a 1.5% agarose gels. The gels were stained with MidoriGreen (Nippon), and were visualized under UV light by using the Gel doc system (Biorad). The size marker was a 100 bp DNA ladder (Invitrogen). The PCR products were purified with a NucleoSpin® Gel and a PCR Clean-up kit (Macherey-Nagel), following the manufacturer's instructions. PCR products of the EF-1α regions were sequenced by Sanger sequencing (Sanger *et al*., 1977) directly from the PCR products, without a cloning step, using Applied Biosystems BigDye Kit v3.1 and the primers used for PCR amplification of the fragments. Sequencing was performed in the direction (forward/reverse) for each amplicon. Sequencing was carried out by Gene Life Sciences.

The sequences obtained were analyzed and cleaned using the CHROMAS PRO software, and were then compared with those from the GenBank database using the BLAST Program (https://blast.ncbi.nlm.nih.gov/Blast.cgi Blast) to identify the isolates based on percentage homology with reference strains. A dendrogram was established using the UPGMA method algorithm to show the genetic diversity of the isolated fungi.

Assessment of Koch's postulates for representative fungi

To verify the pathogenicity of *Fusarium* spp. isolates, five species [*F. redolens* (FR), *F. solani* (FS), *F. oxysporum* (FO), *Fusarium oxysporum* f. sp. *ciceris* (FOC), and *F. oxysporum* f. sp. *lactuceae* (FOL)] were inoculated individually onto plants of cultivar ILC-482 from ICARDA. The seeds were surface sterilized, and then pre-germinated on moist cotton wool, which provided favorable conditions for seedling germination (ISTA, 2015; Korter *et al.,* 2023).

The pre-germinated seeds were then sown in plastic pots (30 × 20 cm) containing a sterile mixture of potting soil and sand (1:1 v:v). For each *Fusarium* sp., three pots each containing four plants were used. Seven d after sowing (3–4 leaf stage), the plants were removed from soil and their root systems were soaked for 30 min in a conidial suspension (10^6 conidia mL^{-1} (Gao *et al*., 1995; Ficcadenti *et al*., 2002). Five pots were used as controls, where the plants were soaked in sterile water without inoculum.

RESULTS AND DISCUSSION

In the assayed chickpea fields, diseased plants were spread throughout each field, with incidence up to 30% (Figure 1, a and b). In addition to wilting and yellowing symptoms, the stems and root xylem tissues of the diseased plants had black discolourations (Figure 2 a). Brown necrotic lesions in the tap roots and necroses of lateral roots (Figure 2 b) also occurred on most of the sampled plants from the west of Algeria. The same symptoms were observed by Jimenez-Fernandez *et al*. (2011).

On PDA, colonies of the isolates had different morphotypes (Figure 3), with differences in colour, growth rates, and aspect of mycelium. All colonies initially had white to cream-coloured mycelium, which turned (after 3 to 7 d incubation) to purple and pink for isolates of *F. redolens*, purple tinged or slightly orange for *F. solani*, or cream or purple for *F. oxysporum* f. sp. *ciceris* and *F. oxysporum*. The mycelium texture was fluffy or appressed.

Microscopic observations of most of the isolates revealed septate mycelium which carried phialides bearing false-headed conidia (Figure 4).

The morphological and cultural characteristics on PDA identified the isolates as *Fusarium* sp., based on the descriptions of Booth (1977).

BLASTn sequence analyses with (https://blast.ncbi.nlm.nih.gov/Blast.cgi) identified the isolates as follows: ten isolates were *F. redolens*, six were *F. oxysporum* f. sp. *ciceris*, nine were *F. oxysporum, five were F. oxysporum* f. sp. *Lactuceae*, and one isolate was *F. solani* (*Ascomycota*, *Pezizomycotina*, *Sordariomycetes*, *Hypocreomycetidae*, *Hypocreales*, *Nectriaceae*) with 94.85 to 100% sequence similarity to the sequences of type isolates from Genbank.

A dendrogram was constructed based on the EF-1α sequences, using the UPGMA method (Sneath and

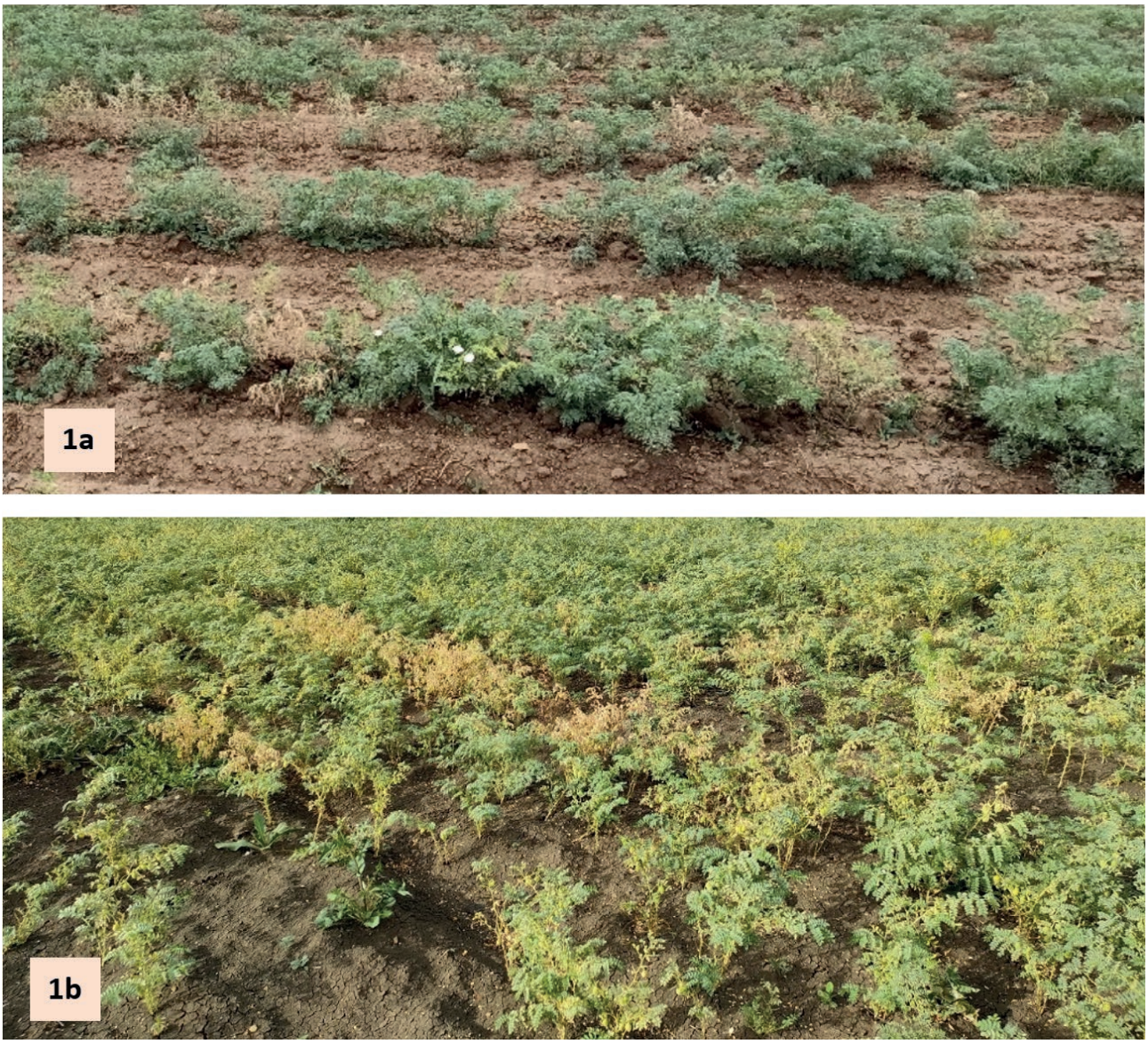

Figure 1. (**1a**) Typical symptoms of Fusarium wilt caused by *Fusarium redolens* on chickpea plants in the Ain Temouchent region (Western Algeria). (**1b**) Typical symptoms of Fusarium wilt caused by *Fusarium oxysporum* f. sp. *ciceris* in chickpea plants in Mila (Eastern region).

Sokal, 1973) to show phylogenetic relationships among the *Fusarium* isolates obtained from different regions of Algeria (Figure 5). The branches of the dendrogram were supported by bootstrap values, demonstrating the robustness of the phylogenetic relationships among these isolates. For 15 isolates from the western region, ten isolates (67%) were FR, four (27%) were FO of one *forma specialis* (*F. oxysporum* f. sp. *lactuceae*), and one isolate (6.7%) was FS. In contrast, among the 16 isolates from the eastern region of Algeria, all were FO, in which two *formae speciales* were identified, six of FOC, and three of FOL (Table 1).

These results indicate that *F. redolens* is dominant in the western region of Algeria, while *F. oxysporum* prevails in the eastern region, where *F. oxysporum* f. sp. *ciceris* was the most frequently identified *forma specialis* among the isolates collected from the east. *Fusarium oxysporum* f. sp. *ciceris* was not isolated from the western region, and *Fusarium redolens* was not isolated from the eastern region of the country (Figure 6).

Koch's postulates were confirmed by inoculating chickpea cultivar ILC-482 and re-isolating the fungi from the inoculated chickpea roots, which indicates that all the *Fusarium* isolates were infectious agents of

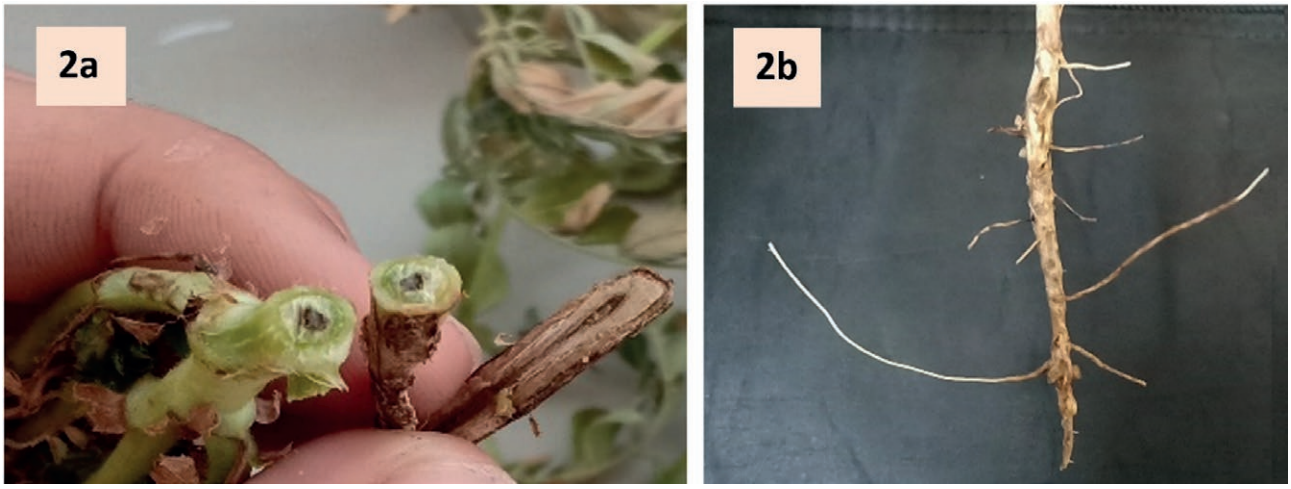

Figure 2. (2a) Cross section of a chickpea stem showing discoloration (black and brown necrosis) of the xylem and pith tissue caused by *Fusarium redolens*. **(2b)** Brown necrotic lesions in the tap root and necrosis of lateral roots showing on chickpea infected with *Fusarium.*

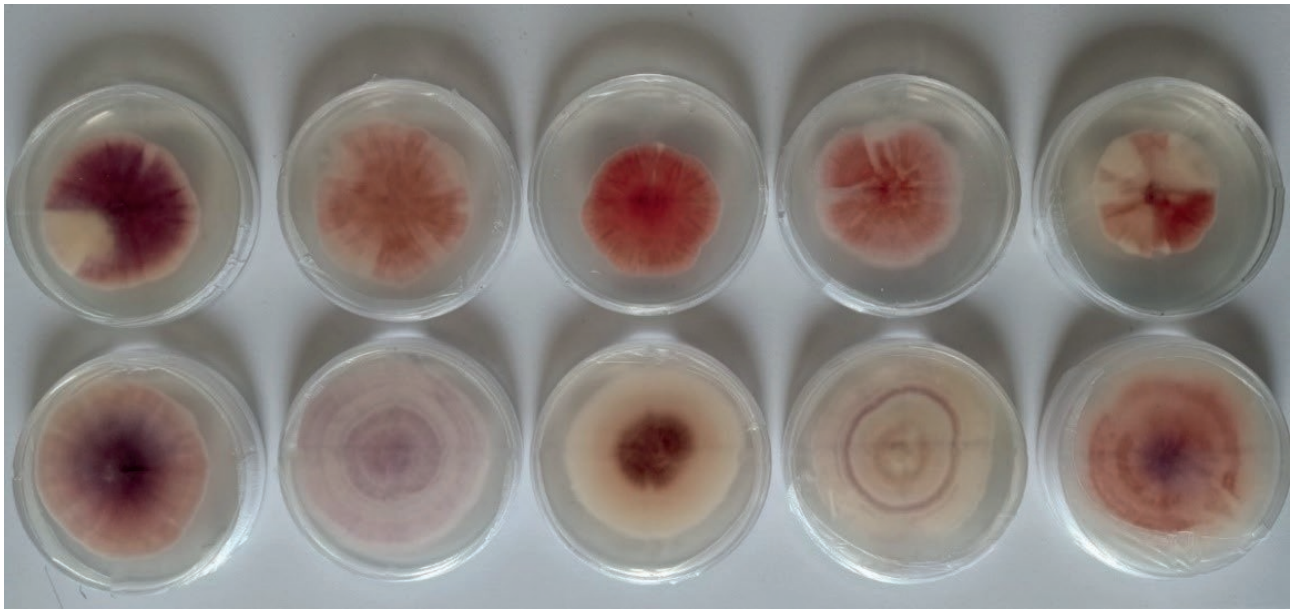

Figure 3. Different morphotypes of *Fusarium* spp. of a colony isolated from chickpea, on PDA medium, after 8 days of incubation.

diseased plants sampled from the chickpea fields. These results show that chickpea culture can be susceptible to different *Fusarium* species, and even to FOL that has been previously shown to be a pathogen of lettuce. All the inoculated plants developed progressive wilting. Although *formae speciales* of *F. oxysporum* are mainly described as highly specific, their host ranges have been found to increase. For example, only 53 of the 106 *formae speciales* listed by Edel-Hermann and Lecomte (2019) remain associated with a unique plant species. Similarly, Ramirez-Suero *et al*. (2010) showed susceptibility of *Medicago truncatula* to several *F. oxysporum formae speciales*, even from non-legume hosts.

In the present study, wilting symptoms appeared on inoculated plants at 21 d after inoculation for all of the *Fusarium* isolates. Leaves at the base of plants initially showed marginal yellowing before wilting (Figure 7). The symptoms then developed progressively towards the upper leaves, and most rapidly in plants inoculated with *F. oxysporum* f. sp. *ciceris* and *F. redolens*. Roots of inoc-

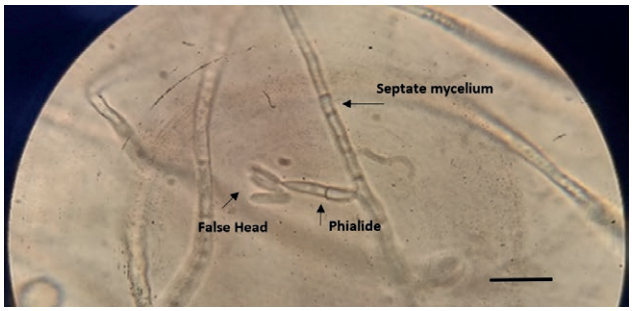

Figure 4. Microscopic features of *Fusarium redolens* (isolate FR1). Note the phialide bearing false-headed conidia on a septate hypha (x 100). Bar = 20 µm.

ulated plants had reduced root hairs and brown/black discolouration, which extended to the plant collars and sometimes caused collar narrowing (Figure 7b).

Longitudinal sections of primary roots of the diseased plants had dark vascular necroses, which were more or less dark according to the inoculated *Fusarium* isolates. Root xylem necroses were sometimes accompanied by wet rots, where plants were inoculated with *F. solani* or *F. redolens* (Figure 8). All non-inoculated (control) plants remained healthy. Symptoms on roots and leaves were more severe on plants inoculated with isolates of FOC or FR than on those inoculated with the other isolates (Figure 7, a and b).

To date, chickpea wilt in the western region of Algeria has been attributed to *Fusarium oxysporum* f. sp. *ciceris,* using morphological characteristics of the pathogenic fungi (Benfreha *et al*., 2014) or Koch's postulates for the chickpea ILC-482 genotype (Tlemsani *et al*., 2015; Zaim, 2016). The present study indicates that FOC does not exist in the western region of Algeria. Using ITS and EF-1α, Zaim and Bekkar (2022) identified only *Fusarium redolens* of 20 *Fusarium* isolates from chickpea in the western region of this country. The present study further confirms the absence of FOC, since among the 15 *Fusarium* isolates that were obtained from the western region, ten were *F. redolens*, and the remaining five were FS (one isolate), FO (two isolate), and FOL (two isolates). Although only 31 of 74 isolates were sequenced in the present study, these results and those of Zaim and Bekkar (2022) confirm that FOC is absent from western Algeria.

Fusarium redolens has been reported to cause wilt of tomato (Edel-Hermann *et al*., 2012), and damping-off of Aleppo pine (*Pinus halepensis*) (Lazreg *et al*., 2013) in the North west of Algeria. Association of *F. redolens* with wilt symptoms of chickpea has been reported in Morocco, Spain, Lebanon, and Pakistan (Jimenez-Fernandez *et al*., 2011), Saskatchewan (Taheri, 2011), Tunisia (Bou-

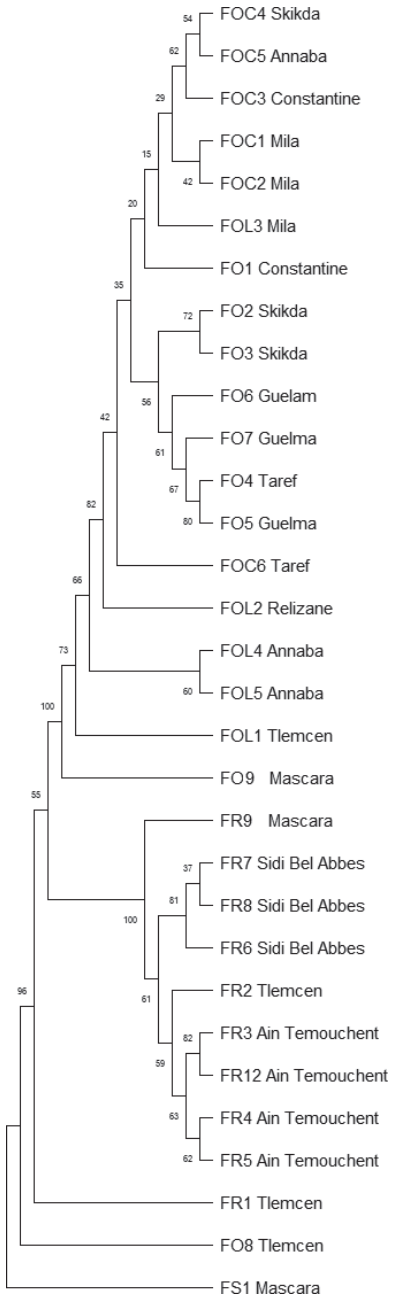

Figure 5. Dendrogram of *Fusarium* wilt species, obtained using the UPGMA method. The bootstrap consensus tree inferred from 1000 replicates (Tamura K. *et al*., 2004) is taken to represent the evolutionary history of the taxa analyzed (Tamura *et al*., 2004). The percentages of replicate trees in which the associated taxa clustered together in the bootstrap test (1000 replicates) are shown next to the branches (Tamura K. *et al*., 2004). The evolutionary distances were computed using the Maximum Composite Likelihood method (Tamura K. *et al*., 2021), and are the numbers of base substitutions per site. This analysis involved 31 nucleotide sequences. Codon positions included were 1st+2nd+3rd+Noncoding. All ambiguous positions were removed for each sequence pair (pairwise deletion option). There were 1042 positions in the final dataset. Evolutionary analyses were conducted in MEGA11 (Felsenstein J., 1985).

Table 1. Identities of *Fusarium* isolates, their sampling site fields, and their EF-1α sequence similarities with reference strains, for isolates from different regions and provinces in Algeria.

Region	Province	Code	Identification	Field coordinates	Percentage similarity	Blast Best Hit ID	Accession number NCBI
Western region	Tlemcen	FOL1	*Fusarium oxysporum* f. sp. *lactuceae*	35°09'54.3"N+1°26'50.7"W	98.64	MK801786.1	PQ899234
		FR1	*Fusarium redolens*	34°56'42.5"N+1°14'59.6"W	94.85	*HQ731060.1*	PV388859
		FR2	*Fusarium redolens*		99.75	*HQ731060.1*	PV388860
		FO8	*Fusarium oxysporum*	35°09'54.3"N+1°26'50.7"W	100.00	*ON703236.1*	PQ899228
	Ain Temouchent	FR12	*Fusarium redolens*	35°13'56.7"N+1°20'50.5"W	99.16	*HQ731063.1*	PV388869
		FR3	*Fusarium redolens*	35°13'56.7"N+1°20'50.5"W	99.58	*MT305223.1*	PV388861
		FR4	*Fusarium redolens*	35°16'36.2"N+1°13'43.1"W	99.58	*OR270920.1*	PV388862
		FR5	*Fusarium redolens*	35°17'43.2"N+1°05'10.6"W	99.57	*OR105855.1*	PV388863
	Sidi Bel Abbes	FR6	*Fusarium redolens*	35°14'18.9"N+0°43'51.5"W	99.79	*OR270920.1*	PV388864
		FR7	*Fusarium redolens*	35°16'15.8"N+0°35'04.5"W	99.79	*OR270920.1*	PV388865
		FR8	*Fusarium redolens*	35°23'25.0"N+0°29'03.4"W	99.85	*MK172061.1*	PV388866
	Mascara	FR9	*Fusarium redolens*	35°26'56.5"N+0°08'48.9"E	99.57	*HQ731060.1*	PV388867
		FS1	*Fusarium solani*	35°24'23.9"N+0°18'27.0"E	99.57	*HE647956.1*	OR234389
		FO9	*Fusarium oxysporum*		97.53	*MW361989.1*	-
	Relizane	FOL2	*Fusarium oxysporum* f. sp. *lactuceae*	35°59'58.4"N+0°52'33.9"E	99.35	*MH412703.1*	PQ899235
Eastern region	Mila	FOC1	*Fusarium oxysporum* f. sp. *ciceris*	36°30'22.9"N+6°16'35.1"E	99.55	FJ538240.1	PQ899229
		FOC2	*Fusarium oxysporum* f. sp. *ciceris*	36°27'54.3"N+6°13'21.8"E	100.00	FJ538240.1	PQ899230
		FOL3	*Fusarium oxysporum* f. sp. *lactuceae*	36°27'21.7"N+6°12'51.0"E	99.85	OP918954.1	PQ899236
	Constantine	FOC3	*Fusarium oxysporum* f. sp. *ciceris*	36°17'58.0"N+6°38'41.8"E	100.00	FJ538241.1	PQ899231
		FO1	*Fusarium oxysporum*	36.294952, 6.641571	98.46	*PP795998.1*	PQ613583
	Skikda	FOC4	*Fusarium oxysporum* f. sp. *ciceris*	36°43'22.0"N+6°51'29.3"E	100.00	FJ538241.1	PQ899232
		FO2	*Fusarium oxysporum*	36°42'43.2"N+6°47'47.8"E	100.00	*OQ511027.1*	PQ613583
		FO3	*Fusarium oxysporum*		99.85	*OQ511027.1*	PQ899231
	Annaba	FOC5	*Fusarium oxysporum* f. sp. *ciceris*		98.85	FJ538241.1	PQ899233
		FOL4	*Fusarium oxysporum* f. sp. *lactuceae*	36°46'38.1"N+7°44'18.4"E	99.57	*MW316853.1*	PQ899237
		FOL5	*Fusarium oxysporum* f. sp. *lactuceae*		99.78	*MW316854.1*	-
	El Taref	FOC6	*Fusarium oxysporum* f. sp. *ciceris*	36°42'28.4"N+7°44'26.5"E	98.81	FJ538240.1	-
		FO4	*Fusarium oxysporum*		99.85	*OQ511027.1*	PQ613586
	Guelma	FO5	*Fusarium oxysporum*	36°39'03.1"N+7°42'35.2"E	99.85	*KF537337.1*	PQ613587
		FO6	*Fusarium oxysporum*		100.00	*OQ511027.1*	PQ613588
		FO7	*Fusarium oxysporum*		99.85	*OQ511027.1*	PQ899227

hadida *et al*., 2017), Turkey (Tekeoğlu *et al*., 2017), and Iran (Chehriand Sattar, 2018).

The present study isolated *F. solani* from the western region of Algeria. This fungus was previously reported to infect chickpea in China, India, Spain, Pakistan, Iran, and other countries (Zhuang *et al*., 2005; Jiménez-Fernández *et al*.,2011). In Algeria, *F. solani* has been reported to cause wilt of potato (*Solanum tuberosum*) (Azil *et al*., 2021) and tomato (*Solanum lycopersicum*) (Abdesselem *et al*., 2016), as well as damping-off of Aleppo pine (*Pinus halepensis*) (Lazreg *et al*., 2014). Therefore, the present study is the first to show that *F. solani* is a chickpea pathogen in Algeria.

While *F. redolens* and *F. oxysporum* f. sp. *ciceris* are known to cause yellowing and wilt of chickpea, the reasons for their distinct geographic distributions in Algeria remains unclear. Several factors could explain this separation of the pathogens, including variations in climate,

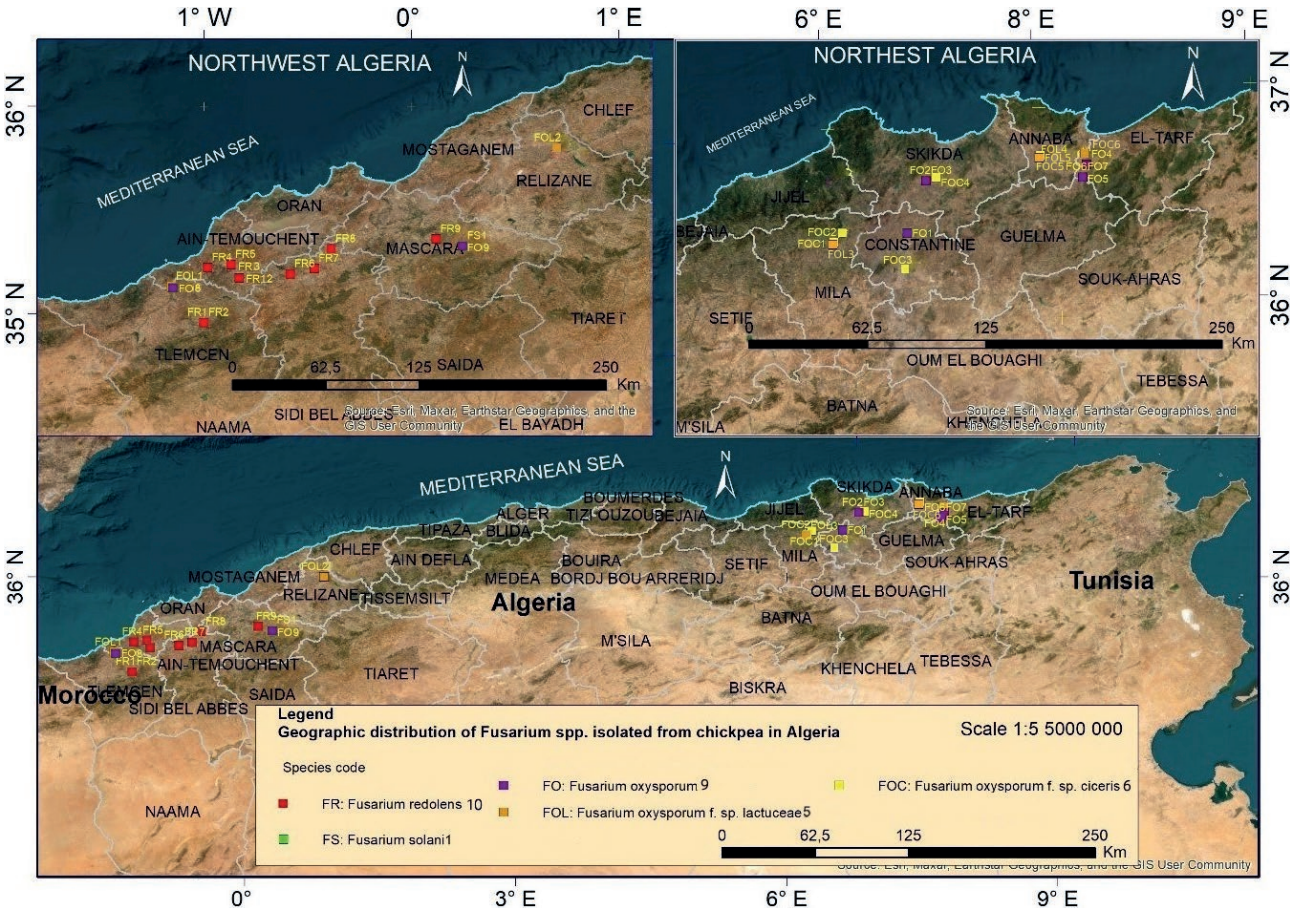

Figure 6. Geographic distribution of *Fusarium* spp. isolated from chickpea in Algeria, recorded with ArcGis software. The numbers after the names of the *Fusarium* species correspond to the numbers of obtained isolates of that species.

soil structure, and cropping systems. Further research is required to confirm these potential influences.

It is well-documented that plant pathogen prevalence can be linked to climatic conditions, such as temperature and rainfall, which differ across geographic regions. For example, *F. graminearum* tends to dominate in warm areas such as parts of the United States of America, while *F. culmorum* is common in cool, maritime regions such as the United Kingdom (Parry *et al*., 1995; Doohan *et al*., 2003). Similarly, optimal temperatures and moisture levels are critical for *Fusarium* sporulation and inoculum dispersal (Rossi *et al*., 2001), suggesting that local environmental factors may play a role in the distributions of FR and FOC.

Soil characteristics, including moisture and pH, also affect *Fusarium* spp. growth and resulting host disease development. Previous studies have shown that soil pH can influence *Fusarium* growth rates and expression of wilt symptoms (Chen *et al*., 2013; Gatch and du Toit, 2017). Additionally, resistance to *Fusarium* wilt has been observed in particular soils, with microbiological interactions such as competition for iron and/or carbon playing important roles (Elad and Baker, 1985b; Couteaudier and Alabouvette, 1990).

To fully understand the geographic distributions of FOC and FR, further research is required on effects on the fungi of soil physicochemical properties, microbial communities, and agricultural practices. It remains that FS and FOC could be serious future threats to chickpea cultivation in Algeria. It would also be worthwhile to test the aggressiveness of *Fusarium* spp. on different chickpea cultivars to understand whether those isolates have cultivar specificities.

The use of morphological traits to differentiate morphologically similar *Fusarium* spp., including *F. oxysporum* and *F. redolens*, may lead to incorrect pathogen identifications. However, accurate identification of pathogenic *Fusarium* spp. and *F. oxysporum formae speciales* is important for efficient management of diseases caused by these fungi, particularly when resistant cultivars are

Figure 7. (7a) Wilt symptoms, on chickpea cultivar ILC482 30 d after inoculation with *Fusarium isolates.* **a,** *F. oxysporum* f. sp. *ciceris;* **b,** *F. redolens;* **c,** *F. solani*; **d,** *F. oxysporum*; **e,** *F. oxysporum* f. sp. *lactucae*; **f,** Inoculation Control. **(7b)** Symptoms on chickpea cultivar ILC482 inoculated with *Fusarium isolates,* 30 days after inoculation: **a,** *F. redolens*; **b,** *F. oxysporum* f. sp. *ciceris;* **c,** *F. oxysporum;* **d,** *F. oxysporum* f. sp. *lactucae*; **e,** *F. solani*; **f,** Inoculation Control.

Figure 8. Symptoms in xylem tissues of chickpea cultivar ILC-482 inoculated with *Fusarium* isolates. **a,** Inoculation Control; **b.** inoculation with *F. oxysporum;* **c,** with *F. oxysporum* f. sp. *lactucae*; **d,** with *F. oxysporum* f. sp. *ciceris*; **e,** with *F. redolens*; **f**, inoculation with *F. solani.*

one of the few and most effective control measures for these diseases, as is the case for *Fusarium* wilt of chickpea (Nene and Reddy, 1987).

Identification of new pathogen species and races would help plant breeders to select appropriate germplasm for development of resistant crop cultivars. Identification of disease-causing *Fusarium* spp. may also help development of cultural practices for management of *Fusarium* wilt, which can be achieved with use of resistant cultivars and adjustment of sowing dates (Jiménez *et al*., 1991; Jalali and Chand, 1992; Jiménez *et al*., 1998; Landa *et al*., 2004; Navas-Cortés *et al*., 1998; Navas-Cortés *et al*., 2000), and appropriate crop rotations (Landa *et al*., 2006).

LITERATURE CITED

Abdesselem S.M., Nisserine H.K., Mebrouk K., Jamal E.H., Jos Eacute S., Eduardo G., 2016. Characterization of *Fusarium oxysporum* isolates from tomato plants in Algeria. *African Journal of Microbiology Research* 10, 1156–1163. https://doi.org/10.5897/ajmr2016.8161

Azil N., Stefanczyk E., Sobkowiak S., Chihat S., Boureghda H., Sliwka, J., 2021. Identification and pathogenicity of *Fusarium* spp. Associated with tuber dry rot and wilt of potato in Algeria. *European Journal Plant Pathology* 159, 495–509. https://doi.org/10.1007/s10658-020-02177-5

Baayen R.P., Gams W., 1988. The Elegans fusaria causing wilt disease of carnation. I. Taxonomy. *Netherlands Journal of Plant Pathology* 94: 273–288.

Benfreha F.Z., Henni D.E., Merzoug A., 2014. *Fusarium* wilt of Chickpea (*Cicer arietinum* L.) in Northwest Algeria. *African Journal of Agricultural Research* Vol. 9(1), 168-175, https://doi.org/10.5897/AJAR2013.6694

Booth C., 1971. *The Genus Fusarium*. Commonwealth Mycological Institute, Kew, Surrey, UK. Reprinted 1977, 237 pp.

Booth C., 1977. *Fusarium Laboratory Guide to the Identification of the Major Species*. Commonwealth Mycological Institute, Kew, Surrey, England, 58 pp.

Bouhadida M., Jendoubi W., Gargouri S., Beji M., Kharrat M., Chen W., 2017. First report of *Fusarium redolens* causing *Fusarium* yellowing and wilt of chickpea in Tunisia. *Plant Disease* 101. https://doi.org/10.1094/PDIS-08-16-1114-PDN

Carbone I., Kohn L.M., 1999. A method for designing primer sets for speciation studies in filamentous ascomycetes. *Mycologia* 91: 553–556. https://doi.org/10.2307/3761358

Chehri K.h., Sattar H.A., 2018. Detection of fumonisin chemotype produced by *Fusarium proliferatum* isolated from nuts in Iraq using specific PCR assays. *Biological Journal of Microorganism* 24: 21–27.

Chen L.H., Huang X.Q., Yang X.M., Shen Q.R., 2013. Modeling the effects of environmental factors on the population of *Fusarium oxysporum* in cucumber continuously cropped soil. Communications in *Soil Science and Plant analysis* 44: 2219–2232.

Couteaudier Y., Alabouvette C., 1990. Quantitative comparison of *Fusarium oxysporum* competitiveness in relation with carbon utilization. *FEMS Microbiology Ecology* 74: 261–268.

Doohan F.M., Brennan J., Cooke B.M., 2003. Influence of climatic factors on *Fusarium* species pathogenic to cereals. *European Journal of Plant Pathology* 109: 755–768. https://doi.org/10.1023/A:1026090626994

Edel-Hermann V., Gautheron N., Steinberg C., 2012. Genetic diversity of *Fusarium oxysporum* and related species pathogenic on tomato in Algeria and other Mediterranean countries. *Plant Pathology* 61: 787–800. https://doi.org/10.1111/j.1365-3059.2011.02551.x

Edel-Hermann V., Lecomte C., 2019. Current status of *Fusarium oxysporum* formae speciales and races. *Phytopathology* 109: 512–530. https://doi.org/10.1094/PHYTO-08-18-0320-RVW

Elad Y., Baker R., 1985b. The role of competition for iron and carbon in suppression of chlamydospores germination of *Fusarium* spp. by *Pseudomonas* spp. *Phytopathology* 75: 1053–1059.

Felsenstein J., 1985. Confidence limits on phylogenies: An approach using the bootstrap. *Evolution* 39: 783–791.

Ficcadenti N., Sestili S., Annibali S., Campanelli G., Belisario A., ... Corazza L., 2002. Resistance to *Fusarium oxysporum* f. sp. *melonis* Race 1, 2 in Muskmelon Lines. *Plant Disease*, 86: 897–900.

Gao H., Beckman C.H., Mueller W.C., 1995. The rate of vascular colonisation as a measure of the genotypic interaction between various cultivars of tomato various formae or races of *Fusarium oxysporum*. *Physiological Molecular Plant Pathology* 46: 29–43.

Gatch E.W., du Toit L.J., 2017. Limestone-mediated suppression of *Fusarium* wilt in spinach seed crops. *Plant Disease* 101: 81–94. https://doi.org/10.1094/PDIS-04-16-0423-RE

Gordon W.L., 1952. The occurrence of *Fusarium* species in Canada, II. Prevalence and taxonomy of *Fusarium* species in cereal seeds. *Canadian Journal of Botany* 30: 236–238.

ISTA, 2015. *International Rules for Seed Testing*. International Seed Testing Association, Bassersdorf, Switzerland.

Jalali B.L., Chand H., 1992. Chickpea wilt. In: *Plant Diseases of International Importance.. Diseases of Cereals and Pulses*. Vol. I (Singh U.S., Mukhopadhayay A.N., Kumar J., Chaube H.S., ed). Prentice Hall, Englewood Cliffs, NJ, USA. 429–444.

Jimenez-Diaz R.M., Singh K.B., Trapero-Casas A., 1989. Races of *Fusarium oxysporum* f. sp. *ciceri* infecting chickpeas in southern Spain. In: *Vascular Wilt Diseases of Plants* (Tjamos E.C., Beckman C.H. ed.), NATO ASI Ser., Springer-Berlin, 1989, vol. H28, 515–520.

Jiménez-Díaz, R.M., Porta-Puglia A., Tivoli B., 1998. New approaches in the integrated management of legume diseases: Toward sustainable crop health. Pages 89–93. In: *European Conference Grain Legumes*, 3rd. Opportunities for High Quality, Healthy and Added-value Crops to Meet European Demands. European Association for Grain Legumes, ed. Valladolid, Spain.

Jiménez-Díaz R.M., Singh K.B., Trapero-Casas A., Trapero-Casas, JL, 1991. Resistance in kabuli chickpeas to *Fusarium* wilt. *Plant Disease* 75: 914–918.

Jimenez-Fernandez D., Navas-Cortes J.A., Montes-Borrego M., Jiménez-Díaz RM, Landa B.B., 2011. Molecular and pathogenic characterization of *Fusarium redolens*, a new causal agent of *Fusarium* yellows in chickpea. *Plant Disease* 95: 860–870. https://doi.org/10.1094/PDIS-12-10-0946

Jiménez-Gasco M.M., Jiménez-Díaz R.M., 2003. Development of a specific polymerase chain reaction based-assay for the identification of *Fusarium oxysporum* f. sp. *ciceris* and its pathogenic races 0, 1A, 5 and 6. *Phytopathology* 93: 200–209. https://doi.org/10.1094/PHYTO.2003.93.2.200

Korter G.O., Sunday A.A., Ehiagwina F.O., Lawal P.O., Akinola T.E., Kolawole S.K., 2023. Comparative studies of rockwool and cotton wool for tomatoes production: Nutrient balance, plant growth and fruit quality. *International Research Journal of Modernization in Engineering Technology and Science* 5: 19–25.

Landa B.B., Navas-Cortés J.A., Jiménez-Díaz R.M., 2004. Integrated management of *Fusarium* wilt of chickpea with sowing date, host resistance, and biological control. *Phytopathology* 94: 946–960. https://doi.org/10.1094/PHYTO.2004.94.9.946

Landa B.B., Navas-Cortés J.A., Jiménez-Gasco M.M., Katan J., Retig B., Jiménez-Díaz R.M., 2006. Temperature response of chickpea cultivars to races of *Fusarium oxysporum* f. sp. *ciceris*, causal agent of *Fusarium* wilt. *Plant Disease* 90: 365–374. https://doi.org/10.1094/PD-90-0365

Lazreg F., Belabid L., Sanchez J., Gallego E., Bayaa B., 2014. Pathogenicity of *Fusarium* spp. associated with diseases of Aleppo-pine seedlings in Algerian forest nurseries. *Journal of Forest Science* 60:1 15–120.

Lazreg F., Belabid L., Sanchez J., Gallego E., Garrido-Cardenas J.A., Elhaitoum A., 2013. First Report of *Fusarium redolens* as a Causal Agent of Aleppo Pine Damping-Off in Algeria. *Plant Disease* 97: 997. https://doi.org/10.1094/PDIS-12-12-1169-PDN

Leslie J.F., Zeller K.A., Summerell B.A., 2001. Icebergs and species in populations of Fusarium. *Physiological and Molecular Plant Pathology*. 59: 107–117. https://doi.org/10.1006/pmpp.2001.0351

Merga B., Haji J., 2019. Economic importance of chickpea: production, value, and world trade. *Cogent Food & Agriculture*, vol. 5 (1). https://doi.org/10.1080/23311932.2019.1615718

Navas-Cortés J.A., Hau B., Jiménez-Díaz, R.M., 1998. Effect of sowing date, host cultivar, and race of *Fusarium oxysporum* f. sp. *ciceris* on development of Fusarium wilt of chickpea. *Phytopathology* 88: 1338–1346. https://doi.org/10.1094/PHYTO.1998.88.12.1338

Navas-Cortés J.A., Hau B., Jiménez-Díaz, R.M., 2000. Yield loss in chickpeas in relation to development of *Fusarium* wilt epidemics. *Phytopathology* 90: 1269–1278. https://doi.org/10.1094/PHYTO.2000.90.11.1269

Nelson P.E., Toussoun T.A., Marasas W.F.O., 1983. *Fusarium species: An illustrated Manual for Identification*. Pennsylvania State University Press, University Park, USA.

Nene Y.L., Reddy M.V., 1987. Chickpea diseases and their control. In: *The Chickpea*. (Saxena M.C., Singh K.B., ed.). Oxon, UK. CAB-International, 233–270.

Nene Y.L., Reddy M.V., Haware M.P., Ghanekar A.M., Amin K.S., … Sharma M., 2012. *Field Diagnosis of Chickpea Diseases and their Control. Information Bulletin* No. 28 (revised). International Crops Research Institute for the Semi-Arid Tropics. 60 pp.

Parry D.W., Jenkinson P., McLeod L., 1995. Fusarium ear blight (scab) in small grain cereals – a review. *Plant Pathology*. https://doi.org/10.1111/j.1365-3059.1995.tb02773.x

Ramirez-Suero M., Khanshour A., Martinez Y., Rickauer M., 2010. A study on the susceptibility of the model legume plant *Medicago truncatula* to the soil-borne pathogen *Fusarium oxysporum*. *European Journal Plant Pathology* 126: 517–530. https://doi.org/10.1007/s10658-009-9560-x

Rossi V., Ravanetti A., Pattori E., Giosuè S., 2001. Influence of temperature and humidity on the infection of wheat spikes by some fungi causing *Fusarium* head blight. *Journal of Plant Pathology* 83: 189–198. https://doi.org/10.4454/JPP.V83I3.1128

Sanger F., Nicklen S., Coulson AR, 1977. DNA sequencing with chain-terminating inhibitors. *Proceedings*

National Academy Sciences USA 74 (12): 5463–7. Bib code: 1977PNAS...74.5463S. https://doi.org/10.1073/pnas.74.12.5463. PMC 431765. PMID 271968

Siddique K.H.M., Brinsmead R.B., Knight R., Knights E.J., Paull J.G., Rose I.A., 2000. Adaptation of chickpea (*Cicer arietinum* L.) and faba bean (*Vicia faba* L.) to Australia. In R. Knight (Ed.), *Linking Research and Marketing Opportunities for Pulses in the 21st Century* (289–303). Dordrecht: Kluwe Academic Publishers. https://doi.org/10.1007/978-94-011-4385-1_26

Sneath P.H.A. and Sokal R.R. 1973. *Numerical Taxonomy*. Freeman, San Francisco. 600 pp.

Taheri A.E., 2011. First report of *Fusarium redolens* from Saskatchewan and its comparative pathogenicity. *Canadian Journal Plant Pathology* 33: 559. https://doi.org/10.1080/07060661.2011.620631

Tamura K., Nei M., Kumar S., 2004. Prospects for inferring very large phylogenies by using the neighbor-joining method. *Proceedings of the National Academy of Sciences* (USA) 101: 11030–11035.

Tamura K., Stecher G., Kumar S. 2021. MEGA 11: Molecular Evolutionary Genetics Analysis Version 11. *Molecular Biology and Evolution*. https://doi.org/10.1093/molbev/msab120.

Tekeoğlu M., Özkılınç H., Tunalı B., Kusmenoğlu İ., Chen W., 2017. Molecular identification of *Fusarium* spp. causing wilt of chickpea and the first report of *Fusarium redolens* in Turkey *Mediterranean Agricultural Sciences* 30 (1): 27–33. https://doi.org/10.22268/AJPP-39.4.231240

Tlemsani M., Bellahcene M., Fortas Z., 2015. Behavior study of chickpeas varieties (*Cicer arietinum* L.) against *Fusarium* wilt. *Asian Journal of Biochemical and Pharmaceutical Research*.

Zaim S., 2016. *Essai de lutte biologique contre le Fusarium oxysporum f. sp. ciceris à l'aide des microorganismes de la rhizosphère de la culture du pois chiche*. PhD Thesis, University of Mascara, Mascara, Algeria, 220 pp.

Zaim S., Bekkar A.A., 2022. First report of *Fusarium redolens* causing *Fusarium* yellows on chickpea in Algeria. *Journal of Plant Pathology* 104(2). https://doi.org/10.1007/s42161-022-01044-y

Zhuang W.Y., Guo L., Guo S.Y., Guo Y.L., Mao X.L., ... Zhang X.Q., 2005. *Fungi of Northwestern China*. Ithaca (NY): *Mycotaxon*, 430 pp.

Phytopathologia Mediterranea
The international journal of the
Mediterranean Phytopathological Union

Firenze University Press
www.fupress.com/pm

Research Papers

First report of *Xanthomonas arboricola* on oleander

Attila FODOR[1], László PALKOVICS[2], Anita VÉGH[1,*]

[1] *Hungarian University of Agriculture and Life Sciences, Buda Campus, Institute of Plant Protection, H-1118, Budapest Ménesi Road 44, Hungary*
[2] *Széchenyi István University, Department of Plant Sciences, Albert Kázmér Faculty of Mosonmagyaróvár, 2. Vár square, Mosonmagyaróvár; Hungary; ELKH-SZE PhatoPlant-Lab, Széchenyi István University, 2. H-9200, Mosonmagyaróvár Vár square, Hungary*
*Corresponding author E-mail: karacs.vegh.anita@uni-mate.hu

Summary. *Nerium oleander* L is a long-lasting flowering vegetatively propagated ornamental plant of the Mediterranean region, where it is a major imported flowering pot plant. Only a few bacteria can infect it such as *Pseudomonas savastanoi* pv. *nerii*, *Agrobacterium tumefaciens* and *Xylella fastidiosa*. Between 2018 and 2022 we collected several infected plant parts in our country. In 2020 we observed atypical symptoms on the leaves and stems, which were not clearly similar to the known bacterial infection of oleander. In our work, we aimed to identify the pathogen. The isolates formed yellow-coloured bacterial colonies on King-B and on YDC agar, were Gram-negative, oxidase negative and induced hypersensitive reaction on tobacco leaves. The biochemical properties were determined by API 20E and API 50CH tests. Brown necrosis was observed on oleander leaves in a pathogenicity test. Multilocus sequence analysis was used for molecular identification of the pathogen. Three housekeeping genes (*gyrB*, *fyuA* and *rpoD*) were amplified. According to symptoms, colony morphology, biochemical features, pathogenicity and molecular methods, the pathogen was identified as *Xanthomonas arboricola.* This is the first report of the plant pathogenic *Xanthomonas* spp. on oleander.

Keywords. *Nerium oleander*, *Xanthomonas*, bacterial disease, Hungary.

OPEN ACCESS

Citation: Fodor, A., Palkovics, L. & Végh, A. (2025). First report of *Xanthomonas arboricola* on oleander. *Phytopathologia Mediterranea* 64(1): 101-108. doi: 10.36253/phyto-15575

Accepted: April 28, 2025

Published: May 15, 2025

Data Availability Statement: All relevant data are within the paper and its Supporting Information files.

Competing Interests: The Author(s) declare(s) no conflict of interest.

Editor: Joel L. Vanneste, Plant and Food Research, Sandringham, New Zealand.

ORCID:
AF: 0000-0003-3399-4585
LP: 0000-0002-1850-6750
VA: 0000-0002-5942-038X

INTRODUCTION

Nerium oleander L. is an evergreen tropical and subtropical plant of the *Apocynaceae* family. It is a vegetatively propagated ornamental plant. The plant is appreciated for its striking flower of different colours. Only a few bacteria can infect oleander during cultivation, but only *Pseudomonas savastanoi* pv. *nerii* (Janse) Young, Dye & Wilkie causes significant damage. The typical symptoms are knots or galls on stems, twigs, leaves and seedcases. The knots are few millimetres, soft and green in the early stages of infection. Then it grows to a few centimetres, turns brown (Smith, 1906) and decays as the periderm blocks the source of water and nutrients. The severity of symptoms is influenced by phytohormone production (Themsah *et*

al., 2010). *Xanthomonas (*Dowson 1939*)* is a large genus of plant pathogenic Gram-negative bacteria, which are obligate aerobes and generally rod shaped with a single polar flagellum (Bradbury, 1984). Many members of this genus are yellow-pigmented because of xanthan production (Kennedy and Bradshaw, 1984). The *Xanthomonas* genus comprises 45 species (Parte *et al*., 2020) which show a high degree of host plant specificity. The range of host plants is mostly a single plant or a few plants from the same botanical family (Ryan *et al.,* 2011). However, it is difficult to define the exact range of host plants, as pathogenicity tests are only carried out on a few cultivated plants (Bull and Koike, 2015). The symptoms are ranging from water-soaked spots, wilting to cankers (Rudolph, 1993). *Xanthomonas* spp. cause serious diseases on important crops such as rice, citrus, banana, cabbage, tomato and walnut (Kennedy and Bradshaw, 1984; Ryan *et al.,* 2011). Additionally, *Xanthomonas* produces a polysaccharide called xanthan gum, which is used in industry as a thickener and emulsifier (Backer *et al.,* 1998).

MATERIALS AND METHODS

We have been investigating oleander knot in Hungary since 2018. Only a few cases of atypical symptoms were observed during the nationwide sampling of approximately 300 samples. In 2020 two infected plant samples, one from Southern Great Plain (Kecskemét) and one from Northern Great Plain (Nyírbátor) were collected from hobby gardeners. Symptoms of brown, necrosis on the leaf, and untypical canker on the stem were observed. The symptomatic plant parts were delivered to the laboratory of the Department of Plant Pathology, Hungarian University of Agriculture and Life Sciences. The samples were surface-sterilized, homogenized and streaked onto King's B agar (King *et al.,* 1954). The agar plates were incubated at room temperature (RT) for 48 to 72 h, and pure cultures of bacterial isolates were obtained by colony subculturing. Hypersensitive reaction (HR) was tested on tobacco leaves (*Nicotiana tabacum* L. Xanthi) using pure bacterial suspension of 5×10^7 cells mL^{-1}. The suspension was determined with a spectrophotometer set at $\lambda = 560$ nm. Leaves were assessed at 24 and 48 h post-inoculation. Gram feature was determined by the KOH test (Powers, 1995). Biochemical analysis was performed using the API 20E and API 50CH kit (BioMérieux). Colony morphology was observed on Yeast Extract-Dextrose-Calcium Carbonate agar (YDC). For pathogenicity test 1 year old oleander plants were used. Stem internodes, between the first and the second leaves were injected using sterile syringes containing bacterial suspension of 5×10^7 cells mL^1 and 2 leaves of each plant were also lacerated with the inoculant syringe needle. Sterilized distilled water was used for injection as a negative control. 3 plants were used for each replicate. The inoculated plants were maintained at RT with a relative humidity greater than 90% for 1 week. Symptoms were observed daily for 3-week post-inoculation. To determine host plants specificity of isolates detached leaves of apricot (*Prunus armeniaca* L.), walnut (*Juglans regia* L.), pepper (*Capsicum annum* L.*)*, kohlrabi (*Brassica oleraceae* L convar. *acephala* var. *gongylodes*), cabbage (*B. oleracea* convar. *capitata*), geranium (*Pelargonium zonale* L'Hér ex Aiton), poplars (*Populus alba* L., *P. nigra*) and willow (*Salix alba* L.) were used. The surface-sterilized leaves were infected in two ways: inoculated with bacterial colonies using sterilised toothpicks and transferred with bacterial suspension of 5×10^7 cells mL^1 using a sterilized paintbrush. Positive control leaves were infected with bacteria from Gene Bank of Institute of Plant Protection. Negative control leaves were inoculated with sterilized distilled water. The leaves were incubated at hight relative humidity. 5 leaves were used for replicates. The cabbage and the kohlrabi were bought in a supermarket and the leaves of apricot, walnut, pepper and geranium were collected in a hobby garden. Symptoms were observed daily for 2 weeks after inoculation.

Multilocus sequence analysis (MLSA) was conducted using three housekeeping genes (*fyuA*, *rpoD*, *gyrB*) and forty strains (Table 1). The polymerase chain reaction (PCR) cycling conditions for *fyuA* and *rpoD* genes were 3 min at 94°C, then 30 s at 94°C, 30 s at 54°C, 1 min at 72°C for 30 cycles, then 10 min at 72°C (Young *et al*., 2008). The PCR cycling conditions for *gyrB* were 2.5 min at 94°C, then 30 s at 94°C, 45 s at 50°C, 1 min at 68°C for 34 cycles, then 7 min at 68°C (Parkinson *et al.,* 2007). The re-isolated bacteria were confirmed by 16S rDNA PCR using 63F and 1389R primers. The PCR cycling conditions were 5 min at 94°C, then 15 s at 95°C, 30 s 55°C, 90 s 72°C for 30 cycles, then 10 min at 72°C (Osborn *et al.,* 2000). Primers for partial sequences of *fyuA*, *rpoD gyrB* and 16S rDNA are listed in Table 2. The amplification was visualised on a 1% (w/v) agarose gel in 1 × TBE buffer with ECOSafe (Biocenter). The PCR products were cleaned with the High Pure PCR Product Purification Kit (Roche Diagnostics GmbH). The nucleotide sequence of the PCR amplified DNA fragment was determined and compared with sequences from the National Center for Biotechnology Information (NCBI) database, using the Basic Local Alignment Search Tool (BLAST) program. Homologous sequences from other

Table 1. *Xanthomonas* strains referred to in this study whit collection numbers (CFBP: French Collection for Plant-associated Bacteria, ICMP: International Collection of Microorganisms, LMG: Belgian Coordinated Collections of Microorganisms, NCPPB: National Collection of Plant Pathogenic Bacteria Fera (UK)) or isolate codes (X1, X2, Xp10, KBNS163, KBNS165) and NCBI GenBank database accession numbers.

Strain	*Xanthomonas* spp.	NCBI Accession Numbers		
		gyrB	*fyuA*	*rpoD*
X1	*arboricola*	PQ094467	PQ094469	PQ094471
X2	*arboricola*	PQ094468	PQ094470	PQ094472
CFBP 1159	*arboricola* pv. *corylina*	EU499002	EU498895	EU499121
CFBP 2528	*arboricola* pv. *juglandis*	EU498951	EU498852	EU499070
CFBP 2535	*arboricola* pv. *pruni*	EU498853	EU498854	EU499072
Xp10	*arboricola* pv. *pruni*	MN520634	MN520626	MN520630
CFBP 4924	*axonopodis* pv. *axonopodis*	EU498952	EU498853	EU499071
LMG 982	*axonopodis* pv. *axonopodis*	EU498981	EU498914	EU499100
CFBP 3836	*axonopodis* subsp. *alfalfae*	EU499001	EU498894	EU499120
CFBP 2524	*axonopodis* pv. *begoniae*	EU498962	EU498909	EU499081
ICMP 7493	*axonopodis* pv. *citri*	EU499024	EU498910	EU499143
ICMP 10022	*axonopodis* pv. *citri*	EU499045	EU498930	EU499165
CFBP 2526	*axonopodis* pv. *glycines*	EU499003	EU498896	EU499122
CFBP 7153	*axonopodis* pv. *manihotis*	EU499006	EU498898	EU499125
CFBP 6546	*axonopodis* pv. *phaseoli*	EU499015	EU498904	EU499134
CFBP 7663	*axonopodis* pv. *phaseoli*	EU498968	EU498864	EU499087
ICMP 7462	*axonopodis* pv. *ricini*	EU499023	EU498771	EU499142
LMG 8122	*campestris* pv. *campestris*	EU499018	EU498907	EU499137
CFBP 2350	*campestris* pv. *campestris*	EU498948	EU498849	EU4999067
CFBP 5828	*campestris* pv. *raphani*	EU498982	EU498877	EU499101
CFBP 7270	*dyei*	GQ183103	GQ183117	GQ183090
CFBP 7261	*dyei* pv. *eucalypti*	GQ183102	GQ183115	GQ183088
CFBP 2157	*fragariae*	EU499000	EU498893	EU499119
NCPPB 2949	*fragariae*	EU499012	EU498901	EU499131
ICMP 6646	*fragariae*	EU499019	EU498908	EU499138
ICMP 1661	*hortorum* pv. *hederae*	EU498987	EU498880	EU499106
CFBP 4925	*hortorum* pv. *hederae*	KY984200	KYP984167	KYP984233
KBNS163	*hortorum* pv. *pelargoni*	KP900004	KP899987	KP899953
KBNS165	*hortorum* pv. *pelargoni*	KP900006	KP899889	KP899955
ICMP 12013	*oryzae* pv. *oryzicola*	EU499050	EU498935	EU499170
CFBP 2286	*oryzae* pv. *oryzicola*	EU499007	EU498899	EU499126
ICMP 16690	*euvesicatoria* pv. *perforans*	EU499059	EU498944	EU499179
NCPPB 762	*pisi*	EU498976	EU498872	EU499095
CFBP 3123	*populi*	EU499035	EU498919	EU499155
NCPPB 989	*vasicola*	EU498974	EU498870	EU499093
CFBP 2543	*vasicola*	EU498992	EU498885	EU499111
ICMP 3490	*vasicola*	EU498994	EU498887	EU499113
NCPPB 422	*vesicatoria*	EU498954	EU498855	EU499073
ICMP 696	*vesicatoria*	EU498980	EU498876	EU499099
ICMP 115	*vesicatoria*	EU498956	EU498857	EU499075

members of the *Xanthomonas* spp. were included in the phylogenetic analysis for comparisons. For phylogenetic analysis Mega 11.1 was used (Tamura and Nei, 1993; Tamura *et al*., 2021).

RESULTS AND DISCUSSION

Between 2018 and 2022 we collected several infected oleander plant parts in Hungary. First of all, we brought

Table 2. Primers used in this study (Parkinson *et al.,* 2007; Young *et al.,* 2008).

Sequence	Forward	Reverse
fyuA	XfyuA1F	XfyuA1R
	AGCTACGAYGTGCGYTACGA	GTTCACGCCRAACTGGTAG
rpoD	XrpoD1F	XrpoD1R
	TGGAACAGGGCTATCTGACC	CATTCYAGGTTGGTCTGRTT
gyrB	XgyrPCR2F	Xgyrrsp1
	AAGCAGGGCAAGAGCGAGCTGTA	CAAGGTGCTGAAGATCTGGTC
16S rDNA	63F	1389R
	CAGGCCTAACACATGCAAGTC	ACGGGCGGTGTGTACAAG

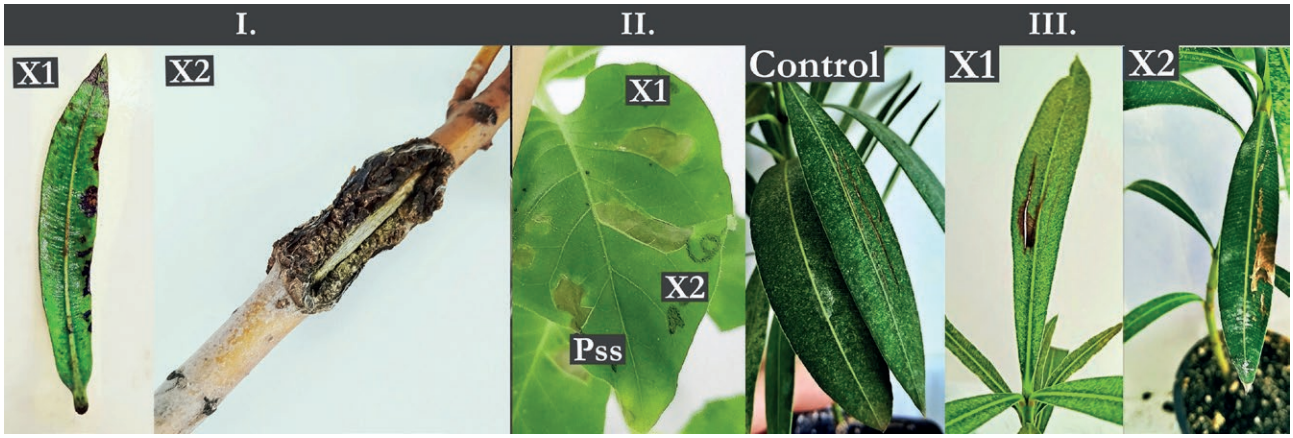

Figure 1. I. The symptoms of the plant parts used for isolation, II. Hypersensitive reactions from infiltration of tobacco leaves 36 h post-inoculation with negative control (*Pseudomonas syringae* pv. *syringae*-Pss) and III. Necrosis on oleander leaves around the points of injections 2 weeks post-inoculation.

into focus *Pseudomonas savastanoi* pv. *nerii*, however other pathogens (among others *Botrytis cinerea*, *Cercospora* spp.) were also investigated. In 2020 we observed two atypical symptoms, one from Southern Great Plain (Kecskemét) and one from Northern Great Plain (Nyírbátor). On the stem splitting of the canker bark were observed, which was not typical symptoms of oleander canker. In addition, there was no isolation of *Pseudomonas* spp. from the sample. On the leaf margins and main stem of the leaf scattered brown spots and watery necrosis were observed (Figure 1). It was assumed that the symptoms were caused by bacteria, which are unknown pathogens of oleander. Our previous research confirmed this hypothesis, as we isolated for the first time the pathogen *Serratia marcescens* bacteria on oleander leaf and seedcase (Fodor *et al.,* 2022). The colonies of both isolates (X1, X2) were yellow-colored, smooth-edged, slightly convex on King-B and on YDC agar. The KOH tests were positive, so both isolates were Gram-negative. The isolates induced HR on tobacco leaves 24 h post-inoculation (Kennedy and Bradshaw, 1984; Trébaol, *et al.,* 2000; Vicente and Holub, 2013) (Figure 1).

There was little variation in the biochemical properties of the isolates. The API 20NE test gave a positive reaction during sixteen reactions (NO_3, GLU, ESC, GEL, PNPG, GLU, ARA, MNE, MAN, NAG, MAL, GNT, CAP, ADI, MLT, CIT). Only the production of arginine dihydrolase (ADH) showed differences (X1-negative, X2-positive) (Table 3). On the API 50CH kit the isolates differed in eight tests (DXYL, ARB, SAL, CEL, MEL, TRE, GLGY, XLT). The X2 isolate showed positive results on D- Xylose, arbutin, cellobiose melibiose, trehalose, glycogen, xylitol, while the X1 isolate showed negative results. On salicin and xylitol tests of the isolate X2 showed a positive reaction, while X1 showed a negative reaction (Table 4). Vauterin and co-authors (1995) studied the biochemical properties of two *X. populi* strains. Our isolates show difference from their isolates in arabinose (ARA) utilization (positive), while in 11 reaction (NAG, CEL, GAL, MAN, TRE, SOR, TUR, XLT, GLY) our isolates were differed their isolates by half and half. The result *X. populi* of López and co-authors (2018) showed differences only in mannitol (MAN) assimilation.

Table 3. Result of API 20NE test (NO_3: nitrate reduction, TRP: tryptophan deaminase, GLU: glucose acidification, ADH: arginine dihydrolase, URE: urease, ESC: esculin ferric citrate, GEL: gelatinase, PNPG: β-galactosidase, ARA: arabinose, MNE: mannose utilization, MAN: mannitol utilization, NAG: N-acetyl glucosamine utilization, MAL: maltose utilization, GNT: gluconic acid utilization:, CAP: capric acid utilization, ADI: adipic acid utilization, MLT: malic acid utilization, CIT: citric acid utilization, PAC: phenylacetic acid utilization).

	NO_3	TRP	GLU	ADH	URE	ESC	GEL	PNPG	GLU	ARA
X1	+	-	+	+	-	+	+	+	+	+
X2	+	-	+	-	-	+	+	+	+	+
	MNE	MAN	NAG	MAL	GNT	CAP	ADI	MLT	CIT	PAC
X1	+	+	+	+	+	+	+	+	+	-
X2	+	+	+	+	+	+	+	+	+	-

Two weeks after inoculation, necrosis was observed on the oleander leaves around the injection points. Control showed no symptoms. Although the isolated bacteria did not cause knots. It is assumed that the X2 isolate did not produce tumour. The pathogen of interest was the only microorganism re-isolated from lesions on the different inoculated plants, which was confirmed by colony morphology and PCR. The Koch's postulates were fulfilled only in the case of X1 isolate. The X2 isolate were also pathogen of oleander, however the symptoms experienced during isolation were not observed during pathogenicity test (Figure 1). Leaves of apricot, walnut, pepper, kohlrabi, cabbage, geranium, poplars and willow did not show symptoms. There was no difference between infected and negative control leaves. However, the positive control isolates caused necrosis around the inoculation points (Figure 2).

The phylogenetic tree was constructed using *fyuA*, *rpoD*, *gyrB* housekeeping genes, which was separated two branches. On one branch *X. oryzae*, *X. pisi*, *X. dey*, *X. vesicatoria, X. fragariae* and pathotypes of *X. axonopodis* were separated. On the other branch, *X. arboricola* and the pathotypes of *X. campestris*, *X. hortorum* and *X. populi* were found. The X1 and X2 isolate were on a separate branch with pathotype of *X. arboricola* (*X arboricola* pv. *corylina*, *X. arboricola* pv. *juglandis*, *X. arboricola* pv. *pruni*) and *X. populi*. Both isolates were similar and related to a *Xanthomonas arboricola* pv. *pruni* isolate from Montenegro (Xp10). They were on the same branch with *X. populi* (CFBP 3123). However, our isolates were different. They did not cause symptoms on *Populus* spp. and *Salix* spp. leaves, which plants are the only host of *X. populi* (De Kam, 1984). This indicates that our isolates may belong to a different pathotype, which needs to be confirmed by further studies- e.g. molecular test-

Table 4. Result of API 20NE test (0: Control, GLY: Glycerol, ERY: Erythritol, DARA: D-Arabinose, LARA: L-Arabinose, RIB: Ribose, DXYL: D- Xylose, LXYL: L-Xylose, ADO: Adonithol, MDX: Methyl xyloside, GAL: Galactose, GLU: D-Glucose, FRU: D-Fructose, MNE: D-mannose, SBE: Sorbose, RHA: Rhamnose, DUL: Dulcitol, INO: Inositol, MAN: Mannitol, SOR: Sorbitol, MDM: Methyl-D-mannoside, MDG: Methyl-D-glucoside, NAG: N-acetyl-glucosamine, AMY: Amygdalin, ARB: Arbutin, ESC: Esculine, SAL: Salicin, CEL: Cellobiose, MAL: Maltose, LAC: Lactose, MEL: Melibiose, SAC: Sucrose, TRE: Trehalose, INU: Inulin, MLZ: Melizitose, RAF: D-raffinose, AMD: Starch, GLGY: Glycogen, XLT: Xylitol, GEN: Gentibiose, TUR: Turanose, LYX: Lyxose, TAG: Tagatose, DFUC: D-fucose, LFUC: L-fucose, DARL: D-Arabitol, LARL: L-Arabitol, GNT: Gluconate, 2KG :2, Keto-gluconate, 5KG :5, keto-gluconate).

	0	GLY	ERY	DARA	LARA	RIB	DXYL	LXYL	ADO	MDX	GAL
X1	-	-	-	-	-	-	-	-	-	-	+
X2	-	-	-	-	-	-	+	-	-	-	+
	GLU	FRU	MNE	SBE	RHA	DUL	INO	MAN	SOR	MDM	MDG
X1	+	+	+	-	-	-	-	-	-	-	-
X2	+	+	+	-	-	-	-	-	-	-	-
	NAG	AMY	ARB	ESC	SAL	CEL	MAL	LAC	MEL	SAC	TRE
X1	+	+	-	-	+	-	+	-	-	+	-
X2	+	+	+	-	-	+	+	-	+	+	+
	INU	MLZ	RAF	AMD	GLGY	XLT	GEN	TUR	LYX	TAG	DFUC
X1	-	-	-	+	-	+	-	-	-	-	+
X2	-	-	-	+	+	-	-	-	-	-	+
	LFUC	DARL	LARL	GNT	2KG	5KG					
X1	+	-	-	-	-	-					
X2	+	-	-	-	-	-					

Figure 2. Results from host plant specificity tests: positive controls (I.), negative control (II), inoculated with two *Xanthomonas arboricola* isolates (X2-III., X1-IV.). The first column shows cabbage, the second column kohlrabi, the third column apricot, the fourth column walnut, the fifth column pepper, the sixth column geranium, the seventh and eight column poplars, the ninth column willow leaves at 7 days post-inoculation.

ing, DNS-DNS hybridization, fatty acid analysis. To the best of our knowledge, this is the first report of the *Xanthomonas* as a pathogen of oleander. Additionally, a *Xanthomonas* spp. have been identified from olive (*Olea europaea* L), which caused brown necrosis and canker on the stream (Taylor *et al*., 2001; Young *et al*., 2010). Our isolates caused only on the oleander leaves necrosis in the pathogenicity test. They did not induce canker, although they may play a role in the evolve of on oleander knot symptoms.

ACKNOWLEDGEMENT

This work was supported by the ELKH TKI (project number: 3200107). The research was funded by the "VP4-10.2.2.-20.Ex situ conservation of genetic resources of rare and endangered plant species and microorganisms".

REFERENCES

Backer A., Katzen F., Puhler L., Ielpi L., 1998. Xanthan gum biosynthesis and application: a biochemical/genetic perspective. *Applied Microbiology and Biotechnology* 50: 145–152. https://doi.org/10.1007/s002530051269

Bradbury J.F., 1984. Genus II *Xanthomonas* (Dowson 1939). In: Bergey's Manual of Systematic Bacteriology (Krieg, N.R., Holt, J.G. ed) vol. 1. The Williams & Wilkins Co., Baltimore, 199-210.

Bull C.T., Koike S.T., 2015. Practical benefits of knowing the enemy: modern molecular tools for diagnosing the etiology of bacterial diseases and understanding the taxonomy and diversity of plant-pathogenic bacteria. *Annual Review of Phytopathology* 53: 157–180. https://doi.org/10.1146/annurev-phyto-080614-120122

De Kam M., 1984. *Xanthomonas campestris* pv. *populi*, the causal agent of bark necrosis in poplar. *Nether-*

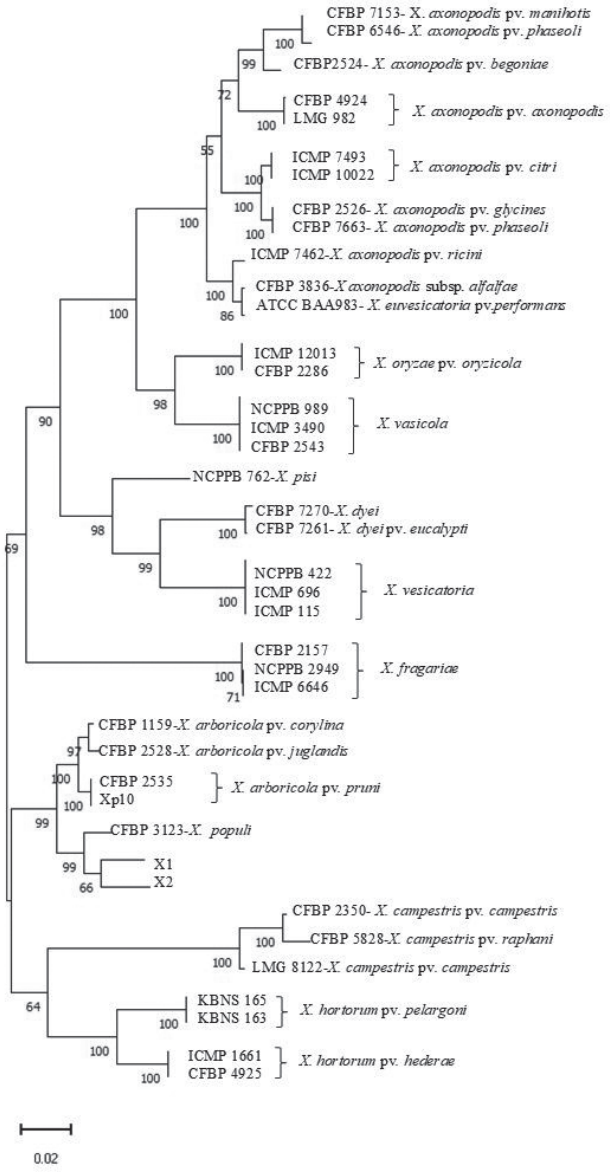

Figure 3. Maximum likelihood tree of concatenated *Xanthomonas* spp. nucleotide sequences for partial *fyuA*, *gyrB* and *rpoD* gene with identifier numbers. Tamura-Nei G5 model was used. The bootstrap values were 1000 samplings. The percentage of trees in which the associated taxa clustered together is shown below the branches. There were a total of 2109 positions in the final dataset (Tamura and Nei, 1993; Tamura *et al*., 2021).

lands Journal of Plant Pathology 90: 13–22. https://doi.org/10.1007/BF02014178

Fodor A., Palkovics L., Végh A., 2022. First report of *Serratia marcescens* from oleander in Hungary. *Phytopathologia Mediterranea* 61: 311–317. https://doi.org/10.36253/phyto-13354

Kennedy J.F., Bradshaw I.J. 1984. Production, properties and applications of xanthan. *Progress in Industrial Microbiology* 19, 319–371.

King E.O., Ward M.K., Raney D.E., 1954. Two simple media for the demonstration of pyocyanin and fluorescin. *Journal of Laboratory and Clinical Medicine* 44: 301–307.

López M.M., Lopez-Soriano P., Garita-Cambronero J., Beltrán C., Taghouti G., … Marco-Noales E., 2018. *Xanthomonas prunicola* sp. nov., a novel pathogen that affects nectarine (*Prunus persica* var. *nectarina*) trees. *International Journal of Systematic and Evolutionary Microbiology* 68(6): 1857–1866. https://doi.org/10.1099/ijsem.0.002743

Osborn A.M., Moore E.R., Timmis K.N., 2000. An evaluation of terminal-restriction fragment length polymorphism (T-RFLP) analysis for the study of microbial community structure and dynamics. *Environmental Microbiology* 2: 39–50. https://doi.org/10.1046/j.14622920.2000.00081.x

Parkinson N., Aritua V., Heeney J., Cowie C., Bew J., Stead D., 2007. Phylogenetic analysis of *Xanthomonas* species by comparison of partial gyrase B gene sequences. *International Journal of Systematic and Evolutionary Microbiology* 57(12): 2881–2887. https://doi.org/10.1099/ijs.0.65220-0

Parte A.C., Carbasse S.J., Meier-Kolthoff J.P., Reimer L.C., Göker M., 2020. List of Prokaryotic names with Standing in Nomenclature (LPSN) moves to the DSMZ. *International Journal of Systematic and Evolutionary Microbiology* 70(11): 5607–5612. https://doi.org/10.1099/ijsem.0.004332

Powers E.M., 1995. Efficacy of the Ryu nonstaining KOH technique for rapidly determining gram reactions of food-borne and waterborne bacteria and yeasts. *Applied and Environmental Microbiology* 61: 3756–3758. https://doi.org/10.1128/aem.61.10.3756-3758.1995

Rudolph K., 1993. Infection of the plant by *Xanthomonas*. In: *Xanthomonas* (Swings J. G., Civerolo E. L. ed) Chapman and Hall, London. 193–264.

Ryan R.P., Vorhölter F.J., Potnis N., Jones J.B., Van Sluys M.A., … Dow, J.M. 2011. Pathogenomics of *Xanthomonas*: understanding bacterium-plant interactions. *Nature Reviews Microbiology* 9(5): 344–355. https://doi.org/10.1038/nrmicro2558

Smith C.O. ,1906. A Bacterial disease of oleander. *Bacillus oleae* (Arcang.) Trev. *Botanical Gazette*, 42(4): 301–310.

Tamura K., Nei M., 1993. Estimation of the number of nucleotide substitutions in the control region of mitochondrial DNA in humans and chimpanzees. *Molecular Biology and Evolution* 10(3): 512–526. https://doi.org/10.1093/oxfordjournals.molbev.a040023

Tamura K., Stecher G., Kumar S., 2021. MEGA 11: Molecular Evolutionary Genetics Analysis Version 11. *Molecular Biology and Evolution*. 38(7): 3022–3027. https://doi.org/10.1093/molbev/msab120

Taylor R.K., Hale C.N., Hartill, W.F.T., 2001. A stem canker disease of olive (*Olea europaea*) in New Zealand. *New Zealand Journal of Crop and Horticultural Science* 29(3): 219–228. https://doi.org/10.1080/01140671.2001.9514181

Temsah M., Hanna L., Saad A.T., 2010. Histological pathogenesis of *Pseudomonas savastanoi* on *Nerium oleander*. *Journal of Plant Pathology* 92(2): 407–413.

Trébaol G., Gardan L., Manceau C., Tanguy J. L., Tirilly Y., Boury S., 2000. Genomic and phenotypic characterization of *Xanthomonas cynarae* sp. nov., a new species that causes bacterial bract spot of artichoke (*Cynara scolymus* L.). *International Journal of Systematic and Evolutionary Microbiology* 50(4): 1471–1478.

Vauterin L., Hoste B., Kersters K., Swings J., 1995. Reclassification of *Xanthomonas*. *International Journal of Systematic and Evolutionary Microbiology* 45(3): 472–489. https://doi.org/10.1099/00207713-45-3-472

Vicente J.G., Holub E.B., 2013. *Xanthomonas campestris* pv. *campestris* (cause of black rot of crucifers) in the genomic era is still a worldwide threat to brassica crops. *Molecular Plant Pathology* 14(1): 2–18. https://doi.org/10.1111/j.1364-3703.2012.00833.x

Young J.M., Park, D.C., Shearman H.M., Fargier E., 2008. A multilocus sequence analysis of the genus *Xanthomonas*. *Systematic and Applied Microbiology* 31(5): 366–377. https://doi.org/10.1016/j.syapm.2008.06.004

Young J.M., Wilkie J.P., Park D.C., Watson D.R.W., 2010. New Zealand strains of plant pathogenic bacteria classified by multi-locus sequence analysis; proposal of *Xanthomonas dyei* sp. nov. *Plant Pathology* 59(2): 270–281. https://doi.org/10.1111/j.1365-3059.2009.02210.x

Phytopathologia Mediterranea
The international journal of the
Mediterranean Phytopathological Union

Firenze University Press
www.fupress.com/pm

Research Papers

Antifungal efficacy of four plant-derived essential oils against *Botrytis cinerea*: chemical profiles and biological activities

Faiçal AOUJIL[1,2], Loubna DRA[1], Chaimae EL GHDAICH[1], Sarah TOUFIQ[3], Hiba YAHYAOUI[1,2], Majida HAFIDI[2], Aziz AZIZ[4], Khaoula HABBADI[2,*]

[1] *Phytobacteriolgy and Biological Control Laboratory, Regional Center of Agricultural Research of Meknes, National Institute of Agricultural Research, Avenue Ennasr, BP 415 Rabat Principal, Rabat 10090, Morocco*
[2] *Laboratory of Biotechnology and Bio-Resources Valorization, Faculty of Sciences, Moulay Ismail University, Meknes 50000, Morocco*
[3] *Faculty of Agricultural Science, University of Hohenheim, Stuttgart 70593, Germany*
[4] *Research Unit "Induced Resistance and Plant Bioprotection", RIBP-USC INRAe 1488, University of Reims Champagne-Ardenne, 51100 Reims, France*
* Corresponding author. E-mail: khaoula.habbadi@inra.ma

Summary. Chemical compositions and the antifungal efficacy of essential oils derived from *Origanum elongatum, Mentha pulegium, Thymus vulgaris*, or *Corymbia citriodora* were assessed against the grapevine gray mold pathogen *Botrytis cinerea*, isolated from Moroccan vineyards. Gas chromatography-mass spectrometry (GC-MS) analyses identified the major constituents of these oils as carvacrol (61.8%) from *O. elongatum*, pulegone (91.2%) from *M. pulegium*, thymol (47.8%) from *T. vulgaris*, and cineol (78.11%) from *C. citriodora*. All these essential oils had antifungal activity, inhibiting *in vitro* colony radial growth and conidium germination of *B. cinerea*. Among the essential oils, that from *O. elongatum* exhibited the greatest inhibition of mycelium growth, with minimum inhibitory concentrations (MICs) and effective concentrations (EC_{50}), respectively, of 252.5 µL L^{-1} and 33.27 µL L^{-1} in direct contact, and 56.17 µL L^{-1} and 12.75 µL L^{-1} in fumigation. At 125 µL L^{-1}, origanum essential oil completely inhibited *B. cinerea* conidium germination. *In vivo* tests with detached leaves of two grapevine cultivars and grape berries showed that essential oils from *M. pulegium* and *O. elongatum* reduced the lesion diameters by, respectively, 78% and 72% on the leaves, and by 58% and 50% on grape berries. The results indicate the potential of using these essential oils as natural and effective alternatives to chemical fungicides for control of *B. cinerea*, offering a promising strategy for sustainable and environmentally friendly disease management practices.

Keywords. *Vitis vinifera,* plant extracts, chemical composition, sustainable agriculture.

OPEN ACCESS

Citation: Aoujil, F., Dra, L., El Ghdaich, C., Toufiq, S., Yahyaoui, H., Hafidi, M., Aziz, A. & Habbadi, K. (2025). Antifungal efficacy of four plant-derived essential oils against *Botrytis cinerea*: chemical profiles and biological activities. *Phytopathologia Mediterranea* 64(1): 109-127. doi: 10.36253/phyto-15566

Accepted: February 2, 2025

Published: May 15, 2025

Data Availability Statement: All relevant data are within the paper and its Supporting Information files.

Competing Interests: The Author(s) declare(s) no conflict of interest.

Editor: Antonio Evidente, University of Naples Federico II, Italy.

ORCID:
FA: 0009-0004-3763-9841
CEG: 0009-0005-0469-8105
ST: 0009-0008-2293-9007
MH: 0000-0002-6207-2822
AA: 0000-0003-1602-2506
KH: 0000-0002-1890-4601

INTRODUCTION

Gray mold, caused by the necrotrophic fungus *Botrytis cinerea*, adversely affects a wide range of host plants, both pre- and post-harvest, including important horticultural crops in temperate and subtropical regions (Wil-

liamson *et al*., 2007). This widespread impact makes *B. cinerea* the second most important phytopathogenic fungus (Bi *et al*., 2023). Annual economic impacts of *B. cinerea* have been estimated to exceed 10 billion dollars (Boddy, 2016). Additionally, the annual expenditure for botrytis control exceeds 1 billion euros (Hua *et al*., 2018). In grapevine, gray mold is an important disease, causing 10 to 70% of losses (Orozco-Mosqueda *et al*., 2023), reducing the quality of fresh grapes (Xueuan *et al*., 2018) and posing major postharvest challenges (Xu *et al*., 2007; Adaskaveg *et al*., 2022).

In recent decades, synthetic fungicides have been used to prevent the onset of fungal diseases (Yu *et al*., 2020), and synthetic fungicides (e.g. fludioxonil, fenhexamid, iprodione, boscalid) are utilized manage diseases caused by *B. cinerea* (Notte *et al*., 2021).However, application of these chemicals has led to development and prevalence of resistant pathogen strains (Shao *et al*., 2021). There are also risks of food contamination with pesticide residues, which can pose threats to human health and the environment due to their high toxicity and persistence (Aoujil *et al*., 2024). Consequently, there is need to develop fungicides that are safe, biodegradable, and derived from natural sources for managing *B. cinerea*. Essential oils derived from plants (EOs) have promise for protecting plants against fungal pathogens, and mitigating the harmful effects of chemical fungicides, due to their biocompatibility, biodegradability, and cost-effectiveness (Chang *et al*., 2022).

EOs, characterized by their hydrophobic composition and volatility, are natural secondary metabolites produced by aromatic plants (Nazzaro *et al*., 2017). They have diverse chemical structures, including phenylpropanoids, aliphatic hydrocarbons, terpenoids, and phenolic compounds (Maurya *et al*., 2021), and these phytochemicals are responsible for EO inhibitory effects (Moghaddam and Mehdizadeh, 2016).

EOs inhibit fungal pathogens by directly reducing mycelium growth and spore germination, and by modifying cellular metabolism, mainly through metabolic disruptions and cellular damage (Tang *et al*., 2018). They can also affect cellular pH and electrochemical gradients of plant plasma membranes (Li *et al*., 2017; Yang *et al*., 2022), and can interfere with metabolic processes associated with changes in gene expression (Singh *et al*., 2024). Numerous studies have shown that EOs have antifungal properties that are effective against *B. cinerea* infections in different fruits, including tomatoes, apples, strawberries, and grapes (Šernaitė *et al*., 2020; Almasaudi *et al*., 2022; Di Francesco *et al*., 2022; Hong *et al*., 2023). However, the effectiveness of EOs in reducing gray mold on grapevine fruit and vegetative organs has not been assessed.

The present study aimed to evaluate the antifungal properties of EOs derived from the aerial parts of three *Lamiaceae* plants (*Origanum elongatum*, *Mentha pulegium*, *Thymus vulgaris*) and one *Myrtaceae* plant (*Corymbia citriodora*). These EOs were selected from an initial screening of 18 EOs (see supplementary file S1), against *B. cinerea*. The chemical compositions of the four EOs were first characterized using GC/MS analysis. Their effects on *B. cinerea* conidium germination and hyphal growth were assessed, through direct and vapour contact assays. *In vivo* efficacy of these EOs for managing gray mold infections was also evaluated on detached grapevine leaves and grape berries.

MATERIALS AND METHODS

Fungal isolate

Botrytis cinerea strain BC53 used in this study was obtained from the mycotheque collection of the National Institute of Agronomic Research, Unit of Plant Protection (CRRAM) Laboratory. This strain was isolated from infected grape berries during the 2021–2022 agricultural season. After cultivation on potato dextrose agar (PDA) and monoconidium subculture on water agar, the isolate was identified based on morphological characteristics and molecular analysis using the primer pairs G3PDHfor and G3PDHrev, which amplify partial fragments of glyceraldehyde-3-phosphate dehydrogenase. The nucleotide sequences obtained were compared with those available from the National Center for Biotechnology Information (NCBI) database, using the Basic Local Alignment Search Tool (BLAST) (Aoujil *et al*., unpublished data). For long-term preservation, mycelia of this isolate were stored at -80°C, in cryovials containing 25% glycerol.

Plant material and extraction of essential oil

Aerial parts of the four medicinal and aromatic plants (MAPs) under study were collected from locations in Morocco between February and April 2024 (Table 1). The plant samples were each cleaned, air-dried in the shade (except for eucalyptus, which was used fresh), and were then stored in the dark at 4°C until further use. EOs were each extracted from the plant samples by hydrodistillation for 2 h using a Clevenger-type apparatus. The extracted EOs were then each separated by decantation, dried over anhydrous sodium sulfate, and then stored in a dark glass bottle at 4°C. The extraction yields were calculated as the ratio of the mass of the EOs to the mass of the original plant material.

Table 1. Information on the classifications and origins of the medicinal and aromatic plants used in this study.

Common name	Botanical name	Plant family	Phenological stage	Sampling site
Oregano	*Origanum elongatum*	*Lamiaceae*	Flowering stage	Bouiblane
Pennyroyal	*Mentha pulegium*	*Lamiaceae*	Vegetative stage	Meknes
Thyme	*Thymus vulgaris*	*Lamiaceae*	Flowering stage	Sefrou
Lemon Eucalyptus	*Corymbia citriodora*	*Myrtaceae*	Vegetative stage	Sidi yahya gharb

Gas chromatography-mass spectrometry analyses of essential oils

Gas chromatography-mass spectrometry (GC-MS) analyses were carried out to determine the chemical composition of each EO. These analyses were performed using a Hewlett Packard model HP6890 gas chromatograph (Agilent Technologies) equipped with a DB-5MS capillary column (30 m × 0.25 mm i.d., film thickness 0.25 µm; Agilent Technologies) coupled to an HP model 5973 mass selective detector. The chromatographic conditions involved an initial oven temperature of 50°C, which was ramped up at 7°C min^{-1} until reaching 300°C. The injector temperature was maintained at 290°C. Helium gas served as the carrier with a flow rate of 1 mL min^{-1}, and a split ratio of 60:1 was employed. Mass spectra were obtained in electron ionization (EI) mode at 70eV ionization energy, covering a mass range from m/z 35 to 400. For each EO sample, 10 µL was diluted in 990 µL of pure hexane, and 1 µL of this solution was injected into the GC-MS system for analysis. Instrument control and data processing were carried out using "HP ChemStation Software" G1701BA, version B.01.00. To aid compound identification, Kovats retention indices (RI) were calculated using a standard mixture of n-alkanes (C8 to C26, Sigma-Aldrich Co.) analyzed under identical conditions. Identification of EO constituents was achieved by comparing their RI values and mass spectra with literature data (Adams, 2007), and by computer matching against standard reference databases (NIST98, Wiley275, and CNRS libraries).

Effects of essential oils on in vitro *mycelium growth of* Botrytis cinerea

Direct contact assay Antifungal activity of the four EOs against *B. cinerea* was determined according to the method of Fontana *et al.* (2021). Sterile molten PDA, cooled to 45°C, was supplemented with the EOs to obtain the following concentrations: 0.97, 1.91, 3.93, 7.88, 15.77, 31.56, 63.12, 126.25, 252.5, 505, 1010 or 2020 µL L^{-1}, in Tween 80 (1%) to increase the solubility of the EOs (Figure 1) (López-Meneses *et al.*, 2017). PDA containing Tween 80 (1%) was used as an experimental control. EO amended and non-amended agar plates were each inoculated with a 6 mm diam. *B. cinerea* mycelium plug taken from a 3-day old culture. The agar plates were then closed, sealed with Parafilm and incubated at 21 ± 1°C.

Vapour phase assay to determine the effects of volatile phase, 90 mm Petri dishes were filled with 20 mL of PDA, resulting in a 40 mL air space after adding the agar medium. The middle of each Petri dish was inoculated as previously described. The EOs were pipetted onto sterile filter paper discs (8 mm diameter) to achieve final concentrations of 5.61, 11.23, 22.47, 44.94, 56.17, 67.41, 89.88, and 112.35 µL L^{-1} of the Petri dish clearance volume (Figure 1) (Zhao *et al.*, 2021). The treated discs were attached to the Petri dish lids (one disc per lid). The dishes were then inverted, immediately sealed with parafilm to prevent the loss of volatile compounds and incubated in the dark at 21 ± 1°C.

For both assays, the mean radial mycelium growth of the pathogen was assessed by measuring colony diameters in two perpendicularly opposite directions, once the surfaces of control Petri dishes were completely covered by the fungus. The inhibition rate of mycelium growth was calculated using the equation (Chen and Dai, 2012):

$$\%\text{inhibition} = \frac{D1-D2}{D2} \times 100$$

where (%) is the percentage inhibition of mycelial growth; D1 is the mean value of the colony radius (mm) grown in the PDA-Tween control; and D2 is the colony diameter of the treated fungi.

The fungal growth observed on the last day of cultivation was used to determine the minimum inhibitory concentrations (MIC) and the effective concentrations (EC_{50} and EC_{90}) of the four essential oils. The MIC was defined as the lowest concentration of EO that completely inhibited mycelium growth of *B. cinerea* (Parikh *et al.*, 2021). The EC_{50} and EC_{90}, the concentrations, respectively, at which mycelium growth

was inhibited by 50% and 90%. were calculated with dose-response analyses, using R statistical software (Ritz *et al*., 2015). Three replicates of each treatment were performed in these experiments, and the experiment was carried out twice, with each Petri dish considered as the experimental unit.

Conidium germination assays

Botrytis cinerea was cultured on PDA Petri dishes for 14 d to produce conidia. The conidia were then collected to prepare a conidium suspension, which was adjusted to contain 10^5 conidia mL^{-1} using a hemocytometer. Petri dishes were prepared containing water agar and different concentrations of EO (2500, 2000, 1500, 1000, 500, 250, 125, 62.5, and 31.25 µL L^{-1}) dissolved in 1.0% Tween 80 (1%). An aliquot of 40 µL of the *B. cinerea* conidia solution was added to the agar surface of each dish (Figure 1). Experimental control dishes contained conidia exposed only to Tween 80 (1%). Dishes were then sealed with parafilm to prevent evaporation, and were incubated at 21 ± 1°C for 20 h. Conidium germination was assessed by counting at least 100 randomly selected conidia per replicate using an optical microscope. Conidia were considered to have germinated if the lengths of the germ tubes were equal to, or greater than, the diameter of the conidia (Parikh *et al*., 2021). The results were expressed as the percentage of conidium germination, which was calculated as follows:

$$\text{Conidium germination rate } (\%) = \frac{\text{Number of germinated conidia}}{\text{Total number of conidia}} \times 100$$

Antifungal efficacy of EOs on detached grapevine leaves

The effectiveness of the four EOs for protecting *Vitis vinifera* L. 'Chardonnay' and 'Cabernet Sauvignon' leaves was assessed using inoculation tests with *B. cinerea* mycelium agar plugs. Young leaves from commercial vineyards, treated with 3 kg ha^{-1} copper at the time of collection and free of disease lesions, were thoroughly washed with water, then immersed in 1% sodium hypochlorite for 2 min, rinsed three times with sterile distilled water, and were then dried on filter paper. EO treatments were applied by immersing leaves for 1 min in the appropriate solutions, following the experimental design detailed in Table 2 and Figure 1. After treatment, the leaves were each wounded with a sterile needle (four wounds per leaf). Subsequently, 5 mm agar plugs containing fresh mycelium from the edge of actively growing *B. cinerea* fungal colonies on PDA plates were placed on the wounds, mycelium side down. The inoculated leaves were incubated in closed plastic boxes at 21°C and with a 16 h photoperiod, with filter paper soaked in water to maintain humidity. The effects of the treatments were evaluated by measuring lesion diameters at 120 h post-inoculation (hpi).

Table 2. Experimental design to assess *in vivo* effects of essential oils on disease development on the grapevine leaves and berries.

Code	Treatment
T-	Treated with sterile distilled water (SDW) + Tween 80 (1%)
T+	Treated with fungicide (fenhexamid)
EC_{50}	Treated simultaneously with the fungus and the EO at EC_{50}
EC_{90}	Treated simultaneously with the fungus and the EO at EC_{90}
EC_{50}+1	Treated with EO at EC_{50} 24 h before fungal inoculation
EC_{90}+1	Treated with EO at EC_{90} 1 24 h before fungal inoculation

Antifungal efficacy of EOs on grape berries

The effects of the four EOs on grape berries was investigated using the methods outlined by Fontana *et al.* (2021), with slight modifications. Healthy table grapes, *Vitis vinifera* L. 'Muscat of Italy', from contaminants or injuries, were randomly selected and purchased in Meknes City, Morocco. These berries were washed under running water, surface-sterilized with a 1% sodium hypochlorite solution, rinsed three times with distilled water, and then air-dried in a laminar flow hood. (Table 2), the berries were placed in 90 mm diam. Petri dishes without lids, and were secured using double-sided tape, with 12 fruits per treatment. Inoculations were carried out injecting a 10 µL aliquot of a *B. cinerea* conidium suspension containing 10^5 conidia mL^{-1} into the equatorial region of each fruit (Figure 1). The inoculated fruits were then incubated in closed plastic boxes (to maintain high humidity conditions) at 22°C with a 16 h photoperiod. On the final day of evaluation, disease incidence and lesion diameters were analysed. Incidence was determined as presence or absence of typical disease symptoms. Lesion diameter was calculated from the average length and width (cm) of each lesion.

Statistical analyses

All calculations were performed using R statistical software (version 4.3.1), and Data were arcsine-transformed where necessary before statistical analysis. Analyses of variance (ANOVA) were carried out at $P \leq$

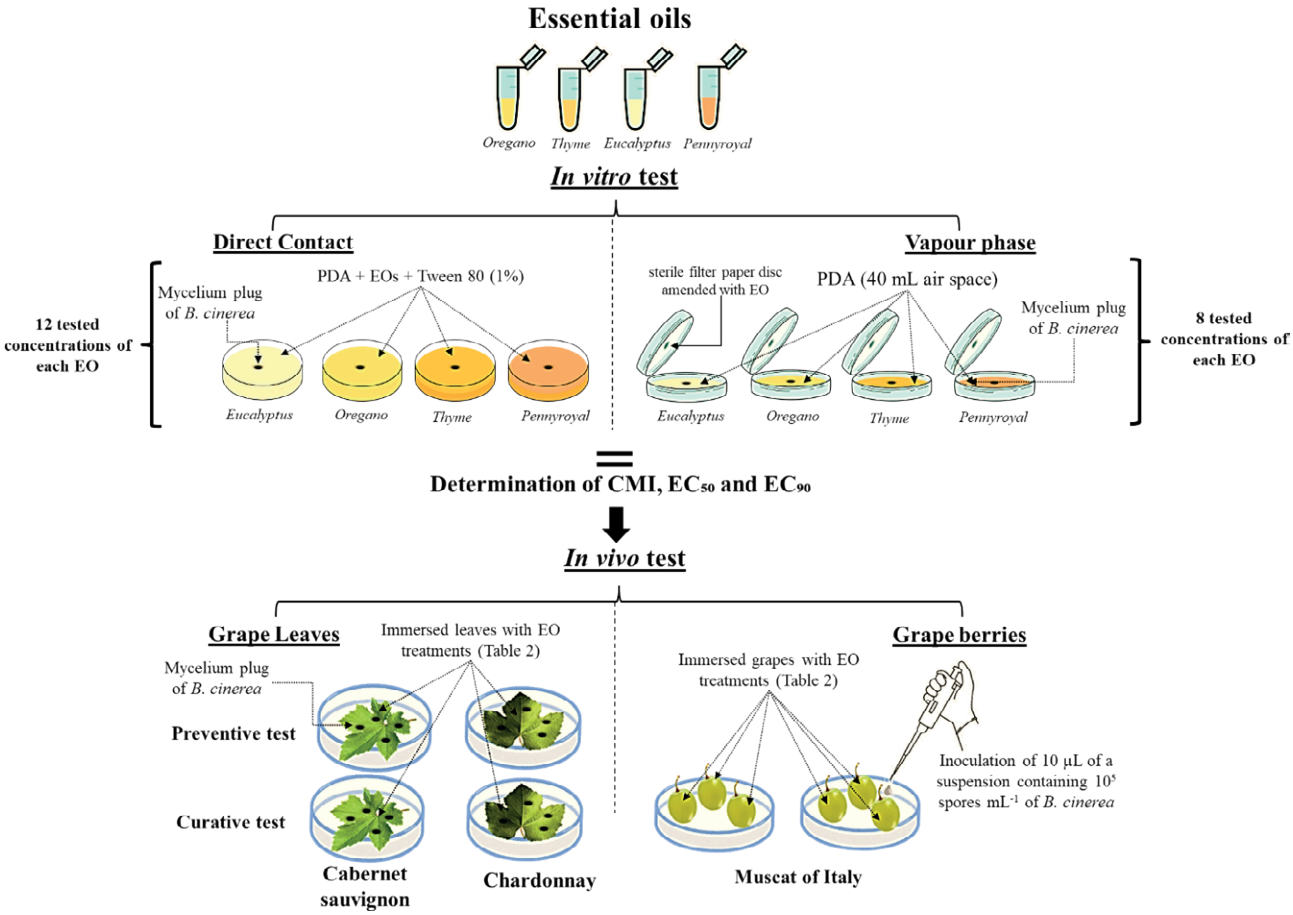

Figure 1. Experiment setup for the *in vitro* and *in vivo* tests to assess effects on *Botrytis cinerea* of treatments of grapevine leaves or berries with four Eos.

0.05. Tukey's HSD test was used to separate means when appropriate ($P \leq 0.05$). The EC_{50} and EC_{90} values for each assessed EO were calculated using the 'drc' package, based on percentage inhibition of mycelium growth. All the histograms presented below were generated using the 'ggplot2' package.

RESULTS

Yields and chemical compositions of essential oils

The EOs, extracted through hydrodistillation, ranged in colour from light yellow to brown, with each possessing a distinctive aroma. The yields of these oils varied depending on the plant species. *Oreganum elongatum* produced the greatest yield (3%), followed by *C. citriodora* (2.7%, *M. pulegium* at 3.2, and *T. vulgaris* (0.7%). The main components of the different EOs assessed in this study are presented in Table 3. Gas chromatography-mass spectrometry (GC-MS) analyses revealed distinct chemical compositions among the EOs. Forty-eight compounds were identified, with 35, 26, 11 and nine compounds detected, respectively, from *T. vulgaris*, *O. elongatum*, *M. pulegium*, and *C. citriodora*, representing, respectively, 98.4%, 98.9%, 98.67%, and 98.7% of the total oil for *T. vulgaris*, *O. elongatum*, *M. pulegium*, and *C. citriodora*. The primary constituents of the *T. vulgaris* EO were thymol (47.8%), p-cymene (24.1%), γ-terpinene (8.2%), and carvacrol (5%). The EO of *O. elongatum* was primarily composed of carvacrol (61.8%), γ-terpinene (12.5%), p-cymene (8.2%), and thymol (7%). The *M. pulegium* EO was predominantly pulegone (91.2%), while that from *C. citriodora* consisted mainly of cineole (78.1%) and α-pinene (12.2%). The main chemical classes identified in the analyses were monoterpenoid phenols (thymol, carvacrol), monoterpenes (γ-terpinene, p-cymene, and α-pinene), monoterpenoid ketone (pulegone), and monoterpenoid ether (cineole).

Table 3. Chemical compositions (%) and yields of essential oils analysed by GC-MS.

Compound	Essential oil				Identification
	Origanum elongatum	*Mentha pulegium*	*Thymus vulgaris*	*Corymbia citriodora*	
Thujene	0.92	-	0.57	-	RI and MS
α-Pinene	0.59	0.19	0.54	**12.21**	RI and MS
Camphene	0.08	-	0.16	-	RI and MS
β-Pinene	0.12	0.21	0.11	0.58	RI and MS
Octen-3-ol	1.17	-	0.32	-	RI and MS
3-Octanone	0.10	-	0.06	-	RI and MS
Myrcene	**1.43**	-	1.34	0.4	RI and MS
3-Octanol	-	0.41	0.06	-	RI and MS
α-Phellandrene	0.22	-	0.16	-	RI and MS
δ-3-Carene	0.08	-	0.07	-	RI and MS
Cineole (Eucalyptol)	-	-	-	**78.11**	RI and MS
Cis-β-Ocimene	0.13	-	-	-	RI and MS
α-Terpinene	**1.85**	0.53	1.72	-	RI and MS
γ-Terpinene	**12.46**	-	**8.19**	-	RI and MS
Terpinolene	0.08	-	0.10	-	RI and MS
cyclohexanone	-	0.30	-	-	RI and MS
Isomaylisovalerate	-	-	-	-	RI and MS
trans-isopulegone	-	1.43	-	-	RI and MS
1-oxaspiro-2,5-octane-4-one	-	0.94	-	-	RI and MS
Pulegone	-	**91.18**	-	-	RI and MS
Pipertenone	-	1.41	-	-	RI and MS
Cyclopentane	-	0.42	-	-	RI and MS
ρ-Cymene	**8.21**	-	**24.13**	**0.79**	RI and MS
Trans-Ocimene	-	-	-	-	RI and MS
Limonene	0.23	1.55	0.38	-	RI and MS
Cis-Linalool Oxide	-	-	0.09	-	RI and MS
Linalool	0.86	-	**3.06**	-	RI and MS
p-Cymenene	-	-	0.07	-	RI and MS
1,8-Cineole	-	-	0.12	-	RI and MS
Camphor	-	-	0.05	-	RI and MS
Borneol	0.14	-	0.45	-	RI and MS
Terpinen-4-ol	0.42	-	0.59	-	RI and MS
2-β-pinene	-	-	-	**5.27**	RI and MS
Cis-Dishydro Carvone	0.06	-	0.06	-	RI and MS
Thymol Methyl Ether	-	-	0.04	-	RI and MS
Carvacrol Methyl Ether	-	-	0.05	-	RI and MS
Carvacrol	**61.78**	-	**5.03**	-	RI and MS
Thymol	**7.01**	-	**47.79**	-	RI and MS
(E)Caryophyllene	**1.47**	-	1.76	-	RI and MS
α-Humulene	0.06	-	0.06	-	RI and MS
α-Selinene	-	-	0.04	-	RI and MS
α-Murolene	-	-	0.01	-	RI and MS
β-Bisabolene	0.13	-	0.05	-	RI and MS
γ-Cadinene	0.03	-	0.07	-	RI and MS
δ-Cadinene	0.06	-	0.16	-	RI and MS
Caryophyllene Oxide	-	-	0.80	-	RI and MS
Isoaromadendrene	-	-	-	0.33	RI and MS

(Continued)

Table 3. (Continued).

Compound	Essential oil				Identification
	Origanum elongatum	*Mentha pulegium*	*Thymus vulgaris*	*Corymbia citriodora*	
Aromadendrene	-	-	-	1	RI and MS
δ- gurjunene	-	-	-	0.35	RI and MS
Total	98.89	98.57	98.35	98.69	RI and MS
Yield (%)	3.00	2.17	0.7	2.67	

RI: Retention index. MS: Comparison of the mass spectra with the NIST98 NIST98, Wiley275, and CNRS libraries.

Effects of essential oils on in vitro mycelium growth of Botrytis cinerea

The *in vitro* direct contact (DC) antifungal activities of EOs from *O. elongatum, M. pulegium, T. vulgaris,* and *C. citriodora* at different concentrations against *B. cinerea* are presented in Figure 2. The minimum inhibitory concentration (MIC), defined as the lowest concentration that inhibited 100% of fungal growth, was 253 μL L^{-1} for the oils from oregano and thyme, and 1010 μL L^{-1} for those from pennyroyal and eucalyptus. Mycelium growth (colony diameter) was reduced ($P < 0.05$) with increasing concentrations of EOs, indicating dose-dependent activities. The mean inhibition zone diameters obtained from determinations of the EO MICs against on *B. cinerea* are presented in Table 4.

The negative control (0 μL L^{-1} of essential oil) gave no inhibition zone formation, suggesting that the diluent (Tween 80) had no antifungal activity, and did not interfere with the MIC analysis. The EO of *O. elongatum* was the most suppressive of *B. cinerea*, reducing growth of *B. cinerea* at low concentrations. At 7.8 μL L^{-1}, differences ($P < 0.05$) were observed, with 21.1% inhibition for the oil of *O. elongatum*, whereas oils from *M. pulegium*, *T. vulgaris*, and *C. citriodora*, gave inhibition rates, respectively, of 0.8, 0.5, and 3.5%. At 31.56 μL L^{-1}, the oregano essential oil gave 50.5% inhibition of the fungus, while the inhibition rates from oils of *M. pulegium*, *T. vulgaris*, and *C. citriodora* were, respectively, 11.1, 19.5, and 18.5%.

The mean essential oil EC_{50} and EC_{90} for inhibition of colony size of *B. cinerea* on PDA after 4 d of incubation are shown in Table 4. These values were derived from dose-response curve regression equations, and are expressed in μL L^{-1}. Oregano oil gave the greatest inhibition of the fungus (mean EC_{50} = 33.27 μL L^{-1}, mean EC_{90} = 139.17 μL L^{-1}. The greatest values were from the pennyroyal oil (mean EC_{50} = 221.74 μL L^{-1}; mean EC_{90} = 828.26 μL L^{-1}.

In the vapour contact (VC) assays, the fumigant activities of the EOs from *O. elongatum*, *M. pulegium, T. vulgaris,* and *C. citriodora* against *B. cinerea* were also determined (Figure 3). This activity is different from that assessed in traditional DC assays. Although the antifungal activity trends in the VC assays were similar to those in the DC assays, the inhibitory effects of the oils in the VC assays were significantly more potent. All the assessed EOs inhibited mycelium growth of *B. cinerea* in dose-dependent ways. Oregano and thyme EOs were more inhibitory effects than those from pennyroyal or Eucalyptus at all the assessed *in vitro* concentrations.

At 44.94 μL L^{-1}, the inhibitory effect of oregano oil was 98.43%, and that of thyme oil was 84.82%, whereas the inhibitory effects of oils from eucalyptus and pennyroyal were, respectively, 48.97% and 26.81%. The mean MICs were 56.17 μL L^{-1} for oregano EO, 89.88 μL L^{-1} for thyme EO, and 112.35 μL L^{-1} for eucalyptus and pennyroyal EOs.

The mean EC_{50} were estimated using a regression model (Table 4). In VC assays, the mean EC_{50} were lower than those obtained in the DC assays. The lowest mean EC_{50} (12.85 μL L^{-1}) resulted from oregano oil, followed by those from thyme EO (19.08 μL L^{-1}), eucalyptus EO (48.11 μL L^{-1}), and pennyroyal EO (61.35 μL L^{-1}).

Effects of essential oils on Botrytis cinerea *conidium germination*

The effects of different concentrations of the four EOs on the *B. cinerea* conidium germination of were assessed using direct contact assays. The results presented in Figure 4 indicate that among the EOs tested, only that of oregano completely inhibited conidium germination at 125 μL L^{-1}. In contrast, at the same concentration, the EOs from *M. pulegium, T. vulgaris*, and C. *citriodora* gave mean conidium germination rates not exceeding, respectively 29.0%, 47.4%, and 28.7%. At 250 μL L^{-1} and greater, toxicity of the EOs to conidia was high, as the germination percentages were 0% for all the EOs except that from *C. citriodora*, which gave 12.5% germination. It was only at a concentration of 2000 μL L^{-1} that the *C. citriodora* EO completely inhibited conidium germination.

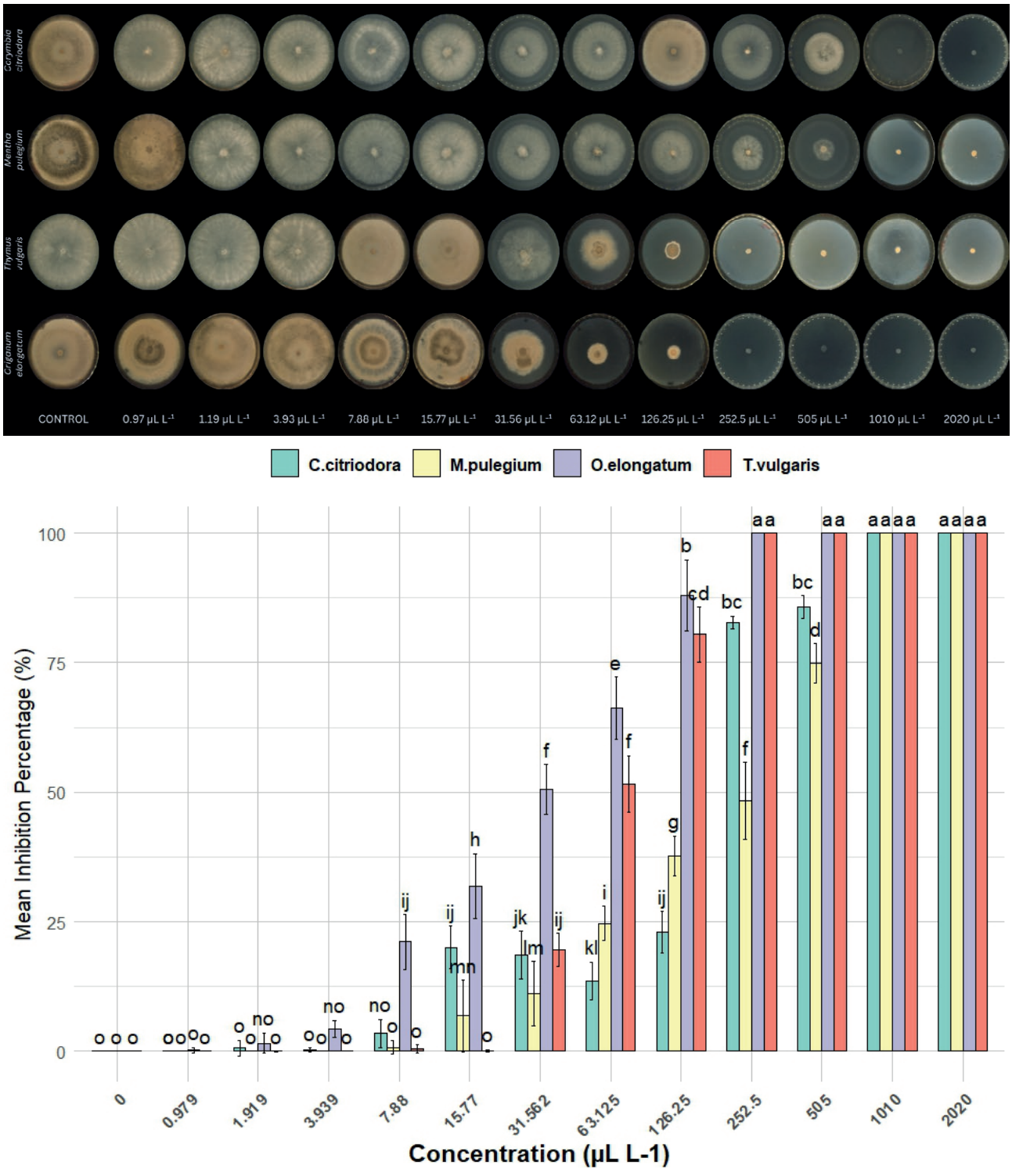

Figure 2. *In vitro* antifungal activities of the four essential oils (EOs) indicated from direct contact assays against mycelium growth of *Botrytis cinerea*, after 4 d of incubation at 24 ± 1 °C. Top: Mycelium growth in Petri dishes containing different concentrations of each EO in agars plates, in the direct contact assay. Bottom: Mean percentage inhibition of mycelium growth at different concentrations of the tested EOs. Different letters above bars indicate differences ($P < 0.05$), according to Tukey's high significance difference (HSD) test. All the data are means ± SD.

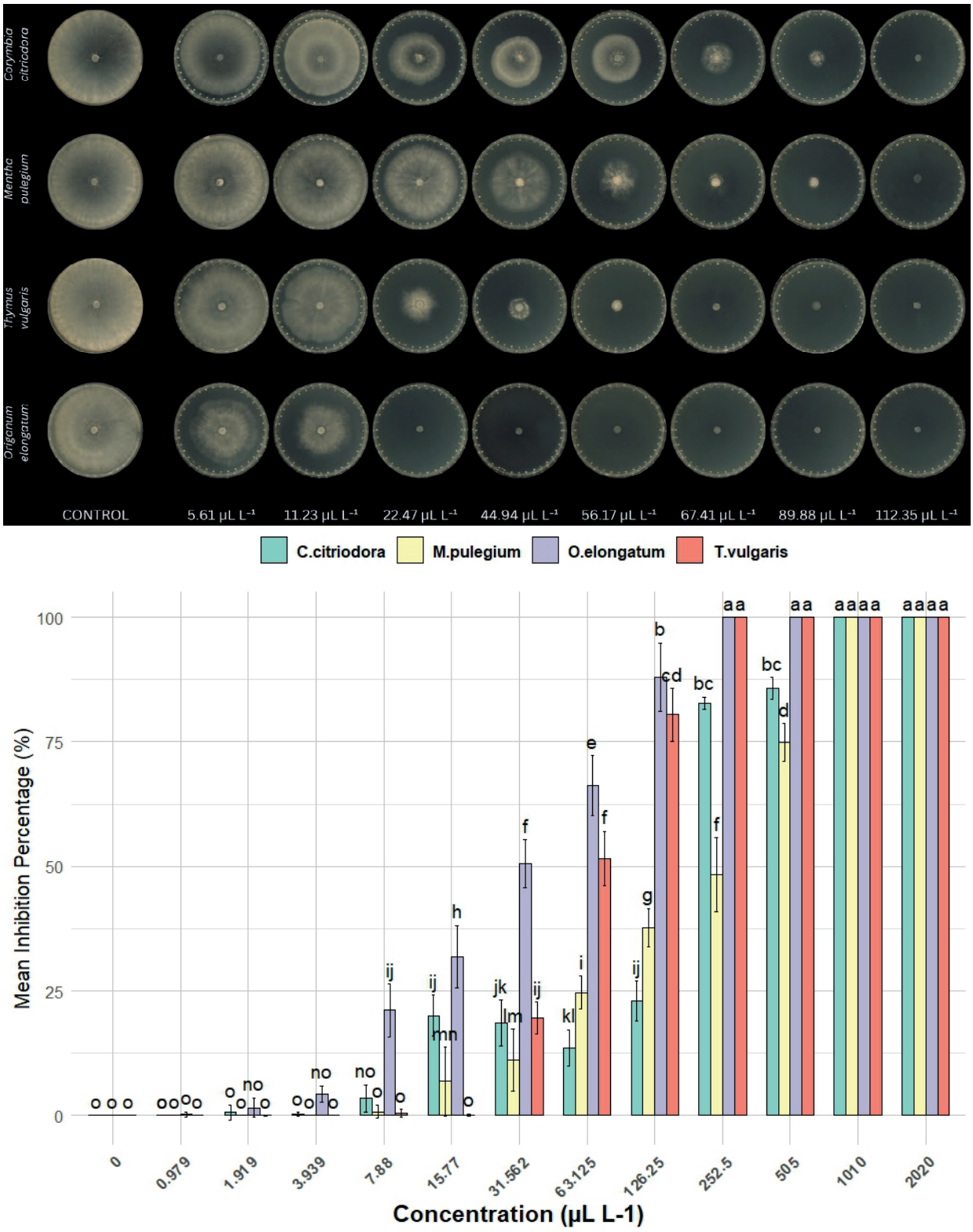

Figure 3. *In vitro* antifungal activities of the four essential oils (EOs) indicated from vapor-phase assays against mycelium growth of *Botrytis cinerea*, after 4 d incubation at 24 ± 1 °C. Top: Mycelium growth in Petri dishes containing different concentrations of each EO in the direct contact assay. Bottom: Mean percentages of inhibition of mycelium growth at different concentrations of the tested EOs. Different letters above bars indicate differences ($P < 0.05$), according to Tukey's high significance difference (HSD) test. All data are means ± SD.

Table 4. mean minimum inhibitory concentrations (MIC) and mean effective concentrations (EC_{50} and EC_{90}) from essential oils from of *Oreganum elongatum*, *Mentha pulegium*, *Thymus vulgaris* and *Corymbia citriodora* against mycelium growth of *Botrytis cinerea*.

Essential oil	Methods	R^{2*}	MIC (µL L^{-1})	EC_{50} (µL L^{-1})	95%Confidence Limits (µL L^{-1})	EC_{90} (µL L^{-1})	95% Confidence Limits (µL L^{-1})
O. elongatum	DC*	0.99	252.5	33.27	[30.13-36.41]	139.17	[121.46-156.88]
	VC*	0.95	56.17	12.75	[11.07-14.44]	26.56	[21.76-31.35]
M. pulegium	DC	0.97	1010	223.867	[194.62-253.11]	816.763	[644.44-986.08]
	VC	0.97	112.35	61.347	[55.30-67.39]	99.5098	[81.59-117.42]
T. vulgaris	DC	0.99	252.5	59.799	[53.90-65.69]	142.040	[132.68-151.39]
	VC	0.96	89.88	18.495	[1652-20.47]	42.995	[30.38-55.60]
C. citriodora	DC	0.94	1010	176.455	[137.73-215.17]	258.78	[238.71-278.84]
	VC	0.97	112.35	53.708	[41.48-65.93]	99.90	[64.28-135.51]

*R^2: Coefficient of determination. DC = Direct contact assay. VC = Vapor contact assay.

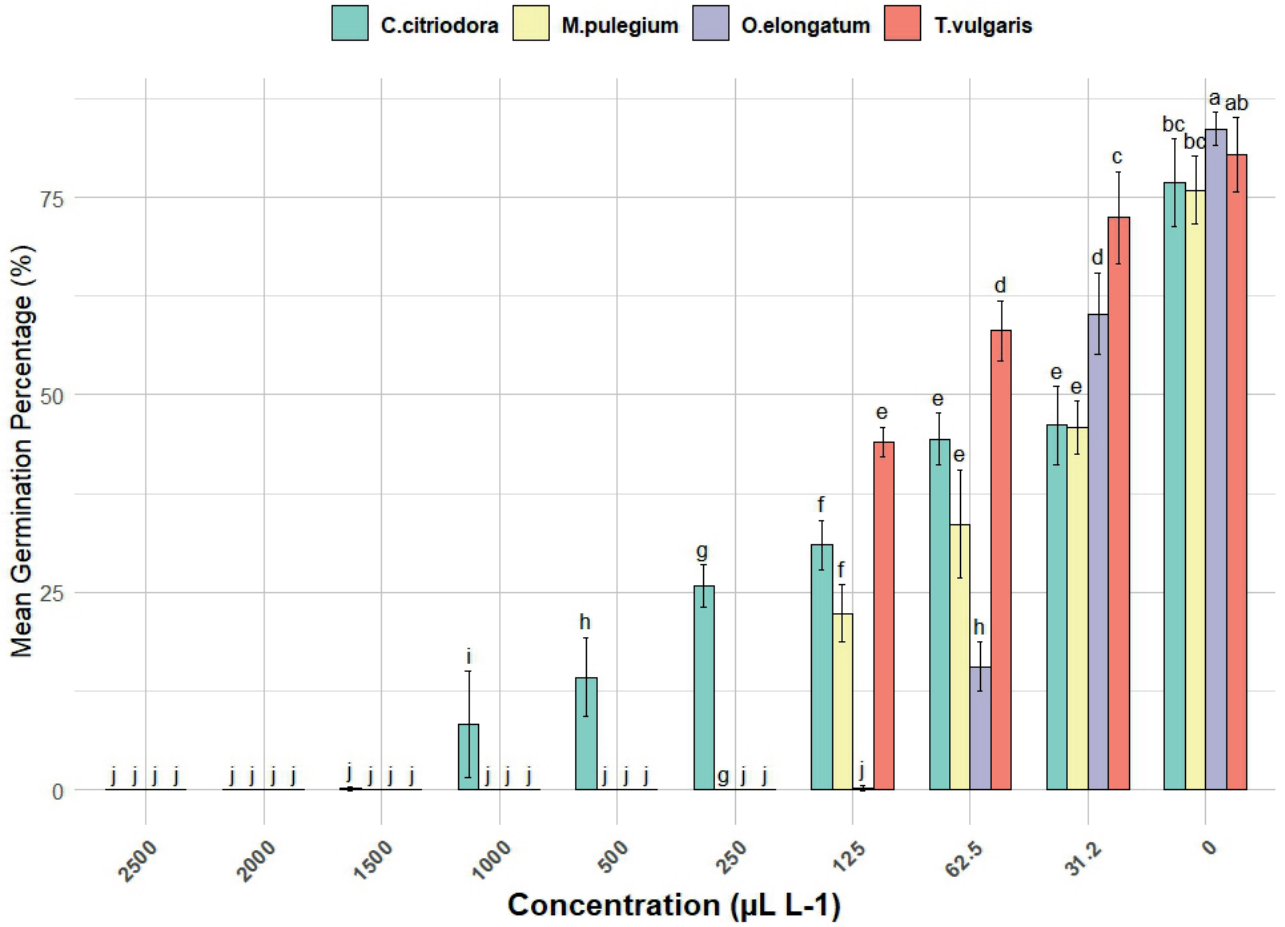

Figure 4. Effect of different concentrations of essential oils on conidial germination in contact phases. Letters (a, b, c, d, e, f, g, h, i, j) indicate homogeneous groups of means based on the high significant difference (HSD) test for each variable ($P < 0.05$). Arcsine transformation was performed prior to statistical analyses.

These results also showed that the EO of *C. citriodora* did not prevent, or only slightly reduced, *B. cinerea* conidium germination, even at high concentrations (1500 µL L^{-1}). In contrast, the oregano EO was the most effective against the fungus, even at low concentrations. For all control treatments, which contained only 1% Tween 80, conidium germination exceeded 75%.

In vivo *Antifungal assays*

Protection assays on detached grapevine leaves

Disease development was also monitored *in vivo* using the EC_{50} and EC_{90} concentrations of each EO that was determined from the *in vitro* assessments. The test was conducted on 'Chardonnay' and 'Cabernet Sauvignon' grapevines, which are, respectively, highly susceptible and less susceptible to *Botrytis cinerea* (Jeandet et al., 1992).

Illustration of the *in vivo* fungicidal activity of different concentrations of the four EOs against *B. cinerea* is presented in Figure 5. The *B. cinerea* isolate used in this experiment causes disease in grape berries. In the direct contact treatment trial, all four EOs applied preventively or simultaneously showed strong antifungal activity compared to untreated leaves, and significantly ($P < 0.05$) reduced lesion areas.

For all treatments, the effectiveness of the EOs was greatest for 'Cabernet Sauvignon', with mean lesion size reductions of 84.2% for *M. pulegium* essential oil, 72.4% for that from *T. vulgaris*, 68.9% for that from *C. citriodora*, and 68.6% for the EO from *O. elongatum* EOs, compared to their respective negative controls. For 'Chardonnay', the reductions in mean lesion sizes were 74.6% for the oil from *O. elongatum*, 72.7% for that from *M. pulegium*, 68.2% for the oil from *T. vulgaris*, and 62.6% for the EO from *C. citriodora*. Ranking of the EOs according to their impacts on leaf lesion sizes in the two grapevine varieties was as follows: The *M. pulegium* EO (78.5%) was the most effective, followed by that from *O. elongatum* (71.6%), from *T. vulgaris* (70.3%) and from *C. citriodora* (65.7%).

Protection assays on berry grapevine

The effects of EOs from *O. elongatum, M. pulegium, T. vulgaris* and *C. citriodora* on development of *Botrytis cinerea* in wound-inoculated grape berries of 'Muscat of Italy' are shown in Figure 6. All treatments reduced the incidence and development of gray mold at 22°C over a 6 d storage period. All the grape berries not treated with the EOs were almost completely infected by the fungus. The results showed that the four EOs inhibited fungal growth, but their effectiveness varied. The most effective EO was from *M. pulegium* causing a 57.7% reduction in mean lesion diameter, followed by the EO from *O. elongatum* (49.7% reduction), then *T. vulgaris* (40.1%) and *C. citriodora* with 31.7% reduction, compared with the negative experimental controls. The most effective treatment was the preventive application of Eucalyptus, pennyroyal and thymus EOs, which reduced average lesion diameters in grape berries. For the oregano EO, the treatment resulted in the smallest lesions. The EOs showed no phytotoxic effects on the grape fruit tissues at all studied concentrations.

DISCUSSION

Essential oils from plants and their chemical components have long been studied for their antifungal activities, particularly within sustainable environmental practices to enhance agricultural yields and food storage durability (Carrubba and Catalano, 2009; El-Mohamedy, 2017; Habbadi *et al*., 2018; Cheng *et al*., 2024; Nunes *et al*., 2024; Wike *et al*., 2024). Grapevine has also been the subject of research into alternative treatments using EOs to treat fungal infections, particularly gray mold, which is a major cause of fruit losses (Antonov *et al*., 1997; Walter *et al*., 2001; Tripathi *et al*., 2008; Burggraf and Rienth, 2020). Although numerous studies have reported inhibition of *B. cinerea* by EOs *in vitro*, none have assessed the *in vivo* protective effects of EOs on grape berries and vegetative organs of the grape varieties, 'Cabernet Sauvignon' and 'Chardonnay', which have, respectively, intermediate resistance and susceptibility to *B. cinerea* (Jeandet *et al*., 1992). The present study investigated the chemical composition and *in vitro* antifungal activity of EOs from *O. elongatum*, *M. pulegium*, *T. vulgaris* and *C. citriodora* in direct contact and vapour contact *B. cinerea* mycelium growth and spore germination assays. The study also evaluated effects of these EOs on detached grapevine leaves of two grapevine varieties and on grape berries *in vivo*.

The main constituents of the four EOs found in the present study (Table 2) corroborate those reported in the literature. Lemon eucalyptus EO was contained cineole and α-pinene (Low *et al*., 1974; Ramezani *et al*., 2002), while carvacrol was prominent in *O. elongatum* EO, and thymol in *T. vulgaris* EO. These results are comparable with previous research (Sivropoulou *et al*., 1996; Dorman *et al*., 2000; Aligiannis *et al*., 2001; Burt, 2004). However, other studies have shown that the chemical composition of thyme and oregano EOs can vary greatly depending on the plant chemotype assessed, and that the antifungal activity of the EO can vary significantly (Daferera *et al*., 2003; Della Pepa *et al*., 2019; Drioiche *et al*., 2022). Pennyroyal is associated with pulegone (see figure S2). This high concentration of pulegone is supported by numerous studies, which also report pulegone as the main constituent (Kokkini *et al*., 2002; Stoyanova *et al*., 2005), while other studies have reported lower pulegone levels but high amounts of menthone/isomen-

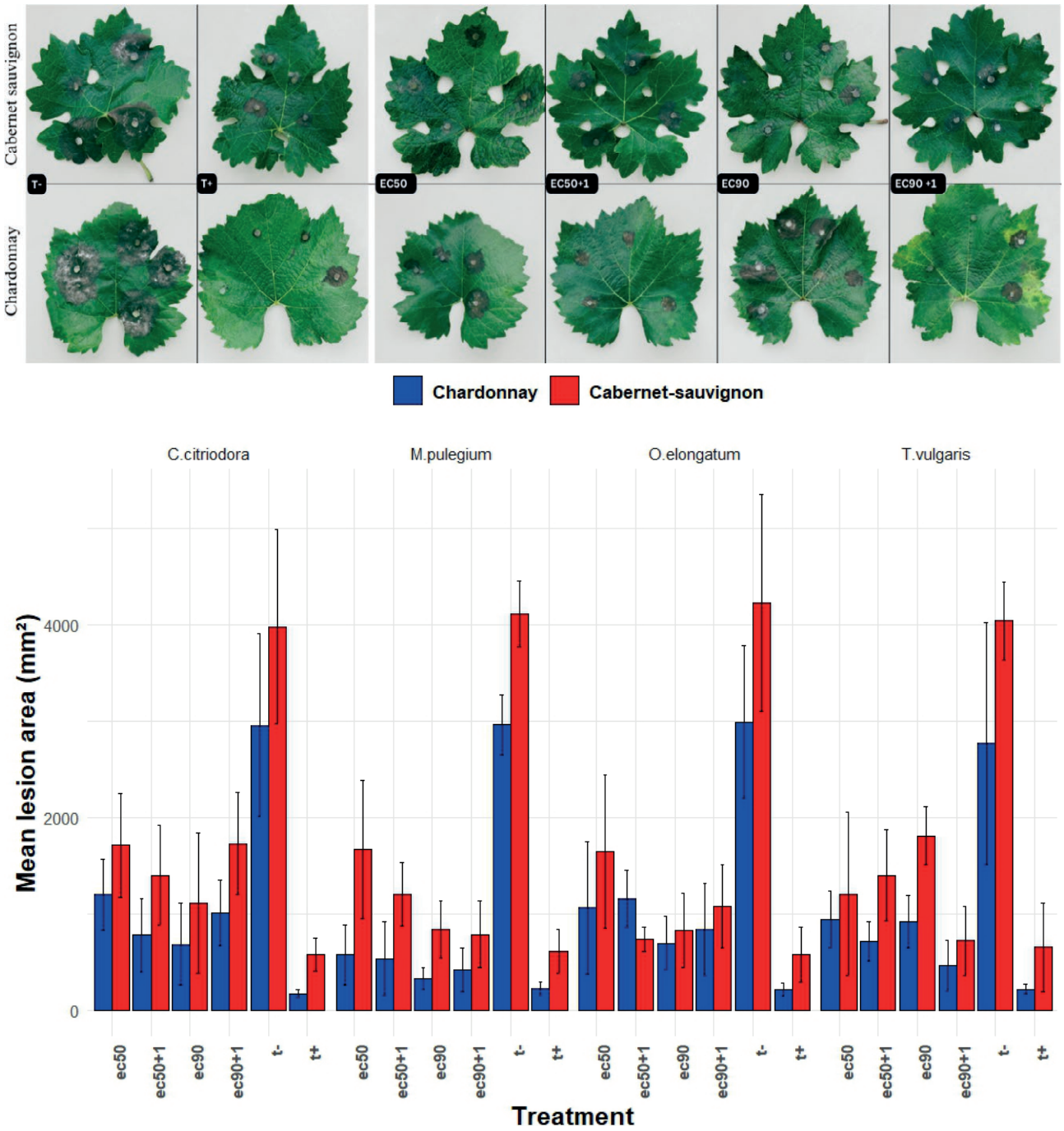

Figure 5. Top: Representative grapevine leaves that had been inoculated with *Botrytis cinerea* and treated with two concentrations (EC_{50} or EC_{90}) of essential oils from four different plants, in preventive and simultaneous applications, with fungicide fenhexamid as the positive experimental control. Bottom: Mean lesion surface areas caused by *B. cinerea* on two grapevine varieties treated with the essential oils *in vivo* by direct contact. All the data are expressed as means ± SD.

thone, piperitenone/piperitone, or piperitone (Lorenzo *et al.*, 2002; El-Ghorab, 2006; Ait-Ouazzou *et al.*, 2012; Abdelli *et al.*, 2016; Brahmi *et al.*, 2016). Variabilities in chemical composition could be related to effects of geographical location, genetic factors, collection period, and extraction techniques (Mechergui *et al.*, 2016; Elansary *et al.*, 2018). Data from the present study indicate qualitative and quantitative variations in the EO com-

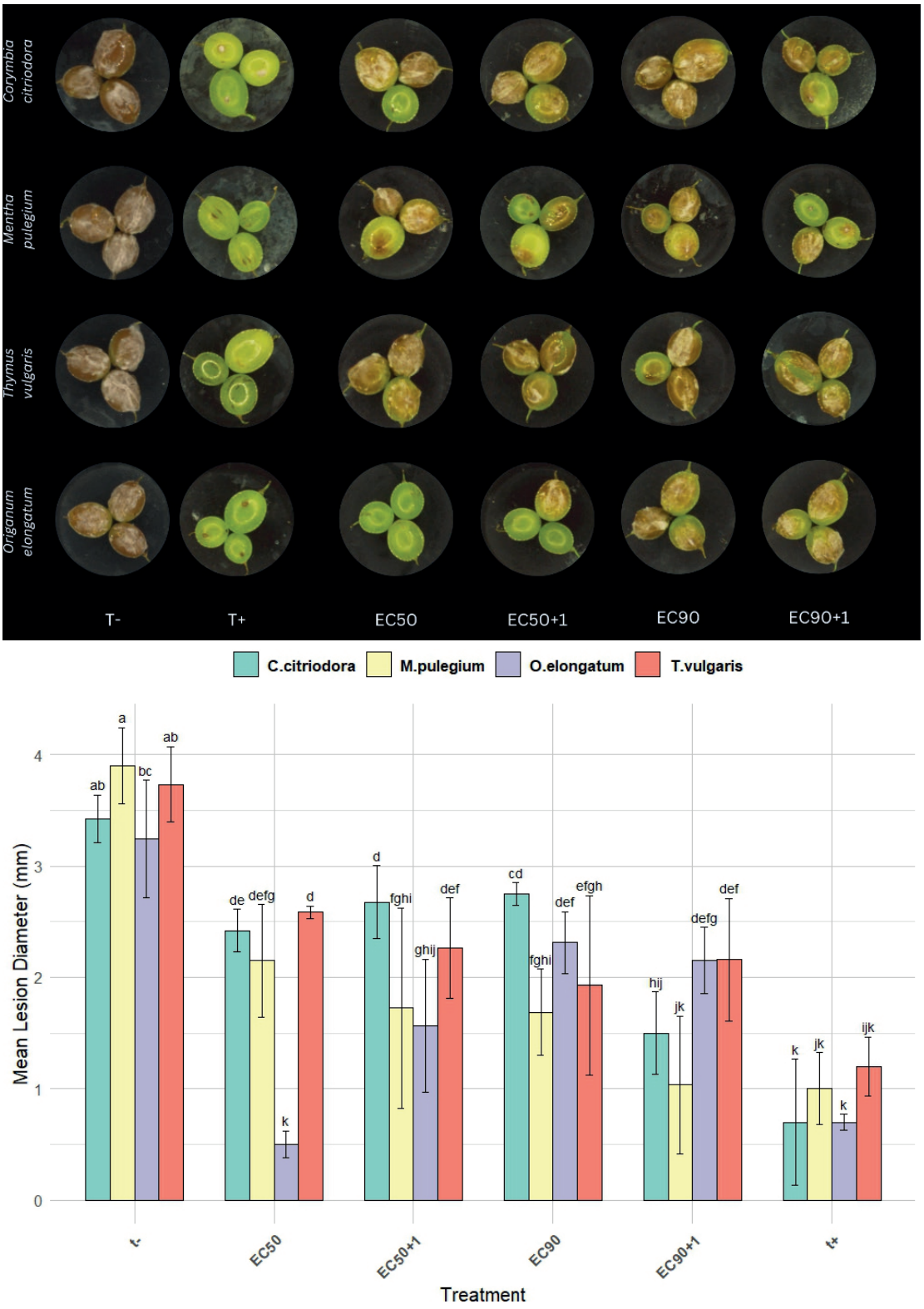

Figure 6. Top: Visual differences in *Botrytis cinerea* mycelium growth and fruit desiccation of detached 'Muscat of Italy' berries after 6 d of treatment. These images were captured at the end of the *in vivo* trial. Bottom: Mean *in vivo* antifungal activities of four essential oils against *B. cinerea* on detached grapes berries. Letters accompanying the means indicate homogeneous groups based on the Tukey HSD test for each variable at ($P < 0.05$).

positions of the four investigated plant species. However, GC-MS analyses have shown that terpenoids and terpenes predominate in all the four oils examined.

The present study presents *in vitro* inhibition proportions of *B. cinerea* through direct contact of the pathogen with different EOs at various concentrations. The MIC at which no fungal growth was observed for the oregano oil was is 252.5 µL L^{-1}, greater than 125 µL L^{-1} reported by Zhao *et al.* (2021), and that obtained by Yilmaz *et al.* (2016), but less than the 0.5 mg mL^{-1} obtained by Hou *et al.* (2020) for *O. vulgare* EO. For thyme EO, the MIC was also 252.5 µL L^{-1}, which is less than the 800 µL L^{-1} obtained by Abdolahi *et al.* (2010) , the 400 µL L^{-1} obtained by Fathi *et al.* (2012), but similar to the 200 µg mL^{-1} reported by Daferera *et al.* (2003). The MIC for pennyroyal is 1010 µL L^{-1}, which is less than the 2660 µL L^{-1} obtained by Aouadi *et al.* (2022), but greater than the 250 ppm obtained by Singh and Pandey (2018). Similarly, the MIC for lemon Eucalyptus oil was 1010 µL L^{-1}, which is greater than the MIC reported by Tripathi *et al.* (2008).

The present study results show that oregano and thyme EOs were effective against *B. cinerea*, even at very low concentrations. This efficacy may be due to the presence of thymol and carvacrol (see figure S2) as major components in these two EOs. This observation is supported by the results of Zhang *et al.* (2019), who showed that thymol and carvacrol had antifungal activity against *B. cinerea* at low concentrations compared to crude EO (Hou *et al*., 2020), inducing clear morphological changes in fungus hyphae. Zhao *et al.* (2021) also obtained similar results, where thymol and carvacrol at 125 mg L^{-1} completely suppressed gray mold. In addition, p-cymene, present as a major component in the two EOs, completely inhibited *B. cinerea* growth at 80.0 µg L^{-1}, as observed in the study by Pinto *et al.* (2020). Efficacy of Eucalyptus and pennyroyal EOs requires high concentrations to maintain significant *in vitro* inhibition of *B. cinerea*.

In the vapour contact assays, oregano EO gave an MIC of 44.9 µL L^{-1}, differing from the value of 31.25 mg L^{-1} obtained by Zhao *et al.* (2021). For thyme EO, the MIC was 89.88 µL L^{-1}, greater than the 45.45 µL L^{-1} reported by Álvarez-García *et al.* (2023). These results confirm those obtained through the direct contact method, demonstrating that, of the four oils studied, that from oregano EO was the most inhibitory of *B. cinerea*, followed by the EO from thyme. This efficacy is likely to be due to thymol and carvacrol, which induce morphological changes by disrupting the *B. cinerea* mycelium and hyphal structure (Abbaszadeh *et al*., 2014; Elshafie *et al*., 2015), whereas the oils from pennyroyal and eucalyptus had reduced efficacy at low concentrations. However, the inhibitory effects of the oils in the vapor contact assays were stronger. To explain this toxicity difference, the pathogen may have been more exposed to the volatile substances released in the closed environment of the VC assay, whereas in a DC assay, the mycelia are only exposed to a small portion of a substance on the surface of the agar in assay plates. Consequently, inhibitory effects on the mycelium growth of *B. cinerea* in the VC assays was greater than in the DC assays, as was confirmed by Soylu *et al.* (2010).

Inhibition of conidium germination is crucial for evaluating the efficacy of EOs, as conidium germination is the starting point for fungal infection (Agrios, 2008). Additionally, germination leads to eventual multiplication and dissemination of pathogenic fungi. Previous studies have shown that *T. vulgaris* oil suppresses the germination of *B. cinerea* at 1000 µL L^{-1} (Fincheira *et al*., 2023), a concentration greater than the 250 µL L^{-1} obtained in the present study with the same EO. For the oregano oil, the values obtained were 250 µL L^{-1}, which is less than the 3.2 µg mL^{-1} reported by Soylu *et al.* (2010) for oregano oil. For the inhibitory effect of Eucalyptus EO on conidium germination, Aguiar *et al.* (2014) found that at 150 mg L^{-1}, spore germination of three assessed fungi was completely inhibited. Inhibition of fungal spore germination strongly depends on the applied EO and its concentration (Fincheira *et al*., 2023). Therefore, it is likely that suppression of spore germination by EO treatments could contribute to limiting the spread of *B. cinerea* by reducing the conidium load.

Grapevine leaves were chosen in the present study for the *in vivo* test because young leaves emerging at bud burst are the primary sources of *B. cinerea* inoculum (Balasubramaniam, 1997). The objective of the test was to evaluate whether the potential of EOs depends on the grape variety tested and the mode of application (simultaneous or preventive). The experiment showed that 'Cabernet Sauvignon' was better protected by the direct application of EOs, regardless of the treatment, compared to 'Chardonnay'.

The treatments applied during the tests did not inhibit fungal growth in a dose-dependent manner. For treatments with the EC_{50} doses, the preventive treatments (EC_{50}+1) were more effective than the concomitant treatments. However, for the EC_{90} doses, the concomitant treatments were more effective. Although all EOs were effective in reducing fungal infections, the *M. pulegium* EO was the most effective in controlling infections caused by *B. cinerea* on detached leaves of both grapevine varieties. Aouadi *et al.* (2022) reported in a subsequent study that, during *in vivo* tests, *M. pulegium* EO completely suppressed, by direct contact, gray mold

on strawberries previously inoculated with *B. cinerea* conidia. Oumzil *et al.* (2002) demonstrated that pulegone inhibited all tested microorganisms and was the most effective against three assessed fungi. De Sousa Barros *et al.* (2015) studied the functional properties of EOs from different *Mentha* species, demonstrating that oils rich in pulegone exhibited significant antifungal activity against *Microsporum canis* and *Trichophyton rubrum*. Pulegone, a monoterpene ketone, is the principal component of *Mentha pulegium* EO. This compound has an important role in the antimicrobial activity of the EO (Areco *et al.*, 2024). The second *in vivo* experiment of the present study was carried out on detached grape berries, to determine effectiveness of direct contact treatments. All the applied treatments resulted in reductions in *B. cinerea* lesion diameter. Inhibition of fungal growth on the berries varied according to the different EOs and treatments. These results are consistent with those from other studies conducted on harvested fruits and vegetables from growing plants. Soylu *et al.*, (2010) demonstrated the ability of EOs from oregano, lavender and rosemary, applied in contact and vapour forms, to reduce disease on tomatoes infected by *B. cinerea*.

The present study did not assess *in vivo* fumigation effectiveness of EOs against *B. cinerea* on leaves and grapes berries. Further research is therefore required to investigate the vapour contact effects against *B. cinerea* of EOs on grape berries. It would be particularly interesting to conduct *in vivo* fumigation tests to avoid direct contact of the EOs with food commodities, therefore maintaining the organoleptic features of these oils and avoiding the alterations that occur during soaking treatments. Increasing resistance of pathogens to fungicides, and awareness of the dangers associated with the intensive use of pesticides indicate that EOs from oregano, thyme, pennyroyal and lemon Eucalyptus have potential to be effective and sustainable alternatives to conventional phytosanitary products. The present study confirms the antifungal activity of the EOs tested, which at low doses effectively protected grapevine organs against gray mold under controlled conditions. These results pave the way for more extensive studies to evaluate their long-term effectiveness of these oils under field conditions.

CONCLUSIONS

In this study, the essential oils of *Origanum elongatum*, *Mentha pulegium*, *Thymus vulgaris*, and *Corymbia citriodora* exhibited strong antifungal activity against *Botrytis cinerea*, a phytopathogenic fungus of major importance. *In vitro* and *in vivo* tests both confirmed effectiveness of these oils, suggesting that they could serve as viable alternatives to synthetic chemical fungicides for disease management. However, further innovation is needed to develop practical application techniques for the use of essential oils in agriculture and food production industries.

ACKNOWLEDGMENTS

This research was funded by PRIMA-MiDiVine project 1564 coordinated by Aziz Aziz, 2021/2025 (https://www.univ-reims.fr/MiDiVine/, accessed on 1 January 2025) (Innovative Approaches Promoting Functional Microbial Diversity for Sustainable Grapevine Health and Productivity in Vineyard Systems of Mediterranean Areas), supported by the European Union, with co-funding by MESRSI (Morocco).

LITERATURE CITED

Abbaszadeh S., Sharifzadeh A., Shokri H., Khosravi A.R., Abbaszadeh A., 2014. Antifungal efficacy of thymol, carvacrol, eugenol and menthol as alternative agents to control the growth of food-relevant fungi. *Journal de Mycologie Médicale* 24: e51–e56. https://doi.org/10.1016/j.mycmed.2014.01.063

Abdelli M., Moghrani H., Aboun A., Maachi R., 2016. Algerian *Mentha pulegium* L. leaves essential oil: Chemical composition, antimicrobial, insecticidal and antioxidant activities. *Industrial Crops and Products* 94: 197–205. https://doi.org/10.1016/j.indcrop.2016.08.042

Abdolahi A., Hassani A., Ghuosta Y., Bernousi I., Meshkatalsadat M.H., 2010. *In vitro* efficacy of four plant essential oils against *Botrytis cinerea* Pers.:Fr. and *Mucor piriformis* A. Fischer. *Journal of Essential Oil Bearing Plants* 13: 97–107. https://doi.org/10.1080/0972060X.2010.10643796

Adams R.P., 2007. Identification of essential oil components by gas chromatography mass spectroscopy. Carol stream, Ill, Allured publishing corporation, 804 pp.

Adaskaveg J.E., Förster H., Prusky D.B. (eds), 2022. Postharvest pathology of fruit and nut crops. *The American Phytopathological Society*.

Agrios G.N., 2008. *Plant Pathology*. Amsterdam, Elsevier Academic Press, 922 pp.

Aguiar R.W.D.S., Ootani M.A., Ascencio S.D., Ferreira T.P.S., Santos M.M.D., Santos G.R.D., 2014. Fumigant Antifungal Activity of *Corymbia citriodora* and *Cymbopogon nardus* Essential Oils and Citronellal against

Three Fungal Species. *The Scientific World Journal* 2014: 1–8. https://doi.org/10.1155/2014/492138

Ait-Ouazzou A., Lorán S., Arakrak A., Laglaoui A., Rota C., … Conchello P., 2012. Evaluation of the chemical composition and antimicrobial activity of *Mentha pulegium*, *Juniperus phoenicea*, and *Cyperus longus* essential oils from Morocco. *Food Research International* 45: 313–319. https://doi.org/10.1016/j.foodres.2011.09.004

Aligiannis N., Kalpoutzakis E., Mitaku S., Chinou I.B., 2001. Composition and antimicrobial activity of the essential oils of two *Origanum* species. *Journal of Agricultural and Food Chemistry* 49: 4168–4170. https://doi.org/10.1021/jf001494m

Almasaudi N.M., Al-Qurashi A.D., Elsayed M.I., Abo-Elyousr K.A.M., 2022. Essential oils of *oregano* and *cinnamon* as an alternative method for control of gray mold disease of table grapes caused by *Botrytis cinerea*. *Journal of Plant Pathology* 104: 317–328. https://doi.org/10.1007/s42161-021-01008-8

Álvarez-García S., Moumni M., Romanazzi G., 2023. Antifungal activity of volatile organic compounds from essential oils against the postharvest pathogens *Botrytis cinerea*, *Monilinia fructicola*, *Monilinia fructigena*, and *Monilinia laxa*. *Frontiers in Plant Science* 14: 1274770. https://doi.org/10.3389/fpls.2023.1274770

Antonov A., Stewart A., Walter M., 1997. Inhibition of conidium germination and mycelial growth of *Botrytis cinerea* by natural products. *Proceedings of the New Zealand Plant Protection Conference* 50: 159–164. https://doi.org/10.30843/nzpp.1997.50.11289

Aouadi G., Grami L.K., Taibi F., Bouhlal R., Elkahoui S., … Mediouni Ben Jemâa J., 2022. Assessment of the efficiency of *Mentha pulegium* essential oil to suppress contamination of stored fruits by *Botrytis cinerea*. *Journal of Plant Diseases and Protection* 129: 881–893. https://doi.org/10.1007/s41348-022-00623-6

Aoujil F., Litskas V., Yahyaoui H., El Allaoui N., Benbouazza A., … Habbadi K., 2024. Sustainability indicators for the environmental impact assessment of plant protection products use in Moroccan vineyards. *Horticulturae* 10: 473. https://doi.org/10.3390/horticulturae10050473

Areco V.A., Achimón F., Almirón C., Nally M.C., Zunino M.P., Yaryura P., 2024. Antifungal activity of essential oils rich in ketones against *Botrytis cinerea:* New strategy for biocontrol. *Biocatalysis and Agricultural Biotechnology* 59: 103233. https://doi.org/10.1016/j.bcab.2024.103233

Balasubramaniam A., 1997. Neuropeptide Y Family of Hormones: Receptor subtypes and antagonists. *Peptides* 18: 445–457. https://doi.org/10.1016/S0196-9781(96)00347-6

Bi K., Liang Y., Mengiste T., Sharon A., 2023. Killing softly: a roadmap of *Botrytis cinerea* pathogenicity. *Trends in Plant Science* 28: 211–222. https://doi.org/10.1016/j.tplants.2022.08.024

Boddy L., 2016. Pathogens of Autotrophs. In: *The Fungi*, Elsevier, 245–292.

Brahmi F., Abdenour A., Bruno M., Silvia P., Alessandra P., … Mohamed C., 2016. Chemical composition and *in vitro* antimicrobial, insecticidal and antioxidant activities of the essential oils of *Mentha pulegium* L. and *Mentha rotundifolia* (L.) Huds growing in Algeria. *Industrial Crops and Products* 88: 96–105. https://doi.org/10.1016/j.indcrop.2016.03.002

Burggraf A., Rienth M., 2020. Origanum vulgare essential oil vapor impedes *Botrytis cinerea* development on grapevine (*Vitis vinifera*) fruit. *Phytopathologia Mediterranea* 59: 331–344. https://doi.org/10.14601/Phyto-11605

Burt S., 2004. Essential oils: their antibacterial properties and potential applications in foods – a review. *International Journal of Food Microbiology* 94: 223–253. https://doi.org/10.1016/j.ijfoodmicro.2004.03.022

Carrubba A., Catalano C., 2009. Essential oil crops for sustainable agriculture – A Review. In: *Climate Change, Intercropping, Pest Control and Beneficial Microorganisms* (E. Lichtfouse, ed.), Dordrecht, Springer Netherlands, 137–187.

Chang Y., Harmon P.F., Treadwell D.D., Carrillo D., Sarkhosh A., Brecht J.K., 2022. Biocontrol Potential of essential oils in organic Horticulture systems: From Farm to Fork. *Frontiers in Nutrition* 8: 805138. https://doi.org/10.3389/fnut.2021.805138

Chen Y., Dai G., 2012. Antifungal activity of plant extracts against *Colletotrichum lagenarium*, the causal agent of anthracnose in cucumber. *Journal of the Science of Food and Agriculture* 92: 1937–1943. https://doi.org/10.1002/jsfa.5565

Cheng C., He X., Li H., Zhang Y., Sun S., … Li Y., 2024. Study on the antibacterial activity of *Litsea* essential oil nanoemulsion and its effect on the storage quality of duck meat. *Journal of Molecular Liquids* 410: 125610. https://doi.org/10.1016/j.molliq.2024.125610

Daferera D.J., Ziogas B.N., Polissiou M.G., 2003. The effectiveness of plant essential oils on the growth of *Botrytis cinerea*, *Fusarium* sp. and *Clavibacter michiganensis* subsp. michiganensis. *Crop Protection* 22: 39–44. https://doi.org/10.1016/S0261-2194(02)00095-9

De Sousa Barros A., De Morais S.M., Ferreira P.A.T., Vieira Í.G.P., Craveiro A.A., … De Sousa H.A., 2015.

Chemical composition and functional properties of essential oils from *Mentha species*. *Industrial Crops and Products* 76: 557–564. https://doi.org/10.1016/j.indcrop.2015.07.004

Della Pepa T., Elshafie H.S., Capasso R., De Feo V., Camele I., ... Caputo L., 2019. Antimicrobial and phytotoxic activity of *Origanum heracleoticum* and *O. majorana* Essential oils growing in Cilento (Southern Italy). *Molecules* 24: 2576. https://doi.org/10.3390/molecules24142576

Di Francesco A., Aprea E., Gasperi F., Parenti A., Placì N., ... Baraldi E., 2022. Apple pathogens: Organic essential oils as an alternative solution. *Scientia Horticulturae* 300: 111075. https://doi.org/10.1016/j.scienta.2022.111075

Dorman H.J.D., Figueiredo A.C., Barroso J.G., Deans S.G., 2000. *In vitro* evaluation of antioxidant activity of essential oils and their components. *Flavour and Fragrance Journal* 15: 12–16. https://doi.org/10.1002/(SICI)1099-1026(200001/02)15:1<12::AID-FFJ858>3.0.CO;2-V

Drioiche A., Zahra Radi F., Ailli A., Bouzoubaa A., Boutakiout A., ... Zair T., 2022. Correlation between the chemical composition and the antimicrobial properties of seven samples of essential oils of endemic Thymes in Morocco against multi-resistant bacteria and pathogenic fungi. *Saudi Pharmaceutical Journal* 30: 1200–1214. https://doi.org/10.1016/j.jsps.2022.06.022

Elansary H.O., Abdelgaleil S.A.M., Mahmoud E.A., Yessoufou K., Elhindi K., El-Hendawy S., 2018. Effective antioxidant, antimicrobial and anticancer activities of essential oils of horticultural aromatic crops in northern Egypt. *BMC Complementary and Alternative Medicine* 18: 214. https://doi.org/10.1186/s12906-018-2262-1

El-Ghorab A.H., 2006. The Chemical Composition of the *Mentha pulegium* L. Essential oil from Egypt and its antioxidant activity. *Journal of Essential Oil Bearing Plants* 9: 183–195. https://doi.org/10.1080/0972060X.2006.10643491

El-Mohamedy R.S.R., 2017. Plant essential oils for controlling plant pathogenic Fungi. In: *Volatiles and Food Security* (D.K. Choudhary, A.K. Sharma, P. Agarwal, A. Varma and N. Tuteja, ed.), *Singapore, Springer Singapore*, 171–198.

Elshafie H.S., Mancini E., Camele I., Martino L.D., De Feo V., 2015. *In vivo* antifungal activity of two essential oils from Mediterranean plants against postharvest brown rot disease of peach fruit. *Industrial Crops and Products* 66: 11–15. https://doi.org/10.1016/j.indcrop.2014.12.031

Fathi Z., Hassani A., Ghosta Y., Abdollahi A., Meshkatalsadat M.H., 2012. The potential of Thyme, Clove, Cinnamon and Ajowan essential oils in inhibiting the growth of *Botrytis cinerea* and *Monilinia fructicola*. *Journal of Essential Oil Bearing Plants* 15: 38–47. https://doi.org/10.1080/0972060X.2012.10644017

Fincheira P., Jofré I., Espinoza J., Levío-Raimán M., Tortella G., ... Rubilar O., 2023. The efficient activity of plant essential oils for inhibiting *Botrytis cinerea* and *Penicillium expansum*: Mechanistic insights into antifungal activity. *Microbiological Research* 277: 127486. https://doi.org/10.1016/j.micres.2023.127486

Fontana D.C., Neto D.D., Pretto M.M., Mariotto A.B., Caron B.O., ... Schmidt D., 2021. Using essential oils to control diseases in strawberries and peaches. *International Journal of Food Microbiology* 338: 108980. https://doi.org/10.1016/j.ijfoodmicro.2020.108980

Habbadi K., Meyer T., Vial L., Gaillard V., Benkirane R., ... Lavire C., 2018. Essential oils of *Origanum compactum* and *Thymus vulgaris* exert a protective effect against the phytopathogen *Allorhizobium vitis*. *Environmental Science and Pollution Research* 25: 29943–29952. https://doi.org/10.1007/s11356-017-1008-9

Hong J.K., Sook Jo Y., Jeong D.H., Woo S.M., Park J.Y., ... Park C.-J., 2023. Vapors from plant essential oils to manage tomato grey mold caused by *Botrytis cinerea*. *Fungal Biology* 127: 985–996. https://doi.org/10.1016/j.funbio.2023.02.002

Hou H., Zhang X., Zhao T., Zhou L., 2020. Effects of *Origanum vulgare* essential oil and its two main components, carvacrol and thymol, on the plant pathogen *Botrytis cinerea*. *PeerJ* 8: e9626. https://doi.org/10.7717/peerj.9626

Hua L., Yong C., Zhanquan Z., Boqiang L., Guozheng Q., Shiping T., 2018. Pathogenic mechanisms and control strategies of *Botrytis cinerea* causing post-harvest decay in fruits and vegetables. *Food Quality and Safety* 2: 111–119. https://doi.org/10.1093/fqsafe/fyy016

Jeandet P., Sbaghi M., Bessis R., 1992. The production of resveratrol (3,5,4'-trihydroxystilbene) by grapevine *in vitro* cultures, and its application to screening for grey mold resistance. *Journal of Wine Research* 3: 47–57. https://doi.org/10.1080/09571269208717914

Kokkini S., Hanlidou E., Karousou R., Lanaras T., 2002. Variation of pulegone content in Pennyroyal (*Mentha pulegium* L.) Plants growing wild in Greece. *Journal of Essential Oil Research* 14: 224–227. https://doi.org/10.1080/10412905.2002.9699830

Li Y., Shao X., Xu J., Wei Y., Xu F., Wang H., 2017. Tea tree oil exhibits antifungal activity against *Botrytis cinerea* by affecting mitochondria. *Food Chem-*

istry 234: 62–67. https://doi.org/10.1016/j.foodchem.2017.04.172

López-Meneses A.K., Sánchez-Mariñez R.I., Quintana-Obregón E.A., Parra-Vergara N.V., González-Aguilar G.A., … Cortez-Rocha M.O., 2017. *In vitro* Antifungal activity of essential oils and major components against fungi plant pathogens. *Journal of Phytopathology* 165: 232–237. https://doi.org/10.1111/jph.12554

Lorenzo D., Paz D., Dellacassa E., Davies P., Vila R., Cañigueral S., 2002. Essential oils of *Mentha pulegium* and *Mentha rotundifolia* from Uruguay. *Brazilian Archives of Biology and Technology* 45: 519–524. https://doi.org/10.1590/S1516-89132002000600016

Low D., Rawal B., Griffin W., 1974. Antibacterial action of the essential oils of some australian myrtaceae with special references to the activity of chromatographic fractions of oil of *eucalyptus citriodora*. *Planta Medica* 26: 184–189. https://doi.org/10.1055/s-0028-1097987

Maurya A., Prasad J., Das S., Dwivedy A.K., 2021. Essential oils and their application in food safety. *Frontiers in Sustainable Food Systems* 5: 653420. https://doi.org/10.3389/fsufs.2021.653420

Mechergui K., Jaouadi W., Coelho J.P., Khouja M.L., 2016. Effect of harvest year on production, chemical composition and antioxidant activities of essential oil of oregano (*Origanum vulgare* subsp glandulosum (Desf.) Ietswaart) growing in North Africa. *Industrial Crops and Products* 90: 32–37. https://doi.org/10.1016/j.indcrop.2016.06.011

Moghaddam M., Mehdizadeh L., 2016. Essential oil and antifungal therapy. In: *Recent Trends in Antifungal Agents and Antifungal Therapy* (A. Basak, R. Chakraborty and S.M. Mandal, eds.), *New Delhi, Springer India*, 29–74.

Nazzaro F., Fratianni F., Coppola R., Feo V.D., 2017. Essential oils and antifungal activity. *Pharmaceuticals* 10: 86. https://doi.org/10.3390/ph10040086

Notte A.-M., Plaza V., Marambio-Alvarado B., Olivares-Urbina L., Poblete-Morales M., … Castillo L., 2021. Molecular identification and characterization of *Botrytis cinerea* associated to the endemic flora of semi-desert climate in Chile. *Current Research in Microbial Sciences* 2: 100049. https://doi.org/10.1016/j.crmicr.2021.100049

Nunes M.R., Agostinetto L., Da Rosa C.G., Sganzerla W.G., Pires M.F., … Zinger F.D., 2024. Application of nanoparticles entrapped orange essential oil to inhibit the incidence of phytopathogenic fungi during storage of agroecological maize seeds. *Food Research International* 175: 113738. https://doi.org/10.1016/j.foodres.2023.113738

Orozco-Mosqueda Ma.D.C., Kumar A., Fadiji A.E., Babalola O.O., Puopolo G., Santoyo G., 2023. Agroecological management of the grey mold fungus *Botrytis cinerea* by Plant Growth-Promoting Bacteria. *Plants* 12: 637. https://doi.org/10.3390/plants12030637

Oumzil H., Ghoulami S., Rhajaoui M., Ilidrissi A., Fkih-Tetouani S., … Benjouad A., 2002. Antibacterial and antifungal activity of essential oils of *Mentha suaveolens*. *Phytotherapy Research* 16: 727–731. https://doi.org/10.1002/ptr.1045

Parikh L., Agindotan B.O., Burrows M.E., 2021. Antifungal activity of plant-derived essential oils on pathogens of pulse crops. *Plant Disease* 105: 1692–1701. https://doi.org/10.1094/PDIS-06-20-1401-RE

Pinto L., Bonifacio M.A., De Giglio E., Cometa S., Logrieco A.F., Baruzzi F., 2020. Unravelling the antifungal effect of red Thyme oil (*Thymus vulgaris* L.) Compounds in vapor phase. *Molecules* 25: 4761. https://doi.org/10.3390/molecules25204761

Ramezani H., Singh H.P., Batish D.R., Kohli R.K., 2002. Antifungal activity of the volatile oil of *Eucalyptus citriodora*. *Fitoterapia* 73: 261–262. https://doi.org/10.1016/S0367-326X(02)00065-5

Ritz C., Baty F., Streibig J.C., Gerhard D., 2015. Dose-response analysis using R. *PLOS ONE* (Y. Xia, ed.) 10: e0146021. https://doi.org/10.1371/journal.pone.0146021

Šernaitė L., Rasiukevičiūtė N., Valiuškaitė A., 2020. The extracts of Cinnamon and Clove as potential biofungicides against strawberry Grey Mold. *Plants* 9: 613. https://doi.org/10.3390/plants9050613

Shao W., Zhao Y., Ma Z., 2021. Advances in understanding fungicide resistance in *Botrytis cinerea* in China. *Phytopathology*® 111: 455–463. https://doi.org/10.1094/PHYTO-07-20-0313-IA

Singh K., Deepa N., Chauhan S., Tandon S., Verma R.S., Singh A., 2024. Antifungal action of 1,8 cineole, a major component of *Eucalyptus globulus* essential oil against *Alternaria tenuissima* via overproduction of reactive oxygen species and downregulation of virulence and ergosterol biosynthetic genes. *Industrial Crops and Products* 214: 118580. https://doi.org/10.1016/j.indcrop.2024.118580

Singh P., Pandey A.K., 2018. Prospective of essential oils of the *Genus Mentha* as biopesticides: A Review. *Frontiers in Plant Science* 9: 1295. https://doi.org/10.3389/fpls.2018.01295

Sivropoulou A., Papanikolaou E., Nikolaou C., Kokkini S., Lanaras T., Arsenakis M., 1996. Antimicrobial and cytotoxic activities of *Origanum* Essential Oils. *Journal of Agricultural and Food Chemistry* 44: 1202–1205. https://doi.org/10.1021/jf950540t

Soylu E.M., Kurt Ş., Soylu S., 2010. *In vitro* and *in vivo* antifungal activities of the essential oils of various plants against tomato grey mold disease agent *Botrytis cinerea*. *International Journal of Food Microbiology* 143: 183–189. https://doi.org/10.1016/j.ijfoodmicro.2010.08.015

Stoyanova A., Georgiev E., Kula J., Majda T., 2005. Chemical composition of the essential oil of *Mentha pulegium* L. from Bulgaria. *Journal of Essential Oil Research* 17: 475–476. https://doi.org/10.1080/10412905.2005.9698968

Tang X., Shao Y.-L., Tang Y.-J., Zhou W.-W., 2018. Antifungal activity of essential oil compounds (Geraniol and Citral) and inhibitory mechanisms on grain pathogens (*Aspergillus flavus* and *Aspergillus ochraceus*). *Molecules* 23: 2108. https://doi.org/10.3390/molecules23092108

Tripathi P., Dubey N.K., Shukla A.K., 2008. Use of some essential oils as post-harvest botanical fungicides in the management of grey mold of grapes caused by *Botrytis cinerea*. *World Journal of Microbiology and Biotechnology* 24: 39–46. https://doi.org/10.1007/s11274-007-9435-2

Walter M., Jaspers M.V., Eade K., Frampton C.M., Stewart A., 2001. Control of *Botrytis cinerea* in grape using thyme oil. *Australasian Plant Pathology* 30: 21–25. https://doi.org/10.1071/AP0059

Wike N.Y., Olaniyan O.T., Adetunji C.O., Adetunji J.B., Akinbo O., ... Yerima M.B., 2024. Stability of essential oil during different types of food processing and storage and their role in postharvest management of fruits and vegetables. In: *Applications of Essential Oils in the Food Industry*, *Elsevier*, 281–284.

Williamson B., Tudzynski B., Tudzynski P., Van Kan J.A.L., 2007. *Botrytis cinerea*: the cause of grey mold disease. *Molecular Plant Pathology* 8: 561–580. https://doi.org/10.1111/j.1364-3703.2007.00417.x

Xu W.-T., Huang K.-L., Guo F., Qu W., Yang J.-J., ... Luo Y.-B., 2007. Postharvest grapefruit seed extract and chitosan treatments of table grapes to control *Botrytis cinerea*. *Postharvest Biology and Technology* 46: 86–94. https://doi.org/10.1016/j.postharvbio.2007.03.019

Xueuan R., Dandan S., Zhuo L., Qingjun K., 2018. Effect of mint oil against *Botrytis cinerea* on table grapes and its possible mechanism of action. *European Journal of Plant Pathology* 151: 321–328. https://doi.org/10.1007/s10658-017-1375-6

Yang F., Mi J., Huang F., Pienpinijtham P., Guo Y., ... Xie Y., 2022. Trans-cinnamaldehyde inhibits *Penicillium italicum* by damaging mitochondria and inducing apoptosis mechanisms. *Food Science and Human Wellness* 11: 975–981. https://doi.org/10.1016/j.fshw.2022.03.022

Yilmaz A, Ermis E, Boyraz N, 2016. AFL_Investigation of *in vitro* and *in vivo* anti fungal activities of different plan. *Journal of Food Safety and Food Quality* 122–131. https://doi.org/10.2376/0003-925X-67-122

Yu L., Qiao N., Zhao J., Zhang H., Tian F., ... Chen W., 2020. Postharvest control of *Penicillium expansum* in fruits: A review. *Food Bioscience* 36: 100633. https://doi.org/10.1016/j.fbio.2020.100633

Zhang J., Ma S., Du S., Chen S., Sun H., 2019. Antifungal activity of thymol and carvacrol against postharvest pathogens *Botrytis cinerea*. *Journal of Food Science and Technology* 56: 2611–2620. https://doi.org/10.1007/s13197-019-03747-0

Zhao Y., Yang Y.-H., Ye M., Wang K.-B., Fan L.-M., Su F.-W., 2021. Chemical composition and antifungal activity of essential oil from *Origanum vulgare* against *Botrytis cinerea*. *Food Chemistry* 365: 130506. https://doi.org/10.1016/j.foodchem.2021.130506

Phytopathologia Mediterranea
The international journal of the
Mediterranean Phytopathological Union

Firenze University Press
www.fupress.com/pm

Research Papers

Microbiota dynamic communities in sweet orange infected by "huanglongbing" in Iran

Shiva SAFARPOUR KAPOURCHALI[1], Mojdeh MALEKI[2,*], Ali ALIZADEH ALIABADI[3,*], Saeideh RAJAEI[4], Mohammad MEHDI FAGHIHI[5], Mehdi NASR ESFAHANI[6]

[1] *Department of Plant Protection, Islamic Azad University, Varamin, Pishva Branch, Varamin, Iran*
[2] *Department of Plant Pathology, Islamic Azad University, Varamin, Pishva Branch, Varamin, Iran*
[3] *Iranian Research Institute of Plant Protection, AREEO, Tehran, Iran*
[4] *The National Institute of Genetic Engineering and Biotechnology, NIGEB, Tehran, Iran*
[5] *Plant Protection Research Department, Fars Agricultural and Natural Resources Research and Education Center, AREEO, Zarghan, Iran*
[6] *Plant Protection Research Department, Isfahan Agricultural and Natural Resources Research and Education Center, AREEO, Isfahan, Iran*
*Corresponding authors. E-mail: mojdehmaleki@yahoo.com; aalizadeh1340@yahoo.com

Summary. "Huanglongbing"-(HLB) or citrus-greening is one of the most serious citrus diseases worldwide. This study aimed to investigate the bacterial-communities associated with HLB-symptomatic sweet orange trees (*Citrus sinensis*) from different geographical regions in southern Iran. The 16S rRNA gene amplicon metagenomics sequencing of DNA extracted from the midrib and petiole tissues of symptomatic plants confirmed that the '*Candidatus* Liberibacter asiaticus', was spread along the citrus-plantation regions in southern Iran, including Kerman, Sistan and Baluchistan, Fars, Hormozgan, and Khuzestan Provinces. The frequency of Operational Taxonomic Units (OTUs) related to '*Ca.* L. asiaticus' was remarkable in the HLB symptomatic tree in the Fars region. No OTUs of '*Ca.* Liberibacter' or '*Ca.* Phytoplasma' were detected in the asymptomatic samples in the Kerman region. However, in asymptomatic materials representatives of the class Bacilli, including *Lactobacillus* spp. and *Bacillus* spp., showed 12- and 4-fold presence compared to the symptomatic samples of Kerman groves. Furthermore, the presence of OTUs belonging to '*Ca.* L. europaeus' and '*Ca.* Phytoplasma aurantifolia' was detected in sweet oranges. The simultaneous occurrence of '*Ca.* L. asiaticus', '*Ca.* L. europaeus', and '*Ca.* P. aurantifolia' in HLB symptomatic orange trees in the Fars groves provided worthwhile insights for further research, although their epidemiological role in co-infections remains unknown. Microbial dataset in relation to variables associated with the plant health, defense, and disease helps to understand how these variables shape the citrus microbial community and identify individual that play a role in HLB suppression or promotion.

Keywords. '*Candidatus* Liberibacter' species, plant microbiota, Valencia sweet orange.

OPEN ACCESS

Citation: Safarpour Kapourchali, S., Maleki, M., Alizadeh Aliabadi, A., Rajaei, S., Faghihi, M. M. & Nasr Esfahani, M. (2025). Microbiota dynamic communities in sweet orange infected by "huanglongbing" in Iran. *Phytopathologia Mediterranea* 64(1): 129-143. doi: 10.36253/phyto-15662

Accepted: April 28, 2025

Published: May 15, 2025

Data Availability Statement: All relevant data are within the paper and its Supporting Information files.

Competing Interests: The Author(s) declare(s) no conflict of interest.

Editor: Assunta Bertaccini, Alma Mater Studiorum, University of Bologna, Italy.

ORCID:
SSK: 0009-0006-6434-5608
MM: 0000-0001-5355-8049
AAA: 0000-0003-0636-7674

INTRODUCTION

Citrus fruits are economically significant crops for Iran. They are grown in two commercial citrus-growing areas, including the Caspian Sea belt (Mazandaran and Guilan provinces) and the southern inland belt scattered through the low valleys of the Southern Zagros mountain range, particularly in the provinces of Fars, Kerman, Hormozgan and Khuzestan. Statistics show that Iran is the world's seventh-largest citrus fruit producer and ranks eighth in farmland under citrus fruit cultivation (Cochran and Samadi, 1976).

"Huanglongbing" (HLB), previously known as citrus greening, is the most devastating disease of citrus worldwide which is associated with three phloem limited Gram-negative α-proteobacteria, '*Candidatus* Liberibacter asiaticus', '*Ca*. L. africanus', and '*Ca*. L. americanus' (Bove, 2006; Hu *et al*., 2011). Both '*Ca*. L. asiatisus' and '*Ca*. L. americanum' are transmitted by the Asian citrus psyllid, *Diaphorina citri* Kuwayama (Sternorrhyncha, Liviidae), while '*Ca*. L. africanus' is transmitted by the African citrus psyllid *Trioza erytreae* Del Guercio (Sternorrhyncha, Triozidae). HLB-infected trees show different symptoms including blotchy mottle and corky vein in leaves, defoliation, yellowing and die back as well as small misshapen fruits, with color inversion (Bendix and Lewis, 2018; da Graça, 2008). The disease results in phloem malfunction, root decline, and altered plant source-sink relationships, leading to a deficient plant with minimal yield before it dies (Limayem *et al*., 2024). HLB disease, in Florida alone, has caused $7 billion in crop losses and over 8,000 jobs lost in a 7-year period (2007–2014) (Hodges *et al*., 2017). HLB disease was first observed in China in the late 19th century and was called "huanglongbing" (which means yellow dragon tail). Then after, in 1928, it was noticed in South Africa and called greening and was also reported from other Asian and African countries. Until 2004, it was reported in orange trees (*Citrus sinensis*) in Brazil and a year later on pomelo trees (*Citrus maxima*) in Florida (Filho *et al*., 2004; Halbert, 2005).

In Iran, *D. citri* was first observed in 1997 in an area close to the Pakistan border, and since then, high populations of the insect have been reported frequently in citrus plantations of Hormozgan and Kerman Provinces suggesting the possible presence of '*Ca*. L. asiaticus' that was detected and confirmed in various locations of Sistan-Baluchistan and Hormozgan Provinces in Valencia sweet orange trees (*C. sinensis*) and over 50 psyllid samples (Faghihi *et al*., 2009). The Asian HLB bacterium has been detected in citrus growing areas in southern Iran in Sistan and Baluchistan, Kerman, Hormozgan, and Fars Provinces and its presence has been confirmed employing DNA-based methods (Faghihi *et al*., 2009; Mohkami *et al*., 2011; Salehi *et al*., 2012, Faghihi *et al*., 2016; Salehi and Rasoulpour, 2016). The disease is one of the agents associated with citrus decline in some areas of southern Iran, such as mandarin decline in Siyahoo in Hormozgan Province of Iran (Faghihi, 2018; Alizadeh *et al*., 2022). Since 2010, almost 10% of losses have emerged in citrus cultivated trees belonging to different citrus species in various groves of Kerman Province, Iran (Passera *et al*., 2018). Moreover, emergence and spread of the citrus HLB indicating that the disease expanded and spread in citrus cultivation areas in the south parts of Iran with a gradual slope in the recent years. The reduction of the disease-carrying psyllid population seems to be effective in slowing down the spread of the disease accordingly (Alizadeh *et al*., 2020).

So far, no definitive treatment for HLB has been identified. The only way to grow high-yielding citrus where the disease is prevalent is to manage it using integrated management strategies. These include obtaining healthy seedlings from infection-free nurseries to prevent the spread of infection to trees in uninfected areas; focusing on reducing the initial source of infection by removing infected trees or branches, and controlling vectors and keeping the pest population at the lowest possible level. However, one of the most effective ways to manage this disease is to find cultivars that have a high degree of resistance to HLB. Safarpour *et al*. (2022) evaluated the response of seedlings of ten Iranian commercial citrus cultivars inoculated with '*Ca*. L. asiaticus' using conventional grafting. In this regard, the cultivar Mexican lime was the most tolerant, while Valencia orange and Orlando tangelo were the most susceptible ones to HLB.

The symptoms of HLB have been related by callose accumulation and depositions in the phloem sieve plates as a mechanism of defense against invasive tissue pathogens that inhibit nutrient uptake and transport (Bendix and Lewis, 2018). Phloem-limited pathogens represent a significant research challenge because they are difficult to detect within plants and induce disease symptoms to develop and emerge slowly in infected plants

Recent developments in high-throughput DNA sequencing technology have opened new ways to investigate plant-associated microbial communities in the '*Ca*. L. asiaticus' infected trees (Zhang *et al*., 2017; Tedersoo *et al*., 2019). Plant phyllosphere hosts a variety of bacteria which can play a positive role in the performance of the host plant. These bacterial communities are influenced by both biotic (host species, genotype, pathogens, and leaf age) and abiotic (mainly related to geographical location) factors that can play significant roles in plant growth and disease resistance. The study of plant-associated microbial

communities may result in identification of synergistic and antagonistic agents against pathogens from a similar niche (Bodenhausen *et al*., 2013; Monazzah *et al*., 2022).

Recent research on the citrus microbiome has established a foundation of data concerning the rhizosphere- or leaf-associated microbes in citrus plants affected by HLB (Blaustein *et al*., 2017; Trivedi *et al*., 2010; Zhang *et al*., 2017; Xu *et al*., 2018). Blaustein *et al*. (2017) proposed that the diversity of bacterial communities within leaf tissues diminishes as HLB symptoms progress and that the relative abundance of '*Ca*. Liberibacter' species exhibited a negative correlation with the α-diversity of the bacterial community in leaf tissues. They also anticipated adverse interactions between '*Ca*. Liberibacter' species and specific bacterial families found within the native leaf bacteriome of citrus, which could extend to the entire tree level.

Research on microbiota dynamics in sweet oranges infected with HLB (exhibiting decline symptoms) indicated that the families *Micrococcaeae*, *Gemellaceae*, and *Streptococcaeae* were significantly prevalent in asymptomatic trees compared to those displaying symptoms, while the families *Coriobacteriaceae*, *Lachnospiraceae*, *Ruminococcaceae*, *Erysipelotrichaceae*, and *Desulfovibrionaceae* showed a markedly higher abundance in symptomatic trees in comparison to the asymptomatic ones (Passera *et al*., 2018).

Today, a few studies have been conducted in terms of the microbial communities associated with citrus HLB for managing the disease in Iran. Therefore, given the importance of this disease in citrus orchards in Iran and its increasing spread, this study aimed to investigate the bacterial communities of midribs and petiole tissues of HLB symptomatic orange (*C. sinensis*) trees from five major groves located in different geographical regions in southern Iran including Kerman, Sistan and Baluchistan, Fars, Hormozgan, and Khuzestan Provinces, so that the management strategy and breeding programs can be planned accordingly. Moreover, there is a critical need to analyze and characterize the bacterial communities in HLB-affected citrus trees using 16S rRNA gene amplicon sequencing and to explore the presence of co-infecting and or co-existing bacterial taxa, including potential pathogenic or beneficial bacteria.

MATERIALS AND METHOD

Plant samples collection

Sampling methods are critical for the detection, identification, and quantification of '*Ca*. Liberibacter' species since their distribution in host plants can be irregular. Sweet orange trees infected may have symptomatic leaves only on some branches and others may remain free of symptoms or have low bacterial concentration. In the initial phase of the study, in October 2017, totally 75 leaf samples of Valencia sweet orange (*C. sinensis*) trees exhibiting symptoms of the HLB disease were collected from orchards located in the provinces of Fars (Darab), Hormozgan (Rudan), Kerman (Jiroft), Sistan and Baluchestan (Sarbaz), and Khuzestan (Dezful). Subsequently, the presence of infection was confirmed by PCR assay for '*Ca*. L. asiaticus', and the infected trees were identified in each region. Following the identification of the infected trees, composite leaf sampling was taken from three infected orange trees in each area in December 2017. Additionally, a composite leaf sample was obtained from three healthy orange trees (confirmed by PCR and quantitative PCR) located in Kerman Province. The trees targeted for sampling were almost at the same age and growing stage. In total, five composite leaf samples were collected from infected trees across the mentioned provinces (Suppl. Table 1), along with one composite leaf sample from healthy trees in Kerman Province (Figure 1). The leaf samples were placed in separated bags and transferred to the laboratory under cold conditions.

Plant samples preparation

The preparation of the midrib and petiole tissues was done after a proper surface sterilization to strictly ensure that only endophytic bacterial communities were present. Thus, the collected midrib and petiole tissues were surface sterilized separately. The related segments (approx. 60 mm long) were washed in mild liquid soap solution and rinsed thoroughly with running tap water. Surface sterilization was achieved by sequentially submerging each segment in 70% ethanol for 1 min and 0.625% sodium hypochlorite (10% Clorox, the Clorox Company, Oakland, CA, USA) solution for 4 min, followed by 3 sequential immersions in sterile distilled water. Surface sterilization was verified by pressing disinfected midrib and petiole segments along with aliquots of the sterile distilled water used in the final rinse. For more confidence, again the midrib and petiole tissues were rinsed five times in sterile distilled water and allowed to drain. Then, the related midribs and petioles were cut into small pieces and were flash-frozen accordingly.

DNA extraction, PCR amplification, and microbiome sequencing

The surface sterilized flash-frozen tissues of the collected symptomatic and asymptomatic tree samples were

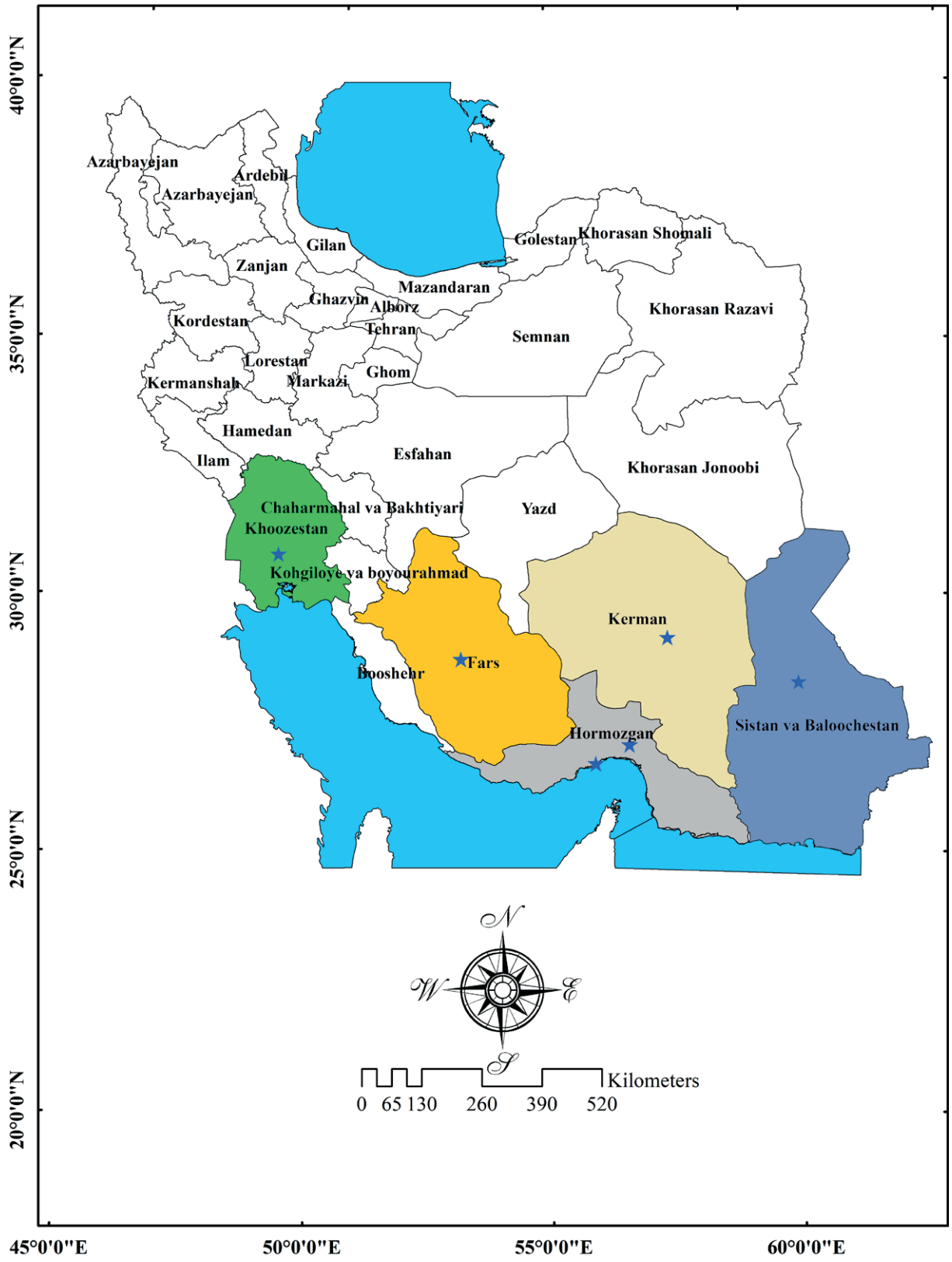

Figure 1. The geographical location of the sampling areas in the provinces of Fars, Hormozgan, Kerman, Khuzestan and Sistan & Baluchistan in southern Iran.

ground separately with sterile pestle and to ensure that the data only reflected endophytic or phloem-associated bacterial communities. Genomic DNA was extracted from 0.5 g of petioles and midribs using the DENAzist Plant DNA Isolation Kit (DENAzist, Iran) according to the manufacturer's instructions. The quantity and purity of total DNA was evaluated using a NanoDrop™ 2000/2000c Spectrophotometers (Thermo Fisher Scientific).

The identity of the HLB-associated bacterium was confirmed through PCR amplification of a specific fragment of the ribosomal protein *rplKAJL rpoBC* gene of '*Ca.* L. asiticus' using the primer pair A2/J5 (Villechanoux *et al*., 1993; Hocquellet *et al*., 1999). The DNA extracted from leaves of healthy sweet orange trees and sterile distilled water were used as negative controls. PCR was conducted in 20 µL of reaction mixture containing 10 µL 2X PCR Master Mix (Ampliqon, Denmark), 1 µL of each primer (10 µM), 1–2 µL of template DNA (ca. 100 ng) and 6 µL sterile distilled water. The thermocycling program included an initial denaturation step at 95°C for 4 min, succeeded by 35 cycles comprising denaturation at 94°C for 30 s, annealing at 59°C for 30 s and extension at 72°C for 60 s, with a final extension step at 72°C for 10 min. Two PCR products were directly sequenced in both directions. The sequences were compared with GenBank sequences using BLAST search (https://blast.ncbi.nlm.nih.gov/Blast.cgi) to identify and confirm the identity of '*Ca.* L. asiaticus'.

It was designed a custom set of 10-base pair indices specifically tailored for the preparation of libraries from amplicons derived from the V3-V4 region of the 16S rRNA gene for the analysis of the microbial composition through sequencing on the Illumina MiSeq and HiSeq platforms. The 16S rRNA gene sequencing (V3-V4 region) was used to identify bacterial taxa to capture bacterial diversity.

Amplicon libraries were prepared for the V3–V4 region of 16S rRNA genes with PCRs that incorporated Illumina-compatible universal bacteria/archaeal primers, 341F and 805R (Klindworth *et al*., 2013). Amplicon libraries were sequenced using a MiSeq sequencer (Microsynth AG, Switzerland). This analysis was based on data obtained from 16S rRNA metagenomic sequencing conducted on the Illumina MiSeq and HiSeq sequencing platforms.

Data availability

Raw sequencing reads were deposited in the NCBI's Sequence Read Archive under the accession number PRJNA578610 (SRX7033691-5).

Data analysis

The obtained forward and reverse DNA reads were analyzed using the QIIME v.1.8. pipeline (Bolyen *et al*., 2019). The reads were processed with Cutadapt (https://github.com/marcelm/cutadapt) and Sickle (https://github.com/najoshi/sickle) to remove residual Illumina adapters and primer sequences, truncate the sequences at the first N position, and trim the sequences at a base pair with a PHRED score below 30. The paired-end reads were joined using Eautils (https://github.com/ExpressionAnalysis/ea-utils) with the requirements of a minimum overlap of 30 bp and a 3% maximum difference in the overlap region. The names of the samples were added to the definition lines of the sequencing reads using the sed command and concatenated into one FASTA file to make them compatible for analysis in QIIME v.1.8. OTU clustering was performed at the 97% similarity threshold in QIIME, and taxonomy assignments were made by mapping to the Silva reference database version 132 limited to bacterial taxa (Swisher *et al*., 2018). In this study, the OTU clustering and taxonomic assignment are limited to bacterial taxa analysis to avoid broader microbial communities.

Unassigned OTUs and those identified as mitochondrial or plastid DNA were removed from further analyses. The total counts of OTUs and assigned taxa for each taxonomic rank were transformed to relative abundance values. The microbial communities' structure was analyzed with Phyloseq and plotted with ggplot2 in R v.3.2.1. (Wickham, 2016; Warnes *et al*., 2020).

Phylogenetic analysis of identified 'Ca. Liberibacter' species

The evolutionary analyses of the identified '*Ca.* Liberibacter' species were conducted in MEGA X (Kumar *et al*., 2018). The 420 bp partial sequences of 16S rDNA fragments belonging to the three identified '*Ca.* Liberibacter' species were aligned with strains from GenBank, and phylogenetic analysis was performed using maximum likelihood methodology coupled with the Tamura-Nei model (Tamura and Nei, 1993) and 1000 replicates of the bootstrap for the statistical support of evolutionary branch lengths.

RESULTS

PCR detection of 'Ca. L. asiaticus'

DNA extracted from the leaf midribs of symptomatic and asymptomatic sweet orange trees were tested

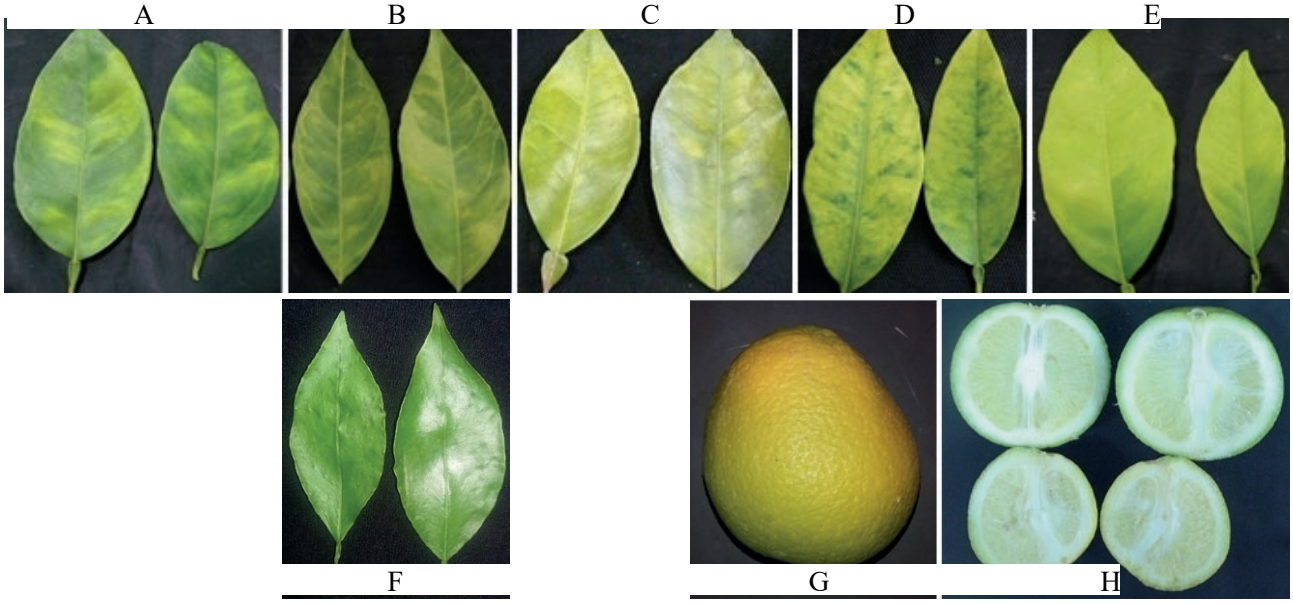

Figure 2. The "huanglongbing" symptoms in sweet orange (*Citrus sinensis*) including blotchy mottle of leaves with yellow discolorations emerging in asymmetric patterns relative to the central vein for A: Khuzestan, B: Kerman, C: Hormozgan, D: Fars, E: Sistan and Baluchistan, and F: Asymptomatic leaves from Kerman, G: Misshaping and color inversion in the fruit of HLB infected trees; the bottom of the fruit remains green, H: Misshaping and asymmetrical fruits sectioned.

for the presence of '*Ca*. L. asiaticus' by PCR using primer pair A2/J5. Amplicons of approximately 700 bp of the ribosomal protein *rplKAJL rpoBC* gene were obtained from all symptomatic but not from symptomless trees. Two PCR amplicons were directly sequenced and edited. The sequences were 100% identical to each other, and the BLAST analysis confirmed that the nucleotide sequences of the fragments exhibited 100% identity with the corresponding sequences from strains of '*Ca*. L. asiaticus' available in the NCBI database (GenBank accession numbers AP014595, CP145497, KP210461). The infected trees showed symptoms of blotchy mottle, yellowing shoot, as well as small misshapen fruits, usually with color inversion (Figure 1).

OTU clustering and beta diversity

After removing the residual contaminant sequences from the quality-filtered libraries, 91 bacterial OTUs were obtained, including 1332 assigned reads (Suppl. Table 2, Figure 6). A number of 975, 137, 131, 55, 42, and 10 OTUs were identified from the surface-sterilized midrib and petiole tissue samples of Fars, Khuzestan, Hormozgan, Kerman (symptomatic), Kerman (asymptomatic), and Sistan and Baluchistan Provinces, respectively. These results indicate significantly reduced OTUs in average relative abundance in Khuzestan (7.11), Hormozgan (7.44) and Sistan and Baluchistan (17.72) provinces compared to the Far Province with the highest OTUs of 975.

The microbial community distances (beta diversity) of the samples is depicted in Figure 3. Concerning the OTU-level PCoA (principal coordinates analysis) based on Bray-Curtis distances, the bacterial community structures of the five provinces differed from each other. Nonetheless, both samples including the infected (symptomatic) and non-infected (asymptomatic) samples from Kerman Province clustered together (Figure 3). PCo1 and PCo2 explained 30% and 24% of the variation in bacterial OTUs, respectively.

Microbial community structures of individual samples

The taxonomic distribution revealed that *Alphaproteobacteria* were the prevalent class in the Fars samples bacterial communities, accounting for 75.3% of all the detected taxa. Other well-represented phyla included 17.74% Bacilli, 2.36% Gamma-proteobacteria, 1.64% Mollicutes, 0.72% Bacteroidetes, 0.31% Clostridia, and 0.1% Actinobacteria (Suppl. Table 2, Figure 6). Similar trends are observed here, as seen in the OTU clustering and beta diversity analysis, indicating that Fars Province displays significantly different microbial community structure at the phylum and class level.

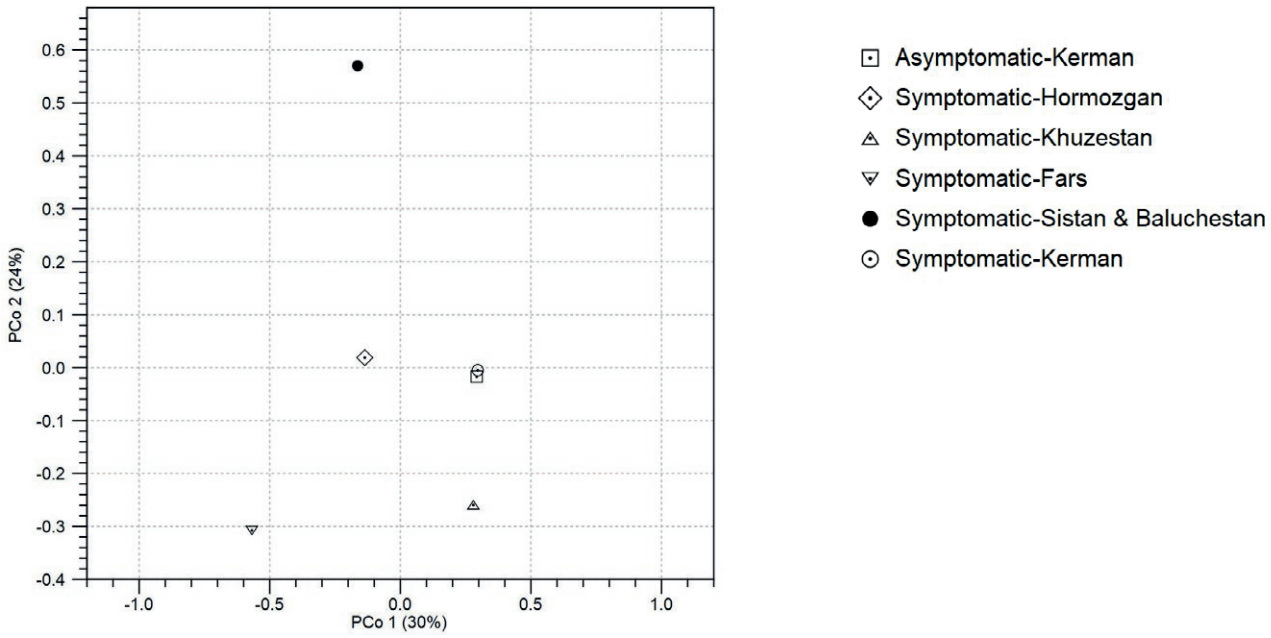

Figure 3. Principal component analysis of bacterial species based on OTUs. X-axis, first principal component; Y-axis, second principal component. Numbers between parentheses represent the contributions of the principal components to differences among the samples. This plot was made with ade4 package (v3.1.1).

Overall, 75% of the microbial communities of the Fars samples were constituted mostly by '*Ca*. Liberibacter' and 15.48% by *Staphylococcus* genera (Suppl. Table 2, all, 75% of the Figure 6). Furthermore, the most prevalent bacterial taxa in this region may not be the species with significant potential for inhibiting the colonization of '*Ca*. L. asiaticus' particularly in relation to its impact on disease outcomes.

The presence of '*Ca*. L. asiaticus' was confirmed not only in the Fars samples, but also in the other four symptomatic samples (Suppl. Table 2, Figure 6). Moreover, with the clustering of the OTUs at the 97% similarity threshold, two different OTUs were identified for '*Ca*. L. asiaticus', presenting an evolutionary distance in the phylogenetic tree, as shown in Figure 4. With respect to the clustering of the OTUs at the 97% similarity threshold, '*Ca*. Liberibacter europaeus' was detected in the symptomatic Fars samples. Moreover, the NCBI nucleotide blast of the 420 bp partial 16S sequenced rDNA fragment and the phylogenetic tree confirmed the similarity of the identified OTU to the reported '*Ca*. L. europaeus' database (GenBank accession numbers JX629241, JX244259, MN176610) (Figure 4). Further, '*Candidatus* Phytoplasma aurantifolia = citri' was detected in the microbial communities of the Fars samples. Multiple factors may play a role in simultaneous occurrence and development of '*Ca*. L. europaeus' alongside other species, including '*Ca*. P. aurantifolia' in this Province.

In general, the 16S amplicon metagenomic sequencing of DNA extracted from midrib and petiole tissues verified the presence of '*Ca* L. asiaticus' in all five composite samples collected from the symptomatic sweet orange trees. No OTU of '*Ca*. Liberibacter' and '*Ca*. Phytoplasma' were found in the asymptomatic samples obtained from the Kerman groves.

The microbial communities of samples from Khuzestan Province consisted of 51.43% *Actinobacteria*, 17.14% *Alphaproteobacteria*, 14.29% *Clostridia*, 10% *Bacteroidia*, 5% *Gamma-proteobacteria*, and 2.14% *Negativicutes*. Among *Actinobacteria*, OTU belonging to *Leifsonia kafniensis* had the highest abundance in the microbial communities. In this region, the predominant bacterial taxa, especially *L. kafniensis*, along with other potentially relevant bacterial species, may play a significant role in influencing disease outcomes. This influence could be attributed to their ability to inhibit the colonization of '*Ca*. L. asiaticus', which may explain the reduced incidence of this pathogen.

The bacterial communities of midrib and petiole tissues in the Sistan and Baluchistan samples contained 60% *Gamma-proteobacteria* and 40% *Alphaproteobacteria*. In this region, the most abundant bacterial taxa, *Gamma-proteobacteria* and *Alphaproteobacteria* may not be to that extent as the potentially relevant bacteria which could be influencing the disease outcomes by promoting or inhibiting '*Ca*. L. asiaticus' colonization.

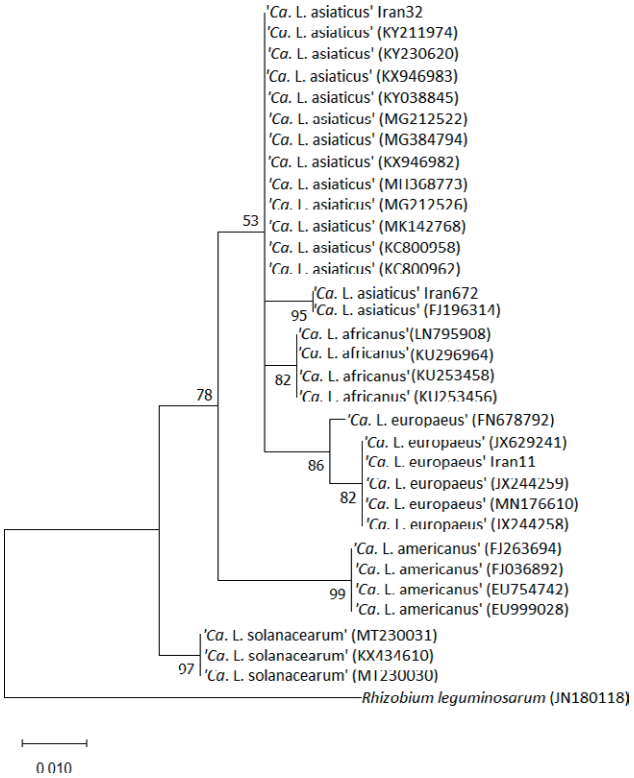

Figure 4. The phylogenetic comparison tree generated from the alignment of partial 16S rDNA sequences of '*Ca.* Liberibacter' species in the infected Valencia sweet orange in Iran with selected strains from GenBank. The evolutionary analyses were inferred by using the maximum likelihood method and the Tamura-Nei model that were conducted in MEGA X. *Rhizobium leguminosarum* was added as an outgroup. Bootstrap values (1000 replications) are shown at the nodes.

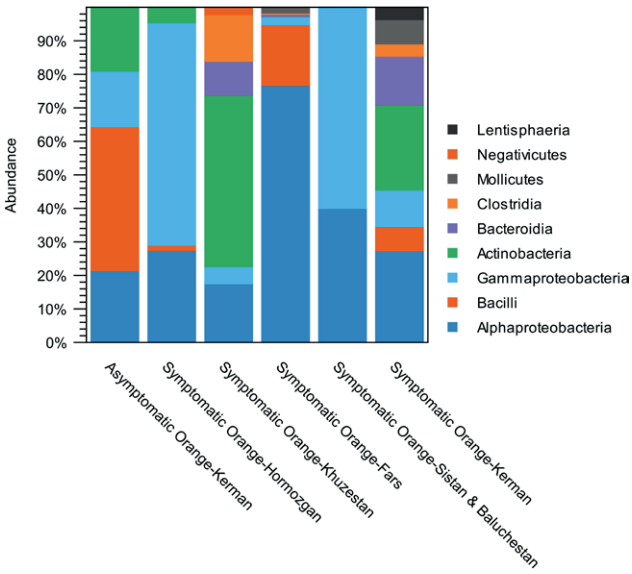

Figure 5. The stacked bar chart of the microbial communities at the phylum and class levels for orange (*Citrus sinensis*) midrib and petiole tissues.

The midrib and petiole bacterial of the Kerman Province samples comprised 26.79% *Actinobacteria*, 26.79% *Alphaproteobacteria*, 14.3% *Bacteroidia*, 10.71% *Gamma-proteobacteria*, 7.14% *Bacilli*, 7.14% *Mollicutes*, 3.57% *Clostridia*, and 3.57% *Lentisphaeria*. However, the uninfected samples from Kerman Province contained 42.86% *Bacilli*, 21.43% *Alphaproteobacteria*, 19% *Actinobacteria*, and 16.67% *Gamma-proteobacteria*. The presence of the most abundant bacterial taxa, 42.86% *Bacilli* in the uninfected samples in this region in comparison with infected ones indicates the potential of the relevant bacterial species such as *Bacillus* spp. could be influencing the disease outcomes by inhibiting '*Ca.* L. asiaticus' colonization.

An analysis of the bacterial community structure in symptomless samples from Kerman Province revealed a higher frequency of certain genera in comparison to symptomatic samples. The representatives of the class *Bacilli*, i.e. *Lactobacillus* spp. and *Bacillus* spp., in the symptomless sweet oranges in Kerman Province exhibited 12- and 4-fold changes compared to the infected samples from this province. These bacteria could be influencing the disease outcomes by inhibiting '*Ca.* L. asiaticus' colonization. It may be in interaction with the prevailing climatic condition in this particular region

The bacterial communities of midrib and petiole tissues in the Hormozgan samples contained 66.4% *Gamma-proteobacteria*, 27.4% *Alphaproteobacteria*, 4.6% *Actinobacteria*, and 1.5% *Bacilli*. Approximately, 20% of the bacterial communities of the samples were constituted mostly by '*Ca.* Liberibacter' species enclosing '*Ca.* L. europaeus' in the sweet orange tree samples. The diverse bacterial taxa present in this region may not significantly impact disease outcomes by either promoting or inhibiting the colonization of '*Ca.* L. asiaticus.'

DISCUSSION

In this study, microbial communities in the midrib and petiole tissues of HLB-infected sweet orange trees were investigated using 16S rRNA gene metagenomics sequencing. In previous report, the presence of '*Ca.* L. asiaticus' in sweet orange and other local varieties of citrus trees was described in Sistan and Baluchistan and Hormozgan provinces, Iran (Faghihi *et al.*, 2009). Both '*Ca.* L. asiaticus' and phytoplasmas were detected in HLB-infected citrus trees. The HLB-associated phytoplasma from this study was a member of peanut

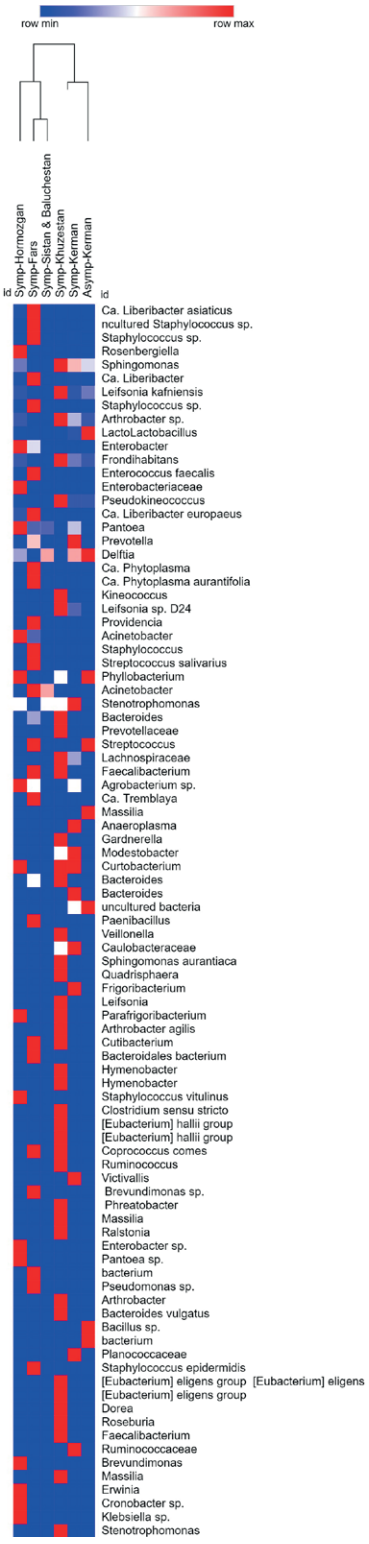

Figure 6. The microbiome heat map showing the core bacterial in the petiole and midrib tissues of oranges. The heat map depicts the differential abundance of microbial taxa among orange samples. Rows (microbial taxa at each level) and columns (samples) were ordered with hierarchical clustering.

witches' broom (16SrII) phytoplasma group. The results presented here not only confirmed that '*Ca*. L. asiaticus' is present in HLB disease under sampling groves in southern Iran, but also revealed that citrus midrib and petiole tissues could be colonized with a variety of bacteria. This variation could be defined as the influence of the geographical climatic parameters including temperature, precipitation and relative humidity percentage. This finding is in agreement with Camerota *et al*. (2012) and Daranas *et al*. (2019) in influence of the geographical climatic parameters and establishment of the biological control of bacterial plant diseases reported for *Lactobacillus plantarum* strains selected for their broad-spectrum activity (Montero Castillo *et al*., 2015).

It is plausible that the progression and development of the disease in orange trees varied at the time of sampling, and it may be related to variations in the microbial populations associated with each region. Research has indicated that the composition of endophytic bacteria during the initial phases of '*Ca*. L. asiaticus' infection differs from that observed in the later stages of the disease.

In this research, the highest identified microbial communities associated with the midrib and petiole tissues of HLB symptomatic sweet orange trees samples of Fars Province may stem from a variety of factors including disease development, vector activity, and climatic conditions. The various geographical regions of sample collection and the key climatic parameters such as average temperature, relative-humidity and the average annual precipitation in each region may be influenced the presence and distribution of the bacterial-communities associated with HLB-symptomatic orange-trees (Fitzpatrick *et al*., 2018; Grady *et al*., 2019). Moreover, the immune system, and interactions between microbes play a crucial role in shaping the structures of microbial communities (Naylor & Coleman-Derr, 2018).

The incidence and severity of the HLB disease may be affected by different geographical and climatic parameters in southern Iran. The disease is widespread in certain citrus-producing regions in the southern part of the country, notably in areas such as Jiroft (in orange) in Kerman Province and the Siyahoo region (in mandarin) in Hormozgan Province. In some orchards, the disease occurrence exceeds 50%, and even in these regions, orchards exposed to elevated levels of infection have been recorded.

The 16S amplicon metagenomics sequencing of DNA extracted from midrib and petiole tissues confirmed the presence of '*Ca*. L. asiaticus' in all the five composite samples taken from the symptomatic sweet orange trees. No OTU of '*Ca*. Liberibacter' and '*Ca*. Phytoplasma' was detected in the asymptomatic samples

belonging to the Kerman groves. There was an overall increase in the bacterial richness in the symptomatic Fars samples, mostly belonging to the class alpha-proteobacteria, especially '*Ca*. L. asiaticus' species. The relative abundance of this bacterium in the Fars samples was 75% of the total identified OTUs, in agreement with the intensity of infection in the samples. The relative abundances of '*Ca*. L. asiaticus' in Sistan and Baluchistan, Kerman, and Khuzestan provinces were 40, 3.5, and 0.7%, respectively.

With OTU clustering at the 97% similarity threshold, a '*Ca*. Liberibacter europaeus' was identified in the symptomatic Fars samples (0.9% relative abundance). Moreover, the NCBI nucleotide blast of the 420 bp partial 16S sequenced rDNA fragment and the phylogenetic tree confirmed the similarity of the identified OTU with those previously reported. This is the first report of '*Ca*. L. europaeus' in HLB-infected citrus (sweet orange) tree. This bacterium was first described in 2010 in asymptomatic pear trees in Italy (Raddadi *et al*., 2011). Nevertheless, it was also associated with mild symptoms when it was detected in Scotch broom shrub (*Cytisus scoparius*) in New Zealand (Thompson *et al*., 2013).

It is thought that '*Ca*. L. europaeus' possibly co-exist with '*Ca*. Phytoplasma' since both are found in the same vector, *Cacopsylla pyri* (Camerota *et al*., 2012). Interestingly, OTU of '*Candidatus* Phytoplasma' was also identified in the Fars samples. The simultaneous incidence of multiple pathogens has been commonly observed in the vascular tissues of a single plant (Križanac *et al*., 2010; Nicolaisen *et al*., 2011; Arratia-Castro *et al*., 2016; Satta *et al*., 2016; Swisher *et al*., 2018). Likewise, different species/strains of phytopathogens may be hosted by the same individual insect vector, possibly being transferred together to the host plant. Occasionally, insect vectors are infected with various pathogens through feeding a variety of host plant species (Križanac *et al*., 2010; Raddadi *et al*., 2011; Swisher *et al*., 2018). The bacterial communities of insect vectors include a complex network of bacteria which have a significant influence on the biology of hosts (Ahmed *et al*., 2009; Camerota *et al*., 2012). Polyphagy as the ability of insects to feed from a variety of plants possibly influences the chance of plants to be infected by different pathogens. Microbial interactions inside insect vectors are highly complicated. However, the study of such multipartite interactions can help to develop microbial-based control strategies (Crotti *et al*., 2012; Saldaña *et al*., 2017). The simultaneous occurrence of '*Ca*. P. aurantifolia=citri', '*Ca*. L. asiaticus', and '*Ca*. L. europaeus' in the Fars citrus plants and their epidemiological role remain unknown, although it provides insights for further research.

Genome analysis indicates that '*Ca*. L. asiaticus' lacks genes encoding some essential enzymes and other proteins, and relies on the presence of other microbiota within citrus phloem for its survival. Moreover, it is not cultured in axenic conditions and has only recently been successfully co-cultured within a microbial consortium, suggesting that its growth is likely highly reliant on associated microbial communities (Fujiwara *et al*., 2018).

Concerning other members of the orange bacterial communities, *Staphylococcus* spp., especially *S. epidermidis,* was detected as the second dominant microorganism in the Fars samples. *Staphylococci*, particularly *S. epidermidis*, are currently the most studied microorganisms due to their biofilm formation capacity. It has been suggested that phloem-limited phytopathogenic bacteria (e.g., '*Ca*. Phytoplasma' and '*Ca*. Liberibacter') depend on other phloem microbiota and phloem nutrients for the colonization of the plant host. It means that the biofilm formation of *Staphylococci* in host plants may facilitate the colonization of '*Ca*. Liberibacter'. However, mechanisms underlying such associations have not been well understood yet (Ahmed *et al*., 2009). Various reports have shown that the infection of citrus with HLB has a profound effect on the structure and composition of the citrus-associated bacterial communities (Fujiwara *et al*., 2018). The results of the current investigation open a new perspective for study on the function of plant bacterial communities on HLB synergistic and antagonistic agents. Co-infection with '*Ca*. Phytoplasma' provides a solid hypothesis about its role in HLB-infected trees. No OTUs of '*Ca*. Liberibacter' or '*Ca*. Phytoplasma' were identified in the asymptomatic samples from the Kerman region. The analysis of the bacterial community's composition in the asymptomatic (non-infected or healthy plant) samples from Kerman Province demonstrated that the frequency of certain genera, known as plant growth-promoting bacteria, was higher compared to the symptomatic samples. In this regard, the fold change of OTUs related to *Bacillus* spp. and *Lactobacillus* spp. in the non-infected samples from Kerman Province increased four and 12 times, respectively, compared to the symptomatic samples. *Bacillus* spp. and *Lactobacillus* spp. were previously identified from roots and leaves of '*Ca*. L. asiaticus'-infected or uninfected citrus trees (Ginnan *et al*., 2018). Nevertheless, the higher frequency of both genera in the asymptomatic tree suggested a possible role of the mentioned bacteria in strengthening the citrus tree bacterial communities against pathogens. Today, it has been proved that plant bacterial communities are involved in plant health aspects such as growth, nutrition, immunity, infection, and protection against diseases under biotic

and abiotic stresses (Vorholt, 2012; Mendes *et al*., 2013). *Lactobacillus* is a lactic acid bacterium with antagonistic activity. Generally, lactic acid bacteria produce antimicrobial compounds, inhibiting the growth of some bacterial species, and also, show antagonistic activities against some fungi (Daranas *et al*., 2019). It was mentioned earlier that biofilm-producing bacteria may have the ability to facilitate the colonization of phloem limited bacteria. It can be presumed that the antagonistic activity of *Lactobacillus* against certain groups like *Staphylococcus* spp. may indirectly control the phloem limited bacteria like '*Ca.* Liberibacter'. (Montero Castillo *et al*., 2015). It has been also demonstrated that treating citrus grafts and rootstocks with surfactin (SFC) of *Bacillus subtilis* indicated an effective antibacterial (eliminating or suppressing) activity against '*Ca*. L. asiaticus'. SFC can also interact with plant cells by stimulating the induction of systemic immune resistance (Yang *et al*., 2018).

Bacterial cells situated in close proximity may have the capacity to alter their microenvironment. The composition of the microbial community plays a crucial role in the ability of '*Ca*. L. asiaticus' to drive the progression of HLB. Other research groups have also documented the microbial diversity associated with HLBin planta. Certain plant growth-promoting bacteria, including *Bacillus* and *Burkholderia*, were identified in '*Ca*. L. asiaticus' free leaf samples. In contrast, bacteria like *Methylobacterium* and *Sphingobacterium* were found in root samples taken from trees affected by HLB (Trivedi *et al*., 2011).

Some microorganisms extracted from plant tissues demonstrate potential as biocontrol agents against phytopathogens, as well as the ability to enhance plant growth and development.

A higher prevalence of *Alcaligenaceae* has been observed in asymptomatic samples compared to symptomatic samples from '*Ca*. L. asiaticus' -infected citrus (Zhang *et al*., 2013). Some species may play a crucial role in mitigating the symptoms of HLB disease. Nevertheless, *Methylobacterium* was also identified in the root samples of citrus trees affected by HLB. The genus *Methylobacterium* was found to inhabit the xylem vessels of citrus plants, and the presence of abundant *Methylobacterium* species in citrus plants induces Citrus variegated chlorosis (CVC) disease through a synergistic interaction with *Xylella fastidiosa* (Araujo *et al*., 2002; Zhang *et al*., 2013). Consequently, the prevalence of the endophytic *Methylobacterium* may be linked to the HLB development.

Several additional factors may influence the population dynamics of plant endophytes. Even within a single plant species, the population density and concentration of endophytic bacteria may vary at various stages of disease progression.

It is plausible that the progression and development of the disease in orange trees varied at the time of sampling, and it may be related to variations in the microbial populations associated with each region. Research has indicated that the composition of endophytic bacteria during the initial phases of '*Ca*. L. asiaticus' infection differs from that observed in the later stages of the disease. For instance, the bacterial populations of *Methylobacterium* spp. and *Hymenobacter* spp. were found to be more abundant in the leaf communities of trees exhibiting low disease levels. Conversely, their relative abundances were significantly diminished during the later stages of the disease (Ginnan *et al*., 2020).

The three predominant bacterial phyla including Proteobacteria, Bacteroidetes, and Actinobacteria, showed pronounced alterations in their relative abundance within the leaf and stem tissues as the severity of the disease increased (Ginnan *et al*., 2020).

The genus *Massilia* was identified in the non-infected samples from Kerman province, which were described recently in highly diverse environments, and certain species exhibited *in vitro* attributes related to plant growth promotion, including IAA production, siderophore production, and antagonistic activity toward *Phytophthora infestans* (Ofek *et al*., 2012). In addition, here also the most abundant bacterial taxa *Lactobacillus* spp. and *Bacillus* spp. in this region may influence the disease outcomes by inhibiting '*Ca*. L. asiaticus' colonization (Ginnan *et al*., 2020).

A comprehensive comparison of the microbial communities among the different samples demonstrated that '*Ca.* Liberibacter' was present in all the symptomatic samples. Due to focusing only on midrib and petiole tissues in the current study, a high number of OTUs was not really expected, especially since the surfaces of the leaf samples were well washed and sterilized before DNA extraction. As demonstrated by PCoA analysis based on Bray-Curtis dissimilarity distances, the bacterial community's structures of the samples were different from each other. Nonetheless, the infected (symptomatic) and non-infected (asymptomatic) trees from Kerman Province clustered together, giving the impression that the geographical situation as significant abiotic factor has probably a substantial impact on the structure of the plant microbial communities.

The plant-associated microbiome is shaped by complex interactions between the plant host, microorganisms, and their surrounding environment.

A sustainable management strategy entails leveraging the citrus microbiome, as this microbial community is inherently compatible with the host plant. By occupying similar ecological niches as pathogens, the microbi-

ome can effectively bolster the overall health of the plant and its defense mechanisms.

Future research aimed at elucidating the mechanistic interactions between antagonistic microbes and '*Ca*. L. asiaticus' will facilitate the widespread implementation of sustainable management practices that utilize the microbiome to mitigate the progression of HLB disease.

CONCLUSIONS

This study aimed to investigate the bacterial communities of midribs and petiole tissues of HLB symptomatic orange (*C. sinensis*) trees from five major groves located in different geographical regions in southern Iran including Kerman, Sistan and Baluchistan, Fars, Hormozgan, and Khuzestan Provinces. Significant differences in the relative abundance of important bacterial species between HLB-infected sweet orange trees from different regions, highlight the impact of the geographic location on microbial community structure. The diverse geographical regions selected for sample collection, along with essential climatic factors including temperature, relative humidity, and average annual precipitation, significantly affected the presence and distribution of bacterial communities associated with HLB-symptomatic orange trees. This study marks the first detection of OTUs of '*Ca*. L. europaeus' in sweet orange in Iran. The concurrent presence of '*Ca*. L. asiaticus', '*Ca*. L. europaeus' and '*Ca*. P. aurantifolia=citri' in certain orange trees exhibiting symptoms of HLB offers valuable insights for future research endeavors. Due to the lack of control of healthy samples from other provinces in the country, making conclusions about similar microbial patterns under HLB diseases was impossible. In fact, understanding how the bacterial community's influences and interacts with the citrus tree entails the implementation of multiple targeted experiments, aiming to understand plant-microbe and microbe-microbe interactions associated with HLB. Preparing a large microbial dataset in relation to variables associated with the plant health, defense, and disease could help to understand how these variables shape the citrus bacterial communities and identify individual microorganisms or consortia that play a role in HLB suppression or promotion by performing.

CONTRIBUTIONS

This article was a part of PhD dissertation of Shiva Safarpour Kapourchali, PhD candidate of Islamic Azad University of Iran, Varamin-Pishva Branch. Mojdeh Malek organized the team members, submitted the proposal at the university and officially and scientifically supported the team. Ali Alizadeh Aliabadi designed the study, prepared samples, strongly and scientifically supported the team and revised the manuscript. Saeideh Rajaei conducted bioinformatic analysis, prepared laboratory space and revised the manuscript. Mohammad Mehdi Faghihi supported samples preparation, revised the manuscript and supported scenically the team. Mehdi Nasr Esfahani revised the manuscript and data curation. All authors read and approved the final manuscript.

LITERATURE CITED

Ahmed N.A., Petersen F.C., Scheie A., 2009. AI-2/LuxS is involved in increased biofilm formation by *Streptococcus intermedius* in the presence of antibiotics. *Antimicrobial Agents and Chemotherapy* 53(10): 4258–4263. https://doi.org/10.1128/AAC.00546-09

Alizadeh Aliabadi A., Foroutan A., Golmohamadi M., 2010. Occurrence of citrus greening caused by *Candidatus* Liberibacter asiaticus in Sistan-Baluchestan province. *19th Iranian Plant Protection Congress*, 31 July-3 August 2010. Tehran. Iran. p. 525. (in Persian with English summary)

Alizadeh Aliabadi A., Ghasemi A., Salehi M., Faghihi M.M., Forootan A., 2013. Identification and distribution of citrus greening disease in Iran. Approved number: 14-16-16-8802-88001 and Farvast number: 44237 dated 16/04/2013.

Alizadeh A.A., Faghihi M.M., Salehi M., Ghasemi A., 2022. Dynamics of emergence and spread of citrus huanglongbing disease in Iran. *Plant Pathology Science* 11(2): 11–21. https://doi.org/10.2982/PPS.11.2.11

Araujo W., Marcon J., Maccheroni W Jr, Elsas JD, Vuurde JWL, *et al*., 2002. Diversity of endophytic bacterial populations and their interaction with *Xylella fastidiosa* in citrus plants. *Applied Environmental Microbiology* 68: 4906–4914. https://doi.org/10.1128/AEM.68.10.4906-4914.2002

Arratia-Castro A.A., Santos-Cervantes M.E., Arce-Leal Á.P., *et al*., 2016. Detection and quantification of '*Candidatus* Phytoplasma asteris' and '*Candidatus* Liberibacter asiaticus' at early and late stages of Huanglongbing disease development. *Canadian Journal of Plant Pathology 38*(4): 411–421. https://doi.org/10.1080/07060661.2016.1243586

Bazany K.E, Delgado-Baquerzo M, Thompson A, Wang J-T, Otto K, Adair R.C., *et al*. 2022. Management

induce shifts in rhizosphere bacterial communities contribute to the control of pathogen causing citrus greenin disease. *Journal of Sustainable Agriculture and Environment* 1: 275–286. https://doi.org/10.1002/sae2.12029

Bendix C., Lewis J.D., 2018. The enemy within: phloem-limited pathogens. *Molecular Plant Pathology* 19: 238–254. https://doi.org/10.1111/mpp.12526

Blaustein R.A., Lorca G.L., Meyer J.L., Gonzalez C.F., Teplitski M., 2017. Defining the core citrus leaf- and root-associated microbiota: Factors associated with community structure and implications for managing huanglongbing (citrus greening) disease. *Applied Environmental Microbiology* 83: e00210-17. https://doi.org/10.1128/AEM.00210-17

Bodenhausen N., Horton M.W., Bergelson J., 2013. Bacterial communities associated with the leaves and the roots of *Arabidopsis thaliana*. *PloS One* 8(2): e56329. https://doi.org/10.1371/journal.pone.0056329

Bolyen E., Rideout J.R., Dillon M.R., *et al.,* 2019. QIIME 2: Reproducible, interactive, scalable, and extensible microbiome data science (2167-9843). *Nature Biotechnology* 37: 852–857. https://doi.org/10.1038/s41587-019-0209-9

Bosco D., D'Amelio R., Weintraub P., Jones P., 2009. Transmission specificity and competition of multiple phytoplasmas in the insect vector. *Phytoplasmas: Genomes, Plant Hosts and Vectors*, 293–308. https://doi.org/10.1079/9781845935306.02

Bové J.M., 2006. Huanglongbing: a destructive, newly-emerging, century-old disease of citrus. *Journal of Plant Pathology* 88: 7–37. https://doi.org/10.4454/jpp.v88i1.828

Camerota C., Raddadi N., Pizzinat A., … Alma A., 2012. Incidence of '*Candidatus* Liberibacter europaeus' and phytoplasmas in *Cacopsylla* species and their host plants. *Phytoparasitica* 40(3): 213–221. https://doi.org/10.1007/s12600-012-0225-5

Cochran L., Samadi, M., 1976. Distribution of stubborn disease in Iran. *International Organization of Citrus Virologists Conference Proceedings* (1957–2010). https://doi.org/10.5070/C53tn9w703

Crotti E., Balloi A., Hamdi C., … Daffonchio D., 2012. Microbial symbionts: a resource for the management of insect-related problems. *Microbial Biotechnology* 5(3): 307–317. https://doi.org/10.1111/j.1751-7915.2011.00312.x

Dala-Paula B.M., Plotto A., Bai J., Manthey J.A., Baldwin E.A., … Gloria M.B.A., 2019. Effect of huanglongbing or greening disease on orange juice quality, a review. *Frontiers in Plant Science* 9: 1976. https://doi.org/10.3389/fpls.2018.01976

da Graça J.V., 1991. Citrus greening disease. *Annual Review of Phytopathology* 29: 109–136. https://doi.org/10.1146/annurev.py.29.090191.000545

da Graça J.V., 2008. Biology, history and world status of Huanglongbing. Texas A & M University-Kingsville, Citrus Center, Weslaco TX 78596, USA.

Daranas N., Roselló G., Cabrefiga J., Donati I., 2019. Biological control of bacterial plant diseases with Lactobacillus plantarum strains selected for their broad-spectrum activity. *Annals of Applied Biology,* 174(1): 92–105. https://doi.org/10.1111/aab.12476

Dominguez J.; Jayachandran K.; Stover E.; Krystel J.; Shetty K.G., 2023. Endophytes and plant extracts as potential antimicrobial agents against '*Candidatus* Liberibacter asiaticus', causal agent of huanglongbing. *Microorganisms* 11: 1529. https://doi.org/10.3390/microorganisms11061529

Faghihi M.M., 2018. Investigation of association of phloem-limited prokaryotes with Siyahoo tangerine trees showing misshapen and inverted color change symptoms in fruit. *23rd Iranian Plant Protection Congress.* 27–30 August 2018, Gorgan. IRAN.

Faghihi M., Salehi M., Bagheri A., Izadpanah K., 2009. First report of citrus huanglongbing disease on orange in Iran. *Plant Pathology* 58(4): 793–793. https://doi.org/10.1111/j.1365-3059.2009.02051.x

Faghihi M.M., Taghavi S.M., Salehi M., Golmohammadi M., 2016. First report of huanglongbing disease on Mexican lime in iran. In: *Proceedings of the 20th International Organization of Citrus Virologist* (IOCV) conference, April 10–15, 2016, Chongqing, China. p. 45.

Fitzpatrick C.R.; Copeland J.; Wang P.W.; Guttman D.S.; Kotanen P.M.; Johnson M.T.J., 2018. Assembly and ecological function of the root microbiome across angiosperm plant species. *Proceedings of the National Academy of Sciences USA.* 115, E1157–E1165. https://doi.org/10.1073/pnas.1717617115

Fujiwara K., Iwanami T., Fujikawa T., 2018. Alterations of '*Candidatus* Liberibacter asiaticus'-associated microbiota decrease survival of *Ca.* L. asiaticus in *in vitro* assays. *Frontiers in Microbiology* 9: 3089. https://doi.org/10.3389/fmicb.2018.03089

Ginnan N.A., Dang T., Bodaghi S., … Borneman J., 2018. Bacterial and fungal next generation sequencing datasets and metadata from citrus infected with '*Candidatus* Liberibacter asiaticus'. *Phytobiomes* 2(2): 64–70. https://doi.org/10.1094/PBIOMES-08-17-0032-A

Grady K.L., Sorensen J.W., Stopnisek N., Guittar J., Shade A., 2019. Assembly and seasonality of core phyllosphere microbiota on perennial biofuel crops. *Nature*

Communications 10: 4135. https://doi.org/10.1038/s41467-019-11974-4

Hocquellet A., Toorawa P., Bové J.M., Garnier M., 1999. Detection and identification of the two *Candidatus* Liberobacter' species associated with citrus huanglongbing by PCR amplification of ribosomal protein genes of the b operon. *Molecular and Cellular Probes* 13: 373–379. https://doi.org/10.1006/mcpr.1999.0263

Hu W., Wang X., Zhou Y., Li Z., Tang K., Zhou C., 2011. Diversity of the *omp* gene in *Candidatus* Liberibacter asiaticus in China. *Journal of Plant Pathology* 93(1): 211–214. https://doi.org/10.4454/jpp.v93i1.294

Klindworth A., Pruesse E., Schweer T., … Glöckner F.O., 2013. Evaluation of general 16S ribosomal RNA gene PCR primers for classical and next-generation sequencing-based diversity studies. *Nucleic Acids Research* 41(1): e1. https://doi.org/10.1093/nar/gks808

Križanac I., Mikec I., Budinščak Ž., Musić M.Š., Škorić D., 2010. Diversity of phytoplasmas infecting fruit trees and their vectors in Croatia. *Journal of Plant Diseases and Protection* 117(5): 206–213. https://doi.org/10.1007/BF03356362

Kumar Ghosh D., Bhose S., Motghare M., Gowa S., 2015. Genetic diversity of the Indian populations of '*Candidatus* Liberibacter asiaticus' based on the tandem repeat variability in a genomic locus. *Phytopathology*. 105(8):1043–1049. https://doi.org/10.1094/PHYTO-09-14-0253-R

Kumar S., Stecher G., Li M., Knyaz C., Tamura K., 2018. MEGA X: molecular evolutionary genetics analysis across computing platforms. *Molecular Biology and Evolution* 35(6): 1547–1549. https://doi.org/10.1093/molbev/msy096

Limayem A., Martin E.M., Shankar S., 2024. Study on the citrus greening disease: Current challenges and novel therapies. *Microbial Pathogenesis* 192: 106688. https://doi.org/10.1016/j.micpath.2024.106688

Mendes R., Garbeva P., Raaijmakers J.M., 2013. The rhizosphere microbiome: significance of plant beneficial, plant pathogenic, and human pathogenic microorganisms. *FEMS Microbiology Reviews* 37(5): 634–663. https://doi.org/10.1111/1574-6976.12028

Mohkami A., Sattari R., Lori Z., Ehsani A., Nazemi A., 2011. First report of citrus huanglongbing in the Orzooiyeh region in Kerman province (Orzooiyeh). *Iranian Journal of Plant Pathology* 47: 105.

Montero Castillo P.M., Díaz A., 2015. Antagonistic action of *Lactobacillus* spp. against *Staphylococcus aureus* in cheese from Mompox-Colombia. *Revista Facultad Nacional de Agronomía Medellín* 68(2): 7721–7727. https://doi.org/10.15446/rfnam.v68n2.50991

Monazzah M., Nasr Esfahani M., Tahmasebi S., 2022. Genetic structure and proteomic analysis associated in potato to *Rhizoctonia solani* AG-3PT-stem canker and black scurf. *Physiological and Molecular Plant Pathology* 122: 101905. https://doi.org/10.1016/j.pmpp.2022.101905

Murray R., Schleifer K., 1994. Taxonomic notes: a proposal for recording the properties of putative taxa of procaryotes. *International Journal of Systematic and Evolutionary Microbiology* 44(1): 174–176. https://doi.org/10.1099/00207713-44-1-174

Naylor D., Coleman-Derr D., 2018. Drought stress and root-associated bacterial communities. *Frontiers in Plant Science* 8: 303756. https://doi.org/10.3389/fpls.2017.02223

Nicolaisen M., Contaldo N., Makarova O., Paltrinieri S., Bertaccini A., 2011. Deep amplicon sequencing reveals mixed phytoplasma infection within single grapevine plants. *Bulletin of Insectology* 64: S35–S36.

Ofek M., Hadar Y., Minz D., 2012. Ecology of root colonizing *Massilia* (Oxalobacteraceae). *PloS One 7*(7): e40117. https://doi.org/10.1371/journal.pone.0040117

Passera, A., Alizadeh, H., Azadvar, M., … Bianco P.A., 2018. Studies of microbiota dynamics reveals association of '*Candidatus* Liberibacter asiaticus' infection with citrus decline. *International Journal of Molecular Sciences* 19(6): 1817. https://doi.org/10.3390/ijms19061817

Raddadi N., Gonella E., Camerota C., … Alma A., 2011. '*Candidatus* Liberibacter europaeus' sp. nov. that is associated with and transmitted by the psyllid *Cacopsylla pyri*. *Environmental Microbiology* 13(2): 414–426. https://doi.org/10.1111/j.1462-2920.2010.02347.x

Rajaei S., Farshi R.S., Jazi M.M., Seyedi S., 2017. Efficient strategies for elimination of phenolic compounds during DNA extraction from *Pistacia vera* L. *Agrivita Journal of Agricultural Science* 39(3): 279–287. https://doi.org/10.17503/agrivita.v39i3.734

Saldaña M.A., Hegde S., Hughes G.L., 2017. Microbial control of arthropod-borne disease. *Memórias do Instituto Oswaldo Cruz* 112(2): 81–93. https://doi.org/10.1590/0074-02760160373

Salehi M., Rasoulpour R., 2016. First report of '*Candidatus* Liberibacter asiaticus' associated with huanglongbing in Fars province. *Iranian Journal of Plant Pathology* 51(4): 563–566.

Salehi M., Faghihi M.M., Khanchezar A., Bagheri A., Izadpanah K., 2012. Distributioin of citrus huanglongbing disease and its vector in southern Iran. *Iranian Journal of Plant Pathology* 48(2): 195–208.

Satta E., Ramirez A.S., Paltrinieri S., Contaldo N., 2016. Simultaneous detection of mixed '*Candi-*

datus Phytoplasma asteris' and '*Ca*. Liberibacter solanacearum'infection in carrot. *Phytopathologia Mediterranea* 55(3): 401–409. https://doi.org/10.14601/Phytopathol_Mediterr-18683

Safarpour K.S., Alizadeh Aliabadi A., Faghihi M.M., Rajaei S., Maleki M., 2022. Evaluation of ten citrus cultivars' susceptibility to '*Candidatus* Liberibacter asiaticus', citrus huanglongbing. *Plant Protection* 44: 1–18. https://doi.org/10.22055/ppr.2021.17131

Sagaram U.S., DeAngelis, K.M., Trivedi P., Andersen G.L., Lu S.E., Wang N., 2009. Bacterial diversity analysis of huanglongbing pathogen-infected citrus, using PhyloChip arrays and 16S rRNA gene clone library sequencing. *Applied Environmental and Microbiology* 75: 1566–1574. https://doi.org/10.1128/AEM.02404-08

Swisher K., Munyaneza J., Velásquez-Valle R., 2018. Detection of pathogens associated with psyllids and leafhoppers in *Capsicum annuum* L. in the Mexican states of Zacatecas, and Michoacan. *Plant Disease* 102: 146–153. https://doi.org/10.1094/PDIS-05-17-0758-RE

Tamura K., Nei M.,1993. Estimation of the number of nucleotide substitutions in the control region of mitochondrial DNA in humans and chimpanzees. *Molecular Biology and Evolution* 10(3): 512–526. Https://doi.org/10.1093/oxfordjournals.molbev.a040023

Tedersoo L., Drenkhan R., Anslan S., Morales-Rodriguez C., Cleary M., 2019. High-throughput identification and diagnostics of pathogens and pests: overview and practical recommendations. *Molecular Ecology Resources* 19(1): 47–76. https://doi.org/10.1111/1755-0998.12959

Thompson S., Fletcher J., Ziebell H., ... Pitman, A.R., 2013. First report of '*Candidatus* Liberibacter europaeus' associated with psyllid infested Scotch broom. *New Disease Reports* 27(6): 2044-0588.2013. https://doi.org/10.5197/j.2044-0588.2013.027.006

Trivedi P., Duan Y., Wang N., 2010. Huanglongbing, a systemic disease, restructures the bacterial community associated with citrus roots. *Applied Environmental and Microbiology* 76: 3427–3436.https://doi.org/10.1128/AEM.02901-09

Villechanoux S., Garnier M., Renaudin J., Bovè J.M., 1993. The genome of the non-cultured bacterial-like organism associated with citrus greening disease contains the *nusGrplKAJL-rpoBC* gene cluster and the gene for a bacteriophage DNA polymerase. *Current Microbiology* 26:161–166. https://doi.org/10.1007/BF01577372

Vorholt J.A., 2012. Microbial life in the phyllosphere. *Nature Reviews Microbiology* 10(12): 828–840. https://doi.org/10.1038/nrmicro2910

Wickham H., 2016. *Ggplot2: Elegant Graphics for Data Analysis*. Springer; New York, NY, USA.

Warnes G.R., Bolker B., Bonebakker L., Gentleman R., Huber W., Liaw A., Lumley T., ... Galili T., 2020. Gplots: Various R Programming Tools for Plotting Data. Package version 3.0.1.1. Available online: https://CRAN.R-project.org/package=gplots

Xu J., Zhang Y., Zhang P., Trivedi P., Riera N., Wang Y., ... Wang N., 2018. The structure and function of the global citrus rhizosphere microbiome. *Nature Communications* 9: 4894. https://doi.org/10.1038/s41467-018-07343-2

Yang C., Zhong Y., Powell C.A., ... Zhang M., 2018. Antimicrobial compounds effective against '*Candidatus* Liberibacter asiaticus' discovered via graft-based assay in citrus. *Scientific Reports* 8(1): 1–11. https://doi.org/10.1038/s41598-018-35461-w

Zhang M., Powell C.A., Benyon L.S., Zhou H., Duan Y., 2013. Deciphering the bacterial microbiome of citrus plants in response to '*Candidatus* Liberibacter asiaticus'-infection and antibiotic treatments. *PLoS One* 8(11): e76331. https://doi.org/10.1371/journal.pone.0076331

Phytopathologia Mediterranea
The international journal of the
Mediterranean Phytopathological Union

Firenze University Press
www.fupress.com/pm

Research Papers

First reports of *Xiphinema rivesi* and *Xiphinema incertum* (Nematoda: Longidoridae) in Bosnia-Herzegovina

Elena FANELLI[1,A], Alessio VOVLAS[1,A], Branimir NJEŽIĆ[2], Alberto TROCCOLI[1], Andrija VASILIC[2], Radijana ĐEKANOVIĆ[2], Francesca DE LUCA[1]

[1] *Institute for Sustainable Plant Protection-CNR, Via Amendola 122/D, 70126 Bari, Italy*
[2] *University of Banja Luka, Faculty of Agriculture, Bulevar vojvode Petra Bojovica 1A, 78000 Banja Luka, Bosnia-Herzegovina*
[a] authors contributed equally.
*Corresponding author. E-mail: francesca.deluca@cnr.it

Summary. A nematode survey was carried out (in 2020) in apple and poplar orchards in Banja Luka, Bosnia-Herzegovina detected two nematode species belonging to the *Xiphinema americanum*-group. Polyphasic identification, combining morphological, molecular and phylogenetic analyses identified the nematodes as *X. rivesi* in apple orchards and *X. incertum* in poplar trees. Sequence and phylogenetic analyses used two rRNA genes (D2-D3 expansion segments of 28S rRNA, and ITS regions), and partial mitochondrial COI region detected high intra- and inter-specific variability within *X. rivesi*. These are the first reports of *X. rivesi* and *X. incertum* in Bosnia-Herzegovina, which extend the geographical distribution of these species in Europe.

Keywords. Integrative taxonomy, Longidorids, *Malus domestica*, mitochondrial COI, *Populus* sp., rRNA genes.

OPEN ACCESS

Citation: Fanelli, E., Vovlas, A., Nježić, B., Troccoli, A., Vasilic, A., Đekanović, R. & De Luca, F. (2025). First reports of *Xiphinema rivesi* and *Xiphinema incertum* (Nematoda: Longidoridae) in Bosnia-Herzegovina. *Phytopathologia Mediterranea* 64(1): 145-159. doi: 10.36253/phyto-15951

Accepted: April 29, 2025

Published: May 15, 2025

Data Availability Statement: All relevant data are within the paper and its Supporting Information files.

Competing Interests: The Author(s) declare(s) no conflict of interest.

Editor: Isabel Abrantes, University of Coimbra, Portugal.

ORCID:
EF: 0000-0002-3132-3908
AV: 0000-0003-1682-7101
BN: 0000-0003-2091-7134
AT: 0000-0002-3582-8209
FDL: 0000-0002-6646-8066

INTRODUCTION

Xiphinema is a cosmopolitan nematode genus within the Longidoridae, which includes more than 290 described species (Archidona-Yuste *et al*., 2020; Ali *et al*., 2024; Kornobis *et al*., 2025). Nematodes in the *X. americanum* group (more than 60 species) are studied because they have well-conserved and overlapping morphometrics, and some species transmit by economically important nepoviruses (genus Nepovirus, family Comoviridae) (Taylor and Brown, 1997; Decraemer and Robbins, 2007).

Polyphasic identification of members of the *X. americanum* group provides the most efficient discrimination between virus vector or quarantine species, and to develop effective control strategies (Širca *et al*., 2007; Archidona-Yuste *et al*., 2016; Troccoli *et al*., 2024).

A survey carried out in Bosnia-Herzegovina, in 2020, of *Malus domestica* Borkh., 1803 (apple) and *Populus* sp. (poplar) plantations revealed the pres-

ence of two *Xiphinema* populations belonging to the *X. americanum* group. Initial hypotheses based on morphological observations showed that the two matched with *X. rivesi* and *X. pachtaicum* subgroup within the *X. americanum* group.

Xiphinema rivesi Dalmasso 1969 is widespread in Europe, and has been recorded in France, Germany (Sturhan, 2014), Italy (De Luca and Agostinelli, 2011; Troccoli *et al.,* 2024), Moldova (Poiras, 2012), Portugal (Gutiérrez-Gutiérrez *et al*., 2016), Slovenia (Urek *et al*., 2003), and Spain (Bello *et al*., 2005; Gutiérrez-Gutiérrez *et al*., 2011). The *X. pachtaicum* subgroup includes eight species (*X. fortuitum* Roca, Lamberti & Agostinelli, 1988, *X. incertum* Lamberti, Choleva & Agostinelli, 1983, *X. madeirense* Brown, Faria, Lamberti, Halbrendt, Agostinelli & Jones, 1993, *X. opisthohysterum* Siddiqi, 1961, *X. pachtaicum* (Tulaganov, 1938) Kirjanova, 1951, *X. pachydermum* Sturhan, 1984, *X. simile* Lamberti, Choleva & Agostinelli, 1983, and *X. utahense* Lamberti & Bleve-Zacheo, 1979), which have similar morphologies but different molecular and phylogenetic characteristics (Archidona-Yuste *et al*., 2016; Lazarova *et al*., 2016; Troccoli *et al*., 2024). Lazarova *et al*., 2016 suggested the occurrence of the *X. simile*-subgroup including *X. simile*, *X. parasimile*, *X. browni* and *X. vallense*. *Xiphinema incertum* can be misidentified as *X. pachtaicum* due to conserved gross morphology. *Xiphinema incertum* has been reported from Bulgaria (Lamberti *et al*., 1983), Croatia (Barsi, 1989), Slovenia (Barsi, 1994), Serbia (Barsi and Lamberti, 2002), Spain (Gutiérrez-Gutiérrez *et al*., 2012; Archidona-Yuste *et al*., 2016) and Italy (Troccoli *et al*., 2024), and *X. simile*, *X. densispinatum* Barsi, Lamberti & Agostinelli, 1998 and *X. pachtaicum* have been recorded in Bosnia-Herzegovina (Barsi *et al*., 1998; Barsi and Lamberti, 2004; Milašin *et al.,* 2024).

The objectives of the present study were to provide accurate identification of the two nematodes found in the Bosnia-Herzegovina survey, using an integrative approach, combining morphological, molecular, phylogenetic, and multivariate analyses. Phylogenetic relationships of the nematodes were inferred by their D2-D3 expansion segments of the 28S rRNA gene, the ITS, and the partial mitochondrial COI.

MATERIALS AND METHODS

Nematode samples and their morphologies

Soil samples were obtained from rhizospheres of apple and poplar trees in the Botanical Garden of the University of Banja Luka, Bosnia-Herzegovina. The samples were taken with an auger from 30 cm depth. Nematodes were extracted from 500 cm^3 of soil from each sample using the Flegg and Cobb technique (Flegg, 1967). *Xiphinema* specimens were killed by gentle heat, then fixed in a solution of 4% formaldehyde + 1% propionic acid, and then processed in pure glycerine using Seinhorst's (1962) method. Light micrographs were captured, and measurements were made using a Leica compound microscope equipped with a Leica DFC7000 T digital camera, and with Leica Las® version 2.6 software. All abbreviations used are as defined by Jairajpuri and Ahmad (1992).

Multivariate morphometric analyses

Principal Component Analysis (PCA) of the morphological traits within the *X. americanum* group and the *X. pachtaicum* subgroup, according to the subgroups indicated by Lamberti and Ciancio, 1993, were assessed with particular attention to *X. rivesi*, *X. incertum*, and *X. penevi* Lazarova, Peneva & Kumari, 2016. Two distinct PCA analyses were conducted for *X. rivesi* and for *X. pacthtaicum*-subgroup in XLSTAT (Addinsoft, 2007). Statistical analyses were carried out using PAST v. 4.03 (Hammer and Harper, 2001). Measurements obtained from literature used the mean value for each population (Supplementary Table 1). Measurements were normalized through PAST software before analyses. PCA for the *X. americanum* group was carried out using 13 diagnostic characters, including: body length (L), 'de Man's indices' (a, b, c, c′), percentage distance from anterior end to vulva/body length (V), odontostyle (ODS) and odontophore (ODP) lengths, oral aperture to guided ring distance (OA/gr), tail length (T), body diameters at lip region (LRD) and mid-body (MDB), and J tail length (JTA). PCA for the *X. pachtaicum*-subgroup analysed fourteen features, adding body diameter (ABD). Scores for the first three components (PC1, PC2 and PC3) were determined to form a two-dimensional plot for each nematode population, based on default parameters of the software.

DNA extractions, PCR and sequencing

For molecular analyses, and to exclude the cases of mixed populations in the same sample, total DNA was extracted from individual juvenile specimens, as described by De Luca *et al*. (2004). The ITS1-5.8S-ITS2 regions were amplified using the forward primer 18S (5′-GTTTCCGTAGGTGAACCTGC-3′) and the reverse primer 26S (5′-ATATGCTTAAGTTCAGCGGGT-3′) (Vrain *et al*., 1992). The D2-D3 expansion segments

Figure 1. Photomicrographs of *Xiphenema rivesi* Dalmasso, 1969 (A B and C), and *X. incertum* Lamberti, Choleva & Agostinelli, 1983 (D and E), from Bosnia-Herzegovina. A, female anterior region; B, detail of a female lip region; C, female tail region; D, female anterior region; E, female tail region. (Scale bars: A = 50 µm; B to E = 20 µm).

of the 28S rRNA gene were amplified using the primers D2A (5′-ACAAGTACCGTGGGGAAAGTTG-3′) and D3B (5′-TCGGAAGGAACCAGCTACTA-3′) (Nunn, 1992). The portion of the mitochondrial cytochrome oxidase c subunit 1 (*mt*COI) gene was amplified with this primer set COI-F1 (5′-CCTACTATGATTGGTGGTTTTGGTAATTG-3′) and COI-R2 (5′-GTAGCAGCAGTAAAATAAGCACG-3′) (Kanzaki and Futai, 2002). The PCR cycling conditions used for amplifications were an initial denaturation at 94°C for 5 min, followed by 35 cycles of denaturation each at 94°C for 50 s, annealing at 55°C for 50 s and extension at 72°C for 1 min, and a final step at 72°C for 7 min. PCR products of the ITS, D2-D3 expansion domains of 28S rRNA gene regions, and the partial mitochondrial COI from three individual nematodes were purified using the protocol suggested by the manufacturer (Nucleospin Gel and PCR Clean-up, Macherey-Nagel). Purified D2-D3 amplicons were directly sequenced using specific primers, while ITS and COI purified DNA fragments were cloned in pGEM-T Vector System II kit (Promega). Positive clones were sent for sequencing, in both directions, to MWG-Eurofins (Germany). The obtained sequences were submitted to GenBank database under the accession numbers: PV397451, PV397455-PV397458, PV461875-PV461878.

Evolutionary divergence between sequences

The pairwise distances within the D2-D3 expansion domains and mitochondrial COI sequences of *X. rivesi* populations were determined using the MEGA-X software package (Kumar *et al*., 2018). All positions with gaps and missing data were excluded. The D2-D3 expansion domains involved 32 nucleotide sequences, and the COI analyses involved 21 sequences.

Phylogenetic analyses

To assess the genetic variability within the *X. americanum* group and *X. pachtaicum*-subgroup nematodes, sequences from different geographical populations were included in a phylogenetic analysis. The newly obtained sequences of *X. rivesi* and *X. incertum* were aligned with the corresponding sequences present in GenBank, using MAFFT software 7 with default parameters (Katoh and Standley, 2013). Sequence alignments were manually edited using BioEdit 7.2.5 (Hall *et al*., 1999). Phylogenetic analyses of the sequence datasets were carried out with Bayesian inference (BI) using MrBayes 3.1.2 (Ronquist and Huelsenbeck, 2003). The best-fit model of DNA evolution was obtained using JModelTest V.2.1.7 (Darriba *et al*., 2012) with the Akaike information criterion (AIC). The best-fit model, the base frequency, the proportion of invariable sites, and the gamma distribution shape parameters and substitution rates in the AIC were then used in MrBayes for the phylogenetic analyses. The Markov chains were sampled at intervals of 100 generations and two runs were conducted for each analysis. After discarding burn-in samples of 25% and evaluating convergence, the remaining samples were retained for in-depth analyses. The topologies were used to generate a 50% majority rule consensus tree. Posterior prob-

abilities (PP) were given on appropriate clades. Trees from all analyses were visualized using FigTree software version v.1.42 (Rambaut *et al*., 2014). D2-D3 alignment of sequences belonging to *X. americanum* group included 101 sequences, and *Tylencholaimus mirabilis* (Bütschli, 1873) De Man, 1876 was included as the outgroup. COI alignment of corresponding sequences belonging to the *X. americanum* group included 45 sequences and *X. chambersi*, and *X. browni* Lazarova, Peneva & Kumari, 2016 were used as the outgroups.

RESULTS

Survey for occurrence of Xiphinema *species in Bosnia-Herzegovina*

In 2020, apple and poplar trees in the Botanical Garden of the University of Banja Luka, Banja Luka, Bosnia-Herzegovina, were sampled to ascertain the occurrence of dagger nematodes. *Xiphinema rivesi* was associated with apple trees, and *X. incertum* with poplar trees. These are the first reports of the two nematodes for Bosnia-Herzegovina, extending the geographical distribution of these species in Europe.

Bosnia-Herzegovina (BH) populations of Xiphinema rivesi *and* X. incertum

Morphometrics of *X. rivesi* (Table 1) and *X. incertum* (Table 2) from Bosnia-Herzegovina were compared with the closest reported populations for both species. Morphometrics of BH *X. rivesi* aligned with the descriptions of Italian and Slovenian populations, showed small variations in comparisons with other populations of *X. rivesi*. The BH and Slovenian populations had similar V ratio (respectively, 53.9 *vs* 53.5%) (Urek *et al*., 2005), while the BH population had more posterior vulva compared to *X. rivesi* from Italy (respectively, 53.9 *vs* 52.6%) (Troccoli *et al*., 2024) or from Portugal (respectively 53.9 *vs* 52.0%) (Lamberti *et al*., 1994). The BH population of *X. rivesi* had longer odontostyle (95.7 µm) and tail (36.7 µm) compared to all other previously described populations (Fadaei *et al*., 2003; Urek *et al*., 2005; De Luca and Agostinelli, 2011; Gutiérrez-Gutiérrez *et al*., 2012; Handoo *et al*., 2015; Troccoli *et al*., 2024). Furthermore, Table 1 clearly showed that *X. rivesi* from Egypt is the most different population compared to the others reported in this study.

Morphology and morphometrics of the BH *X. incertum* population agreed with the type population described by Lamberti *et al*. (1983) (Table 2). The lip regions were slightly expanded and set off by constrictions and separated from the bodies by depressions. Female tails were conoid, each with a narrowly rounded terminus, as has been previously described for European populations (Barsi, 1994; Barsi and Lamberti, 2002; Gutiérrez-Gutiérrez *et al*., 2012). The main differences between the BH population and the type population of *X. incertum* from Bulgaria were: slightly longer body length (1952 *vs* 1900 µm), slightly lower V ratio (respectively, 55.4 *vs* 57.0%), and moderately lower c value (57 *vs* 69.0%). There was a lower a and c ratio for the BH nematodes when compared with *X. incertum* from Croatia and Serbia (Table 2). BH *X. incertum* had more anterior vulva (55.4%) compared to other populations, except for that from Spain (52.4%). The BH population had shorter odontostyles (mean = 75.2 µm) compared with specimens from Spain (92.2 µm) and the type population from Bulgaria (92.0 µm). The BH *X. incertum* also had similarities with *X. penevi*, *X. parasimile*, and *X. pachtaicum*, but can be distinguished from *X. penevi* (Lazarova *et al*., 2016) by body length (L = 1952.2 µm *cf*. 1687 µm), a (54.3 *cf*. 55.4%), V values (61 *cf*. 57.1%), and tail shape (rounded *cf*. pointed termini). The BH *X. incertum* can be distinguished from *X. parasimile* (Barsi and Lamberti, 2004) by smaller a and c' values (54.3 and 57.6 *vs* 70.5 and 59.9), and longer odontostyles (means = 75.2 *vs* 69.7 µm). When compared to *X. pachtaicum*, several characters showed overlapping ranges, with stylet lengths being the most significant differentiating feature for *X. pachtaicum* from Serbia (75.2 *vs* 88.3 µm) and for *X. pachtaicum* from Italy (75.2 *vs* 87.3 µm).

Multivariate morphometric analyses

In the PCA analyses built with species of the *X. americanum* group belonging to clade I, an accumulated variability of 68.34% of the total variance was measured for *X. rivesi* compared with other populations of this species (Figure 2). The contributions of PC1 were 32.47%, for PC2 was 21.84% and for PC3 was 14.02%. Kaiser Meyer Olkin's (KMO) measure of sampling indicated a KMO value of 0.608. The loading factors for each character were used to interpret biological meaning of the factors. The c ratio (r = 0.418), odontophore length (r = 0.40), body (r = 0.396) and oral aperture to guided ring length (r = 0.378), had greatest coefficients of correlation, and were responsible for the significant variability of the F1. For the F2, almost all characters showed positive correlations except for body and odontostyle lengths, and all the de Man indices. This component is associated with the general nematode size. F2 was also dominated by the greatest coefficient of correlation for lip region

Table 1. Morphometrics comparisons in *Xiphinema rivesi* Dalmasso, 1969 populations and locations where they were detected. Measurements of females obtained in the present study versus measurements reported from other previous studies. All measurements in µm, except body length in mm and in the form: mean±sd (range).

Character	*X. rivesi*	*X. rivesi*	*X. rivesi*	*X. rivesi*	*X. rivesi*	*X. rivesi*	*X. rivesi*	*X. rivesi*
	Bosnia-Herzegovina	Italy	Italy	Spain	Slovenia	Egypt	Iran	Portugal
		Troccoli *et al.*, 2024	De Luca and Agostinelli, 2011	Gutiérrez-Gutiérrez *et al.*, 2012	Urek *et al.*, 2005	Handoo *et al.*, 2015	Fadaei *et al.*, 2003	Lamberti *et al.*, 1994
n	11	18	10	10	11	10	13	5
L	1874.4 ± 50.7 (1808.1-1967.7)	1892.8 ± 133.4 (1607-2166.7)	2000 ± 0.12 (1900-2200)	1886 ± 127 (1583-2055)	1960 (1780-1070)	1600.6 ± 75.5 (1480-1660)	1700 ± 0.08 (1500-1800)	2000 (1900-2000)
a	52.2 ± 2.5 (47.0-55.7)	49.4 ± 2.1 (45.3-53.5)	55 ± 2.39 (50-58)	45.7 ± 3.3 (37.2-48.4)	45.39 (36.44-53.34)	35.1 ± 1.3 (32.7-37)	44.7 ± 2.9 (38.5-50)	53 (50-55)
b	-	8.4 ± 0.7 (7.2-9.7)	6.4 ± 0.61 (5.5-7.5)	7.4 ± 0.9 (6.4-8.4)	6.00 (5.08-7.05)	6.6 ± 0.7 (5.5-7.4)	6.4 ± 0.5 (5.5-7)	7.0 (5.5-7.0)
c	51.2 ± 4.0 (43.6-56.5)	58.8 ± 5.5 (50.2-67.7)	63.3 ± 4.99 (56.9-69.8)	53.4 ± 3.3 (49.1-58.5)	57.95 (51.12-66.82)	56.0 ± 3.4 (50.2-59.5)	55.2 ± 3.0 (49.5-60)	61 (59-63)
c’	1.6 ± 0.1 (1.5-1.8)	1.4 ± 0.1 (1.2-1.7)	1.4 ± 0.09 (1.2-1.5)	1.4 ± 0.1 (1.2-1.5)	1.44 (1.27-1.59)	1.0 ± 0.1 (1.0-1.1)	1.3 ± 0.07 (1.2-1.4)	1.5 (1.4-1.6)
V (%)	53.9 ± 0.8 (53.1-55.1)	52.6 ± 0.9 (50.9-54.2)	52 ± 0.85 (50-53)	53.0 ± 1.0 (52-55)	53.5 (52.6-54.4)	52.1 ± 1.4 (50.4-54)	52.2 ± 0.7 (51-53.5)	52 (50-55)
Odontostyle length	95.8 ± 0.9 (94.5-96.9)	90.8 ± 2.3 (86.4-94.1)	93.6 ± 1.60 (90.8-94.8)	92.1 ± 5.9 (79.0-98.5)	91.9 (84.9-96.3)	87.5 ± 2.0 (85-90)	81.5 ± 2.8 (73.5-86)	91 (88-95)
Odontophore length	46.4 ± 1.0 (44.0-47.2)	51.2 ± 2.3 (48.4-56.1)	53.3 ± 1.80 (50.6-55.7)	51.7 ± 3.8 (43.5-56.5)	51.8 (48.1-55.4)	52.8 ± 2.9 (50-57)	46.2 ± 1.8 (42-48.5)	50 (47-53)
Oral aperture – guide ring	73.2 ± 1.2 (70.6-74.6)	76.8 ± 2.6 (72.2-84.5)	75.4 ± 1.14 (73.6-77.6)	79.3 ± 6.1 (65.5-87.0)	78.6 (74.4-84.2)	72.2 ± 4.0 (65-75)	66.2 ± 2.0 (63-70)	73 (72-73.5)
Tail length	36.7 ± 2.9 (32.8-42.9)	32.4 ± 2.8 (28.4-38.9)	32.2 ± 1.25 (30.5-35.0)	35.4 ± 2.5 (31.5-39.0)	34.0 (30.4-37.9)	28.6 ± 1.9 (25-30)	30.8 ± 1.9 (28-33.5)	33 (31-34)
J tail	-	8.3 ± 1.2 (5.8-11.6)	7.4 ± 0.83 (6.3-8.6)	8.6 ± 0.7 (7.5-8.5)	-	9.1 ± 1.5 (8-12)	9.4 ± 0.8 (8-11)	9 (8-10)
Body diam. at lip region	-	8.9 ± 0.5 (8-9.9)	10.3 ± 0.00 (10-10)	9.9 ± 0.9 (8.5-12.0)	-	-	11.1 ± 0.4 (10.5-12)	9 (9-9)
Body diam. at guide ring	-	27.5 ± 1.3 (25.6-30.5)	-	-	-	-	25.6 ± 0.9 (25-27)	
Body diam. at mid-body	22.9 ± 1.0 (21.4-24.4)	38.3 ± 3.1 (33.8-43.5)	36.9 ± 1.58 (34.5-38.5)	-	43.8 (34.4-52.7)	45.7 ± 3.3 (40-50)	38.2 ± 3.3 (33.5-46.5)	
Body diam. at anus	-	23.8 ± 1.9 (21.1-28.4)	23.6 ± 0.81 (22.4-25.3)	-	-	-	23.2 ± 1.1 (21.5-25)	
Body diam. at beginning of J	-	10.4 ± 1.0 (8.8-11.8)	10.2 ± 0.47 (9.2-10.9)	-	-	12.6 ± 1.2 (11.5-15)	10.9 ± 0.8 (10-12.5)	

Table 2. Morphometrics comparisons in *Xiphinema incertum* Lamberti, Choleva & Agostinelli, 1983, *X. penevi* Lazarova, Peneva & Kumari, 2016, *X. parasimile* Barsi & Lamberti, 2004, and *X. pachtaicum* (Tulaganov, 1938) Kirjanova, 1951 populations and locations where they were detected. Measurements of females obtained in the present study versus measurements reported from other previous studies. All measurements in µm, except body length in mm and in the form: mean ± sd (range).

Character	*X. incertum*	*X. incertum*	*X. incertum*	*X. incertum*	*X. incertum*	*X. penevi*	*X. parasimile*	*X. pachtaicum*	*X. pachtaicum*
	Bosnia – Herzegovina	Spain	Bulgaria	Croatia	Serbia	Morocco	Serbia	Serbia	Italy
		Gutiérrez-Gutiérrez *et al.*, 2012	Lamberti *et al.*, 1983	Barsi, 1994	Barsi and Lamberti, 2002	Lazarova *et al.*, 2016	Barsi and Lamberti, 2004	Barsi and Lamberti, 2002	Troccoli *et al.*, 2024
n	8	6	4	2	2	6	53	30	10
L	1952.2 ± 89.3 (1858–2126.4)	1844 ± 52 (1788–1922)	1900 (1800–2000)	1910–1960	1920–2050	1687 ± 100 (1532–1846)	1990 ± 130 (1750-2260)	1990 ± 100 (1810-2190)	1926.9 ± 113.5 (1789 - 2091)
a	54.3 ± 1.7 (52.5–58.3)	49.7 ± 3.0 (44.6–52.5)	57 (54–64)	65.3–60.6	63.8–65.6	61.0 ± 2.6 (57.2–65.0)	70.5 ± 3.81 (61.0–76.1)	66.7 ± 3.70 (60.7-75.1)	61.9 ± 2.8 (57.8 - 66.3)
b	–	9.0 ± 1.4 (7.7–11.0)	6.4 (5.9–6.8)	6.2–6.4	6.0–5.9	6.1 ± 1.1 (5.0–7.0)	7.0 ± 0.49 (6.1–8.1)	5.8 ± 0.43 (4.8-7.0)	6.4 ± 0.5 (5.8 - 7.2)
c	57.6 ± 1.9 (55.5–61.2)	64.5 ± 2.7 (61.8–68.6)	69 (62–78)	67.6–78.2	72.5–81.3	57.7 ± 3.9 (50.8–61.5)	59.9 ± 4.51 (50.9–69.8)	61.5 ± 5.50 (51.6-71.8)	61.6 ± 5.1 (54.0 - 70.2)
c’	1.7 ± 0.1 (1.6–1.9)	1.2 ± 0.1 (0.9–1.3)	1.5 (1.4–1.7)	1.61–1.42	1.51–1.33	1.8 ± 0.1 (1.6–1.9)	2.02 ± 0.12 (1.79–2.28)	1.77 ± 0.14 (1.58-2.00)	1.7 ± 0.1 (1.6 - 1.9)
V	55.4 ± 2.1 (51.4–58.8)	52.4 ± 1.1 (51–54)	57 (56–58)	58.8–58.6	58.0–58.1	57.1 ± 0.6 (55.9–58.1)	55.5 ± 1.38 (52.2–58.7)	57.0 ± 1.33 (54.8-59.2)	56.8 ± 1.2 (55.1 - 59.4)
Odontostyle lenght	75.2 ± 2.5 (71.6–79.2)	92.2 ± 3.4 (88.0–97.0)	92 (87–97)	90.5–90.5	88.7–90.0	76.7 ± 2.1 (72–79)	69.7 ± 2.22 (64.4–73.7)	88.3 ± 2.58 (83.7 -93.7)	87.3 ± 2.7 (83.5 - 90.9)
Odontophore lenght	53.4 ± 4.1 (45.0–57.9)	49.7 ± 3.0 (46.0–53.5)	51 (50–54)	50.3–49	46.3–47.5	47.7 ± 1.8 (44–50)	41.6 ± 1.21 (38.8–43.8)	48.9 ± 1.34 (46.3-51.3)	51.2 ± 1.5 (48.4 - 53.3)
Oral aperture–guiding ring	70.0 ± 1.2 (68.8–72.4)	76.4 ± 4.8 (70.0–82.0)	71 (64–82)	81.7 –84.2	80.6–82.5	68.0 ± 0.6 (66–71)	62.6 ± 1.72 (59.4–66.3)	80.5 ± 2.39 (77.3-85.6)	80.1 ± 3.0 (75.8 - 83.8)
Tail lenght	33.9 ± 1.9 (31.2–36.5)	28.6 ± 1.2 (27.0–30.5)	28 (26–32)	28.3–25.1	26.4–25.0	29.3 ± 1.9 (26–32)	33.3 ± 1.62 (30.3 -37.1)	32.6 ± 2.60 (28.6-38.2)	31.4 ± 1.5 (29.8 - 33.7)
J (hyaline portion of tail)	–	6.5 ± 1.0 (5.5–8.5)	7 (6–9)	7.5–8.2	8.8–6.3	8.4 ± 0.7 (8–10)	8.2 ± 0.88 (6.3 -10.0)	10.1 ± 0.94 (8.1-12.5)	9.3 ± 0.4 (8.4 - 9.8)
Body diam. at lip region	–	9.5 ± 0.5 (8.5–10.0)	9 (8–9)	8.8–8.8	8.8–8.8	8.3 ± 0.3 (8–9)	9.0 ± 0.24 (8.4–9.7)	9.1 ± 030 (8.4-9.7)	8.7 ± 0.5 (8.3 - 9.7)
Body diam. at mid–body	35.9 ± 1.2 (34.8–38.7)	–	34 (29–37)	29.3–32.4	30–31.3	27.6 ± 1.4 (25–31)	28.3 ± 1.26 (24.7–30.6)	29.9 ± 1.45 (27.5-33.8)	31.2 ± 2.0 (28.0 - 34.8)
Body diam. at anus	19.7 ± 1.1 (18.4–22.2)	–	19 (18–19)	17.6–17.6	17.5–18.8	16.2 ± 0.7 (15–17)	16.5 ± 0.65 (15.0 -17.7)	18.4 ± 0.71 (16.9-20.0)	18.0 ± 0.5 (17.2 - 18.7)
Body diam. at be beginning of J	–	–	10 (9–10)	10–9.7	11.7–10.0	7.1 ± 0.4 (7–8)	7.1 ± 0.51 (6.3 -8.1)	8.5 ± 0.79 (6.9-103)	–

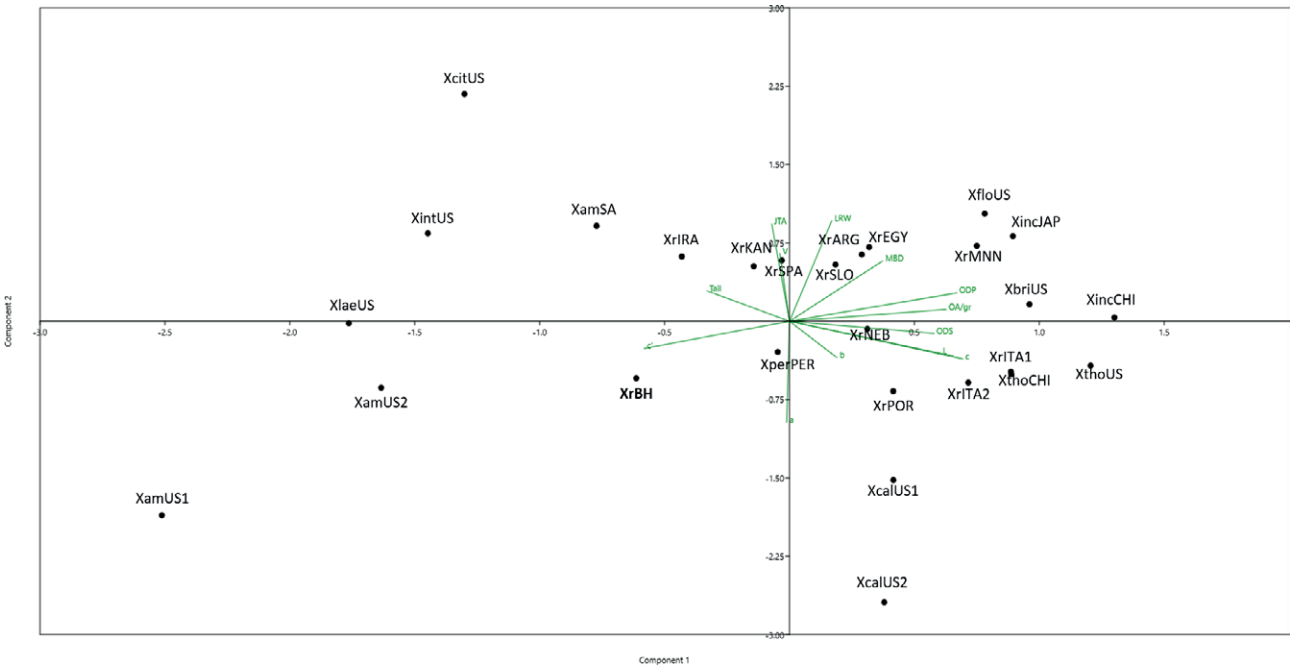

Figure 2. Principal component based on morphometric parameters of *Xiphinema rivesi* Dalmasso, 1969 from Bosnia-Herzegovina and other *X. americanum*-subgroup species from all over the world. Correlation biplot based on a PCA of the morphometric characters of *X. rivesi* from Bosnia-Herzegovina (XrBH) compared with population previous descripted in literature: XrARG (*X. rivesi*, Argentina; Chaves and Mondino, 2013); XrEGY (*X. rivesi*, Egypt; Handoo *et al*., 2015); XrIRA (*X. rivesi*, Iran; Fadaei *et al*., 2003); XrITA1 (*X. rivesi*, Italy; De Luca and Agostinelli, 2011); XrITA2 (*X. rivesi*, Italy; Troccoli *et al*., 2024); XrKAN (*X. rivesi*, USA; Lamberti and Bleve, 1979); XrMNN (*X. rivesi*, USA; Orlando *et al*., 2016); XrNEB (*X. rivesi*, USA; Lamberti and Bleve, 1979); XrPOR (*X. rivesi*, Portugal; Lamberti *et al*., 1994); XrSLO (*X. rivesi*, Slovenia; Urek *et al*., 2005); XrSPA (*X. rivesi*, Spain; Gutierrez-Gutierrez *et al.* 2012); XthoUS (*X. thornei*, USA; Lamberti and Golden 1986); XthoCHI (*X. thornei*, China; Wang *et al*., 1996); XincJAP (*X. incertum*, Japan, Lamberti and Bleve, 1979): XincCHI (*X. thornei*, China; Wang *et al*., 1996); XfloUS (*X. floridae*, USA; Lamberti and Bleve, 1979); XperPER (*X. peruvianum*, USA; Lamberti and Bleve, 1979); XlaeUS (*X. laevistriatum,* USA; Lamberti and Bleve, 1979); Xcal1US (*X. californicum,* USA; Lamberti and Bleve, 1979); Xcal2US (*X. californicum,* USA; Orlando *et al*., 2016); XintUS (*X. intermedium,* USA; Lamberti and Bleve, 1979); XcitUS (*X. citricolum,* USA; Lamberti and Bleve, 1979); XbriUS (*X. bricolense,* Canada*;* Ebsary *et al*., 1989); XamUSA1 (*X. americanum,* USA; Cobb, 1913); XamUSA2 (*X. americanum,* USA; Lamberti and Golden, 1984); XamSA (*X. americanum,* South Africa; Loots and Heyns, 1984).

diameter (r = 0.474) and J tail length (r = 0.459), as well as a high negative correlation for a ratio (r = -0.478). F3 was mainly dominated by a high positive correlation for tail length ratio (r = 0.493) and V ratio (r = 0.489). Specimens of species were not casually situated, and a widespread spatial separation was observed among the *Xiphinema* populations. *Xiphinema rivesi* populations clustered together in the middle of the diagram confirming the morphological similarity among populations. The values of vulva position, oral aperture to guided ring distance and the *a* ratio increased along y-axis (PC2) contributing to the variability among *X. rivesi* populations.

The PCA, built on the *X. pachtaicum*-subgroup species, showed an accumulated variability of 68.50% for total variance, with the contribution of PC1 of 31.21%, for PC2 of 22.18% and for PC3 of 15.11%. The KMO value was 0.583, indicating that the sample size was suitable for the analysis. The loading factors for each character were used to interpret their biological validities. For PC1, almost all the characters had positive correlations, except for tail length (r = - 0.008), a (r = - 0.113) and c′ ratio (r = - 0.301). PC2 was positively correlated with body length L (r = 0.464), c (r = 0.462) and b ratio (r = 0.431), with a gradual increase in values associated with body dimensions and general nematode size. For PC3, a strong positive correlation was found for tail length (r = 0.613) and c′ ratio (r = 0.389), but negative correlations to V (r = -0.432). *Xiphinema pachtaicum* and *X. incertum* grouped on the right side of the diagram, forming a closely related morphocluster, while *X. simile* and *X. parasimile* clustered together on the left side of the diagram clearly separated from the *X. pachtaicum*-subgroup. This spatial separation was mainly dominated by the PC1, grouping the species according to body width, distance of oral aperture to guided ring, odontostyle, and odontophore length.

Molecular characterization

The length of the amplified products of the D2-D3 expansion segments, ITS region and of the partial *mt*COI gene are reported in Table 3.

Low intra-population variability of D2-D3 region of *X. rivesi* sequences included in the present study was observed (2 to 12 nt). Blast NCBI searches using D2-D3 domains of BH *X. rivesi* showed 100% similarity with *X. rivesi* isolates from Italy, Chile (JX912150, OR683648) and the USA (KU680972), and 99% similarity with the remaining sequences of *X. rivesi* present in the Genbank database. Pairwise distances among D2-D3 sequences of *X. rivesi* ranged from 0 to 32 nucleotides, only *X. inaequale* (HM163210) differed between 3 to 40 bp (Supplementary Table S3). Blast search revealed that ITS sequences of *X. rivesi* from BH apple samples had 100% similarity with *X. rivesi* from Chile (OR698922) and *X. inaequale* Khan & Ahmad, 1975 (GQ231530), 99% similarity with *X. rivesi* from Italy (OR698913-OR698921; FR878063-66; 8-16 nt differences; 2-11 gaps), 98% similarity with *X. thornei* Lamberti & Morgan Golden, 1986 (27 nt differences; 21 gaps) and *X. rivesi* from USA (MT524488), and 94 to 96% similarity with all the remaining Genbank sequences for *X. rivesi*. The three individuals of the BH *X. rivesi* population that were amplified produced 435 bp COI fragments. Amplified products were cloned and two clones for each specimen were sequenced. Sequence analyses showed greatest similarity with Italian *X. rivesi*, differing by 1 to 5 bp (99 to 100% similarity). Pairwise distances of all *Xiphinema* COI present in the subgroup A ranged from 0 to 21% (from 0 to 70 nucleotides) (Supplementary Table S4).

D2-D3 sequences of the BH population of *X. incertum* showed 100% similarity with *X. penevi* from Morocco (KU250157), and *X. incertum* from Spain (KX244908) ; 99% similarity with Italian and other Spanish *X. incertum* (1-7 nt differences), and 96 to 98% similarity with corresponding sequences of *X. pachtaicum* and other species belonging to the *X. americanum*-group, confirming the considerable sequence similarity within the *Xiphinema americanum*-group.

Phylogenetic analyses

The D2-D3 phylogenetic tree produced two main clades: clade I containing all *X. rivesi* sequences and the closest species of the *X. americanum* group; and clade II containing all sequences of the *X. pachtaicum*-subgroup including *X. incertum* sequences (Figure 3). Clade I, as previously reported by Troccoli *et al*. (2024), showed different subgrouping for *X. rivesi*. Sequences of *X. rivesi* from Spain and the USA grouped together and separated from other subgroupings. The BH sequences formed a separated subgrouping due to nucleotide variability within *X. rivesi* populations. Clade II contained all sequences belonging to the *X. pachtaicum*-subgroup including *X. incertum* sequences. The subgrouping of *X. incertum* sequences also included *X. penevi* from Morocco, with high support. This indicates that *X. incertum* and *X. penevi* requires further investigation to clarify whether they are distinct or the same species.

The COI phylogenetic tree showed different subgroupings within the *X. americanum* group and within *X. rivesi* populations, separating according to geographical origins (Figure 4; A-D subgroupings). COI sequences of *X. rivesi* formed a well-supported subgroup (97% similarity), in which Italian and BH *X. rivesi* subgrouped together (Figure 4 A).

DISCUSSION

The present study reports previously unrecorded occurrences of *X. rivesi* and *X. incertum* nematodes in

Table 3. Populations of *Xiphinema* characterized in the present study.

Species	Location	Host	Sample code	Genbank accession number			Source
				D2D3	ITS	COI	
X. rivesi	Banja Luka, Bosnia and Herzegovina	*Malus domestica*	N 6_10	-	PV397451	-	B. Nježić
X. rivesi	Banja Luka, Bosnia and Herzegovina	*Malus domestica*	10_11BH	PV397456	-	-	B. Nježić
X. rivesi	Banja Luka, Bosnia and Herzegovina	*Malus domestica*	17_D2	PV397457	-	-	B. Nježić
X. rivesi	Banja Luka, Bosnia and Herzegovina	*Malus domestica*	21_BH	PV397458	-	-	B. Nježić
X. rivesi	Banja Luka, Bosnia and Herzegovina	*Malus domestica*	47_COIF	-	-	PV461875	B. Nježić
X. rivesi	Banja Luka, Bosnia and Herzegovina	*Malus domestica*	51_COIF	-	-	PV461876	B. Nježić
X. rivesi	Banja Luka, Bosnia and Herzegovina	*Malus domestica*	52_COIF	-	-	PV461877	B. Nježić
X. rivesi	Banja Luka, Bosnia and Herzegovina	*Malus domestica*	53_COIF	-	-	PV461878	B. Nježić
X. incertum	Banja Luka, Bosnia and Herzegovina	*Populus* sp.	XI_2_BH	PV397455	-	-	B. Nježić

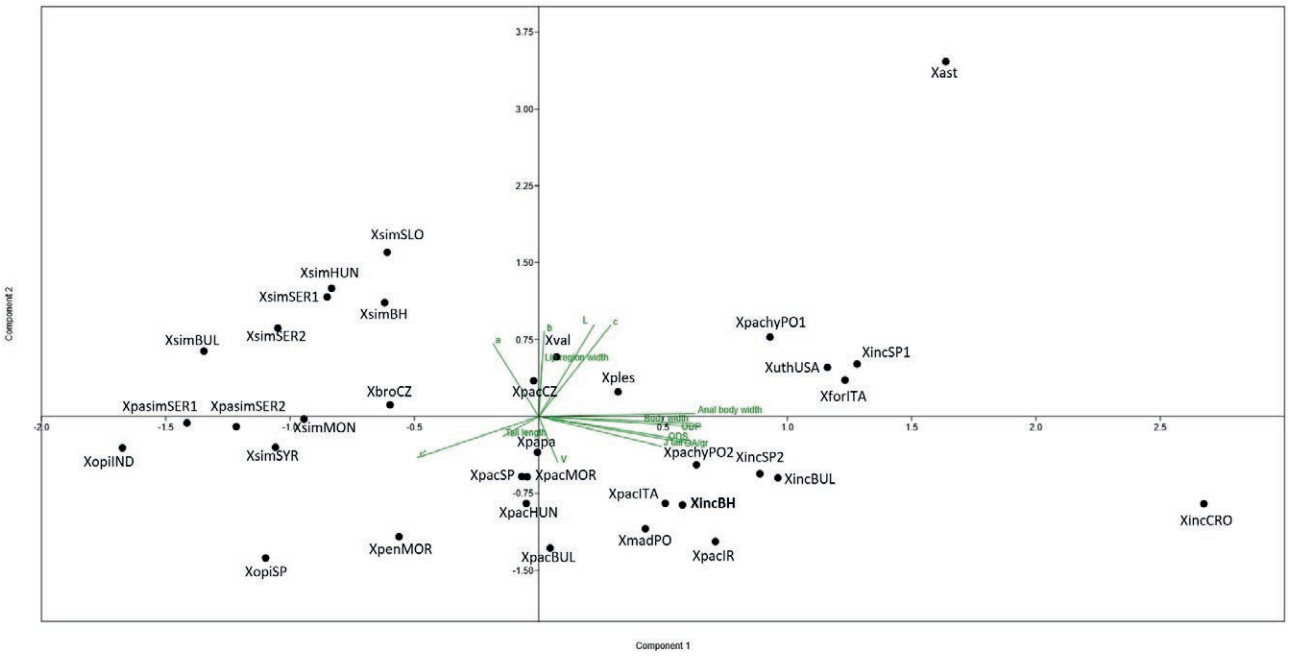

Figure 3. Principal component analysis based on morphometric parameters of *Xiphinema incertum* Lamberti, Choleva & Agostinelli, 1983 from Bosnia-Herzegovina and other *X. pachtaicum*-subgroup species from other geographic regions. The Correlation biplot based on a PCA of the morphometric characters of *X. incertum* from Bosnia-Herzegovina (XincBH) compared with previously described populations: XforITA (*X. fortuitum*, Italy; Roca *et al*., 1987); XuthUSA (*X. utahense*, United States of America; Lamberti and Bleve, 1979); XincBUL (*X. incertum*, Bulgaria; Lamberti *et al*., 1983); XincCRO (*X. incertum*, Croatia; Barsi, 1994); XincSP1 (*X. incertum*, Spain; Gutiérrez-Gutiérrez *et al*., 2012); XincSP2 (*X. incertum*, Spain; Archidona-Yuste *et al*., 2016); XmadPO (*X. madeirense,* Portugal; Lamberti *et al*., 1993); XpachyPO1- XpachyPO2 (*X. pachydermum,* Portugal; Lamberti *et al*., 1994); XopiIND (*X. opisthohysterum,* India; Siddiqi, 1961) XopiSPA (*X. opisthohysterum,* Spain; Archidona-Yuste *et al*., 2016); XsimBUL (*X. simile,* Bulgaria; Lamberti *et al*., 1993); XsimMON (*X. simile,* Montenegro; Barsi, 1994); XsimSER1 (*X. simile,* Serbia; Barsi, 1994); XsimSER2 (*X. simile,* Serbia; Barsi and De Luca, 2008); XsimBH (*X. simile,* Bosnia and Herzegovina; Barsi and Lamberti, 2004); XsimSLO (*X. simile*, Slovakia; Lamberti *et al*., 1999); XsimHUN (*X. simile,* Hungary; Repasi *et al*., 2008); XsimSYR (*X. simile*, Syria; Ali *et al*., 2024); XpasimSER1 (*X. parasimile*, Serbia; Barsi and Lamberti 2004); XpasimSER2 (*X. parasimile*, Serbia; Barsi and De Luca, 2008); XpenMOR (*X. penevi,* Morocco; Lazarova *et al*., 2016); XbroCZR (*X. browni*, Czech Republic; Lazarova *et al*., 2016); Xpapa (*X. parapachydermum,* Spain; Gutiérrez-Gutiérrez *et al*., 2012); Xast (*X. astaregiense,* Spain; Archidona-Yuste *et al*., 2016); Xples (*X. plesiopachtaicum,* Spain; Archidona-Yuste *et al*., 2016); Xval (*X. vallense,* Spain; Archidona-Yuste *et al*., 2016); XpacHUN (*X. pachtaicum,* Hungary; Repasi *et al*., 2008); XpacBUL (*X. pachtaicum,* Bulgaria; Lazarova *et al*., 2016); XpacMOR (*X. pachtaicum,* Morocco; Mokrini and Dababat, 2019); XpacIR (*X. pachtaicum,* Iran; Mobasseri *et al*., 2019); XpacSP (*X. pachtaicum,* Spain; Archidona-Yuste *et al.,* 2016); XpacITA (*X. pachtaicum,* Italy; Troccoli *et al*., 2024); XpacCZ (*X.pachtaicum,* Czech Republic; Kumari, 2006).

Bosnia-Herzegovina (BH), extending incidences of these nematodes in Europe. Morphometric comparisons of the two nematodes from this country with the type and other descriptions of these species confirmed the high intraspecific variability in both species (Tables 1 and 2). Multivariate analyses of *X. rivesi* populations, including the BH population, shared some overlapping characters along with morphometric differences, which may be due to their geographical origins and phenotypic plasticity (Figure 2). PCA of *X. incertum* showed that BH *X. incertum* shared overlapping characters with *X. incertum* populations from Bulgaria and Spain, and several species of the *X. pachtaicum* subgroup for size and body length. The Croatian population of *X. incertum* was closely related but separated from the BH and Bulgarian populations for posterior vulva position and having longer hyaline tails. *Xiphinema penevi* from Morocco was distant from BH *X. incertum* (Figure 3). These results have confirmed the existence of the *X. pachtaicum*-subgroup (Gutiérrez-Gutiérrez *et al*., 2012; Palomares-Rius *et al*., 2014; 2017), and the difficulty to correctly identify these nematode species. Sequence analyses of the BH *X. rivesi* markers confirmed the high interspecific variability within the species (Troccoli *et al*., 2024). For BH *X. incertum*, the D2-D3 sequence had low intra- and inter-specific variability among *X. incertum, X. penevi* (0-7 nt differences) and *X. pachtaicum* populations.

The phylogenetic trees based on D2-D3 showed two main clades, in agreement with previous reports (Archidona-Yuste *et al*., 2016; 2020; Orlando *et al*., 2016; Mobasseri *et al*., 2019; Troccoli *et al*., 2024).

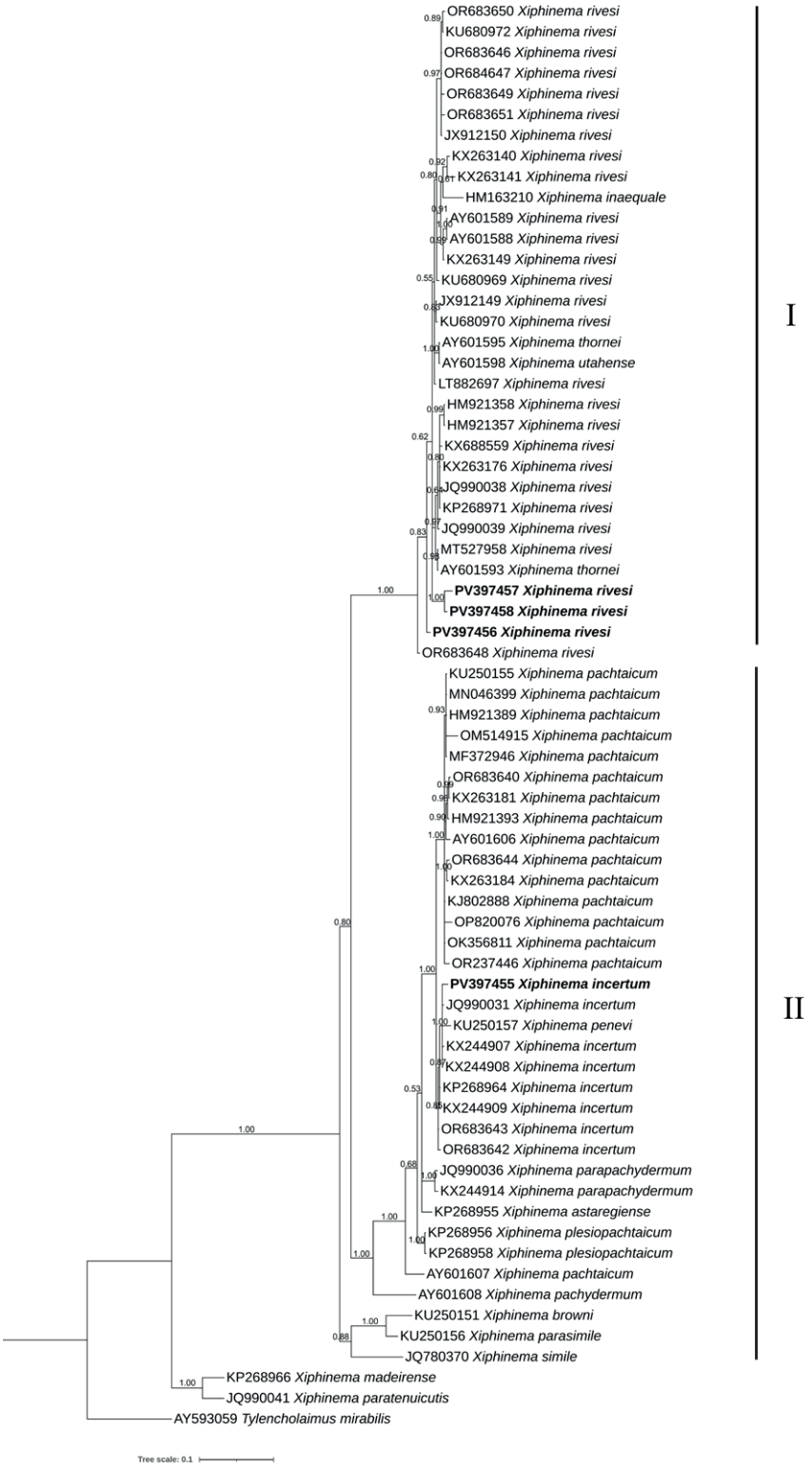

Figure 4. Phylogenetic relationships among *Xiphinema rivesi* Dalmasso, 1969 and *Xiphinema incertum* Lamberti, Choleva & Agostinelli, 1983 populations, indicated from the Bayesian 50% majority rule consensus tree as inferred from D2-D3 expansion domains of the 28S rRNA sequence alignment under a transversional, with correction for invariable sites and a gamma-shaped distribution model (GTR+I+G). Posterior probabilities of more than 0.50 are given for appropriate clades. Newly obtained sequences in the present study are shown in bold font. The scale bar indicates expected changes per site.

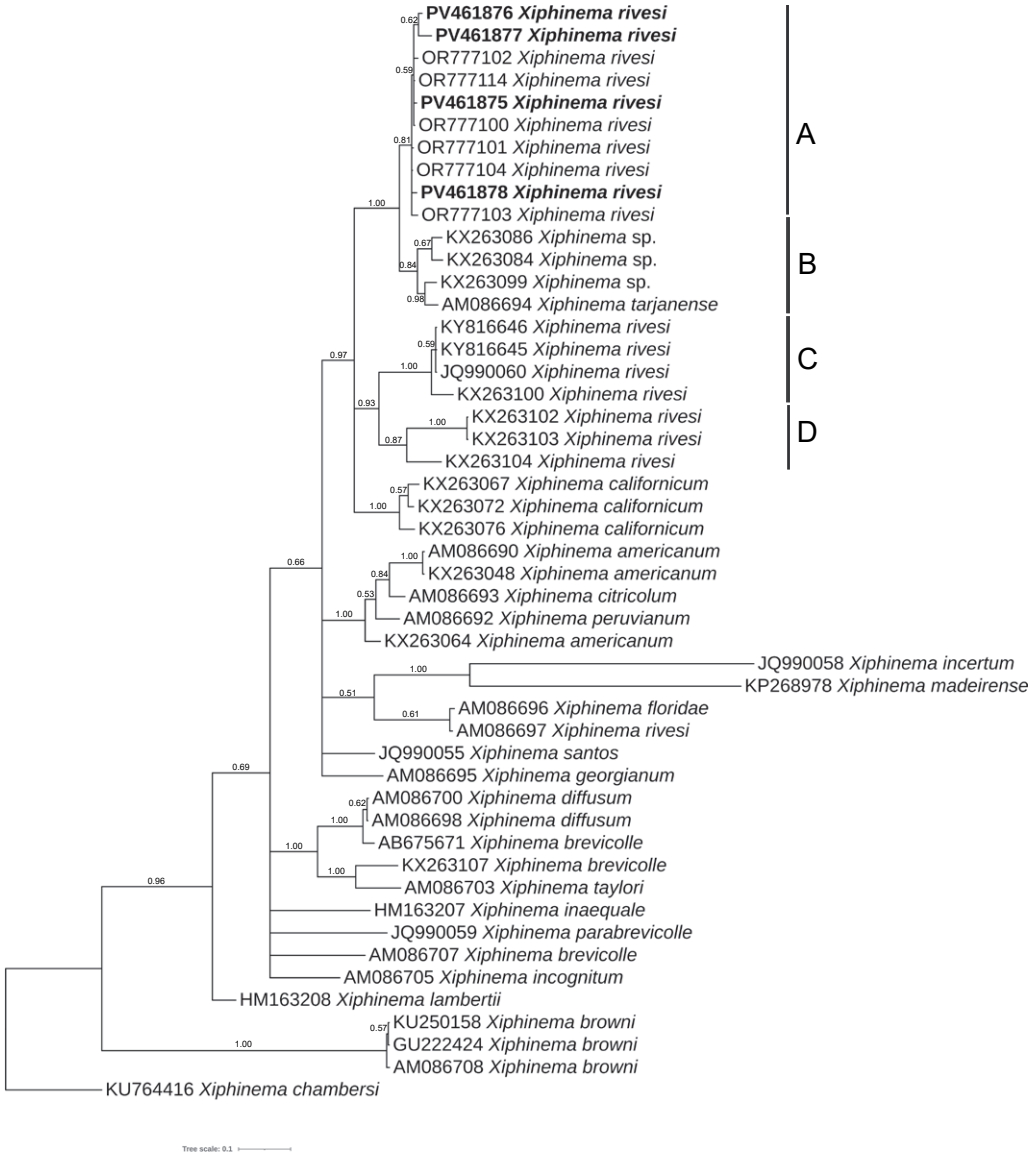

Figure 5. Phylogenetic relationships among *Xiphinema rivesi* Dalmasso, 1969 and *Xiphinema incertum* Lamberti, Choleva & Agostinelli, 1983 populations, indicated from Bayesian 50% majority rule consensus tree as inferred from mitochondrial COI sequence alignment under a transversional, with correction for invariable sites and a gamma-shaped distribution model (GTR+I+G). Posterior probabilities of more than 0.50 are given for appropriate clades. Newly obtained sequences in this study are shown in bold font. The scale bar indicates expected changes per site.

Clade I consisted of several subgroupings of *X. rivesi*, in particular the BH *X. rivesi* had high variability. Clade II grouped all sequences belonging to the *X. pachtaicum*-subgroup (Figure 4). *Xiphinema incertum* populations, including the BH population, and X. *penevi* formed a well-supported subgrouping, despite the PCA results placing *X. penevi* distant from *X. incertum* populations. This result confirms existence of different evolutionary rates of molecular and morphological mechanisms and indicates that *X. penevi* may represent a recent speciation event, as the D2-D3 sequences showed 100% similarity with those of *X. incertum*.

In the phylogenetic tree of COI sequences, different subgroupings of *X. rivesi* populations occurred (Figure 5). BH and Italian *X. rivesi* subgrouped together (Figure 5A), while *Xiphinema* sp. 1 and *X. tarjanense* were in a separate subgroup (Figure 5B) showing sister relationships with subgroup A. *Xiphinema rivesi* from Spain and United States of America were in separate subgroupings (Figure 5, C and D). These results demonstrate

the occurrence of different haplotypes within *X. rivesi*, probably resulting from different mutation rates in the mitochondrial genomes among the different geographical populations. Therefore, the COI marker was useful for population and intraspecific genetic variation studies among *X. americanum* group populations.

In conclusion, the present study shows new occurrence of *X. rivesi* and *X. incertum* in Bosnia-Herzegovina, extending their distribution in Europe. Particular attention is required when identifying *X. pachtaicum*, because of the existence of species complexes. Regarding to *X. incertum* and *X. penevi*, more molecular data are required to verify the occurrence of cryptic species or variability within *X. incertum*, as *X penevi* has only been described from Morocco. Knowledge of intra- and inter-specific molecular variability is important to detect misidentification or cryptic speciation within the *X. americanum* group. Use of COI for integrative nematode taxonomy can delimit species within *Nematoda*, but the high nucleotide variability of mitochondrial COI within the *X. americanum* group suggests high mutation rates, that can represent potential for development of cryptic species or the ability of these species to adapt to climate and environmental changes.

AUTHOR CONTRIBUTIONS

EF and AV equally contributed to molecular and phylogenetic analyses; AT and BN carried out morphological measurements; AV and RD contributed to sampling and nematode recovery; AV, AT, EF and BN reviewed and edited the paper manuscript; FDL contributed to the study design, writing of the original draft, and review and editing; FDL contributed to fund acquisition. The first draft of the manuscript was commented on by all authors, and they all approved the final manuscript.

DATA AVAILABILITY

All sequences described in this paper are freely available from the GenBank database.

LITERATURE CITED

Addinsoft, 2007. XLSTAT 2007 Data analysis and statistics software for Microsoft Excel. Paris, France.

Ali N., Vicente C.S., Mota M., Gutiérrez-Gutiérrez C., 2024. First report of four dagger nematode species of the genus *Xiphinema* (Nematoda: Longidoridae) from banana in Syria using an integrative approach. *European Journal of Plant Pathology* 169(4): 727–753. https://doi.org/10.1007/s10658-024-02868-3

Archidona-Yuste A., Navas-Cortés J.A., Cantalapiedra-Navarrete C., Palomares-Rius J.E., Castillo P., 2016. Cryptic diversity and species delimitation in the *Xiphinema americanum*-group complex (Nematoda: Longidoridae) as inferred from morphometrics and molecular markers. *Zoological Journal of the Linnean Society* 176(2): 231–265. https://doi.org/10.1111/zoj.12316

Archidona-Yuste A., Cai R., Cantalapiedra-Navarrete C., Carreira J.A., Rey A., ... Castillo P., 2020. Morphostatic speciation within the dagger nematode *Xiphinema hispanum*-complex species (Nematoda: Longidoridae). *Plants* 9, 1649. https://doi.org/10.3390/plants9121649

Barsi L., 1989. The Longidoridae (Nematoda: Dorylaimida) in Yugoslavia. I. *Nematologia Mediterranea* 17: 97–108.

Barsi L., 1994. Specimens of the *Xiphinema americanum*-group (Nematoda: Dorylaimida) on the territory of the former Yugoslavia. *Nematologia mediterranea* 22: 25–34.

Barsi L., Lamberti F., Agostinelli A., 1998. *Xiphinema densispinatum* sp. n. from Bosnia and Herzegovina and *X. montenegrinum* sp. n. from Montenegro, Yugoslavia (Nematoda: Dorylaimida) *Nematologia Mediterranea* 26: 67–77.

Barsi L., Lamberti F., 2002. Morphometrics of three putative species of the *Xiphinema americanum* group (Nematoda: Dorylaimida) from the territory of the former Yugoslavia. *Nematologia Mediterranea* 30: 59–72.

Barsi L., Lamberti F., 2004. *Xiphinema parasimile* sp. n. from Serbia and *X. simile*, first record from Bosnia and Herzegovina (Nematoda, Dorylaimida). *Nematologia Mediterranea* 32: 101–109.

Barsi L., De Luca F., 2008. Morphological and molecular characterisation of two putative *Xiphinema americanum*-group species, *X. parasimile* and *X. simile* (Nematoda: Dorylaimida) from Serbia. *Nematology* 10(1): 15–25.

Bello A., Robertson L., Díez-Rojo M.A., Arias M., 2005. A re-evaluation of the geographical distribution of quarantine nematodes reported in Spain. *Nematologia Mediterranea* 33: 209–213.

Cai R., Archidona-Yuste A., Cantalapiedra-Navarrete C., Palomares-Rius J.E., Castillo, P., 2020. New evidence of cryptic speciation in the family Longidoridae (Nematoda: Dorylaimida). *Journal of Zoological Sys-*

tematics and Evolutionary Research 58 (4): 869–899. https://doi.org/10.1111/jzs.12393

Chaves E.J., Mondino, E. A., 2013. Description of some *Xiphinema* species populations (Nematoda) from Argentina. *Nematropica* 43: 68–77.

Cobb N.A., 1913. New nematode genera found inhabiting fresh water and non-brackish soils. *Journal of the Washington Academy of Sciences* 3(16): 432–444.

Dalmasso A., 1969. Etude anatomique et taxonomique des genres *Xiphinema*, *Longidorus* et *Paralongidorus* (Nematoda: Longidoridae). *Mémoires du Muséum National d'Histoire Naturelle*, *Paris, Nouvelle Série A., Zoologie* 61: 33–82.

Darriba D., Taboada G., Doallo R., Posada D., 2012. jModelTest 2: more models, new heuristics and parallel computing. *Nature Methods* 9: 772. https://doi.org/10.1038/nmeth.2109

Decraemer W., Robbins R.T., 2007. The who, what and where of Longidoridae and Trichodoridae. *Jounal Nematology* 39(4):295–297.

De Luca F., Agostinelli A., 2011. Molecular and morphometry identification of plant parasitic nematodes. *Redia* 94: 143–148.

De Luca F., Fanelli E., Di Vito M., Reyes A., De Giorgi C., 2004. Comparisons of the sequences of the D3 expansion of the 26S ribosomal genes reveals different degrees of heterogeneity in different populations and species of *Pratylenchus* from the Mediterranean region. *European Journal of Plant Pathology* 110: 949–957. https://doi.org/10.1007/s10658-004-0813-4.

Ebsary B.A., Vrain T.C., Graham M.B., 1989. Two new species of *Xiphinema* (Nematoda: Longidoridae) from British Columbia vineyards. *Canadian Journal of Zoology* 67(4): 801–804.

Fadaei A.A., Coomans A., Kheiri A., 2003. Three species of the *Xiphinema americanum* lineage (Nematoda: Longidoridae) from Iran. *Nematology* 5(3): 453–461. https://doi.org/10.1163/156854103769224430

Flegg J.J.M., 1967. Extraction of *Xiphinema* and *Longidorus* species from soil by a modification of Cobb's decanting and sieving technique. *Annals of Applied Biology* 60: 429–437.

Guttiérrez-Guttiérrez C., Palomares Rius J.E., Cantalapiedra-Navarrete C., Landa B.B., Castillo P., 2011. Prevalence, polyphasic identification, and molecular phylogeny of dagger and needle nematodes infesting vineyards in southern Spain. *European Journal of Plant Pathology* 129 (3): 427–453.

Gutiérrez-Gutiérrez C., Cantalapiedra-Navarrete C., Decraemer W., Vovlas N., Prior T., ... Castillo P., 2012. Phylogeny, diversity, and species delimitation in some species of the *Xiphinema americanum*-group complex (Nematoda: Longidoridae), as inferred from nuclear and mitochondrial DNA sequences and morphology. *European Journal of Plant Pathology* 134: 561–597. https://doi.org/10.1007/s10658-012-0039-9

Gutiérrez-Gutiérrez C., Bravo M.A., Santos M.T., Vieira P., Mota M., 2016. An update on the genus *Longidorus*, *Paralongidorus* and *Xiphinema* (family Longidoridae) in Portugal. *Zootaxa* 4189 (1): 99–114.

Hall, T.M., Waugh, D.W., Boering, K.A. and Plumb, R.A., 1999. Evaluation of transport in stratospheric models. *Journal of Geophysical Research* 104: 18815–18839. https://doi.org/10.1029/1999JD900226

Hammer, Ø., Harper, D.A., 2001. Past: paleontological statistics software package for education and data anlysis. *Palaeontologia electronica* 4(1): 1.

Handoo Z.A., Ibrahim I.K.A., Chitwood D.J., Mokbel A.A., 2015. First report of *Xiphinema rivesi* Dalmasso, 1969 on citrus in northern Egypt. *Pakistan Journal of Nematology* 33(2): 161–165.

Jairajpuri M.S., Ahmad W., 1992. Dorylaimida: free-living, predaceous and plant-parasitic nematodes. Brill.

Kanzaki N, Futai K., 2002. A PCR primer set for determination of phylogenetic relationships of *Bursaphelenchus* species within the *xylophilus*-group. *Nematology* 4: 35–41. https://doi.org/10.1163/156854102760082186

Katoh K., Standley D.M., 2013. MAFFT multiple sequence alignment software version 7: Improvements in performance and usability. *Molecular Biology and Evolution* 30: 772–780. https://doi.org/10.1093/molbev/mst010

Khan S. H., Ahmad S., 1977. *Xiphinema inaequale* non. nov. (syn. *X. neoamericanum* Khan et Ahmad, 1975). *Nematologia Mediterranea* 5: 93.

Kirjanova E.S., 1951. Soil nematodes in cotton fields and in virgin soil of Golodnaya steppe (Uzbekistan). *Trudy Zoologicheskogo Instituta Akademiya Nauk SSSR* 9: 625–657.

Kornobis F., Osten-Sacken N., Winiszewska G., Castillo P., 2025. Cryptic speciation in the nematode family Longidoridae from South America: description of *Xiphinema cryptocostaricense* sp. nov. from Colombia and notes on *X. seinhorsti*. *European Journal Plant Pathology* 171: 375–389. https://doi.org/10.1007/s10658-024-02947-5

Kumar, S., Stecher, G., Li, M., Knyaz, C., Tamura, K., 2018. MEGA X: Molecular Evolutionary Genetics Analysis across Computing Platforms. *Molecular Biology Evolution* 35(6): 1547–1549. https://doi.org/10.1093/molbev/msy096

Lamberti F., Bleve-Zacheo T., 1979. Studies on *Xiphinema americanum* sensu lato with descriptions of fif-

teen new species (Nematoda, Longidoridae). *Nematologia Mediterranea* 7: 51–106.

Lamberti F., Choleva B., Agostinelli A., 1983. Longidoridae from Bulgaria (Nematoda, Dorylaimida) with description of three new species of *Longidorus* and two new species of *Xiphinema*. *Nematologia Mediterranea* 11: 49–72.

Lamberti F., Golden A.M., 1984. Redescription of *Xiphinema americanum* Cobb, 1913 with comments on its morphometric variations. *Journal of Nematology* 16(2): 204.

Lamberti F., Golden A. M., 1986. On the identity of *Xiphinema americanum* sensu lato in the nematode collection of Gerald Thorne with description of *X. thornei* sp. n. *Nematologia Mediterranea* 14: 163-171.

Lamberti F., Ciancio, A., 1993. Diversity of *Xiphinema americanum*-group species and hierarchical cluster analysis of morphometrics. *Journal of Nematology* 25(3): 332.

Lamberti F., Lemos R.M., Agostinelli A., D'Addabbo T., 1993. The *Xiphinema americanum*-group in the vineyards of the Dao and Douro regions (Portugal) with description of two new species (Nematoda, Dorylaimida). *Nematologia Mediterranea* 21(2): 215–225.

Lamberti F., Bravo M.A., Agostinelli A., Lemos R.M., 1994. The *Xiphinema americanum*-group in Portugal with descriptions of four new species (Nematoda, Dorylaimida). *Nematologia Mediterranea* 22: 189–218

Lazarova S., Peneva V., Kumari S., 2016. Morphological and molecular characterisation, and phylogenetic position of *X. browni* sp. n., *X. penevi* sp. n. and two known species of *Xiphinema americanum*-group (Nematoda, Longidoridae). *Zookeys* 574: 1–42. https://doi.org/10.3897/zookeys.574.8037

Loots G.C., Heyns J., 1984. A study of *Xiphinema americanum* sensu Heyns, 1974 (Nematoda). *Phytophylactica* 16(4): 313–320.

Luc M., Coomans A., Loof P.A.A., Baujard P., 1998. The *Xiphinema americanum* group (Nematoda: Longidoridae). 2. Observations on *Xiphinema brevicollum* Lordello & da Costa, 1961 and comments on the group. *Fundamental and Applied Nematology* 21: 475–490

Milašin R., Voruna M., Matić S., Njezic B., Artimová R., Medo J., Delić D., 2024. Characterisation of *Pythium capillosum* – A new pathogen of *Xiphinema pachtaicum* (Nematoda: Longidoridae). *European Journal Plant Pathology* 168: 497–500. https://doi.org/10.1007/s10658-023-02778-w

Mobasseri M., Hutchinson M.C., Afshar F.J., Pedram M., 2019. New evidence of nematode endosymbiont bacteria coevolution based on one new and one known dagger nematode species of *Xiphinema americanum*-group (Nematoda, Longidoridae). *PLoS ONE* 14(6): e0217506. https://doi.org/10.1371/journal.pone.0217506

Mokrini F., Dababat A., 2019. First report of the dagger nematode *Xiphinema pachtaicum* on onion in Morocco. *Journal of Nematology* 51: e2019-28. https://doi.org/10.21307/jofnem-2019-028

Nunn G.B., 1992. Nematode Molecular Evolution: An Investigation Of Evolutionary Patterns Among Nematodes Based Upon DNA Sequences. Ph.D. Thesis, University of Nottingham, Nottingham.

Orlando V., Chitambar J.J., Dong K., Chizhov V. N., Mollov D., Bert W., Subbotin S.A., 2016. Molecular and morphological characterisation of *Xiphinema americanum*-group species (Nematoda: Dorylaimida) from California, USA, and other regions, and co-evolution of bacteria from the genus *Candidatus xiphinematobacter* with nematodes. *Nematology* 18 (9): 1015–1043. https://doi.org/10.1163/15685411-00003012

Palomares-Rius J.E., Cantalapiedra-Navarrete C., Castillo P., 2014. Cryptic species in plant-parasitic nematodes. *Nematology* 16 (10): 1105–1118. https://doi.org/10.1163/15685411-00002831

Palomares-Rius J.E., Cantalapiedra-Navarrete C., Archidona-Yuste A., Subbotin S.A., Castillo P., 2017. The utility of mtDNA and rDNA for barcoding and phylogeny of plant-parasitic nematodes from Longidoridae (Nematoda, Enoplea). *Science Reports* 7(1): 10905. https://doi.org/10.1038/s41598-017-11085-4

Poiras L., 2012. Species diversity and distribution of free-living and plant parasitic nematodes from order Dorylaimida (Nematoda) in different habitats of the Republic of Moldova. Muzeul Olteniei Craiova. Oltenia. *Studii şi comunicări. Ştiintele Naturii* 28(2): 35–42.

Rambaut A., Suchard M., Xie D., Drummond A., 2014 Tracer v1.6. Computer Program and Documentation Distributed by the Author. https://beast.bio.ed.ac.uk/Tracer

Repasi V., Agostinelli A., Nagy P., Coiro M.I., Hecker K., Lamberti F., 2008. Distribution and morphometrical characterization of *Xiphinema pachtaicum*, *X. simile* and *X. brevicollum* from Hungary. *Helminthologia* 45: 96–102.

Roca F., Lamberti F., Agostinelli A., 1987. *Xiphinema fortuitum*, a new longidorid nematode from Italy. *Nematologia Mediterranea* 15: 219–223.

Ronquist F., Huelsenbeck J.P., 2003. MrBayes 3: Bayesian phylogenetic inference under mixed models. *Bioinformatics* 19(12): 1572–1574.

Seinhorst J.W., 1962. On the killing, fixation and transferring to glycerin of nematodes. *Nematologica* 8: 29–32. https://doi.org/10.1163/187529262X00981

Siddiqi M.R., 1961. On *Xiphinema opisthohysterum* n. sp., and *X. pratense* Loos, 1949, two dorylaimid nematodes attacking fruit trees in India. *Zeitschrift für Parasitenkunde* 20: 457–465.

Širca S., Stare B.G., Pleško I.M., Marn M.V., Urek G., Javornik B., 2007. *Xiphinema rivesi* from Slovenia transmit tobacco ringspot virus and tomato ringspot virus to cucumber bait plants. *Plant Diseases* 91(6): 770. https://doi.org/10.1094/PDIS-91-6-0770B. PMID: 30780499.

Sturhan D., 2014. Plant-parasitic nematodes in Germany - an annotated checklist. *Soil Organisms* 86(3): 177–198.

Taylor C.A., Brown D.J.F., 1997. Nematode vectors of plant viruses. CAB International: Wallingford, UK.

Troccoli A., Vovlas A., Fanelli E. et al., 2024. Integrative characterization and phylogenetic relationships of *Xiphinema rivesi* and *X. pachtaicum* (Nematoda, Longidoridae) associated to vineyards in North Italy. *European Journal Plant Pathology* 169: 137–157. https://doi.org/10.1007/s10658-024-02815-2

Urek G., Širca S., Kox L., Karssen, G., 2003. First report of the dagger nematode *Xiphinema rivesi*, a member of the *X. americanum* group, from Slovenia. *Plant Diseases* 87(1): 100. https://doi.org/10.1094/PDIS.2003.87.1.100A

Urek G., Širca,S., Karssen G., 2005. Morphometrics of *Xiphinema rivesi* Dalmasso, 1969 (Nematoda: Dorylaimida) from Slovenia. *Russian Journal of Nematology* 13: 1–13.

Vrain T.C., Wakarchuk D.A., Lévesque A.C., Hamilton R.I., 1992. Intraspecific rDNA Restriction Fragment Length Polymorphism in the *Xiphinema americanum* group. *Fundamental Applied Nematology* 15(6): 563–573.

Wang S., Chiu W. F., Yu C., Li C., Robbins R.T., 1996. The occurrence and geographical distribution of longidorid and trichodorid nematodes associated with vineyards and orchards in China. *Russian Journal of Nematology* 4: 145–154.

Finito di stampare da
Logo s.r.l. – Borgoricco (PD) – Italia

Mediterranean Phytopathological Union

Founded by Antonio Ciccarone

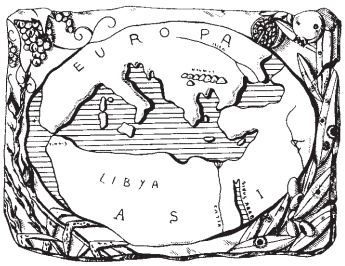

The Mediterranean Phytopathological Union (MPU) is a non-profit society open to organizations and individuals involved in plant pathology with a specific interest in the aspects related to the Mediterranean area considered as an ecological region.
The MPU was created with the aim of stimulating contacts among plant pathologists and facilitating the spread of information, news and scientific material on plant diseases occurring in the area. MPU also intends to facilitate and promote studies and research on diseases of Mediterranean crops and their control.
The MPU is affiliated to the International Society for Plant Pathology.

MPU National Society Members

Croatian Plant Protection Society, https://hdbz.hr/
Egyptian Phytopathological Society
French Society of Plant Pathology, http://www.sfp-asso.org/
Hellenic Phytopathological Society, http://efe.aua.gr/
Israeli Phytopathological Society, http://www.phytopathology.org.il/
Italian Association for Plant Protection, https://aipp.it/
Italian Phytopathological Society, http://www.sipav.org/
Palestinian Plant Production and Protection Society
Plant Protection Society in Bosnia and Herzegovina
Plant Protection Society of Serbia, https://plantprs.org.rs/
Portuguese Phytopathological Society, https://spfitopatologia.pt/
Spanish Phytopathological Society, https://sef.es/en
Turkish Phytopathological Society, https://www.fitopatoloji.org.tr/

MPU Affiliated Members

Arab Society for Plant Protection (ASPP), http://www.asplantprotection.org/
CIHEAM-Mediterranean Agronomic Institute of Bari, https://www.iamb.it/
Italian Society of Nematology, https://www.nematologia.it

2025 Information for authors of the Open Access journal *Phytopathologia Mediterranea*

Only MPU members are eligible to publish according to MPU membership categories (see https://oajournals.fupress.net/index.php/pm/about):

– All authors belonging to an MPU National Society Member (see list above) or to an MPU Affiliated Member (international organizations or networks), that signed a Memorandum of Understanding with MPU, are entitled to publish with a contribution to publication cost (https://oajournals.fupress.net/index.php/pm/about)
– All Individual Members (not in the above categories), including members of profit or non-profit entities, and physical person.

To become an Individual Member see www.mpunion.org or contact phymed@unifi.it

To receive the paper version of the journal please contact phymed@unifi.it

For information visit the MPU web site:
www.mpunion.org
or contact us at: Phone +39 39 055 2755861/862 – E-mail: phymed@unifi.it

Phytopathologia Mediterranea

Volume 64, April, 2025

Contents

Direttore responsabile: Giuseppe Surico • Autorizzazione del Tribunale di Firenze n. 4923 del 5-1-2000 • *Printed by* Logo S.r.l. - Padova, May 2025